DOE/NASA/0290-1
NASA CR-174732

Gas Cooled Fuel Cell Systems Technology Development

Final Report for the First Logical Unit of Work Contract Period: May 1982—May 1983

J.M. Feret
Westinghouse Electric Corporation

August 1983

Prepared for
NATIONAL AERONAUTICS AND SPACE ADMINISTRATION
Lewis Research Center
Under Contract DEN 3-290

for
U.S. DEPARTMENT OF ENERGY
Morgantown Energy Technology Center

DISCLAIMER

Printed in the United States of America

Available from
National Technical Information Service
U.S. Department of Commerce
5285 Port Royal Road
Springfield, VA 22161

NTIS price codes[1]
Printed copy: A15
Microfiche copy: A01

[1]Codes are used for pricing all publications. The code is determined by the number of pages in the publication. Information pertaining to the pricing codes can be found in the current issues of the following publications, which are generally available in most libraries: *Energy Research Abstracts (ERA); Government Reports Announcements* and Index (*GRA* and I); *Scientific and Technical Abstract Reports (STAR);* and publication, NTIS-PR-360 available from NTIS at the above address.

DOE/NASA/0290-1
NASA CR-174732

Gas Cooled Fuel Cell Systems Technology Development

Final Report for the First Logical Unit of Work
Contract Period: May 1982—May 1983

J.M. Feret
Westinghouse Electric Corporation
Advanced Energy Systems Division
Pittsburgh, PA 15236-0864

August 1983

Prepared for
National Aeronautics and Space Administration
Lewis Research Center
Cleveland, Ohio 44135
Under Contract DEN 3-290

for
U.S. DEPARTMENT OF ENERGY
Morgantown Energy Technology Center
Morgantown, West Virginia 26505
Under Interagency Agreement DE-AI21-80ET17088

TABLE OF CONTENTS

Section	Title	Page
1.0	SUMMARY	1-1
2.0	SYSTEMS ENGINEERING	2-1
2.1	DEVELOPMENT SYSTEM REQUIREMENTS	2-1
	2.1.1 SYSTEM ANALYSES	2-1
	2.1.2 FUEL CELL, FUEL PROCESSOR, POWER CONDITIONER AND ROTATING EQUIPMENT SYSTEMS DESIGN REQUIREMENTS	2-15
	2.1.3 FUEL CELL REQUIREMENTS	2-21
	2.1.4 FUEL CELL PROCESSES AND FACILITY REQUIREMENTS	2-29
	2.1.5 FUEL PROCESSOR, POWER CONDITIONER, AND ROTATING EQUIPMENT SYSTEMS TECHNOLOGY ASSESSMENT	2-52
2.2	FUEL CELL SYSTEMS REQUIREMENTS	2-62
	2.2.1 25 kW SHORT STACK FUEL CELL TEST SPECIFICATION	2-62
	2.2.2 FUEL CELL HARDWARE TEST SPECIFICATIONS	2-62
	2.2.3 FUEL CELL MANUFACTURING PROCESS SPECIFICATIONS	2-82
2.3	SYSTEMS INTEGRATION	2-88
	2.3.1 FUEL CELL SYSTEM (FCS) DESIGN	2-88
	2.3.2 FUEL PROCESSOR, POWER CONDITIONER, AND ROTATING EQUIPMENT SYSTEMS DESIGNS	2-100
	2.3.3 SYSTEMS INTERFACE REQUIREMENTS AND CONTROL	2-115
3.0	FUEL CELL DEVELOPMENT AND TEST	3-1
3.1	SUBSCALE FUEL CELL DEVELOPMENT	3-1
	3.1.1 DEVELOPMENT STATUS	3-1
	3.1.2 SUBSCALE FUEL CELL DESIGN DESCRIPTION	3-2
	3.1.3 SUBSCALE FUEL CELL ASSEMBLY	3-5

TABLE OF CONTENTS (CONTINUED)

Section	Title	Page
	3.1.4 SUBSCALE FUEL CELL TESTING	3-5
3.2	NINE-CELL STACK DEVELOPMENT	3-41
	3.2.1 DEVELOPMENT STATUS	3-41
	3.2.2 NINE-CELL STACK DESIGN DESCRIPTION	3-42
	3.2.3 NINE-CELL STACK TESTING	3-45
3.3	10 kW FUEL CELL STACK DEVELOPMENT	3-48
	3.3.1 DEVELOPMENT STATUS	3-48
	3.3.2 10 kW STACK DESIGN DESCRIPTION	3-48
3.4	25 kW SHORT STACK DEVELOPMENT	3-52
	3.4.1 DEVELOPMENT STATUS	3-52
	3.4.2 25 kW STACK DESIGN DESCRIPTION	3-53
	3.4.3 STRUCTURAL ANALYSIS	3-57
3.5	100 kW FULL STACK DEVELOPMENT	3-63
	3.5.1 DEVELOPMENT STATUS	3-63
	3.5.2 100 kW STACK DESIGN DESCRIPTION	3-63
3.6	375 kW MODULE DEVELOPMENT	3-66
	3.6.1 DEVELOPMENT STATUS	3-66
	3.6.2 375 kW MODULE DESIGN DESCRIPTION	3-66
3.7	FUEL CELL MATERIALS CHARACTERIZATION TESTING	3-77
	3.7.1 RAW MATERIAL SPECIFICATIONS	3-77
	3.7.2 PLATE MATERIALS	3-77
	3.7.3 SEAL MATERIALS	3-92

TABLE OF CONTENTS (CONTINUED)

Section	Title	Page
	3.7.4 ELECTRODE MATERIALS	3-99
	3.7.5 MATRIX MATERIALS	3-109
	3.7.6 OTHER STACK MATERIALS	3-117
3.8	ADVANCED FUEL CELL DEVELOPMENT	3-129
	3.8.1 CATALYST AND SUPPORT	3-129
	3.8.2 ACID MANAGEMENT	3-129
	3.8.3 POISON EVALUATION	3-135
	3.8.4 CORROSION ANALYSIS	3-142
	3.8.5 PLATE MOLDING	3-161
4.0	FACILITIES DEVELOPMENT	4-1
	4.1 SUBSCALE 2 x 2 INCH CELL PRESSURIZED TEST FACILITIES	4-1
	4.2 NINE CELL STACK TEST FACILITIES DEVELOPMENT	4-1

LIST OF FIGURES

Figure No.	Title	Page
2.1.1-1	Operating Map for Cathode Air Stoichiometry of 2.0	2-5
2.1.1-2	Domestic U.S. Energy Price Projections in 1983 Dollars	2-10
2.1.1-3	Combustion Turbine Cost of Electricity at Full Load Heat Rate	2-11
2.1.1-4	Optimum Reload Interval and Operating Heat Rate Versus Fuel Price	2-13
2.1.1-5	PAFC Breakeven Total Plant Investment Relative to Combustion Turbine (1983 Dollars)	2-16
2.1.2-1	Operating Map of Cathode Air Stoichiometry of 2.0	2-18
2.1.4-1	Technology Development Logic - PAFC Module	2-30
2.1.5-1	Rotating Equipment Concepts	2-58
2.1.5-2	Rotating Equipment System (RES) Process Flow Schematic	2-60
2.1.5-3	Rotating Equipment System (RES) Arrangement - Top View	2-61
2.2.3-1	Polarization Curves for Five-Cell Stack E-005-001	2-86
2.3.1-1	Fuel Cell Module Design	2-89
2.3.1-2	Fuel Cell System Flow Diagram	2-90
2.3.1-3	Fuel Cell System Conceptual Design	2-93
2.3.1-4	Piping Configuration for the Fuel Cell System Cooling Air	2-96
2.3.2-1	Fuel Processing System (FPS) Flow Schematic (Natural Gas Feed)	2-102
2.3.2-2	Fuel Processing System (FPS) Layout	2-105
2.3.2-3	7.5 MW PAFC Power Plant Power Conditioning System (PCS)	2-107
2.3.2-4	Rotating Equipment System (RES) Flow Schematic	2-111
2.3.2-5	Operating Map of Rotating Equipment System Showing Compressor Surge Limits	2-116
2.3.2-6	Rotating Equipment System Arrangement - Top View	2-117
2.3.2-7	Rotating Equipment System Arrangement - Side View	2-118

LIST OF FIGURES (CONT'D)

Figure No.	Title	Page
2.3.3-1	Interface Control Documents	2-119
2.3.3-2	PAFC Plant Specification Tree	2-121
2.3.3-3	Interface Control Document (ICD) Preparation, Approval and Release Flow Chart	2-122
2.3.3-4	Interface Control Document (ICD) Revision Flow Chart	2-124
3.1.2-1	Subscale 2 x 2 Inch Cell Test Assembly	3-3
3.1.4-1	Polarization Curves for Cells SC-036, 037, 038, and 039	3-11
3.1.4-2	Polarization Curves for Cells SC-041, 042, 043, and 044	3-12
3.1.4-3	Polarization Curves for Cell SC-039, Air, and Oxygen	3-13
3.1.4-4	Polarization Curves for Cell SC-045, Air and Oxygen	3-14
3.1.4-5	Transient Response of Cell Voltage and Internal Resistance with the Variation of Operating Current Density	3-23
3.1.4-6	Variation of Cell Potentials at Constant Current Densities 100, 200, and 325 mA/cm^2 with Operating Temperature	3-25
3.1.4-7	Variation of Cell Voltages with Minor Changes in Operating Currents	3-26
3.1.4-8	Effects of Air Flow Rate on the Measured Cell Voltages at 100, 200, and 325 mA/cm^2	3-28
3.1.4-9	Tafel Plots for Oxygen Reduction in Laminated Porous Cathodes	3-29
3.1.4-10	Cathode Performance Characteristics at Various Air Flow Rates	3-32
3.1.4-11	Variation of Internal Resistance with Air Flow Rate at 100, 200, and 325 mA/cm^2	3-34

LIST OF FIGURES (CONT'D)

Figure No.	Title	Page
3.1.4-12	Subscale Pressurized Test Facility	3-36
3.1.4-13	Variation of Terminal Voltage and IR-Free Cell Voltage at 325 mA/cm^2 with Operating Pressure for Subscale Cell SC-062	3-38
3.1.4-14	Cell Voltage Gain at 200 and 325 mA/cm^2 as a Function of Operating Pressure	3-39
3.2.2-1	Nine-Cell Stack Assembly	3-43
3.3.2-1	PAFC 10 kW Stack Test Assembly	3-50
3.4.2-1	25 kW Stack Design	3-54
3.4.2-2	Baseline Fuel Cell Stack	3-55
3.4.3-1	Analytical Model Used for 25 kW Stack Evaluation	3-59
3.6.1-1	General Seal Test Configuration	3-67
3.6.2-1	Module Cooling Air Flowpath	3-69
3.6.2-2	Module Process Air Flowpath	3-70
3.6.2-3	Fuel Gas Flowpath	3-71
3.6.2-4	Module Flowpaths	3-72
3.7.2-1	PAFC Stack Z-Bipolar and Tree Cooling Plates	3-79
3.7.2-2	General Seal Test Configuration	3-83
3.7.3-1	Compressive Stress Versus Seal Strain for Viton Sponge/Viton Cement at Ambient Temperature Before and After Thermal Cycle	3-95
3.7.3-2	Compressive Stress Versus Seal Strain for Viton Sponge/Viton Cement at Both Ambient and Operating Temperature Conditions	3-96
3.7.3-3	Compressive Stress Versus Seal Strain Pelmor Compound #PLV-10059 Viton 1 Viton/Cement Seal Configuration at Ambient Temperature (60 Durometer Value)	3-98

LIST OF FIGURES (CONT'D)

Figure No.	Title	Page
3.7.4-1	Solution Viscosity Versus Concentration Polyox WSR-301	3-107
3.7.4-2	Brookfield Versus Dip-N-Read Viscosimeter Data Versus Polyox WSR-301 Concentration	3-108
3.7.4-3	Pore Distribution Versus Mercury Intrusion Pressure for Wet Proofed Backing Paper	3-111
3.7.5-1	Relative Flow Rate Versus Pressure for Dry Matrix Materials	3-116
3.7.6-1	Electrode Seal Interface Test Configuration	3-119
3.7.6-2	Nominal Compressive Stress Versus 10-Cell Stack Strain for Dry Stack with Heat Treated Bipolar Plates at Ambient Temperature for Cell Group VI	3-126
3.7.6-3	Nominal Compressive Stress Versus 10-Cell Stack Strain for Dry Stack with Heat Treated Bipolar Plates at Operating Temperature of 200°C for Cell Group VI	3-127
3.7.6-4	Effect Compressive Stress Versus 10-Cell Stack Strain for Dry Stack with Heat Treated Bipolar Plates at Ambient Temperature Cell Group VI	3-128
3.8.2-1	Water Vapor Pressure Versus Temperature for Constant Concentrations (System: H_3PO_4 and water)	3-131
3.8.2-2	Water Vapor Pressure Versus Temperature for Constant Volume (System: H_3PO_4 and water)	3-132
3.8.2-3	AICM-Anode Backing	3-133
3.8.2-4	Apparatus for Characterizing Gas Flow Through A Thin Porous Sheet	3-137
3.8.3-1	Polarization Curves for No-Mat-1 Cell	3-140
3.8.3-2	Comparison of Polarization Curves for No-Mat-1 and Cleared Mat-1 Cells	3-141
3.8.4-1	Results of Corrosion Testing of PLV 10059	3-144
3.8.4-2	Comparison of Corrosion Behavior for A-99 Regrind Material and Standard (A-99) Material	3-146

LIST OF FIGURES (CONT'D)

Figure No.	Title	Page
3.8.4-3	Comparison of Corrosion Behavior for Stackpole Graphite ZZ-144 and Asbury A-99 Plate Material	3-147
3.8.4-4	Comparison of Corrosion Behavior for Poco Graphite and Standard (A-99) Plate Material	3-148
3.8.4-5	Corrosion Tafel Plots for Miscellaneous Materials	3-149
3.8.4-6	Procedure for Introducing a Cross Leak in a Cell	3-153
3.8.4-7	Procedure for Wetting Backing to Create a Continuous Ionic Path	3-154
3.8.4-8	Life Graph of 12-Cell Stack Z-004	3-157
3.8.4-9	Life Graph of 6-Cell Stack Z-003	3-160
3.8.5-1	Molding Parameter Surface (MPS) for the Z-Pattern Flat Plates (Graphite/Resin) with Shoulders (Plate Thickness 0.245 in.)	3-162
3.8.5-2	Molding Parameter Surface (MPS) for the Z-Pattern Flat Plates (Graphite/Resin) with Shoulders (Plate Thickness 0.170 in.)	3-163
3.8.5-3	Warping Characteristics of the Molded and Subsequently 900°C Heat-Treated MK-II Cooler Plate (Materials - A-99 Graphite, Varcum Resin)	3-168
3.8.5-4	Warping Characteristics of the Molded and Subsequently 900°C Heat-Treated MK-II Bipolar Plate (Materials - A-99 Graphite and Varcum Resin)	3-169
3.8.5-5	Micrograph of a Cross-Section of the Rib of a Machined Graphite/Resin Composite Plate	3-170
3.8.5-6	Micrograph of a Cross-Section of the Rib of a Molded Graphite/Resin Composite Plate	3-171
3.8.5-7	Random Graphite Particle Orientation in a Regrind Material/Resin Composite	3-174
4.1-1	2 x 2 Inch Pressurized Test Facility in Operation	4-3

LIST OF TABLES

Table No.	Title	Page
2.1.1-1	Performance Summary	2-3
2.1.1-2	Reliability and Availability Assessment Summary	2-9
2.1.1-3	PAFC Cost and Performance Data	2-14
2.1.2-1	Rotating Equipment System (RES) Operating Requirements	2-22
2.1.3-1	Key PAFC System and Design Constraints	2-25
2.1.3-2	PAFC Development Goals	2-28
2.1.4-1	Experimental Design Variables	2-32
2.1.4-2	Test Variable Measurements Required and Precision Definitions	2-33
2.1.4-3	375 kW Module Performance Requirements	2-37
2.1.4-4	MTF Test Objectives	2-38
2.1.4-5	MTF Test Requirements	2-41
2.1.4-6	MTF Preliminary List of Measurements	2-50
2.1.5-1	Fuel Processing System (FPS) Development Goals	2-53
2.1.5-2	Comparison of Basic Inverter Types	2-55
2.1.5-3	Consolidation Circuitry Control Requirements	2-56
2.1.5-4	Summary Rotating Equipment System (RES) Configurations	2-59
2.2.1-1	25 kW Stack Performance Requirements	2-63
2.2.1-2	Preliminary List of Measurements Required for 25 kW Stack Testing	2-64
2.2.2-1	Test Group Definitions - 2 x 2 Subscale Cells	2-65
2.2.2-2	Areas of Design and Operating Variables	2-67
2.2.2-3	Measurements for Process/Fabrication Control	2-68
2.2.2-4	Measurements for Technology Design Performance	2-69

LIST OF TABLES (CONT'D)

Table No.	Title	Page
2.2.2-5	Measurements to Establish Operation Characteristics	2-70
2.2.2-6	Electrode Comparisons - 2 x 2 Subscale Cell Test Assemblies	2-72
2.2.2-7	Pressurized 2 x 2 Subscale Test Plan Sequence	2-74
2.2.2-8	Pressurized Operating Condition Tests	2-76
2.2.2-9	Mapping Points for Cell to Stack Comparison	2-77
2.2.2-10	Pertinent Parameter Definitions	2-78
2.2.2-11	Measurements for Stack Mechanics	2-80
2.2.2-12	Test Plan Sequence	2-81
2.2.3-1	Summary of Testing for Stack E-005-001	2-84
2.2.3-2	Stack E-005-001 Performance Data	2-87
2.3.1-1	Fuel Cell System Performance Summary	2-91
2.3.1-2	Stress Results for the 0.4 m (16 inch schedule 30) Air Pipes	2-97
2.3.2-1	Fuel Processing System (FPS) Major Equipment	2-104
2.3.2-2	Rotating Equipment System (RES) Operating Requirements	2-112
2.3.2-3	Rotating Equipment System (RES) Power Requirements	2-114
3.1.4-1	Repeating Component Identification	3-7
3.1.4-2	Cell Resistance and Open Circuit Voltage after 100 Hours	3-8
3.1.4-3	Test Time Versus IR-Free Voltage Performance	3-9
3.1.4-4	Analysis of Results of Subscale Cell Reproducibility	3-10
3.1.4-5	Repeating Component Identification for Evaluation of Lot No. 3 Catalyst	3-16
3.1.4-6	IR-Free Voltage (mV) for Cells Built with Lot No. 3 Catalyst	3-17

LIST OF TABLES (CONT'D)

Table No.	Title	Page
3.1.4-7	Data on Cells having Alternate Matrix Material	3-18
3.1.4-8	Effect of Cycling to Ambient Temperature on Cell Performance at 190°C and 200 mA/cm^2	3-20
3.1.4-9	Comparison of Components and Performance of Subscale Cells for Endurance Tests	3-21
3.1.4-10	Effects of Oxygen Content of Kinetic Parameters for Oxygen Reduction at 191°C and Ambient Pressure	3-30
3.1.4-11	Effect of Air Flow Rate on Concentration Overpotential	3-33
3.1.4-12	Pressurized Cell Component Identification	3-37
3.1.4-13	Variation of Performance Characteristics of Pressurized Subscale Cells with Time	3-40
3.2.3-1	Nine-Cell Stacks - W009-04, 05, 06, and 07	3-46
3.2.3-2	Stack Test Program	3-47
3.2.3-3	Nine-Cell Stack Summary	3-49
3.6.1-1	Module Design Parameters	3-68
3.6.2-1	Module Physical Characteristics	3-75
3.6.2-2	Module External Interfaces	3-76
3.7.1-1	Raw Material Specification Status	3-78
3.7.2-1	Preliminary Porosity Data - Bipolar Plates	3-81
3.7.2-2	Electrical Resistivity of Development Plates	3-85
3.7.2-3	Mercury Porosimetry Data for Development Plates	3-86
3.7.2-4	Solvent Extraction and Infrared Spectrographic Data	3-88
3.7.2-5	Plate/Material Thermogravimetric Analysis	3-89
3.7.2-6	X-Ray Diffraction of Graphite Powder and Plate Material	3-91

LIST OF TABLES (CONT'D)

Table No.	Title	Page
3.7.3-1	Cell-To-Cell Seal Test Configuration and Materials	3-94
3.7.3-2	Elastomer Acid Compatibility Screening Test Data	3-100
3.7.4-1	Emission Spectrographic Analyses of Electrode Layers, Catalyst and Catalyst Support Material	3-102
3.7.4-2	Platinum Analysis of Cathodes	3-104
3.7.4-3	Miscellaneous Evaluations of Catalyst and Support	3-105
3.7.4-4	Backing Paper Mercury Porosimetry Data	3-110
3.7.4-5	Electrical Resistance of Compressively Loaded Teflon Backing Paper	3-112
3.7.5-1	Wicking Rate and Acid Content of Matrix Materials	3-114
3.7.5-2	Mercury Porosimetry Data for Matrix Materials	3-115
3.7.6-1	Contact Resistance of Various Collector Plates after Air Exposure at 200°C	3-118
3.7.6-2	Test Parameters for Viton Seal and Support Materials	3-120
3.7.6-3	Summary of Load Versus Deformation Compression Test Data	3-121
3.7.6-4	Summary of Compressive Pressure Required to Initiate Deformation of Support Material	3-122
3.8.2-1	Reproducibility of the AICM Manufacturing Process	3-134
3.8.2-2	Comparison of Acid Pickup in Wetproofed, Non-Wetproofed, and AICM Backing Paper	3-136
3.8.3-1	Chemical Analysis of Fuel Cell Components and Materials Selected for Poison Evaluation	3-138
3.8.4-1	Results of Corrosion Testing and Acid Tolerance Characteristics of Viton Seal Materials	3-143
3.8.4-2	Randomized Cell Arrangement for the 12-Cell Stack Z-004	3-151

LIST OF TABLES (CONT'D)

Table No.	Title	Page
3.8.4-3	Randomized Cell Arrangement for the 6-Cell Stack Z-003	3-152
3.8.4-4	Summary of Testing for Stack Z-004	3-156
3.8.4-5	Summary of Testing for Stack Z-003	3-158
3.8.5-1	Physical Property Measurements of Flat Z-Pattern Plates Molded with Varied Conditions	3-164
3.8.5-2	Dimensional Measurements of 900^{o}C Heat-Treated Machined MK-II Plates	3-165
3.8.5-3	Comparison of Dimensional and Physical Properties for Plates with Varied Molding Cycles	3-166
3.8.5-4	Summary of Heat Treated Experimental Plates Molded with Alternate Graphites	3-172
4.1-1	2 x 2 Inch Cell Pressurized Test Facility Capabilities	4-2
4.1-2	2 x 2 Inch Cell Pressurized Test Facility Verified Operating Conditions	4-4
4.1-3	2 x 2 Inch Performance Data Obtained During Test Facility Check Out (Terminal Voltage)	4-5
4.1-4	2 x 2 Inch Performance Data Obtained During Test Facility Check Out (IR-Free Voltage)	4-6
4.2-1	12 x 17 Inch Stack Pressurized Test Facility Capabilities	4-7
4.2-2	12 x 17 Inch Stack Pressurized Test Facility Design Operating Conditions Range	4-8
4.2-3	Specifications of the Failure Mode Control System for 12 x 17 Inch Stack Pressurized Test Facility	4-9
4.2-4	Progress Report 12 x 17 Inch Pressurized Stack Test Facility	4-10

AE	Architect Engineer
AICM	Acid Inventory Control Members
BOU	Beginning of Use
CCB	Change Control Board
CDIF	Component Development and Integration Facility
COE	Cost of Electricity
DRI	Data Resources, Inc.
EDA	Energy Dispersive Analysis
EOU	End of Use
EPRI	Electric Power Research Institute
ERC	Energy Research Corporation
ESEERCO	Empire State Electric Energy Research Corporation
FCS	Fuel Cell System
FPS	Fuel Processing System
HTS	High Temperature Shift
ICD	Interface Control Documents
ICS	Instrumentation and Control System
LTS	Low Temperature Shift
LVDT	Linear Variable Displacement Transducer
MTF	Module Test Facility
NMP	N Methyl Pyrrolidone
PAFC	Phosphoric Acid Fuel Cell
PCS	Power Conditioning System
PDS	Purchasing Department Specifications
PSD	Primary Control Designer
RES	Rotating Equipment System
SAS	Service Air System
SCS	Steam Condensing System
SD	System Designer
SEM	Scanning Electron Microscopy
SGS	Steam Generator System
SI	System Integration
TDP	Technology Development Program
TGA	Thermogravimetric Analysis
UPP	Utility Power Plant
USE	Utility Station Equipment
WDS	Waste Disposal System
WRS	Water Recovery System
WTS	Water Treatment System

1.0 SUMMARY

The work described in this report addresses the first phase of a planned multiphase program to develop a phosphoric acid fuel cell (PAFC) for electric utility prototype power plant application. The first phase effort in this PAFC Technology Development Program (TDP), funded by the U. S. Department of Energy, Office of Fossil Energy, Morgantown Energy Technology Center, and managed by the NASA Lewis Research Center, was performed by a team comprised primarily of personnel from the Westinghouse Advanced Energy Systems Division and the Energy Research Corporation (a subsidiary of St. Joe Minerals Corporation). The PAFC TDP was performed in parallel with the Utility Power Plant (UPP) Program being sponsored by Westinghouse, the two host utilities, the Electric Power Research Institute, the Empire State Electric Energy Research Corporation, and other participating organizations.

The major technical objectives of the first phase of the PAFC TDP effort were to:

- Establish the preliminary design requirements and system conceptual design for the nominally rated 375 kW PAFC module and its interfacing power plant systems (Fuel Processing, Power Conditioning, and Rotating Equipment Systems).

- Improve the existing PAFC materials data base and establish baseline materials specifications and process procedures for the electrodes, carbon matrix and silicon carbon layer, and bipolar and cooling plates.

- Establish PAFC component and stack performance, endurance, and design parameter data needed for design verification for power plant application. The primary PAFC stack performance goals are:

  An average start of life cell voltage of 680 mV at operating conditions of 70 psia, 190°C, 325 mA/cm^2, 80 percent hydrogen utilization using reformed natural gas and three stoichs of air.

  Endurance consistent with a voltage loss of 2 mV per 1,000 hours and a corrosion rate of five mils per 6,000 hours at the above operating conditions.

- Development of an Acid Management System, economical method of heat treating bipolar and cooling plates, and improved electrode catalyst utilization.

Considerable progress was achieved relative to each of these objectives which is summarized below:

- A number of trade-off studies were performed to determine the proper plant power level, the pressure and temperature level at the rated plant power level, the power level control mode, and the fuel cell system design configuration. As a result of these studies, design parameters were selected for the prototype power plant conceptual design effort that satisfy the various plant economic and performance goals established, such as an installed capital cost of $\$2725/kW_e$ ac net in 1981 dollars, and a heat rate of less than 9000 Btu/kWh of net ac power output using natural gas. The selected design parameters are: (1) a 7.5 MW_e dc plant power output which has about a 7.2 MW_e ac net output, (2) fuel cell system operating points of 70 psia, 190°C, and 325 mA/cm^2, (3) a variable pressure and temperature control mode capability that approximates a constant phosphoric acid concentration, and (4) electrically connect the modules in two parallel banks of ten modules each to produce the 7.5 MW_e dc at about 2240 volts.

  In accordance with the above selected plant design parameters, system level requirements were developed for the fuel cell, power conditioning, rotating equipment, and fuel processing systems. Documented conceptual designs were developed for each of these systems which satisfy the system level requirements as well as plant interfacing requirements. The selected reference baseline conceptual design and other supporting material for each of these systems such as system description, performance characteristics, system arrangement, and instrumentation and control are discussed in detail in Section 2.0.

- An integral part of the manufacture of uniform fuel cell components is a thorough characterization of the raw materials used in component manufacture. Progress was made in this area to establish and improve upon the material data base for the electrodes, matrix, and bipolar and cooling plates. Specifications were developed for the eleven critical materials currently being used in the manufacture of these components. In addition, all process specifications and subassembly and assembly procedures required for the manufacture and assembly of these components were developed and numerous full size components produced and evaluations made that demonstrated repeatability within the acceptance criteria.

- Documented designs of various size stacks were developed in addition to a subscale cell design. Final designs were completed for a 9 cell and 44 cell stack that are nominally rated at 2.5 kW and 10 kW, respectively at operating conditions of 70 psia, 190°C, and 325 mA/cm^2.

The preliminary design of a nominally rated 100 kW stack that consists of 419 cells, and the conceptual design of the nominally rated 375 kW plant module that consists of 1676 cells were completed. Each of these increasing in complexity designs incorporates various design advances conceived such as plastic process gas manifolds, plastic inter-cell edge seals, deflection limited stack design, machining of the bipolar and cooling plate edge surfaces after heat treatment, and various other stack mechanics type improvements.

- To date, testing under this ongoing program has consisted of 122 subscale atmospheric tests for about 110,000 cumulative test hours; 12 subscale cell pressurized tests for about 15,000 cumulative test hours; and 12 pressurized stack tests that contained either 5, 9, or 12 cells each for about 10,000 cumulative test hours. Performance and other improvements realized from this extensive test program are discussed in detail in Section 3.0.

- The design and installation of all needed manufacturing and test facilities to support the planned near term fuel cell development efforts are essentially complete. A fuel cell manufacturing capability is available at Westinghouse to produce the planned subscale cell test assemblies and various size stacks for basic development and design verification purposes. This capability is in addition to that available at ERC.

  Numerous test facilities are available at Westinghouse and ERC. These facilities consist of 45 subscale cell atmospheric test stands (25 at Westinghouse and 20 at ERC), three subscale cell pressurized test loops at ERC and one at Westinghouse, one 6 and 12 cell pressurized test loop at ERC, and two nominally rated 2.5 kW and one 30 kW pressurized test loops at Westinghouse. It should be noted that all Westinghouse manufacturing and test facilities were provided by Westinghouse under the UPP Program to support the TDP.

2.0 SYSTEMS ENGINEERING

The objectives of this task for this period of performance were to develop preliminary requirements and conceptual designs for the fuel cell, fuel processor, power conditioner, and rotating equipment systems (FCS, FPS, PCS, and RES respectively). The following sections summarize the results of analyses and design studies performed.

2.1 DEVELOPMENT SYSTEM REQUIREMENTS

This section summarizes system analyses, technology assessments, and the resulting design requirements for the FCS, FPS, PCS and RES.

2.1.1 SYSTEM ANALYSES

The primary objectives of the system analysis effort were to perform system trade-off studies, performance analyses, operational studies, and economic studies to establish preliminary system level design requirements for the fuel cell, fuel processor, power conditioner, and rotating equipment group systems.

These analyses identified the functional and conceptual interface requirements in conjunction with the Task 1102-04-100 Plant Systems Analyses effort. System level trade-off studies considering heat rate, power level, cost of electricity, operating characteristics, and development risk were performed to select system level design requirements for each of these systems for a prototype power plant that produces 7.5 MW_e dc with a heat rate goal of less than 9500 kJ/kWh (9000 Btu/kWh). The effect upon plant performance and operating characteristics for startup, steady-state, shutdown, and malfunction conditions associated with these systems was determined by utilizing appropriate steady-state, transient, and controllability analyses models.

The prototype power plant cost of electricity utilizing an economic analysis code was determined and cost goals were established for each of the systems. Preliminary failure mode and effects analyses of the systems were performed (in conjunction with the Task 1102-06-300 analysis effort) to evaluate plant safety.

2.1.1.1 PERFORMANCE AND OPERATIONAL STUDIES

A number of trade-off studies were performed to determine the proper plant power level, the pressure and temperature level at the rated plant power level, the power level control mode, and the fuel cell system design configuration. As a result of these studies, design parameters were selected for the prototype power plant conceptual design effort that satisfy the various plant economic and performance goals established, such as an installed capital cost of $\$2725/kW_e$ ac net in 1981 dollars, and a heat rate of less than 9500 kJ/kWh (9000 Btu/kWh) of net ac power output using natural gas. The selected design parameters are: (1) a 7.5 MW_e dc plant power output which has about a 7.1 MW_e ac net output, (2) FCS operating points of 480 kPa, 190°C, and 325 mA/cm^2, (3) a variable pressure and temperature control mode capability, however, the selected control mode is constant temperature and variable pressure, and (4) electrically connect the modules in two parallel banks of ten modules each to produce the 7.5 MW_e dc at about 2240 volts.

Four normal power plant operating points were established. These were (1) full power beginning of use (BOU), (2) full power end of use (EOU), (3) part power BOU, and (4) part power (EOU). The full power BOU point is identified as the baseline prototype power plant design. The EOU condition is defined as 40,000 hours of fuel cell operation at a cell voltage degradation rate of 2 mV/1000 hr. Though the remaining fuel cell operating parameters (temperature, pressure, current density, etc.) remain constant at BOU and EOU for full and part power modes respectively, there is a difference in the operating parameters between full and part power. The full power BOU operating conditions for the fuel cell are 190°C (375°F), 480 kPa (70 psia), and 325 mA/cm^2 producing a cell voltage of 0.680 V (0.600 at EOU). The corresponding part power conditions are 190°C (375°F), 300 kPa (43 psia), and 80 mA/cm^3 which results in a BOU cell voltage of 0.774 V (0.684 V at EOU). The part power operating pressure represents a pressure level where the parasitic losses from the RES do not excessively reduce the heat rate. Part power operation at constant temperature maintains the pressure level of the steam generators. The performance summary for these operating points is given in Table 2.1.1-1.

TABLE 2.1.1-1
PERFORMANCE SUMMARY

	FULL POWER		PART POWER	
	BOU	EOU	BOU	EOU
Cell Voltage	0.680	0.600	0.774	0.694
Pressure, kPa (psia)	480 (70)	480 (70)	300 (43)	300 (43)
Temperature, °C (°F)	190 (376)	190 (376)	190 (376)	190 (376)
Current Density, mA/cm^2	325	325	80	80
Gross dc, kW	7500	6620	2102	1885
Gross ac, kW	7238	6388	1934	1734
Net RES, kW	-46	-58	-169	-145
Net FPS Turbocompressor, kW	+164.0	+146.0	-203.1	-203.1
Parasitic Losses, kW	229	259	56	61
Net ac, kW	7109	6217	1506	1325
Thermal Input, GJ/h (10^6 Btu/h)	63.5 (60.22)	63.5 (60.22)	15.6 (14.82)	15.6 (14.82)
Plant Heat Rate, kJ/kWh (Btu/kWh)	8928 (8471)	10,210 (9687)	10,370 (9843)	11790 (11,186)

The PAFC power plant studies defined the following plant operational modes (COLD STOP, STANDBY, POWER) and transient modes (COLD STARTUP, WARM STARTUP, WARM SHUTDOWN, COLD SHUTDOWN, EMERGENCY SHUTDOWN, EMERGENCY STOP). These modes are described below:

COLD STOP

COLD STOP is a nonpower-producing mode in which the plant reaches essentially ambient temperature and pressure. In this mode, the fuel cell modules will be maintained at 38°C (100°F). All systems will be designed to maintain this mode for indefinite periods. Plant control in this mode will be manual.

STANDBY

STANDBY is a nonpower-producing mode from which the plant can be brought on-line (produce minimum power) in less than one hour. The plant will be capable of STANDBY operation for up to 60 hours. The capability for local or remote automatic plant control in this mode will be provided.

POWER

The POWER mode is the normal plant power-producing mode. All plant systems will be operational and plant electrical output will be in the range from 25 to 100 percent of full power. Plant control during POWER operation will be automatic with the option for manual override. The plant will be capable to respond over the total POWER range at the following rates:

- Up transients up to 7.5 percent of full power per minute.
- Down transients up to 15 percent of full power per minute.

The normal operating power line is shown on Figure 2.1.1-1 with constant average fuel cell temperature and variable pressure.

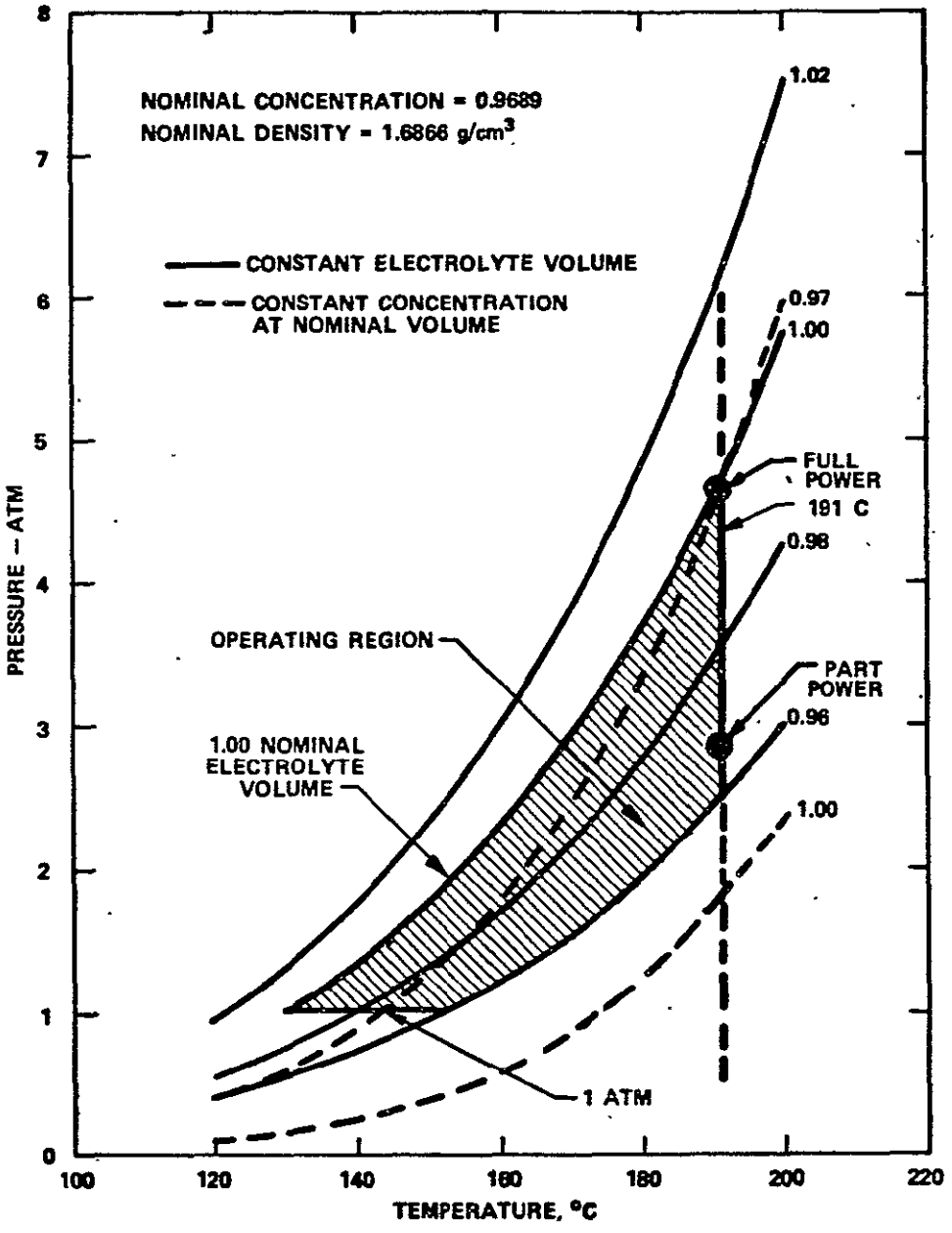

Figure 2.1.1-1 Operating Map for Cathode Air Stoichiometry of 2.0

COLD STARTUP

COLD STARTUP is defined as the plant transient from COLD STOP to STANDBY. The plant will be designed to complete a COLD STARTUP in less than eight hours. Plant control during COLD STARTUP will be manual.

WARM STARTUP

WARM STARTUP is defined as the plant transient from STANDBY to POWER. The plant will be designed for WARM STARTUP to the minimum POWER condition in less than one hour. Plant control during WARM STARTUP will be automatic or manual.

WARM SHUTDOWN

WARM SHUTDOWN is defined as the plant transient from POWER to STANDBY. The plant will be designed to complete a WARM SHUTDOWN from minimum power in less than one hour. Plant control during WARM SHUTDOWN will be automatic or manual.

COLD SHUTDOWN

COLD SHUTDOWN is defined as the plant transient from STANDBY to COLD STOP. The plant will be designed to complete a COLD SHUTDOWN in less than eight hours. Plant control during COLD SHUTDOWN will be manual.

EMERGENCY SHUTDOWN

EMERGENCY SHUTDOWN is defined as the plant transient from a faulted condition during POWER operation to STANDBY. The plant will be designed to complete an EMERGENCY SHUTDOWN in less than 1.5 hours; however, plant electrical power output will be disconnected from the utility transmission line in 0.05 seconds. Plant control during EMERGENCY SHUTDOWN will be automatic.

EMERGENCY STOP

EMERGENCY STOP is defined as the plant transient from a faulted condition during any plant operation or transient to COLD STOP. The plant will be designed to automatically complete an EMERGENCY STOP.

2.1.1.2 PLANT SAFETY

A preliminary plant safety evaluation was conducted to identify areas, components, functions, operations, etc., that should receive early design attention to improve plant safety and operability. The analysis included all the PAFC plant equipment, equipment arrangements, buildings, and the site layout to the extent described in the conceptual design drawings. All of the plant operating modes and maintenance activities were considered in identifying potential equipment malfunctions, failures, hazards, and accidents. The following types of failures, events, and their consequences were considered in this evaluation:

- Those that have the potential for equipment damage
- Those that have the potential for injuring the on-site operating and maintenance personnel
- Those that have the potential for making the plant inoperable and incapable of producing power.

The results of the preliminary assessment of the plant conceptual design identified safety-related events that could potentially lead to equipment damage or personnel injury. Corrective measures were suggested that would reduce the probability or mitigate the consequences of the safety events. In some cases, for example the PCS, intrinsic design features for failure event protection were identified in the equipment conceptual design.

2.1.1.3 AVAILABILITY ASSESSMENT RESULTS

The results of the availability assessment are summarized in Table 2.1.1-2. Except for the fuel cell stacks, the system failure rate and MTTR estimates shown in Table 2.1.1-2 are based on equipment data. The total planned outage is 296 hours per year. Planned outage hours cannot be directly allocated to the individual systems given the present level of design definitions. A minimum acceptable availability, however, for each system can be defined as follows:

$$\text{MAXIMUM ALLOWABLE SYSTEM OUTAGE HOURS} = 296 + \text{SYSTEM UNPLANNED OUTAGE HOURS}$$

$$\text{MINIMUM ACCEPTABLE SYSTEM AVAILABILITY} = 1 - \frac{\text{MAXIMUM ALLOWABLE SYSTEM OUTAGE HOURS}}{\text{PERIOD HOURS}}$$

The overall plant availability goals can be stated from the Table 2.1.1-2 values as:

Unplanned (forced) outage hours per year	580
Inherent availability (reliability), percent	93.4
Forced outage rate, percent	6.9
Planned outage hours per year	296
Planned outage rate, percent	3.4
Overall plant availability, percent	90.0

2.1.1.4 PLANT COST AND ECONOMIC RESULTS

Analyses were performed to define the plant economic characteristics and breakeven capital costs by comparison with competing types of generating units. Combustion turbines, by virtue of their availability in small unit sizes, are considered as competing generating units. Capital cost, operation and maintenance costs, and heat rate data were used to represent combustion turbines. All costs were updated to 1983 dollars. Energy price projections, forecasted by Data Resources, Inc. (DRI) were used and are shown in Figure 2.1.1-2. It is assumed that the natural gas price projection is representative of the fuel used in the combustion turbine and the PAFC power plant. The resulting cost of electricity (COE) for the combustion turbine over a range of fuel prices and capacity factors is shown in Figure 2.1.1-3. The installed capital cost of the combustion turbine, including allowance for funds during construction was $252/kWe. It was assumed that the combustion turbine always operates at its most efficient full load heat rate of 12,100 kJ/kWh (11,500 Btu/kWh) regardless of annual capacity factor.

TABLE 2.1.1-2

RELIABILITY AND AVAILABILITY ASSESSMENT SUMMARY

System	Failure Rate Per 10^6 Hours	Range of Component Mean Time To Repair Or Replace, Hours	System Mean Time to Repair or Replace, Hrs	Unplanned Outage, Hours per Year	System Reliability	Minimum Acceptable System Availability Percent
FHS	80	4 - 42	17	12	0.9987	96.5
FPS	837	4 - 78	14	99	0.9887	95.5
IS	80	2 - 4	3	2	0.9998	96.6
RES	898	4 - 64	24	192	0.9781	94.4
CWRS	127	4 - 36	14	16	0.9982	96.4
SCS	142	4 - 36	13	16	0.9982	96.4
SGS	182	4 - 37	12	19	0.9978	96.4
WTS	241	4 - 63	10	21	0.9976	96.4
FCS (w/o Fuel Cells)	235	8 - 60	35	72	0.9918	95.8
ICS, SAS, WDS PCS, WRS, USE	179 (Average Per System)	4 - 36	13	120 (Total, 6 Systems)	0.9977	96.4
Fuel Cell Stacks	91	14	14	11	0.9987	96.5

Total Unplanned Outage Hours = 580

Planned Outage Hours for Fuel Cell Stack Replacement = 56

Other Planned Outage Hours = 240

Total Annual Planned and Unplanned Outage Hours = 876

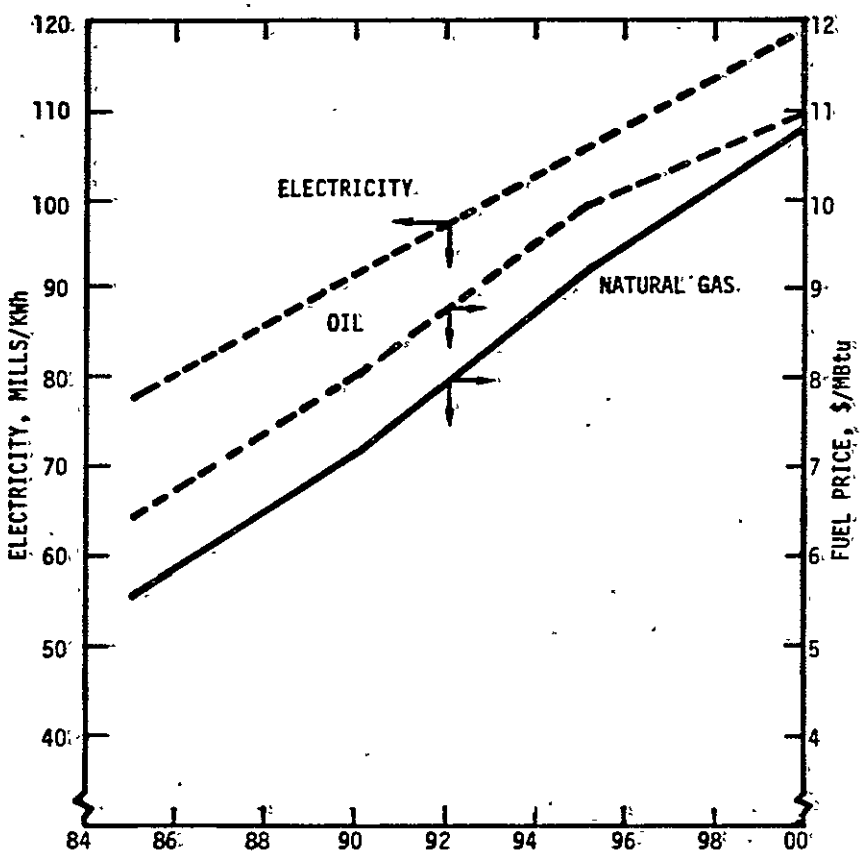

Figure 2.1.1-2. Domestic U.S. Energy Price Projections in 1983 Dollars

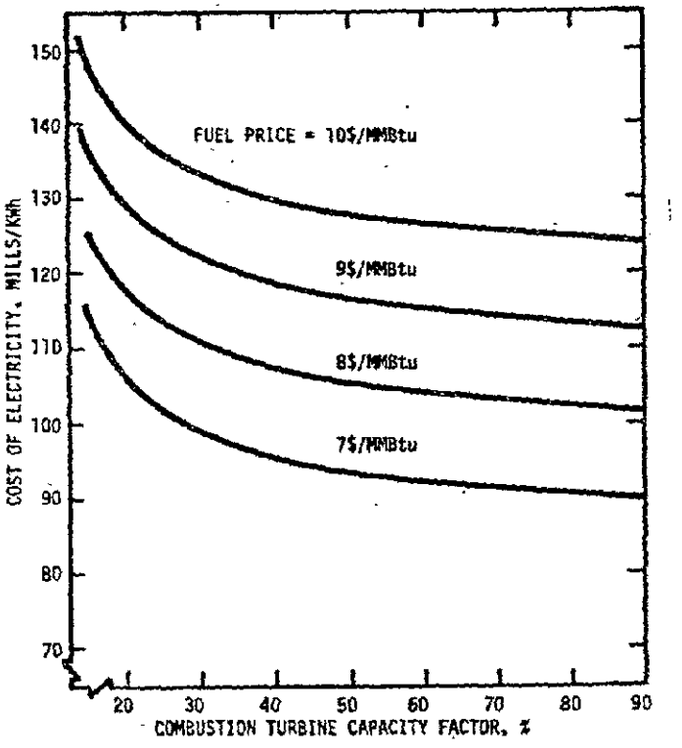

Figure 2.1.1-3. Combustion Turbine Cost of Electricity at Full Load Heat Rate of 12,100 kJ/kWh (11,500 Btu/kWh) (1983 Dollars)

PAFC ECONOMIC DESCRIPTION

The PAFC fuel cell stacks in the power plant will exhibit gradual voltage degradation that increases the overall plant heat rate over a period of time. For an operating plant, this means there will be a trade-off involving increasing fuel costs as degradation occurs, fuel cell remanufacturing costs, and O&M costs to remove and replace degraded fuel cells*. This cost trade-off can be optimized to minimize the COE produced. The optimum reloading interval and the operating heat rate are dependent on the degradation rate and the fuel price. At a 2 mV/1000 hour degradation rate these parameters are shown in Figure 2.1.1-4 for a range of fuel prices. When the fuel price is $8/mmBtu, the optimum reloading interval is close to five years and the operating heat rate is 9555 kJ/kWh (9081 Btu/kWh). Therefore, with a BOU heat rate of 8928 kJ/kWh (8471 Btu/kWh) at initial plant startup, the operating heat rate will rise to 9555 kJ/kWh after two and a half years of operation and to the EOU heat rate representing 80 MV of degradation at the end of the five year period. The plant operator can then replace all of the fuel cell stacks simultaneously and return the plant to the BOU heat rate. As an alternative, the plant operator can, after the first year of plant operation, begin partial reloading of the fuel cell stacks at the rate of four stacks per year in order to maintain the operating heat rate of 9555 kJ/kWh. With escalating fuel prices, it is believed that annual partial reloading of the fuel cell stacks is the more likely scenario.

The economic assumptions, cost data, and performance data is summarized in Table 2.1.1-3. The fuel cell stack remanufacturing cost of $147/kWe for a total reload of the plant is a fully commercialized cost including burden, fee, and round trip shipping costs. The fuel cell stack salvage value of $12/kWe represents the value of the recoverable platinum catalyst less the costs of shipping and recovery. The fixed O&M cost of $7/kWe-yr assumes automatic plant operation but includes an allocation of operator and supervisor costs based on the assumption that even automatic plants require periodic attention by utility operating personnel. The fixed O&M cost estimate includes a maintenance crew at the plant site for 30 days per year and overhead costs.

*Refers to all of the fuel cells contained in a 375 kWe (dc) fuel cell module.

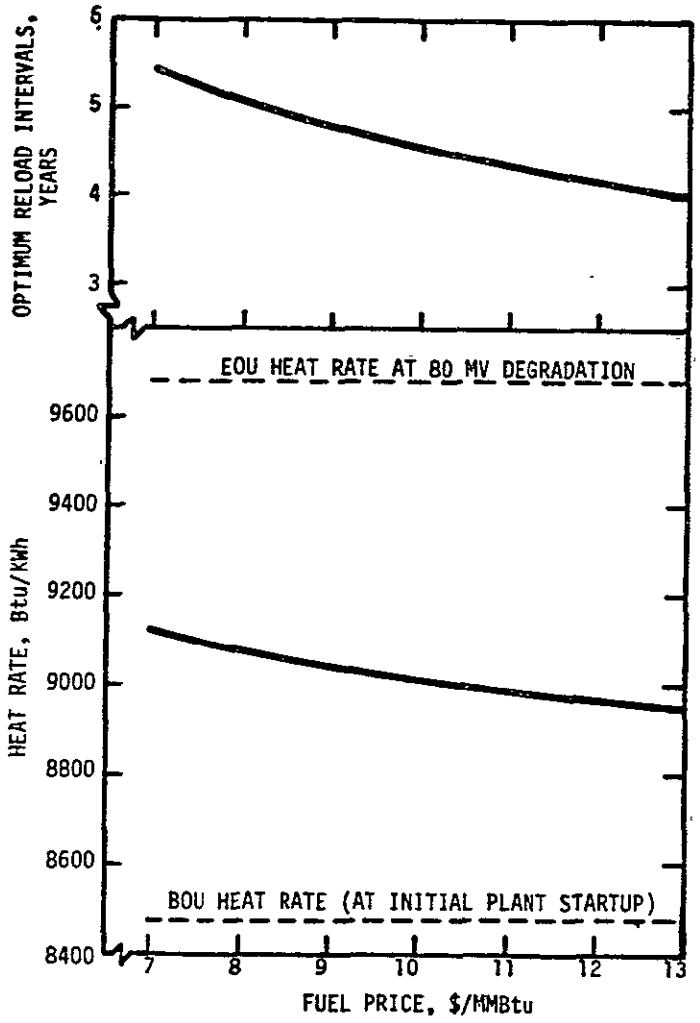

Figure 2.1.1-4. Optimum Reload Interval and Operating Heat Rate Versus Fuel Price

TABLE 2.1.1-3

PAFC COST AND PERFORMANCE DATA

(ALL COSTS IN 1983 DOLLARS)

Fixed Charge Rate, percent	15
Capacity Factor, percent	70
Plant Economic Life, Years	25
Availability, percent	90
Fuel Cell Degradation Rate, mV/1000 hrs	2
Fuel Cell Stack Remanufacturing Cost, $/kWe	147*
Fuel Cell Stack Salvage Value, $/kWe	12
Fixed O&M Costs, $/kWe - YR	7
Heat Rate at Initial Plant Startup, kJ/kWh (Btu/kWh)	8911 (8471)
Net Power Output, kWe (ac)	7108
At a Fuel Price of $8/mmBtu:	
Optimum Reload Interval, years	5
Operating Heat Rate, kJ/kWh (Btu/kWh)	9555 (9081)
Operating Costs in Mills/kWh:	
Fuel	72.65
Fixed O&M	1.14
Variable O&M	1.04
Fuel Cell Reloads	3.67

*Cost incurred at the end of each five year reloading interval. Equivalent partial reloading of four stacks per year would represent an annual cost of 29.4 $/kWe given a net plant output of 7108 kWe (ac).

Variable O&M costs, the cost of the fuel cell reloads, and the plant fuel costs are all a function of the fuel price and the resulting optimum reload interval. These costs in mills per kWh, assuming a fuel price of $8/mmBtu, are shown in Table 2.1.1-3. The variable O&M cost includes plant consumeables and the on-site costs of removing and replacing degraded fuel cell stacks. These on-site costs include the costs of a foreman, mechanical and electrical trades, crane rental, and overhead. The mills per kWh fuel cell reload cost includes the cost of remanufacturing degraded stacks less the salvage value of the stacks at the end of the 25 year plant life.

BREAKEVEN TOTAL INVESTMENT COST

The PAFC breakeven total investment cost at a given fuel price is determined by equating the COE of the plant to the COE of the competing combustion turbine. Since the PAFC fuel, O&M, and stack reloading costs are known, the breakeven total investment cost assuming a 15 percent fixed charge rate can then be calculated. The total investment cost is installed capital cost plus allowance for funds during construction. The PAFC breakeven total investment cost as a function of the competing combustion turbine capacity factor and a range of fuel prices is shown in Figure 2.1.1-5. The PAFC capital cost goals are values equal to or less than the values shown in Figure 2.1.1-5.

2.1.2 FUEL CELL, FUEL PROCESSOR, POWER CONDITIONER AND ROTATING EQUIPMENT SYSTEMS DESIGN REQUIREMENTS

Preliminary system requirements specifications were prepared for the FCS, FPS, PCS, and RES. These specifications include functional, design, operational, configuration, environmental, safety, inspection, maintenance, instrumentation and control, and quality control requirements.

2.1.2.1 FUEL CELL SYSTEM (FCS)

The primary function of the FCS is to produce dc electric power at the performance design conditions specified below using air-cooled fuel cells. The FCS transforms the chemical energy from the fuel and oxidant reaction (hydrogen rich feed gas supplied by the FPS and oxygen in the form of pressurized air

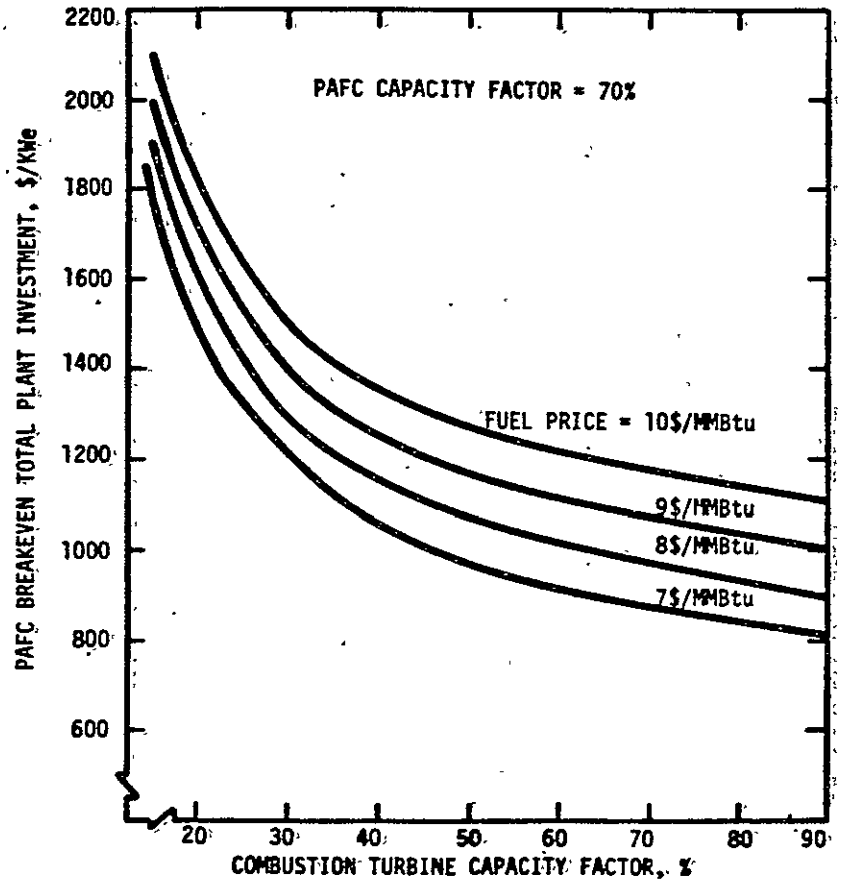

Figure 2.1.1-5. PAFC Breakeven Total Plant Investment Relative to Combustion Turbine (1983 Dollars).

supplied by the RES) into electrical energy. The top level system requirements include:

- The FCS shall provide a gross electrical output of 7.5 MW dc at full power operating conditions at BOU.
- The FCS electrical output shall be based on a constant current output for constant air (oxidant) and fuel flow operation. The design basis for the fuel cell module current is 351 amps.
- The design hydrogen utilization is 83 percent and the design oxygen utilization is 50 percent.
- The FCS operating parameters shall meet an average fuel cell performance degradation objective of 2 mV per 1000 hours of power operation.
- The FCS operation shall maintain the fuel cell phosphoric acid concentration within the boundaries defined in Figure 2.1.2-1.
- The FCS shall have stable operation at power operation conditions and shall respond to the following transient operating conditions:

Cold Start to Standby, hours	< 4
Standby to Minimum Power, hours	< 1/2
Minimum Power to Maximum Power, percent Full Power per minute	7.5
Operating Range, percent Full Power	25-100

- As a design goal the FCS shall be designed to achieve an availability of 95.8 percent and a reliability of 99.2 percent.

2.1.2.2 FUEL PROCESSING SYSTEM (FPS)

The primary function of the FPS is to convert steam and hydrocarbon fuel to a hydrogen-rich gas for use in the fuel cells. Major FPS equipment include a fuel cleanup system to remove impurities detrimental to FPS and fuel cell performance, a steam reformer to convert the hydrocarbon fuels into CO, CO_2 and H_2, shift converters to convert water and CO into additional H_2 and CO_2, and rotating machinery to deliver compressed air and recover waste stream energy. The top level design requirements include the following:

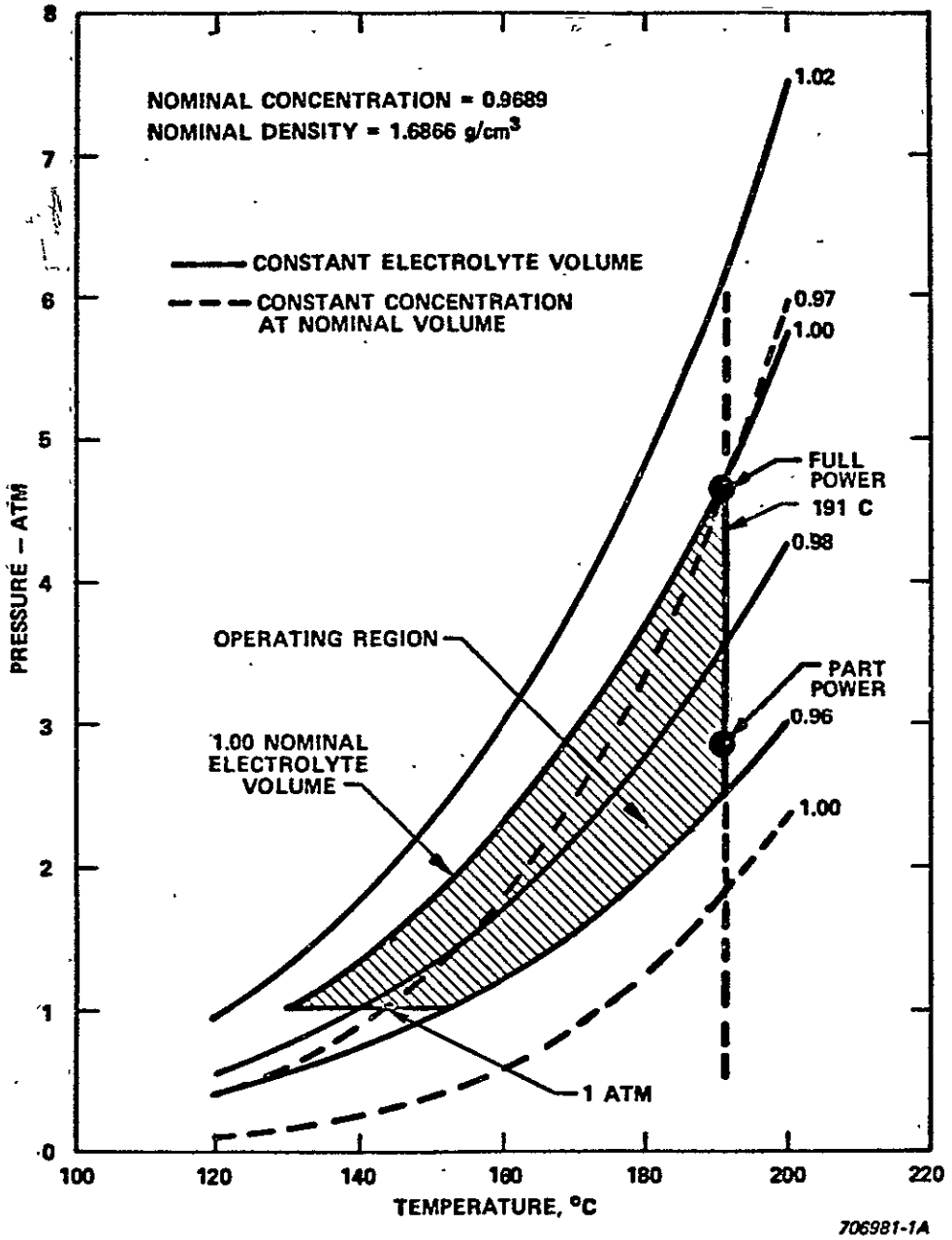

Figure 2.1.2-1 Operating Map for Cathode Air Stoichiometry of 2.0

- PERFORMANCE

H_2 Production Rate, Normal m^3/s (SCFD)	
• Gross	1.53 (4.93 x 10^6)
• Net	1.27 (4.09 x 10^6)
Natural Gas Feedrate*, kg/s (lb/hr)	0.348 (2760)

- OPERATIONAL

Cold Start to Standby, hours	< 4
Standby to Minimum Power, hours	< 1/2
Minimum to Maximum Power, percent Full Power per min	7.5
Operating Range, percent production rate	23-100
Operation	Automatic Dispatch from Standby to Full Power
Start/Stop Cycle (Over Lifetime)	
- Warm Startup/Warm Shutdown	10,000
- Cold Startup/Cold Shutdown	150

- GENERAL

Fuel Capability	Natural Gas/Naphtha
Availability, percent	95.5
Reliability, percent	98.9
Design Life, Years	25
Maximum Plot Plan Area, m^2 (ft^2)	230 (2500)
Maximum Height of Equipment Above Grade, m (ft)	9.1 (30)
Noise Level (db)	55
Transportability	Common Carrier Truck

2.1.2.3 POWER CONDITIONING SYSTEM (PCS)

The primary functions of the PCS are to control the magnitude of the direct current generated in the FCS and to consolidate and convert the current to alternating current at 13.8 kV.

The PCS shall be designed to meet the following major performance requirements:

Power Conversion	
Rated Full Power Input	7.5 MWe dc
Rated Partial Power Input	25 percent of rated full power
Efficiency at Full Power	96 percent
Efficiency at Partial Power	92 percent
Power Factor	Unity or leading at greater than 25 percent power.
Fault Protection	
dc Power	Electronic circuit interruption
ac Power	Circuit breaker
Response Times	Not to limit fluid system transient response times or result in spurious shutdowns.
Manual Control	To bring system to STANDBY condition during plant startup and for system checkout.
Automatic Control	For all normal power operation via plant computer.
Availability	96.4 percent
Reliability	99.8 percent

2.1.2.4 ROTATING EQUIPMENT SYSTEM (RES)

The primary function of the RES is to provide a supply of clean, pressurized air to the FCS to replace air consumed on the cathode side of the fuel cells. The RES receives steam from the SGS and oxygen depleted cathode exhaust air from the FCS. The energy in this stream is converted into mechanical shaft power to drive circulating and compressing equipment. One of the key objectives of the RES design is to help minimize the overall power plant heat rate.

The RES operation is based on using an air circulator, a two-stage centrifugal compressor, a steam turbine, a gas turbine expander, and a variable speed drive electric motor to perform the required functions. This rotating equipment must satisfy the operating parameters for full and part power plant operation summarized in Table 2.1.2-1.

As a design goal, the RES will be designed to achieve an availability of 94.4 percent and a reliability of 97.8 percent.

2.1.3 FUEL CELL REQUIREMENTS

The technical requirements identified for the PAFC system design and operation imposed by current fuel cell technology and the anticipated improvements resulting from a development effort are discussed in this section.

2.1.3.1 APPROACH AND ASSUMPTIONS

The overall objectives of the work in establishing technical requirements were to:

- Establish the existing PAFC technology to permit definition of guidelines and understanding of the constraints imposed upon the design parameters.
- Identify the required performance and needed technology to meet the system requirements.
- Define the design and operating requirements and a suitable development test program to ensure meeting these requirements.

The existing PAFC performance data and currently accepted design and baseline processes were reviewed. A summary of the key design parameters, operating conditions and technology constraints data were developed. Where no specific parameter limits had been defined, the best estimated ranges were identified to facilitate stack and system design efforts. A number of needed parameters could not be established quantitatively. For these, recommendations were made for development testing to establish the needed data.

Table 2.1.2-1
ROTATING EQUIPMENT SYSTEM (RES) OPERATING REQUIREMENTS

	Full Power	Part Power
• Air Circulator		
Flow, kg/hr (lb/hr)	662,840 (1,460,000)	115,089 (253,500)
Inlet Pressure, kPa (psia)	482 (70)	296 (43)
Inlet Temperature, °C (°F)	145 (293)	149 (300)
Outlet Pressure, kPa (psia)	489 (71)	296 (43)
Outlet Temperature, °C (°F)	147 (296)	149 (300)
Fluid	Air	Air
• Centrifugal Compressor* (Two Stages)		
Flow, kg/hr (lb/hr)	28,239 (62,200)	18,160 (40,000)
Inlet Pressure, kPa (psia)	101.3 (14.7)	101.3 (14.7)
Inlet Temperature, °C (°F)	26 (80)	26 (80)
Outlet Pressure, kPa (psia)	482 (70)	296 (43)
Outlet Temperature, °C (°F)	143 (291)	114 (237)
Fluid	Air	Air
• Steam Turbine		
Flow, kg/hr (lb/hr)	8,808 (19,400)	1,226 (2,700)
Inlet Pressure, kPa (psia)	365 (53)	365 (53)
Inlet Temperature, °C (°F)	140 (284)	140 (284)
Outlet Pressure, kPa (psia)	21 (3)	21 (3)
Outlet Temperature, °C (°F)	61 (141)	61 (141)
Fluid	Steam	Steam
• Gas Expander**		
Flow, kg/hr (lb/hr)	28,466 (62,700)	18,205 (40,100)
Inlet Pressure, kPa (psia)	475 (69)	289 (42)
Inlet Temperature, °C (°F)	192 (378)	144 (292)
Outlet Pressure, kPa (psia)	110 (16)	110 (16)
Outlet Temperature, °C (°F)	73 (163)	64 (148)
Fluid	Air (O_2 depleted)	Air (O_2 depleted)

*Bypass flow of 11,214 kg/hr (24,700 lb/hr) to the gas expander is required for part power operation to prevent surge.

Key assumptions made to initiate this effort included the existing ERC and Westinghouse baseline technology and fabrication processes for:

- 12 x 17 inch "Zee" and "tree" bipolar and cooling plates
- Rolled electrodes of Teflon wet-proofed carbon paper with platinum catalyst (0.5 mg Pt/cm^2 nominal + 7 mil nominal SiC coating on the cathode, 0.25 mg Pt/cm^2 nominal on the anode)
- Cooling plates between each five 12 x 17 inch cells with air cooling
- ERC proprietary MAT-1 matrix layer
- H_2 (simulated reformer) fuel oxidized with air

The specified/assumed performance constraints are presented in the Conceptual Design Report, TR 83-1002. These serve as a reference in the definition of functional/technological requirements.

2.1.3.2 TECHNOLOGY ASSESSMENT

To establish a reference PAFC design basis for assessing prototype power plant application, currently available data in the open literature and that developed by ERC, Westinghouse, and others was utilized. This data included the following:

- Materials data such as physical properties, design parameter data, electrical performance data, and chemical performance data
- Fuel cell component production processes and assembly specifications
- Fuel cell configuration and component design
- Fuel cell operating conditions such as pressure, temperature, current density, and fuel utilization
- Principal effects of variation in key design parameter values such as pressure, temperature, current density, flow rates, component compositions, and processes

Most of the parameters needed as identified above were found to have some level of definition, but the impacts of the PAFC selected operating conditions on the life, system performance, economics, and risk were not definable. Therefore, constraints were identified and parameter trade-off sensitivity assessments made to establish the best design parameter data and operating conditions. Some of the pertinent design and operating condition constraints that were identified are presented in Table 2.1.3-1.

Analysis effort was not carried to the point where in all cases definitive results or design values can be established for these constraints. However, sufficient indication of the potential performance and some key parameter sensitivity data were found and provided a basis for defining the potential performance and required design parameter conditions and goals for the development program. The development goals established for the PAFC are presented in Table 2.1.3-2.

2.1.3.3 PRESSURE PERFORMANCE MODEL

The theoretical model used at ERC to predict the effect of system operating pressure on the phosphoric acid fuel cell voltage was submitted to Westinghouse. The following equation is currently used at ERC to calculate the performance changes with pressure.

$$\Delta V = \frac{6 \times 2.303}{4F} RT \text{ Log } \frac{P_2}{P_1}$$

Where:

ΔV = Voltage gain between system operating pressures P_1 and P_2

TABLE 2.1.3-1

KEY PAFC SYSTEM AND DESIGN CONSTRAINTS[1]

Constraint Identity	Time	Level	Origin/Comments
Maximum Voltage (Cell)	Continuous	<800 mV	Corrosion Constraint from life performance required
Minimum Voltage (Cell)		None	Functional Constraint - minimum design voltage required
Current Density (Min)	(TBD) Hrs	0-75 mA/cm^2	Corrosion Constraint - Voltage dependent - requires further development data to set time limit at temperature
Current Density (Min)	Continuous	>75-100 mA/cm^2	Corrosion Constraint - function of temperature and pressure and not yet characterized
Current Density (Max)	Continuous	<400 mA/cm^2	Performance Constraint - low efficiency - requires T.O. - efficiency versus with cost
Temperature (Nom Max)	(TBD) Hrs	220°C (426°F)	Performance Constraint from life requirement and impact of electrolyte loss
Temperature (Max)	Continuous	190-200°C (375-398°F)	Performance Constraint from temperature control - variance and maximum temperature in cell
Temperature (Min)	Continuous	(TBD)	Performance Constraint from temperature control - variance & CO poisoning
Pressure (Max)	Continuous	150 psia	Performance Constraint from trade-off studies - cost versus pressure level needed
Pressure Diff. Containments (Max)	Instant	150 psid	Functional Constraint - design condition imposed on cell assembly and sealing
Temperature Coolant (Max)	Continuous	110-150°C (230-302°F)	Performance Constraint - temperature control of cell and coolant characterization
Temperature Coolant (Max)	(TBD) Hrs	200°C (398°F)	Performance Constraint - life requirement impact from excess cell temperature conditions
Cell Coolant Diff. Press. (Max)	Instant	(TBD)	Functional Constraint - design limit for separation requirement and cell assembly and sealing

TABLE 2.1.3-1

KEY PAFC SYSTEM AND DESIGN CONSTRAINTS[1] (Continued)

Constraint Identity	Time	Level	Origin/Comments
Reactant Diff. Pressure (Max)	Continuous	(TBD)	Functional Constraint - design limit for separation requirement and cell assembly and sealing
Cell Stack Temp Diff. (Max to Min)	(TBD) Hrs	20-50°C (36-90°F)	Performance Constraint - life requirement impact
Cell Stack Temp Diff. (Max to Min)	Continuous	(TBD) ∿20°C	Performance Constraint - life requirement impact
Transient Rates - Power	Startup Shutdown	(TBD) (TBD)	Performance Constraint life requirement impact
Stack Mechanics:			
- Contact Resistances	Continuous	<20mΩ-cm^2	Performance Constraint for practical losses (<2 percent output)
- Clamping Load (Initial)	Continuous	20-60 psi	
- Clamping Load (Min)	Continuous	∿ 1 psi	Performance Constraint - leakage and electrical losses - high contact resistance
- Creep Rates/ Strengths	--	(TBD)	
- Relaxation Rates	--	(TBD)	Performance Constraint - life requirements impact
- Maximum Stack Height (Module Unit)	--	3.3 m	Performance Constraint - truckability
- Maximum Width (Module Unit)	--		Performance Constraint - truckability
- Maximum Weight (Module Unit)	--		Performance Constraint - truckability
- Maximum Output Voltage (Stack)	Instant	<400V dc	Functional Constraint - design limit is fixed as function of number cells in stack at O.C. voltage
- Maximum Output Voltage (Stack)	Continuous	<300V dc	Nominal design condition

TABLE 2.1.3-1

KEY PAFC SYSTEM AND DESIGN CONSTRAINTS[1] (Continued)

Constraint Identity	Time	Level	Origin/Comments
- Minimum Output Voltage (Unit)	Continuous	>2000V dc	Functional Constraint - nominal design condition Performance Constraint - conversion efficiency

(1) Condensed list of key constraints remaining after having assumed fixed process controls and fixed performance parameters for baselined reference design. These parameters are needed for further design and operating requirements definition as derived from functional and/or performance requirements genesis. (The predominating requirement is noted as origin of constraint).

(2) Corrosion impact - not yet understood and varies with temperature.

(3) Amount of H_3PO_4 vaporized; currently perceived upper limit.

TABLE 2.1.3-2

PAFC DEVELOPMENT GOALS

Cell Performance:(1)

Primary

- Efficiency:
  Cell Potential (avg. mV/cell)
  2 x 2 @ Design Cond(2) 705
  12 x 17 @ Design Cond in Stack(2) 680

- Endurance:
  Voltage Loss (mV/1000 hrs) 2
  Corrosion Loss (mil/yr) 2

Secondary

- Catalyst Utilization:
  Anode Loading (mg/cm^2) 0.25
  Cathode Loading (mg/cm^2) 0.50

- Oxidizer Utilization with Air:
  Oxygen Concentration(3) (stoichs) 2

- Operating Temp. of Cell:
  Cell Avg. Temp. (°C) 190

(1) Fixed Parameters:
- Natural gas feedstock with humidified hydrogen
- ERC-Westinghouse Air Cooled System
- Mark II "zee"-"tree" Plates
- Mat-I matrix
- 1981 Process Specs/Fab Controls

(2) Design Conditions (Beginning of Use):
- 70 psia Pressure Level
- 190°C Average Cell Temperature
- 325 mA/cm^2 Average Cell Current Density Loading
- Acid Control Equilibrium
- 80 percent H_2 Utilization
- >2 Stoichs Air

(3) At 3.4 Atmospheres

2.1.4 FUEL CELL PROCESSES AND FACILITY REQUIREMENTS

This section summarizes the establishment of requirements for materials and fabrication processes and facilities needed for the fuel cell development program.

2.1.4.1 APPROACH

The systems study and technology requirements efforts were reviewed and evaluation of needed development testing was initiated. Based upon the system requirements developed from the power plant systems studies, Task 1102-01 and development testing requirements, Task 1102-02, the preliminary design requirements for subscale cells and partial stacks were identified.

These requirements included the subscale cell testing, 9-cell, 10 kW, 25 kW, and 100 kW stack testing and module testing facilities as well as the order of test efforts; resulted in preliminary definition of subscale, stack and module design requirements for testing as presented in Section 3.0. The logic for this development testing is presented in Figure 2.1.4-1.

2.1.4.2 FACILITY REQUIREMENTS FOR PARAMETER DETERMINATION

Review of the fuel cell technology has shown significant uncertainty in not only the understanding of key parameter effects, but sensitivities needed for design. In order to design the fuel cells with some degree of predictability and also to be able to later understand the performance under actual test conditions, it is necessary to determine the key variable and parameter effects and also the interactions among design variables and operating parameters. The number of these variables and parameters could make a test program monumental. However, effective PAFC design from the standpoint of both cost and required performance dictates testing for definition and adequate understanding of these key design parameters.

Experience with the Analysis of Variance as a statistical tool in designing experiments has shown the efficacy of the experimental test design approach. Early assessment of the technology indicated performance of the PAFC was

Establish Design Technology Base

1.0	2.0	3.0	4.0
Materials/ Processes & Procedures Definition	Fuel Cell Baseline Technology Definition	PAFC Stack Baseline Technology Definition	Full Size PAFC Module Design Technology Demonstration
• (A Priori) ERC/(W) & UTC Existing Technology	• 2x2 Subscale Testing Program - Key Design Variables - Basic Technoloyg	• 12x17 Nom. Stacks (9 cell), (10 kW) (25 kW)	• 400 kW Nom. full module Demonstration
• Materials Facilities Exist	• Requires Facilities for Testing Subscale 2x2 Cells - Atmos. and Pressure	• Requires Facilities for Testing Stacks at Pressure	• Requires Full Module System Interfacing Facility

Figure 2.1.4-1 Technology Development Logic - PAFC Module

adequate, however, additional variable and parameter data was required to permit the design of full size stacks with some confidence. The magnitude of the test program and facilities needed to permit definition of these parameter characteristics and sensitivities was of the nature to eliminate this data base development from the early development program. Some estimate of design data could be obtained for early design impact. However, the major variable data was needed. The effort to define the development test program and facilities considers statistical experiment design.

A major effort was made to restrict the tests to the absolute minimum required to obtain satisfactory data in the three areas of most concern. These three areas are: 1) variables and parameters relating to the fabrication process, 2) design variables and related parameters needed for effective design, and 3) operational parameters related to the conditions of operating the test and the fuel cell system.

More than five dozen key process and fabrication variables were also identified, but not included in this test program. These were considered to be controlled by process and procedure specifications to acceptable levels of variance, and therefore not defined as "design or operational variables". Consideration of the pertinent variables and parameters in these three areas resulted in identification of more than two dozen key variables and parameters which needed better definition.

Nine of these key variables and parameters were identified as being required for and essential to satisfactory tradeoff studies. They included two process variables, four design variables, and three operational parameters. These were identified for consideration in the design of the experimental test. The key selected operational parameters and the design variables and parameters that were defined for the test program are shown in Table 2.1.4-1. Measurement requirements for the facility and testing were derived as given in Table 2.1.4-2.

TABLE 2.1.4-1

EXPERIMENTAL DESIGN VARIABLES

Parameter Area	Controlled Variable	Number	Priority
Process Variations:*	1. Substrate Configuration	2	1
	2. Impurities	2	1
	3. Density/Porosity	2	2
	4. Platinum Application	2	2
Design Variations:	1. Cell Size	2	1
	2. Stack Size	3-4	1
	3. Clamping load and compression	3	2
	4. Acid Composition and Amount	2	2
	5. Matrix Thickness	2	2
	6. Current Density	2	1
Operating Variations:	1. Pressure Level	3	1
	2. Temperature	3	2
	3. Flow Rates (Process Gases)	3	1
	4. Loading (power)	3	1
	5. Cycles	3	2
	6. Time	3	1
	7. Voltage	2	2
	8. Gas Composition	2	2

*Assumed control of detailed process functions, i.e., mtls. specs, fabrication procedures, etc., and acceptable consistency of reproducible performance demonstrated and documented for each component used.

TABLE 2.1.4-2

TEST VARIABLE MEASUREMENTS REQUIRED AND PRECISION DEFINITIONS

			Parameter	Precision
1.	Responses -	(cell voltage and cell power output)	• output volts (mV)	1/2%
			• output watts (W)	2%
2.	Controlled Variables -	(conditions that are controlled to obtain designed responses)	• Cell avg. temp. (°C)	2%
			• Time (hr & min.)	
			• Current density (mA/cm^2)	2%
			• Reactant flows (kg/hr)	2%
			• Pressure levels (atm)	2%
			• Pressure differences (in H_2O)	5%
3.	Other Measured Variables	(conditions set for test recorded as specified and monitored)	• Cell resistance (mΩ)	5%
			• Acid concentration (%)	1%
			• H_2O, CO_2, CO level (%)	5%

The initial assessment of the nine selected variables and parameters determined that over twenty-four pertinent interactions needed to be assessed along with the parameter charateristics themselves.

A test plan for subscale 2x2 cell and partial stack (full cell size) desulfurization testing was established with these nine parameters and variables including probable interactions. This would require ninety unique tests. An additional five to ten tests should replicate the key tests for understanding of the reproducibility.

With the assumption that at least sixty tests will be necessary and considering the number of tests needed to assess the time and pressure effects, the distribution is roughly 50% of these tests at low time and low pressure, 40% at mid-time and atmospheric pressure and 10% at high time and high pressure. This is based upon the usual experience in successful evaluation of time dependency using three times (roughly linearly spaced on a log scale at 100, 1000 and 10,000 hours).

With the assumption that the time needed for evaluation of the characteristic performance of the fuel cell would be in the order of a year, considering the design life of five years, the number of tests that must be run in parallel to enable them to be accomplished within the design period would require an additional 10 to 15 subscale test loops. Roughly half of these tests would be run at low pressure and low time.

The experimental test design would be based upon a series of test "sets". These "sets" would be defined in such a way that a maximum input could be obtained for subsequent "sets" in reducing or amplifying the needed parameter information. On this basis two "sets" would be run without the benefit of feedback, but thereafter modification of the following tests could take place to maximize the output. This also would provide some decision points in the full test program. There are four areas of concern. These are indicated below in the order of priority that appears to be most amenable to this learning process.

Major Areas Requiring Characterization Tests

- Fuel Cell Components (Electrodes and Matrix)
- Electrolyte Performance and Control
- Stack Compression and Mechanics
- Process Gas Constituent Control

An attempt was made to identify the size of the stacks and the size of the cells for each of the tests to enable a better estimate of the magnitude of the test effort. Such an estimate can only be approximate until the actual design of the test is undertaken. However, for order of magnitude estimates, the characterization tests were assumed to require mostly subscale size cells, 9 cell stacks and other short stacks. Full size cells in less than 50 cell stacks will comprise most tests, and < 10% would be with 100 full size cells or more. Also, the midterm test may be less than 3000 hrs (of the order of 1,000 hrs) and the long term test (< 10% of the test set) at $\geq$ 10,000 hrs.

In summary, it appears that the best estimate at this time of the minimal experimentally designed subscale test program would include the order of 200 individual subscale tests. Fifty percent of these would be short term, low pressure or atmospheric, and the remaining 50% split about 40% midlife, atmospheric pressure and 10% of long life and high pressure. The latter individual tests, however, would not be necessarily at both high time and high pressure since only the number of tests is considered for these conditions. On the basis of the above, it is estimated that 25 to 30 test loops or (an additional 10-15 subscale cell test loops) will be required. Eight to twelve of these test loops would be needed for the long term testing. Capability to test up to three unit (small) full size cell stack would also be required. These facility requirements are summarized below.

- Fabricate and test up to 200 single subscale cells to establish the existing technology baseline for fuel cell and components for various operating conditions simulating those for a full stack (up to 200°C temp., 400 mA/cm^2 current density and 150 psia press.).

- Fabricate and test up to 20 unit (small) stacks of full size cells to identify key stack design parameters and establish additional technology development needed to meet defined goals. These tests to be up to 200°C temperature, 400 mA/cm^2 current density and 150 psia pressure level for up to 10,000 hours for 2 to 3 units.

2.1.4.3 DEFINITION OF MODULE TEST FACILITY REQUIREMENTS

The requirement for a full size cell and stack demonstration and performance verification dictates a module test facility (MTF). This facility would provide test capabilities to establish full size PAFC stack and module performance and operating characteristics for start-up, steady-state, shutdown, malfunction conditions and servicing using suitable control and instrumentation.

Specifically, the following variables would be evaluated for full size module operation over the design operating range:

- voltages
- current densities (and power)
- fuel type
- fuel utilization
- oxidant utilization
- temperature (mean stack and difference)
- pressure level
- coolant flow and pressure drop
- control of load (external resistance)

The following requirements were established for the MTF:

1. The test facility must have the capability to provide the performance parameters of Table 2.1.4-3, with suitable margins to be determined in the specifications for the facility.

2. Test conditions to be imposed on the facility include the types of operation given in Table 2.1.4-4.

TABLE 2.1.4-3

375 kW MODULE PERFORMANCE REQUIREMENTS

The performance requirements for the 375 kW module design are listed below:

PARAMETER	UNITS	NOMINAL	DESIGN RANGE(1)	MAX.
POWER	KW_{dc}	375	< 480	
TEMPERATURE	°F (°C)			
Oxidant Inlet*		360 (182)	300-400 (149-204)	
Coolant Inlet		290 (143)	230-320 (110-160)	
Fuel Inlet		375 (190)	300-400 (149-204)	
Plate Avg.		375 (190)	300-400 (149-204)	
*Same as coolant outlet.				
PRESSURE	Psia	70	15-70	
FLOW	#/hr			
Fuel		410	< 480	
Oxidant		3100	< 3600	
Coolant (air)		61400	< 72000	
CELL VOLTAGE	mV			
Open Circuit		920		
Operating Limit		800		
Operating Point		680	500-800	
CELL CURRENT DENSITY	mA/cm^2	325	< 4800	
MODULE VOLTAGE	Volts			
Open Circuit		1440	< 1540	
Operating Limit		1260	< 1340	
Operating Point		1080	840-1340	
MODULE CURRENT	Amps	350	< 430	

(1) Provisions are made in this column for 100 more cells.

TABLE 2.1.4-4: MTF TEST OBJECTIVES

A. Performance Testing (Demonstration Units)

Performance testing shall encompass short term steady state tests on a full stack and a demonstration module to verify performance at the following points and other intermediate points.

1. Reference Design Point - BOU Full Power
2. Minimum Power
   Module - Most stringent case for 25% power operation
   Stack - 60 kW
3. Maximum Power - Account for 10% variation in module performance between fresh and nearly spent fuel cell modules

B. Transient Testing (Demonstration Units)

Provide simulation of full stack and module operation over the following normal and abnormal transient events.

1. Cold Iron to Standby
2. Standby to Minimum Power
3. Minimum Power to Full Power
4. Full Power to Minimum Power
5. Minimum Power to Standby
6. Standby to Cold Shutdown
7. Faults
   Open Circuit
   Short Circuit
   Loss of Process Gasses
   Loss of Coolant

TABLE 2.1.4-4: MTF TEST OBJECTIVES (CONT'D)

C. Endurance Testing (Demonstration Units)

Provide trend data of sufficient duration to correlate with 9 cell long term tests.

D. Acceptance Testing (Production Units)

Provide verification tests at selected conditions from performance tests.
Provide initial fuel cell module conditioning.

E. Mechanical Design Tests (Demonstration Units)

Provide test data to verify key full stack mechanical or physical design parameters.

F. Test Cell Check Out and Verification Testing

Provide initial check out testing of facility to verify test cell operation.

G. Fuel Processor Integration Tests (Demonstration Units)

Provide testing to verify integration of fuel processor with fuel cell.

3. System interface requirements are to be imposed on the facility to provide realistic simulation of the following:

   - fuel processor
   - power conditioning
   - rotating equipment
   - system control characteristics
   - stack or module servicing

4. Test conditions to be imposed include the demonstrations and operating map given in Table 2.1.4-5.

5. A preliminary assessment of the measurement requirements is provided in Table 2.1.4-6.

TABLE 2.1.4-5: MTF TEST REQUIREMENTS

A. Performance Testing

Testing shall be performed over the range of parameters defined below.

1. Reference Design Point (BOU Full Power)

Fuel Cell Test Parameters	Stack	Module
Anode Gas Pressure, psia	70 ± 3	70 ± 3
Cooling Air Pressure, psia	70 ± 3	70 ± 3
Cathode Exit Pressure - Anode Exit Pressure, psi	0 to 1.5	0 to 1.5
Anode Gas Exit Temperature, °F	375 ± 25	375 ± 25
Cooling Air Temperature, °F	290 ± 10	290 ± 10
Anode Gas Flow Rate, lbs/hr	100 ± 10	410 ± 40
Air Supply Flow Rate, lbs/hr	780 ± 80	3100 ± 300
Cooling Air Flow Rate, lbs/hr	15,300 ± 1500	61,400 ± 6000
Cathode Exit Flow Rate, lbs/hr	780 ± 80	3100 ± 300
Current, amps	350 ± 5	350 ± 5
Anode Gas Composition (moles %)		
Hydrogen	73 ± 1	73 ± 1
Inert Gas (N_2 or CO_2)	21 ± 1	21 ± 1
CO	1 ± 0.1	1 ± 0.1
H_2O	5 ± 0.5	5 ± 0.5
Voltage (V)	< 270	< 1080
Cooling Air Exit Temperature, °F	360	360
Cathode Gas Exit Temperature, °F	375	375
Power, kW	94	375
Compressor Air Supply Relative Humidity	≤ 100	≤ 100

TABLE 2.1.4-5: MTF TEST REQUIREMENTS (CONT'D)

	Stack	Module
Fuel Processor Supply Parameters		
Natural Gas Flow Rate, lbs/hr	35 ± 4	140 ± 15
Water Flow Rate, lbs/hr	110 ± 15	440 ± 50
Air Flow Rate, lbs/hr	180 ± 20	720 ± 80
2. Minimum Power Point (BOU 25% of Full Power)		
Fuel Cell Test Parameters		
Anode Gas Pressure,** psia	54-70 ± 3	38-70 ± 3
Cooling Air Pressure, psia	54-70 ± 3	38-70 ± 3
Cathode Exit Pressure - Anode Exit Pressure, psi	0 to 1.5	0 to 1.5
Anode Gas Exit Temperature,** °F	357-375 ± 25	338-375 ± 25
Cooling Air Temperature, °F	290 ± 10	290 ± 10
Anode Gas Flow Rate, lbs/hr	*64 ± 6	94 ± 10
Air Supply Flow Rate, lbs/hr	500 ± 50	710 ± 70
Cooling Air Flow Rate, lbs/hr	*9,800 ± 1000	18,000 ± 2000
Cathode Exit Flow Rate, lbs/hr	*500 ± 50	710 ± 70
Current, amps	*225 ± 3	80 ± 1
Anode Gas Composition (moles %)		
Hydrogen	73 ± 1	73 ± 1
Inert Gas (N_2 or CO_2)	21 ± 1	21 ± 1
CO	1 ± 0.1	1 ± 0.1
H_2O	5 ± 0.5	5 ± 0.5
Voltage (V)	< 270	< 1080
Cooling Air Exit Temperature, °F	360	360
Cathode Gas Exit Temperature, °F	357-375	338-375
Power, kW	*60	94
Compressor Air Supply Relative Humidity	≤ 100	≤ 100

*Denotes facility with minimum capacity of 60 kW

** The pressure level at 25% of full power operation may vary from 38 pisa to 70 psia depending on the selected mode of operation. Likewise the temperature level may vary from 338°F to 375°F

TABLE 2.1.4-5: MTF TEST REQUIREMENTS (CONT'D)

	Stack	Module
Fuel Processor Supply Parameters		
Natural Gas Flow Rate lbs/hr	20 ± 2	32 ± 4
Water Flow Rate lbs/hr	50 ± 5	80 ± 10
Air Flow Rate lbs/hr	100 ± 10	160 ± 20
3. Maximum Power		
Fuel Cell Test Parameters		
Anode Gas Pressure, psia	70 ± 3	70 ± 3
Cooling Air Pressure, psia	70 ± 3	70 ± 3
Cathode Exit Pressure - Anode Exit Pressure, psi	0 to 1.5	0 to 1.5
Anode Gas Exit Temperature, °F	375 ± 25	375 ± 25
Cooling Air Temperature, °F	290 ± 10	290 ± 10
Anode Gas Flow Rate, lbs/hr	110 ± 10	450 ± 40
Air Supply Flow Rate, lbs/hr	870 ± 80	3400 ± 300
Cooling Air Flow Rate, lbs/hr	16,200 ± 1600	65,000 ± 6000
Cathode Exit Flow Rate, lbs/hr	870 ± 80	3400 ± 300
Current, amps	390 ± 5	390 ± 5
Anode Gas Composition (moles %)		
Hydrogen	73 ± 1	73 ± 1
Inert Gas (N_2 or CO_2)	21 ± 1	21 ± 1
CO	1 ± 0.1	1 ± 0.1
H_2O	5 ± 0.5	5 ± 0.5
Voltage (V)	< 270	< 1080
Cooling Air Exit Temperature, °F	360	360
Cathode Gas Exit Temperature, °F	375	375
Power, kW	100	400
Compressor Air Supply Relative Humidity	≤ 100	< 100

*Denotes facility with minimum capacity of 60 kW

TABLE 2.1.4-5: MTF TEST REQUIREMENTS (CONT'D)

	Stack	Module
Fuel Processor Supply Parameters		
Natural Gas Flow Rate, lbs/hr	38 ± 4	150 ± 15
Natural Gas Supply Pressure, psia	120	120
Water Flow Rate, lbs/hr	120 ± 15	470 ± 50
Air Flow Rate, lbs/hr	190 ± 20	770 ± 80

TABLE 2.1.4-5: MTF TEST REQUIREMENTS (CONT'D)

B. Transient Testing

The following transients shall be simulated. All operations shall occur at pressures and temperatures that result in acceptable phosphoric acid concentrations.

1. Cold Iron to Standby (in 4 hours)

   a. Introduce nitrogen to anode and cathode channels.
      - Introduce compressed air to the recirculating loop to establish 0.4 psig pressure level
      - Introduce nitrogen to anode stream and cathode gas exit stream between modules and exit control valves to establish 0.5 psig level

   b. Circulate warm air through fuel cell cooling loop and raise FC temperature to > 250°F.
      - Raise module temperature from ambient to 250°F in $\leq$ 3 hours
      - Use heated air in recirculating loop
      - Maintain 0.5 psig pressure level in anode and cathode gas streams using nitrogen gas.

   c. Hold at Standby
      - Switch from manual control to automatic control,
      - Maintain fuel cell temperature at > 250°F and 0.5 psig positive pressure in all lines with nitrogen system for up to a 60 hour period

2. Standby to Minimum Power Point (in < 1 hour)

   a. Connect electrical load

   b. Introduce Process Gas to Anode and Cathode
      - Switch anode gas composition from nitrogen to design fuel composition,
      - Switch cathode process gas from nitrogen to air from recirculating air loop.

   c. Set current demand at minimum operating point which shall simultaneously set anode flow and compressed air supply flow rates corresponding to minimum power levels.

TABLE 2.1.4-5: MTF TEST REQUIREMENTS (CONT'D)

d. Control recirculation flow rate to ramp fuel cell temperature to minimum power operating point.

   - Control fuel cell temperature response at average of 5°F/min. with a maximum of 20°F in 4 minutes.

e. Raise cell pressure to minimum operating pressure.

   - Raise cooling air pressure from 0.5 psig to the minimum power point pressure level, by controlling on cathode exhaust flow. On a demand schedule compatible with acid inventory controls (example - such as constant acid concentration or constant acid volume)
   - Maintain anode and cathode exhaust pressure differential to less than $\pm$ 2 psi by controlling anode exhaust flow

f. Complete steps a to e in 1 hour.

g. Hold at minimum power operating point.

3. Minimum Power to Full Power

   a. Increase current demand from the minimum power operating point to full power operating point at rate of 7.5% to 15% of full current per minute.

   b. Concurrently with step a, the anode fuel flow and the compressed air supply to the recirculation loop shall be increased to the full power point at the same rates.

   c. Control cathode exhaust gas flow rate to either maintain a constant 70 psia pressure or increase pressure from as low as 38 psia at minimum power to 70 psia at 3 to 7 psia/minute rate. (See Figure 2)

   d. Control recirculation rate to either maintain constant temperature or increase temperature from as low as 338°F at minimum power to 375°F at 3 to 6°F/minute rate. (See Figure 2)

   e. Maintain anode and cathode exhaust pressure differential to within $\pm$ 2 psi by controlling anode exhaust flow during transient.

   f. Perform steps a through e in parallel.

   g. Hold at full power operating point.

TABLE 2.1.4-5: MTF TEST REQUIREMENTS (CONT'D)

4. Full Power to Minimum Power

   a. Decrease current demand from the full power to the minimum power operating point at a rate of 7.5% to 15% of full current per minute.

   b. Concurrently with step a, the anode fuel flow and the compressed air supply to the recirculation loop shall be decreased to the minimum power point at the same rate.

   c. Control cathode exhaust gas flow rate to either maintain a constant 70 psia pressure or decrease pressure from 70 psia to as low as 38 psia at 3 to 7 psia/minute rate.

   d. Control recirculation rate to either maintain a constant 375°F temperature or decrease temperature from 375°F to as low as 338°F at 3 to 6°F/minimum rate.

   e. Maintain anode and cathode exhaust pressure differential to within $\pm$ 2 psi by controling anode exhaust flow during transient.

   f. Perform steps a through e in parallel.

   g. Hold at minimum power operating point.

5. Shutdown from Minimum Power to Standby

   a. Lower cooling air pressure and anode gas pressure from minimum operating point to 0.5 psig by controlling cathode exhaust.
      - Maintain anode and cathode exhaust pressure differential to $\pm$ 2 psi during transient.

   b. Reduce fuel cell temperature to 250°F.
      - Vary cooling air recirculating rate to control fuel cell temperature response at -5°F/minute average rate with maximum of -20°F in 4 minutes.

   c. Switch cathode and anode flow from process gas compositions to nitrogen gas. Maintain 0.5 psig positive pressure in lines with nitrogen system by closing cathode exhaust valve.

   d. Disconnect electrical load

   e. Complete steps a through d in less than 1 hour.

   f. Hold at standby for period up to 60 hours.
      - Maintain fuel cell temperature of > 250°F and 0.5 psig positive pressure in all lines using nitrogen system

TABLE 2.1.4-5: MTF TEST REQUIREMENTS (CONT'D)

6. Shutdown from Standby to Cold Iron

   a. Remove heat and continue recirculation of air at flow rate required to cool fuel cell from 250°F to within 20°F of ambient within 8 hours.

   b. Maintain positive pressure (∿ 0.5 psig) using nitrogen system
      - Shutdown all fluid systems

7. Faults

   a. Open Circuit
      - Voltage increases above limit of 1400 V
      - If voltage above limit for 0.5 sec, perform steps a through f in Section 5 to reach standby.

   b. Short Circuit
      - Current increase above limit of 450 A.
      - If current above limit for 0.5 sec, perform steps a through f in Section 5 to go to standby.

   c. Loss of Anode Fuel Supply
      - If voltage drops below 400V for 0.5 sec, perform steps a through f in Section 5 to reach standby.

   d. Loss of Cooling Air
      - If circulator RPM or air pressure decreases below minimum values for > 0.5 sec, perform steps a through f in Section 5 to reach standby, but with reduced temperature cooling rate compatible with circulator or compressor supply ratings.

C. Endurance Testing

1. Stack Testing

   a. Reference Design Point (BOU Full Power)

   b. Minimum Continuous Hours 500

TABLE 2.1.4-5: MTF TEST REQUIREMENTS (CONT'D)

c. Maximum Hours 2000

d. Perform shutdown/startup operational cycle every 500 hours

2. Module Testing

a. BOU Full Power

b. Minimum Continuous Hours 500

c. Maximum Hours > 7000

d. Perform shutdown/startup opeational cycle every 500 hours

D. Acceptance Tests

1. Perform selected performance tests.
2. Run Infant Mortality Tests
   - BOU Full Power for 100 hours.

E. Mechanical Design Tests

Provide full stack displacement and tie bolt strain measurements during performance and transient testing.

F. Test Cell Check Out and Verification Testing

Required by not defined by engineering design requirements.

G. Fuel Processor Integration Tests

Provide measurement of fuel processor performance during steady state and transient tests. Type of measurements and transient operating constraints deferred until fuel processing configuration defined.

TABLE 2.1.4-6: MTF PRELIMINARY LIST OF MEASUREMENTS

REQUIRED MEASURMENTS	SENSOR TYPE	STACK		MODULE	
		OPERATING RANGE	ERROR	OPERATING RANGE	ERROR
ANODE					
1. ΔP, Upper to Lower Manifold, I.V.	Diff. Press Leads	-10 to +10" H_2O	5%	N/A	
2. ΔP, Anode to Cathode, Exit Manifold, I.V.	Diff. Press Leads	± 2 psid	5%	Same	
3. ΔP, Anode to Cathode, Exit, O.V.	Diff. Press Leads	± 5 psid	5%	Same	
4. Anode Gas Press, Exit, O.V.	Press. Taps	0 to 100 psia	5%	Same	
5. Anode Flow Rate, Inlet, O.V.	Flow Meter	10 to 150 lbs/hr	5%	N/A	
6. Anode Gas Temp., Inlet, O.V. (Qty. 1)	T/C	Amb. to 400°F	5%	Same	
7. Anode Gas Temp., Top, Mid., Bot. (Qty. 3), ? Exit Manifold, I.V.	T/C's	Amb. to 400°F	5%	Only 1 per stack	
8. Anode Gas Temp., Exit, O.V. (Qty. 1)	T/C	Amb. to 400°F	5%	Same	
CATHODE					
9. Cathode Gas Temp., Inlet, O.V. (Qty. 1)	T/C	Amb. to 400°F	5%	Same	
10. Cathode Gas Temp., Top, Mid., Bot. (Qty. 3) Exit Manifold, I.V.	T/C's	Amb. to 400°F	5%	Only 1 per stack	
11. Cathode Gas Temp., Exit, O.V. (Qty. 1)	T/C	Amb. to 400°F	5%	Same	
12. Cathode Exhaust Flow Rate, Exit, O.V.?	Flow Meter	50 to 900 lbs/hr	5%	200 to 4000 lbs/hr	
COOLING AIR					
13. Cooling Air Press., Inlet, I.V.	Press. Taps	0 - 100 psia	5%	Same	
14. ΔP, Across Stack, (I.V.?)	Diff. Press Leads	0 - 20" H_2O	5%	Same	
15. ΔP, Cooling Air Inlet to Anode Inlet (I.V.)	Diff. Press Leads	± 5 psid	5%	Same	
16. Cooling Air, Temp., Inlet, O.V. (Qty. 1)	T/C	Amb. to 400°F	5%	Same	
17. Cooling Air, Temp., Exit, O.V. (Qty. 1)	T/C	Amb. to 400°F	5%	Same	
18. Cooling Air, Temp., Exit, I.V. (Qty. 3) Top, Middle, Bottom	T/C	Amb. to 400°F	5%	N/A	
19. Cooling Air, Flow Rate, Inlet, O.V.	Flow Meter	1000 to 20,000 lbs/hr	5%	3500 to 70,000 lbs/hr	

NOTES

I.V. = Inside Vessel O.V. = Outside Vessel

TABLE 2.1.4-6: MTF PRELIMINARY LIST OF MEASUREMENTS (CONT'D)

REQUIRED MEASURMENTS	SENSOR TYPE	STACK		MODULE	
		OPERATING RANGE	ERROR	OPERATING RANGE	ERROR
20. Anode Gas Composition; H_2 Inlet, O.V.	TBD	50% to 80%	5%	Same	
CO	TBD	0 to 4%	5%	Same	
CO_2	TBD	0 to 100%	5%	Same	
21. Anode Gas Composition, H_2 Outlet, O.V.	TBD	80% to 0	5%	N/A	
CO	TBD	0 to 4%	5%	N/A	
CO_2	TBD	0 to 100%	5%	N/A	
22. Air Supply Flow Rate, Inlet, O.V.	Flow Meter	50 to 900 lbs/hr	5%	200 to 4000 lbs/hr	
23. Relative Humidity, Air Supply Inlet	TBD	0 to 100%	5%	Same	
24. Acid Makeup, O.V.	TBD	TBD cc		Same	
25. Fuel Cell Cooling Plates, Temp., I.V. (Qty. 6)	T/C	Amb. to 400°F	5%	Same	
26. Circulator, RPM	Tach.	TBD		TBD	
27. Stack Tie Bolt Loads, Strain Gages, 4 sets	S.G.	585 μ "/"	5%	Same	
28. Stack Tie Bolt Temp., Qty. 4	T/C	Amb. to 400°F		Same	
29. Stack Current, O.V.	Amps	0 - 500 amps	2%	Same	
30. Stack Voltage, Total, I.V.	Leads to @ Plate	400 VDC Max.	0.5 %	Same	
31. Stack Voltage, 5 Cell Groupings, 3 groups/stacks I.V.	Leads to Group	0 - 5 VDC	2%	N/A	
32. Total Module Voltage, Qty. 1, O.V.	Leads to Module	N/A	-	1600 VDC Max., 0.5 %	
33. Fuel Processor	TBD	40 Data Channels	2%	Same	

2.1.5 FUEL PROCESSOR, POWER CONDITIONER, AND ROTATING EQUIPMENT SYSTEMS TECHNOLOGY ASSESSMENT

State-of-the art assessments were performed for conventional fuel processors, power conditioning equipment, and rotating equipment. These assessments were performed to determine the adequacy of existing equipment to meet the requirements for fuel cell power plants and to determine the needs for technological improvements. The results of these assessments are summarized in the following sections.

2.1.5.1 FUEL PROCESSING SYSTEM (FPS)

The FPS for PAFC power plants are represented commercially by conventional hydrogen plants utilizing steam reforming of light hydrocarbons. Steam reforming is a well-known technology, and complete modular, skid-mounted hydrogen plants for capacities up to 10 million SCFD are available from a number of suppliers. Conventional plants are normally conservatively designed, resulting in high reliability, moderate efficiency, and relatively high capital costs. They have long startup periods and poor transient response.

A comparison between the present technology status and PAFC power plant requirements is shown in Table 2.1.5-1. The items requiring the greatest improvement are the thermal efficiency, reformer height, and capital costs. Conventional plant efficiency is limited by the radiant box efficiency of the reformer furnace. Modifications to operating conditions and better waste heat utilization could theoretically increase the efficiency to 85 percent. Higher efficiencies require either an integrated fuel processor/fuel cell system or an advanced reformer design, such as a radiant/convective furnace or an all-convective furnace. The conventional radiant furnace also requires overall heights in excess of the requirements.

2.1.5.2 POWER CONDITIONING SYSTEM (PCS)

A review of the applicable literature, experience with power conversion equipment with comparable requirements, and discussions with design specialists indicated that either of two generic types of an inverter circuit could meet the PCS requirements. These are the current sourced, line commutated and the

TABLE 2.1.5-1

FUEL PROCESSING SYSTEM (FPS) DEVELOPMENT GOALS

	Present Technology	PAFC Requirements
Fuel	Nat. Gas/LPG/Naphtha	Nat. Gas/Naphtha
Efficiency, percent	65-75	90
Operational		
Cold Start to Standby, hrs	4-8	4
Standby to Min Power, hrs	1-2	1
Min to Max Power, percent Load/Min	5-7.5	7.5
Operating Range, percent rated power	25-100	25-100
Operation	Semi-Automatic	Automatic dispatch from standby to full power
Availability, percent	96-99	98
Useful Life, years	15-20	25
Plot Plan Area, ft^2/1000 SCFH H_2	25-45	12
Reformer Height, ft above grade	60-70	30
Capital Cost		
\$/SCFH H_2 rated capacity	12-25	5
\$/kW ac	400-800	130

voltage sourced, forced commutated types. The former is the traditional circuit type used in large power applications such as high voltage dc transmission systems and static VAR generators. The latter inverter type has seen more limited utilization in large ac motor drives, uninterruptible power supplies, and EPRI sponsored battery and fuel cell PCS development programs.

To determine which basic inverter type should be selected for the PAFC power plant application, an evaluation comparing the two types was performed. Table 2.1.5-2 shows how the two compared in seven key areas. The analysis was extended to a total of seventeen areas and when the final assessment was made it was clear that available technology and experience favors using a current sourced, line commutated inverter for this application.

The assessment of the technology available to consolidate or combine the power outputs from multiple fuel cell modules into a two terminal input to the inverter was more difficult. Literature describing circuitry, identifying problems, and suggesting solutions could not be found. The technology assessment consisted of identifying the expected characteristics of the fuel cell modules at steady state and transient, and the desired module operating regimes. Table 2.1.5-3 lists consolidation circuit requirements identified at this time.

2.1.5.3 ROTATING EQUIPMENT SYSTEM (RES)

Over 30 vendors were contacted to obtain data on the availability and characteristics of rotating equipment to meet the typical requirements for PAFC power plants. The following general information was obtained from a vendor survey and follow up meetings with selected vendors.

- A list of rotating equipment suppliers was established; this list represents a good cross-section of suppliers that could meet the RES functional requirements.
- Most of the vendors contacted showed limited interest in supplying a RES as a total package concept and preferred to quote on just one or two special pieces of equipment. Three vendors responded with a total RES package concept.

TABLE 2.1.5-2

COMPARISON OF BASIC INVERTER TYPES

Current Sourced Line Commutated Inverter	Voltage Sourced Forced Commutated Inverter
Efficiency	
95 percent - full load	95 percent - full load
92 percent - 25 percent load	80 percent - 25 percent load (need faster thyristor switching speed for further improvement)
Experience	
3.5 MW for MHD VAR generators of hundred of MVAR Up to 1.8 GW to MVdc	Field proven designs by others limited to about 3 kV and 5 MW
Fault Handling	
Prone to frequency short outages. Fault clearing easier and always automatic.	Commutation not dependent on ac line. Fault clearing and restoration of service always manual.
Input reactors limit rate of rise of dc fault current and make protection easier.	Fuses for dc fault clearing marginally available.
dc Voltage Ratio Capability	
No limitations.	Most work to date at 1.3 to 1 ratio. Inverter cost increases significantly with increase in ratio.
Harmonic Filtering	
Tuned harmonic filter component cost go down with larger sizes.	Most of existing large design per KVAR use phase shifting, summing designs. These transformer costs increase very sharply per kVAR in larger sizes.
Power Factor	
Required correction.	Has reactive power control
Development/Design Time	
18-24 months	30-36 months

TABLE 2.1.5-3

CONSOLIDATION CIRCUITRY CONTROL REQUIREMENTS

- The maximum voltage output of a fuel cell module will be limited to 1400 V dc.
- Consolidation circuitry will be able to carry up to 700A per module for up to ten seconds without damage.
- Reverse voltage of sufficient magnitude to cause reverse current to flow in any module will be prevented.
- Sufficient filtering will be provided in the circuitry to limit any harmonics caused by electronic switching action from damaging fuel cell modules.
- The circuitry will permit the control of the current taken from each module in response to control signals from the central power plant control computer. This control is needed to maximize overall power plant efficiency and to allow for differences in individual module efficiency and to allow for differences in individual module efficiencies due to manufacturing variations and module aging effects.
- The circuitry will provide for the combination of currents from up to ten modules with terminal voltages of up to 150 V apart to be connected to each inverter dc bus. Unequal module terminal voltages will be an inevitable consequence of the overall power plant control scheme based on module current control.
- The consolidation circuitry will be non-dissipative in order not to have an adverse impact on the losses and efficiency of the system.

- All vendors indicated that "off-the-shelf" design equipment is available and that long term RES development work is not warranted with the possible exception of the pressurized circulator.

- The pressurized circulator in the air cooling recirculation stream may require some custom design work. Several vendors quoted fan prices about 25 percent higher in cost than for a design at normal atmospheric operation because of the 0.5 to 1 inch thick steel casing to house the fan.

- The compressor(s) is an off-the-shelf piece of equipment but has varying operational characteristics depending on type and required operating range. The compressor type is important as it affects layout, efficiency, and cost.

- The steam turbine and gas expander components present no problems and can be purchased off-the-shelf.

From the survey and followup meeting with several vendors, seven rotating equipment options illustrated in Figure 2.1.5-1 were selected for a detailed comparative evaluation.

Table 2.1.5-4 summarizes the advantages and disadvantages of all seven equipment options. Of the RES configurations studied, Concept 7 has more advantages than disadvantages over the other vendor concepts. Concept 7 is shown to have the smallest footprint, lightest weight, small number of components, rapid startup and shutdown times, small number of spare parts, lowest cost, and good efficiency at rated conditions. Disadvantages are that bypass flow is required to meet the 25 percent low power operation at the pressure level specified. This bypass causes lower overall plant efficiencies (higher heat rate).

Figure 2.1.5-2 shows the process flow schematic for Concept 7. The process statepoints on the schematic are for rated conditions. A top view arrangement of this concept is shown in Figure 2.1.5-3.

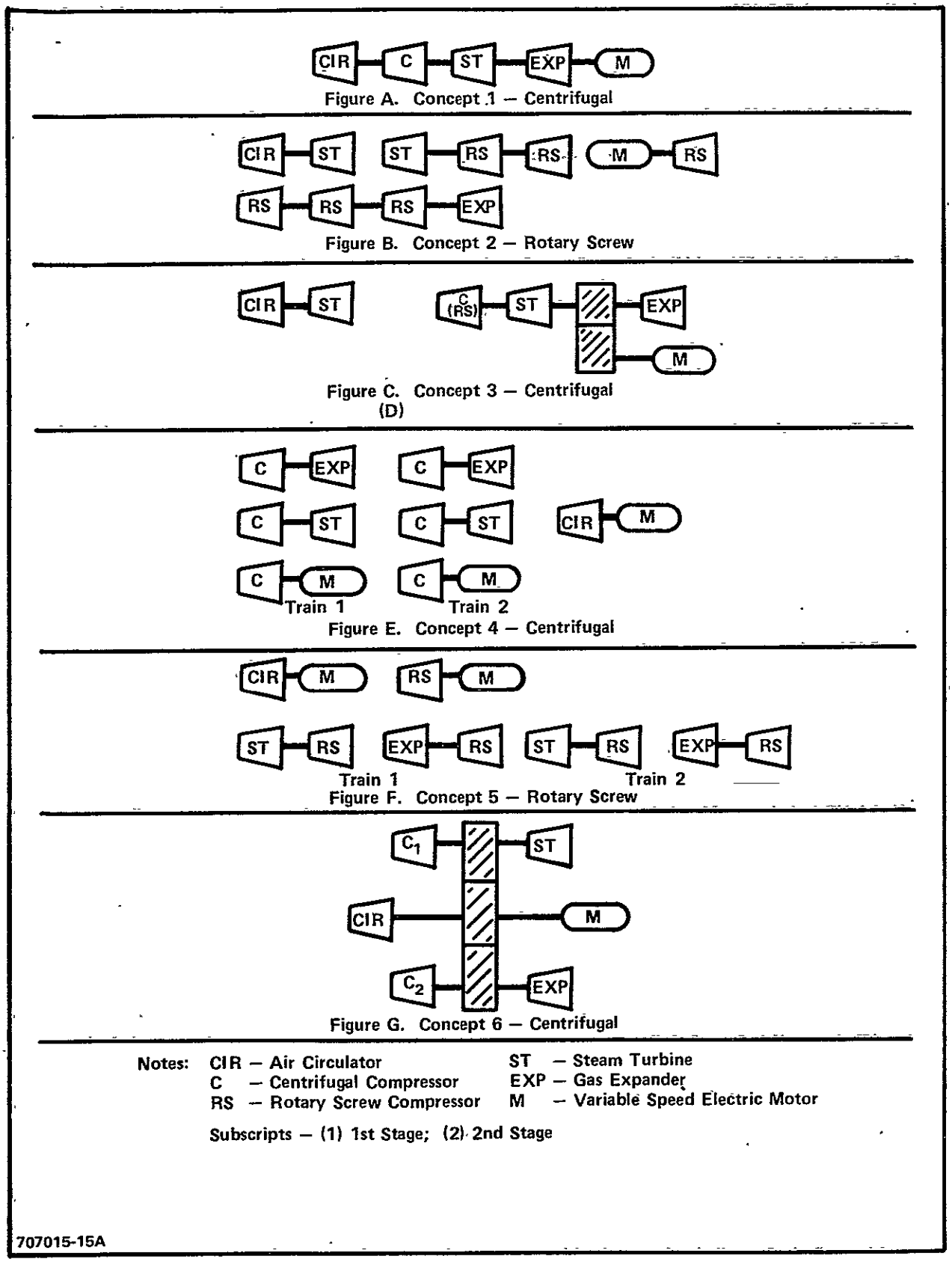

Figure 2.1.5-1. Rotating Equipment Concepts

Table 2.1.5-4

SUMMARY ROTATING EQUIPMENT SYSTEM (RES) CONFIGURATIONS

Concept	Advantages	Disadvantages
1	• Packaged Group of Equipment • Intercooling Available • Good Efficiency at rated conditions • Low Cost	• Must bypass flow to meet 4:1 turndown • Low efficiency at part power
2	• Capable 4:1 Turndown • Separate Shutdown Units • Ease of Operation	• Many components
3	• Single Compressor • Packaged Group of Equipment	• Difficult to meet 4:1 turndown • Low efficiency part power
4	• Capable 4:1 Turndown • Intercooling (two stages) • Ease of Operation • Simple and Compact • At 55 psia single stage compressors available	• Expensive • Two stage compression to reach 70 psia
5	• Good Efficiency at Rated Conditions • Indirect Drive No Gears • Modular Packages • Intercooling	• More difficult to control
6	• Separate Units Which Can Be Shutdown • Ease of Operation • Capable 4:1 Turndown	• 66 psia pressure on single stage • Gear Loss
7	• Packaged Group of Equipment • Intercooling Available • Good Efficiency at Rated Conditions • Low Cost	• Must bypass flow to meet 4:1 turndown • Low efficiency at part power

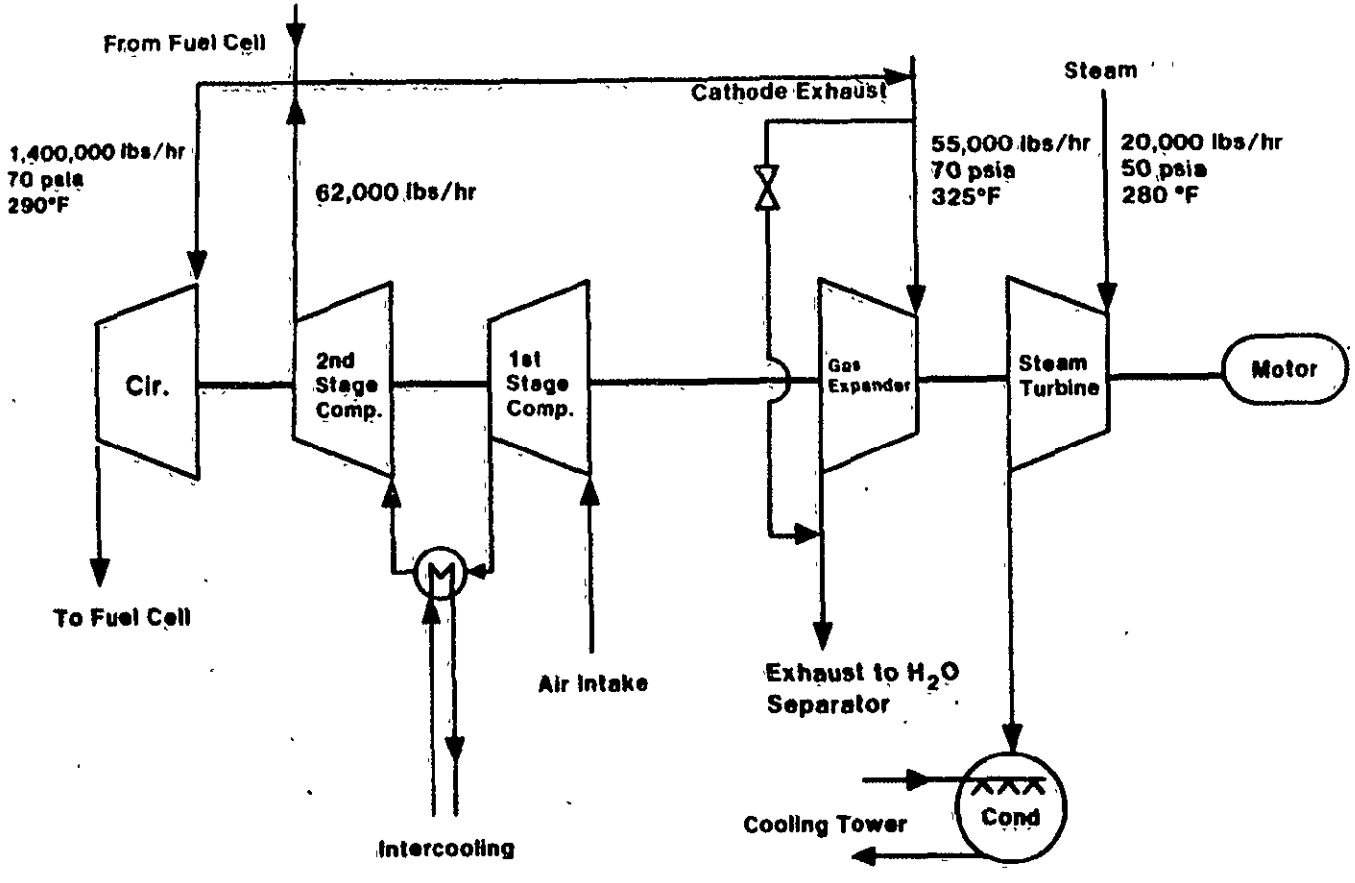

Figure 2.1.5-2. Rotating Equipment System (RES) Process Flow Schematic

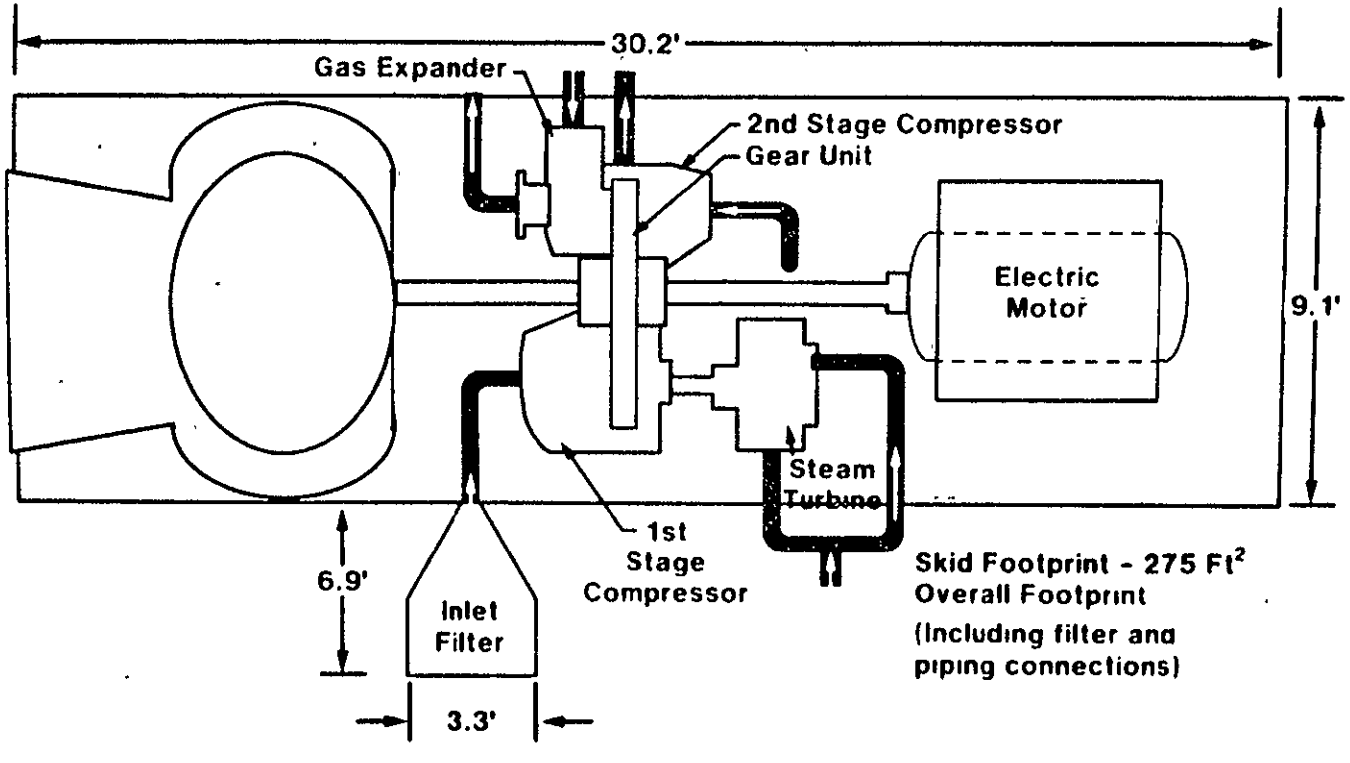

Figure 2.1.5-3. Rotating Equipment System (RES) Arrangement Top View

2.2 FUEL CELL SYSTEMS REQUIREMENTS

The primary objective of this task was to develop test specifications in accordance with the FCS requirements for subscale (2x2 inch) fuel cells, nine-cell stacks, and 10 and the 25 kW stacks. The test specifications included requirements for steady-state and transient performance, endurance, key state-points and gas chemistry. The following sections summarize the results of these efforts.

2.2.1 25 kW STACK FUEL CELL TEST SPECIFICATION

A preliminary test specification was initiated for a 25 kW stack based upon system requirements defined from available design and test data from subscale cell and nine-cell stack tests, system functional analyses and trade-off studies. Limited availability of results from the subscale cell and nine-stack tests has delayed the completion of 25 kW stack design and test requirements and, therefore the completion of the 25 kW short stack test specification. Although a preliminary 25 kW stack test specification was not issued, the system performance requirements and design requirements were identified and documented. The preliminary 25 kW stack performance and instrumentation requirements are summarized in Tables 2.2.1-1 and -2.

2.2.2 FUEL CELL HARDWARE TEST SPECIFICATIONS

The initial subscale cell and nine-cell stack test specifications were issued to perform tests to obtain the technology characterization for fuel cell and stack design and performance prediction. The 10 kW stack test and measurement requirements and testing conditions were also identified. However, the 10 kW stack test specification was not issued pending availability of needed design and operating test results from the subscale cell and nine-cell stack testing.

Subscale cell test specifications were issued for the first group of the technology characterizations needed as noted in Table 2.2.2-1. The purpose of this first group of test specifications was to: (1) verify process and fabrication reproducibility and control, 2) establish comparative capabilities of electrodes and other cell components performance with a few key process

TABLE 2.2.1-1

25 kW STACK PERFORMANCE REQUIREMENTS

Parameter	Units	Nominal	Design Range
POWER	kW dc	25	< 30
TEMPERATURE	°F (°C)		
Oxidant Inlet		363 (184)	300-400 (149-204)
Coolant Inlet		277 (136)	230-320 (110-160)
Fuel Inlet		375 (190)	300-400 (149-204)
Plate Avg.		375 (190)	300-400 (149-204)
PRESSURE	Psia	70	15-100
FLOW	#/hr		
Fuel		8.75	8.75
Oxidant (air)		209	< 418
Coolant (air)		3325	2900-4350
CELL VOLTAGE	mV		
Open Circuit		920	< 1100
Operating Limit		800	
Operating Point		680	500-800
CELL CURRENT DENSITY	mA/cm^2	325	< 400

TABLE 2.2.1-2

PRELIMINARY LIST OF MEASUREMENTS

REQUIRED FOR 25 kW - CELL STACK TESTING

Tentative Req'd Measurements	Tentative Type Sensors	Operating Range Est.	Error Range (% of Max.)**
1. Cell Voltage	Individual leads to each plate	-1.0 to +1.5 volt.	1/2
2. Cell Current	Stack Output Amperage	50 to 500A	2
3. Cell Temperature	T/C's in plates	Amb to 220°C	2
4. Cell Pressure	Press. Taps-Containment	Amb to 100 psia	2
5. Fuel Inlet Pressure	Press. Taps - Manifold	Amb to 100 psia	2
6. Fuel Press. Drop	Diff Press. Leads	0 to +12" H_2O	2
7. Oxidant Inlet Pressure	Press. Taps - Manifold	Amb to 100 psia	2
8. Oxidant Press. Drop	Diff Press. Leads	-10 to +12" H_2O	5
9. Coolant/Manifold Seal ΔP	Diff Press. - Manifold	-50 to +50 psid	5
10. Fuel to Oxidant Press. Diff.	Diff Press. Leads	-10 to +30" H_2O	5
11. Fuel Outlet Pressure	Derived (5 & 6)	Amb to 100 psia	2
12. Oxidant Outlet Pressure	Derived (7 & 8)	Amb to 100 psia	2
13. Coolant Outlet Pressure	Press. Taps-Manifold	Amb to 100 psia	2
14. Oxidant to Fuel - Exit ΔP	Diff Press. Leads	-10 to +30" H_2O	5
15. Coolant ΔP	Diff Press. Leads	0 to +12" H_2O	5
16. Temp Difference - Cells	T/C's Distr. in plates	0 to 60°C	5
17. Temp Increase - Coolant	T/C's in Plenums	0 to 60°C	5
18. Stack Output Voltage	Circuit Voltage	0 to 100 volts	2
19. H_2O fraction - Exhaust	Humidity - fuel exhaust	0 - 100%	2
20. Power Level, Transients	Voltage & Amperage of stack circuit	(> 20 kW/sec) (time constants TBD)	-
21. Cell Internal Resistances	(From Volt. leads)	0 to 1 mΩ	5
22. Stack Resistance*	(Circuit Resist.)	0 to 100 mΩ	5
23. Clamping Load	Strain gages on tie bolts & tie bars	0 to 30,000 psi (0 to 1 mil/in)	5
24. Pressure Level Transient	ΔP transducers	(> 50 psi/sec)	5
25. Oxidant Utilization	Gas Analyzer - Inlet & Outlet Plenums	1.2 to 5 stoichs O_2	5
26. Fuel Utilization	Gas Analyzer - Inlet & Outlet Plenums	50 - 85% H_2	2
27. Oxidant Flow Rate	Flow meters	10 to (TBD) kg/hr	2
28. Fuel Flow Rate	Flow meters	1 to 20 kg/hr	1
29. Fuel Leakage	Coolant Outlet Gas Analysis	0 to (TBD) (% or ppm)	-
30. Stack Creep	Displacements & time	0 to 20 mm	5
31. Acid Addition	Mass added	(TBD) cc	5
32. Acid Loss	Discharge Rate - Outlet Gas Analysis - Outlet	(TBD) cc (TBD) cc	5 5

* Stack capacitance to be checked by Bridge prior to testing

** Operating Range Reference, no instrument

TABLE 2.2.2-1

TEST GROUP DEFINITIONS - 2x2 SUBSCALE CELLS

Principal Characterizations Required:*

1. Electrode - Performance and Life (Reference 1 - baseline technology understanding)

2. Matrix and Electrolyte - Performance & Life

3. Reactant Constituents Effects (Control of key contaminants, air and fuel sources).

4. Physical/Structural Design Effects (Control of key parameters - clamping loads, distortions introduced by tolerances, "shelf" time, handling conditions, etc).

---

*Expected effects due to control of key variables within both design and operating ranges anticipated. Uncertainties in other unknown variables not controllable directly would be included in effect. List is in order of priority. All other variables subsequent to expressed test plan to be constrained by specification or process to keep same (within possible limits).

Reference 1: DRM 115 "Definition of PAFC Subscale Test Plan - Electrode Characterization", Sept. 2, 1982 Revision 1.

variables, 3) establish the test facility and testing compatibilities between Westinghouse and ERC test loops, and 4) to establish pressure effects and input for stack design.

Later subscale cell tests were defined to establish the fuel cell baseline technology, parameter sensitivity understanding and performance characteristics related to process and fabrication control adequacy. Quantitative understanding of the pertinent variables and of the design parameters and effects of operating conditions as noted in Tables 2.2.2-2, -3, -4 and -5 requires both cell and stack testing in a designed test approach.

The voltage and current characteristics with loading and operating conditions (polarization curves) would be established for PAFCs in the first set of tests, with components fabricated to the same specifications. The consistency of the polarization response and cell to cell performance uncertainties for identical cells must be acceptable for the planned variables tests to be successful.

2.2.2.1 REPRODUCIBILITY TESTS

A test specification for identical fabrication and testing of eight identical 2x2 subscale cells was defined to verify reproducibility. These objectives and test plan were defined and the tests were carried out as summarized in Section 3.1.5.

BRIDGING TESTS:

The data requirements and test plan specified that five batches of electrodes were to be made at AESD and subscale 2x2 fuel cells fabricated from these components and tested at AESD. The electrodes were fabricated according to the specified processes, fabrication, and assembly procedures. However, large manufacturing variations in these components were observed. This variation brought into question the ability to obtain the desired data quality and performance consistency required by the tests.

TABLE 2.2.2-2

AREAS OF DESIGN AND OPERATING VARIABLES

1. Hardware Options

- Fabrication Facility
- Furnace Run
- Electrode and Matrix Component "Alternates"
- Testing Facility and Loop

2. Assembly Options

- Facility
- Acid Loading
- Clamping Pressure
- Compression Cycle History

3. Operating Parameter Options

- Current
- Pressure
- Temperature
- O_2 Flow (Stoichs)
- H_2 Flow (Stoichs)
- Fuel Composition
- Impurities
- Transient Conditions
- Cycles

TABLE 2.2.2-3

MEASUREMENTS FOR PROCESS/FABRICATION CONTROL

Test Objective	Measurable Variable	Values: Initial	Values: Final	Values: Oper. Cond.
• Establish cell to cell uniformity - Acceptable Polarization and Life Trends baseline	• Voltage	✓	✓	✓
	• Resistance	✓	✓	✓
	• Corrosion		✓	
	• Catalyst avail/util	✓	✓	
	• Acid condition	✓	✓	
	• Reactants - inlet and outlet condition			✓
	• Times			✓
• Establish stack assembly effects - power output/cell performance baseline	• Current output			✓
	• Voltage output			✓
	• Resistance	✓	✓	✓
	• Pressure			✓
	• Temperature			✓
	• Reactants - inlet and outlet conditions			✓ ✓
• Establish Endurance baseline	• Voltage loss	✓	✓	✓
	• Corrosion loss		✓	
	• Catalyst avail loss	✓	✓	
	• Acid condition	✓	✓	
	• Times			✓

TABLE 2.2.2-4

MEASUREMENTS FOR TECHNOLOGY DESIGN PERFORMANCE

Test Objective	Measurable Variable	Values: Initial	Values: Final	Values: Oper. Cond.
• Establish voltage characteristics and losses	• Stack voltage open cir.	✓	✓	✓
	• Cell voltage open cir.	✓	✓	✓
	• Stack voltage - oper. cond. and during transients			✓
• Establish Polarization characteristics	• Cell voltage	✓	✓	✓
	• Current	✓	✓	✓
	• Pressure			✓
	• Temperature	✓	✓	✓
	• H_2 concentration	✓	✓	✓
	• O_2 concentration	✓	✓	✓
	• CO, CO_2 concentrations	✓	✓	✓
	• Resistance	✓	✓	✓
• Establish performance trend data - voltage degradation	• Voltage	✓	✓	✓
	• Current	✓	✓	✓
	• Time			✓
• Acid Management	• Voltage	✓	✓	✓
	• Current			✓
	• Time			✓
	• Acid added	✓		✓
	• Acid losses	✓	✓	✓
	• Pressure	✓	✓	✓
	• Temperature	✓	✓	✓
	• Process Gas Flow Rates			✓
	• Cell Resistance	✓	✓	✓

TABLE 2.2.2-5

MEASUREMENTS TO ESTABLISH OPERATION CHARACTERISTICS

Test Objective	Measurable Variable	Values Initial	Values Final	Values Oper. Cond.
• Establish voltage characteristics and losses - operating profiles and events	• Stack voltage open cir.	✓	✓	✓
	• Cell voltage open cir.	✓	✓	✓
	• Stack voltage - operating conditions and during transients			✓
• Establish Operating Effects - Polarization characteristics (Short and Long Term)	• Cell voltage			✓
	• Current density			✓
	• Pressure			✓
	• Temperature			✓
	• H_2 concentration			✓
	• O_2 concentration			✓
	• CO concentration			✓
	• Resistance	✓	✓	✓
• Establish performance trend data - voltage degradation with operating conditions	• Voltage	✓	✓	✓
	• Current density	✓	✓	✓
	• Time			✓

To establish the viability of conducting these tests, a "bridging test" was considered necessary. This test was intended to establish the consistency of performance and what performance variation would be expected from cells fabricated from components that were very similar, and those showing the largest observable variations in thickness, weight, and quality (visible flaws, etc). However, other variables in electrode fabrication became significant. The test plan was extended to include a comparison of cell components having the specified area controlled variables at two levels as noted below:

- Non-heat treated and 900°C heat treated PtC catalyst.
- Low (< 0.45 mg) and high (> 0.55 mg) catalyst loading.
- Thin (< 0.005 in.) SiC and thick (> 0.01 in.) SiC coating.
- Wet and dry bond lamination.
- Low viscosity (ERC) and high viscosity (Westinghouse) Polyox mix.

This extended bridging and screening test plan is a partial factorial design of a 2^5 test design that provides all of the direct first order or main effects and second order effects, but assumes that third-order (and higher) interactions are negligible. The test subscale cell unit definitions are given in Table 2.2.2-6.

2.2.2.3 FACILITY COMPARISON TESTS (ROUND-ROBIN):

This test specification defined the testing to compare the performance of 2x2 subscale cells assembled and tested in Westinghouse facility with identical cells assembled and tested in the ERC facility. This test plan will determine the nominal performance variance range and the data repeatability, and establish the capability to directly compare test results obtained from either facility.

TABLE 2.2.2-6

ELECTRODE COMPARISONS - 2x2 SUBSCALE CELL TEST ASSEMBLIES

(2^5 Five Variable Partial Factorial Test)

Test Design	Catalyst Lot #3	Lamination(1)	Cathode Loading(2)	SiC Coating(3)	Percent Polyox(4)
CAS-001.	Non-H.T.	Wet Bond	Low	Thin	W
CAS-002.	900°C H.T.	Wet Bond	Low	Thin	ERC
CAS-003.	Non-H.T.	Wet Bond	High	Thin	ERC
CAS-004.	900°C H.T.	Wet Bond	High	Thin	W
CAS-005.	Non-H.T.	Dry Bond	Low	Thin	ERC
CAS-006.	900°C H.T.	Dry Bond	Low	Thin	W
CAS-007.	Non-H.T.	Dry Bond	High	Thin	W
CAS-008.	900°C H.T.	Dry Bond	High	Thin	ERC
CAS-009.	Non-H.T.	Wet Bond	Low	Thick	ERC
CAS-010.	900°C H.T.	Wet Bond	Low	Thick	W
CAS-011.	Non-H.T.	Wet Bond	High	Thick	W
CAS-012.	900°C H.T.	Wet Bond	High	Thick	ERC
CAS-013.	Non-H.T.	Dry Bond	Low	Thick	W
CAS-014.	900°C H.T.	Dry Bond	Low	Thick	ERC
CAS-015.	Non-H.T.	Dry Bond	High	Thick	ERC
CAS-016.	900°C H.T.	Dry Bond	High	Thick	W

NOTE

1. Per Process Specification
2. Anode loading constant $\sim$ 0.3 mg/cm^2, low cathode load $\leq$ 0.45, high is $\geq$ 0.55.
3. Average of electrode corners, thin $\leq$ 0.005 in., thick $\geq$ 0.01 in.
4. Controlled by source, (Westinghouse or ERC Polyox amount needed for reaching desired viscosity).

This facility, assembly, and testing comparison was accomplished by an exchange of similar subscale test cells between Westinghouse and ERC as defined below.

Test No.	Unit	Assembled	Tested
1	SC-052*	AESD	AESD/ERC
2	SC-053*	AESD	AESD/ERC
3	E-1	ERC	ERC/AESD
4	E-2	ERC	ERC/AESD
5	E-3	ERC	ERC
6	E-4	ERC	AESD

*These test units are sister units assembled and tested by Westinghouse in the earlier Bridging Tests

2.2.2.4 ELECTRODE CHARACTERIZATION TESTS - PRESSURIZED CONDITIONS:

The purpose of this test specification is to extend the subscale cell electrode characterization atmospheric test data matrix to include the effects of pressurized operation to establish the technology base for defining cell design parameters and operating constraints for full size cell stacks.

This pressurized subscale cell test is a designed experiment of two levels of pressure that dovetails the atmospheric pressure tests conducted in the subscale cell electrode tests. For this reason these tests have the same base for temperatures, current levels, and reactant utilization and are conducted with the same test plan, except at the prescribed pressure levels. The test plan sequence is shown in Table 2.2.2-7.

These tests will establish the change in key parameters and the operating characteristics of fuel cell performance with changes in operating pressure level. Specifically, this requires determination of the change in nominal cell measured (and IR free) voltage for the controlled variables.

TABLE 2.2.2-7

PRESSURIZED 2x2 SUBSCALE TEST PLAN SEQUENCE

Atmospheric Tests	Pressurize	Steady State Pressurized	Mapping Depressurize	Shutdown or Additional Optional Test(4)
< 150 Hrs	4 Hrs	300 Hrs	100 Hrs	TBD
• Repeatability(2) • Cell Resistance • OCV • Polarization • O_2 gain • H_2 gain	• Startup to part load (intermediate pressure) • Up to full rated conditions	• Polarization at 3, 30, 300 hours(3) • Conditions per Table 3	• 10 points per Table 4 • Polarization @ end of mapping	• Shutdown • Polarization • OCV • Operational Transients • Endurance • Start/stop Cycles • Development Options

Note: (1) All tests run with 83 percent H_2 utilization SRG (except 100 percent H_2 for H_2 gain)

(2) Verify measurements with installed cells and demonstrate repeatability within uncertainty required by parameter perturbation.

(3) Minimum of four points - H_2 utilization constant, oxidant at constant stoichs for 4 current levels.

(4) Shutdown or TBD options.

The test plan is identified in Table 2.2.2-8. Specific mapping conditions to provide a direct comparison of these data with stack testing for determining scaling effects are defined in Table 2.2.2-9.

NINE-CELL STACK TEST

A test specification for up to 32 nine-cell stacks was issued. The objectives of the nine-cell stack test plan as presented in Reference 1 are to demonstrate PAFC stack performance and determine the operating characteristics of the fuel cells in an in situ stack environment with the smallest logical stack size that would adequately determine individual cell data for:

- Baseline Technology - establish technology base for 12x17 nominal size cells in stack conditions to support larger stack and fuel cell design and performance predictions.
- Key Fuel Cell Parameter Characteristics - develop design and operational understanding of key parameters to support design and operation of fuel cell stacks in a system.
- Interaction Effects - determine relationships of key fuel cell parameters to provide an understanding of effects of their changes in combination on performance characteristics for design and operating guidance.
- Design constraints and operating constraints - establish the performance impact and sensitivities needed to guide design of operating envelopes and control of the PAFC system.

The pertinent test parameters and variables are summarized in Tables 2.2.2-10 and -11. The overall test plan was defined by engineered test designs. This plan permits introduction of additional design or component variables as development proceeds. Four stacks constitute a group to integrate such new variables into the program.

The test plan for the initial group of four stack tests is presented in Table 2.2.2-12.

The objectives of this first group of nine-cell stack tests are to:

TABLE 2.2.2-8

PRESSURIZED OPERATING CONDITION TESTS**

Test No.	Pressure (atm)	Current Density (mA/cm^2)	Temperature (°C)	Test Assembly Components
2	2.4	325	190	CPS-017 See Table
1	4.8	325	190	CPS-021 below for
2	2.4	200	190	CPS-022 Cathode
1	4.8	200	190	CPS-018 Anode
2	2.4	325	200	CPS-019 and
1	4.8	325	200	CPS-023 Matrix
2	2.4	200	200	CPS-024 Description
1	4.8	200	200	CPS-020

**Record data for 30, 300 and 300 hours at stipulated test conditions for reactant conditions of 2.5 stoichs air and 83 percent H_2 with SRG (75 percent H_2, 24 percent CO_2, 1 percent CO, mole percent) except as specified for polarization data (see Test Plan).

Test Unit	Cathode I.D.	Anode I.D.	Matrix I.D.(1)	Comments- Fab & Ass'y.
CPS-017	C136-1	A131-8	M042-7	Dry Bond, Non-H.T. Catalyst
CPS-018	C136-1	A131-8	M042-7	Dry Bond, Non-H.T. Catalyst
CPS-019	C136-1	A131-8	M042-7	Dry Bond, Non-H.T. Catalyst
CPS-020	C136-1	A131-8	M042-7	Dry Bond, Non-H.T. Catalyst
CPS-021	C134-5	A133-3	M042-7	Dry Bond, 900°C H.T. Catalyst
CPS-022	C134-5	A133-3	M042-7	Dry Bond, 900°C H.T. Catalyst
CPS-023	C134-5	A133-3	M042-7	Dry Bond, 900°C H.T. Catalyst
CPS-024	C134-5	A133-3	M042-7	Dry Bond, 900°C H.T. Catalyst

Notes: (1) If needed, a sister equivalent matrix sheet may be substituted.

TABLE 2.2.2-9

MAPPING POINTS FOR CELL TO STACK COMPARISON

Operating Points	Operating Conditions				
	Current Density (mA/cm^2)	Pressure Level (psia)	Temperature Level (°C)	Air* Stoichs	Time** (Hours)
1	325	70	190	2.0	3
2	150	40	170	4.0	3
3	400	40	170	4.0	1
4	150	100	200	4.0	3
5	400	100	200	4.0	1
6	400	40	200	4.0	3
7	150	40	200	4.0	1
8	150	14.7	170	4.0	3
9	400	14.7	170	4.0	1
10	325	70	190	2.0	3
11	325	70	190	4.0	1
12	325	100	190	4.0	1
13	325	40	190	4.0	1
14	325	14.7	190	4.0	1

*All points with 83 percent H_2 utilization with SRG.

**Establish stable operating conditions.

TABLE 2.2.2-10

PERTINENT PARAMETER DEFINITIONS

A. Principal Responses to Be Measured

During Operation:

- Voltages - cells and stack
- Power Output
- Trend Effects with Time

Post Operation:

- Corrosion
- Dimensional changes
- Physical Property changes
- Mechanical integrity of stack and components

B. Principal Variables To Be Controlled*

During Operation:

- Pressure Level
- Temperature Level - Cell (Mean)
- Temperature Levels - Reactants
- Current - (Load)
- Time Histories and Cycling profiles
- Fuel Composition (utilization)
- Flow Rates - (reactants and coolant)

* These are not necessarily the controlled parameters, (i.e., cell/stack temperature may be controlled by control of the air/coolant inlet temperature to meet exit temperature conditions desired.)

- Acid Condition (initial loading inventories, concentrations, or other variable concerns)
- Oxidant Concentrations (stoichs)
- CO Levels
- Reactants Pressure difference

C. Other Controlled Variables:

- Process/fabrication pedigrees
- Gas contaminants - process air & coolant
- Handling/Events (unintended loads, etc.)
- Fuel Composition (H_2O, CO_2, CO, etc.)

D. Variables to Characterize/Define by Nine Cell Stacks

1. Hardware Options	Levels
1. Fabrication Facility	2
2. Furnace Run (Batch)	2
3. Electrode "Alternates" (See Text)	2
4. Testing Loop	2

2. Assembly Options	Levels
1. Acid Loading	2
2. Clamping Pressure	1
3. Compression Cycle History	1

3. Operating Parameter Options	Levels
1. Current	3
2. Pressure	3
3. Temperature	3
4. O_2 Flow (Stoichs)	2
5. H_2 Flow (Stoichs)	2
6. Fuel Composition	2
7. Impurities (TBD)	2
8. Time and Cycles	3

C - 2

TABLE 2.2.2-11

MEASUREMENTS FOR STACK MECHANICS

	Test Objective	Measurable Variable	Values: Initial	Values: Final	Values: Oper. Cond.
1.	Establish dimensional characteristics and stability (creep)	• Dimensions	✓	✓	
		• Displacements			✓
		• Loadings	✓	✓	✓
		• Times			✓
2.	Establish sealing and seal characteristics/ performance	• Leakage rates	✓	✓	
		• Pressure levels	✓	✓	✓
		• Pressure differences	✓	✓	✓
		• Temperature			✓
		• Open circuit voltage	✓	✓	✓
		• Clamping loads	✓	✓	✓
		• Dimensions	✓	✓	
		• Times			✓
3.	Determine Thermally induced displacements and transient impacts	• Dimensions	✓	✓	
		• Displacements		✓	✓
		• Temperatures			✓
		• Loadings	✓	✓	✓
		• Times			✓
4.	Determine flow channel variances and characteristics	• Pressure level			✓
		• Pressure drops			✓
		• Displacements	✓	✓	
		• Dimensions	✓	✓	
5.	Establish design stresses	• Deflections	✓	✓	✓
		• Loads	✓	✓	✓

TABLE 2.2.2-12

TEST PLAN[1] - SEQUENCE

Atmospheric Tests	Startup Pressurize	Steady State Pressurized	Mapping Pressurized	Additional Optional Test[4]
< 50 Hrs	4 Hrs	300 Hrs	100 Hrs	TBD
• Repeatability[2] • OCV • Polarization H_2 300°F 4 ST., 80% H_2 50-200 mA/cm^2	• Expected operating line to 1/4 power point • Increase pressure to full power point	• Polarization at 3, 30, 300 hours[3] • Conditions 375°F 70 psia 2.5 ST., 80% H_2 325 mA/cm^2	• 22 points • Polarization @ end of mapping	• Shutdown • Polarization • OCV • Operational Transients • Electrical Transients • Endurance • Test Cell Exchange • Add mapping • Load Variation (Design) • Start/stop Sequence • Development Options

Noted: (1) All tests run with SRG

(2) Verify measurements and stack control repeatability within uncertainty required.

(3) Minimum of four points - H_2 utilization constant, oxidant flow rate held at steady state condition.

(4) TBD options, transients and continuing development - stacks beyond W-009-07 - will extend these options.

- Establish reference baseline performance of existing technology full-size fuel cells in a stack environment, and determine reproducibility obtained with existing process, fabrication, and assembly controls and specifications.

- Demonstrate stack operating characteristics over operating map and establish measurement repeatability.

- Provide performance "screening" information for heat treated catalyst, dry bonded electrodes, and seal material alternatives using "buffer" fuel cells Numbers 1, 2, 8, and 9 (outside of cooler plates containing five-cell unit stack).

The results of the nine-cell stack testing completed are presented in Section 3.2.5.

2.2.3 FUEL CELL MANUFACTURING PROCESS SPECIFICATIONS

The process specifications listed below for the manufacture of fuel cells were completed and approved by NASA-Lewis.

PS - 598047	Compression Molded Carbon Plates
PS - 598048	Electrode Catalyst Layer
PS - 598049	Electrode Support Layer
PS - 598050	Electrodes
PS - 598054	Electrolyte Matrix

The nine-cell Stack Subassembly Procedure (PAFC-006, Revision 1) and Assembly Procedure (PAFC-007, Revision 1) were completed and approved by NASA Lewis.

A five-cell stack (Number E005-001) was assembled and tested at ERC. The objective of this stack was to compare the Mat-1 layers fabricated at Westinghouse and ERC.

The construction features of this five-cell stack are as follows:

Anodes	:	10 percent Pt/C, 0.3 mg/cm^2 nominal loading, dry pressed
Cathodes	:	10 percent Pt/C, 0.5 mg/cm^2 nominal loading, dry pressed

Mat-1 layers	:	∿ 10 mils thick, cell numbers 2 and 5 supplied by Westinghouse
SiC	:	∿ 7 mils thick
Seals	:	Teflon shim stock
Electrolyte	:	100 - 101 percent 50cc/cell H_3PO_4
Compression	:	56 PSI

A summary of the testing is presented in Table 2.2.3-1. Initial performance at 1 atm. was relatively low (∿ 612 mV/cell at 95 mA/cm^2 and 175°C). Performance increased slowly until it reached 672 mV/cell at 95 mA/cm^2 and 300 hours. At this point the stack was pressurized. The stack was tested for over 100 hours at 5 atm. A polarization curve is presented in Figure 2.2.3-1. A summary of stack data is presented in Table 2.2.3-2. No performance difference was observed between the cells with ERC or Westinghouse Mat-1 layers. After ∿ 500 hours the testing was discontinued. Upon disassembly of the stack, Cell 2 cathode plate and backing paper were found corroded. Cathode plates and backing papers for the other cells were wet with acid.

TABLE 2.2.3-1

SUMMARY OF TESTING FOR STACK E-005-001

Total hours tested 521
Total hours tested at 5 atm. pressure 103

Start-up

Average OCV = 928 mV

Average Cell Voltage = 612 mV at ~95 mA/cm^2, 1 atm, 175°C.

5 hours — T.C.'s at fuel inlet overheating, cell performance low, fuel sensitive. Possible cause: air leaking into fuel.

20 hours — Reactant gases interchanged 4 times in 50 hrs (2 complete cycles) each time sulfur odor detected in H_2 exhaust.

Average cell voltage = 638 mV/cell at ~ 95 mA/cm^2, 1 atm 190°C. — 190 hours

Intermittent Fuel and Oxidant Starvation

Average OCV = 938 mV, 1 atm, 190°C.
Average cell voltage = 672 mV at ~ 95 mA/cm^2, 1 atm, 190°C.
Average cell resistance = 0.20 mΩ — 332 hours

Test Continuing

TABLE 2.2.3-1 (CONTINUED)

Average OCV = 876 mV, 1 atm., 150°C

333 hours — Pressurization and stabilization

Average OCV = 1020 mV, 5 atm., 150°C

336 hours — Endurance started 336 hours

Average Cell voltage = 778 mV at
~95 mA/cm^2, 5 atm., 190°C
80% fuel utilization
50% oxidant utilization
Average Cell Resistance = 0.17 mΩ
Maximum Cell Voltage = 785 mV
(Cell 5)
Minimum Cell Voltage = 771 mV
(Cells 1 and 2)

Average Cell voltage = 774 mV at
~95 mA/cm^2, 5 atm., 190°C

Maximum Cell Voltage = 785 mV
(Cell 5)
Minimum Cell Voltage = 745 mV
(Cell 2)

439 hours — Power failure caused system shutdown and depressurization

454 hours — System restarted

Average Cell Voltage = 608 mV at
~95 mA/cm^2, 1 atm., 190°C

Average Cell Resistance increased from 0.17 mΩ (5 atm.) to 0.52 mΩ (1 atm.), 150°C, no load

521 hours
Testing discontinued

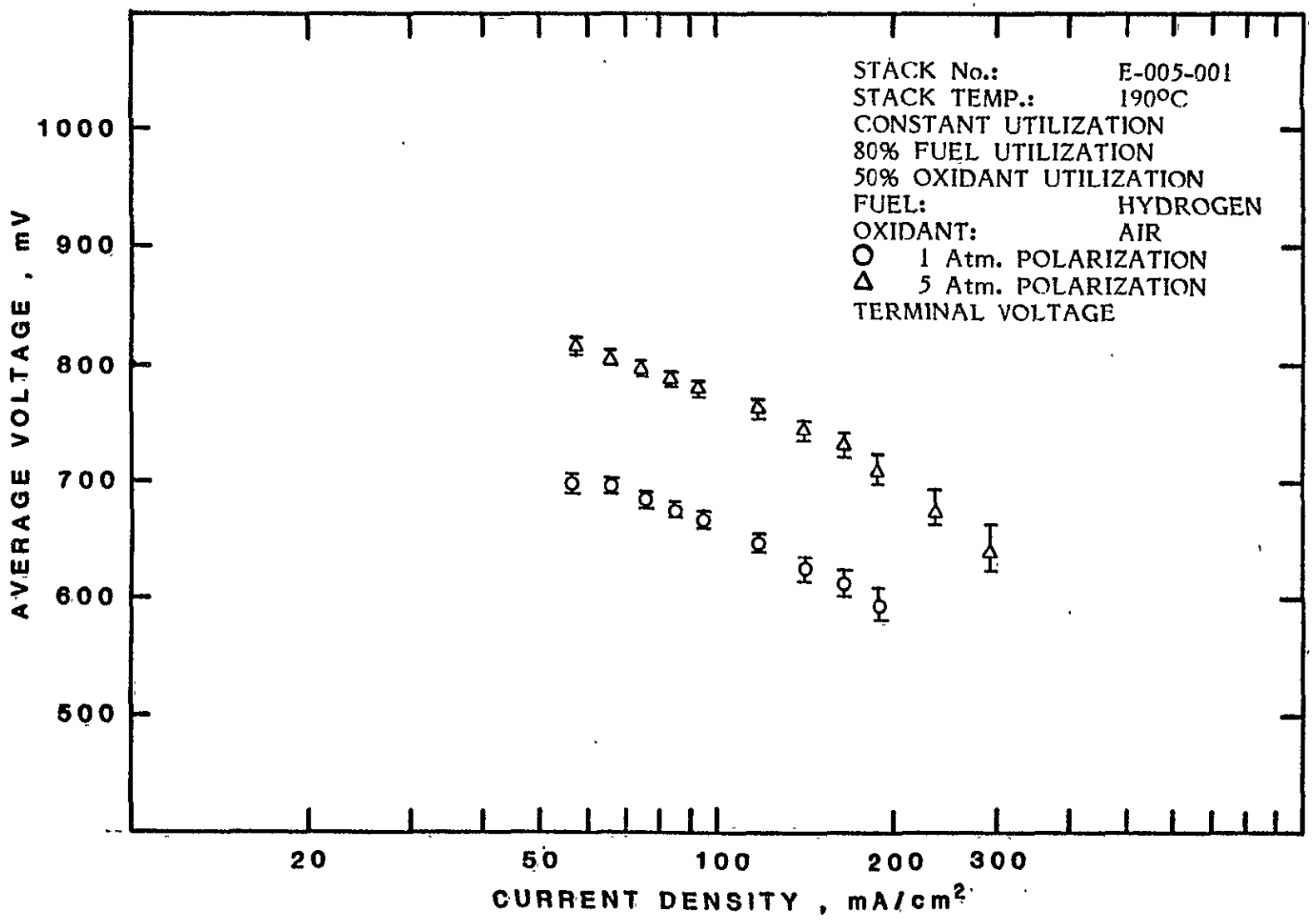

Figure 2.2.3-1. Polarization Curves for Five-Cell Stack E-005-001

TABLE 2.2.3-2

STACK E-005-001 PERFORMANCE DATA

CELL NO	1 ATM INITIAL 200 mA/cm²		1 ATM PREPRESSURE 200 mA/cm²		5 ATM PRESSURE 200 mA/cm²		CELL NO
	TERMINAL mV	IR FREE mV	TERMINAL mV	IR FREE mV	TERMINAL mV	IR FREE mV	
1	555	592	583	619	699	733	1
2	555	592	588	624	703	737	2
3	556	593	591	627	709	743	3
4	575	612	610	646	723	757	4
5	560	597	598	634	716	750	5
AVERAGE	560	597	594	629	710	744	AVERAGE
TOTAL	2800	2984	2970	3148	3550	3722	TOTAL

RESISTANCE: 1 ATM INITIAL - 0.91 mΩ
1 ATM PREPRESSURE- 0.89 mΩ
5 ATM PRESSURE - 0.86 mΩ

TEST CONDITIONS: 190°C - 80% FUEL UTIL 50% OXIDANT UTIL - HYDROGEN/FUEL & AIR/OXIDANT

2.3 SYSTEMS INTEGRATION

This section summarizes the conceptual designs developed for the FCS, FPS, PCS, and RES unit. The approach for defining and controlling system interfaces during subsequent design and fabrication periods is also described.

2.3.1 FUEL CELL SYSTEM (FCS) DESIGN

This section discusses the conceptual design developed for the FCS.

2.3.1.1 SYSTEM DESIGN DESCRIPTION

The FCS design is based on using the fuel cell module illustrated in Figure 2.3.1-1. The module consists of individual fuel cells arrayed in stacks and has a nominal electric output rating of 375 kW at the BOU. The FCS design is illustrated schematically in Figure 2.3.1-2. Twenty fuel cell modules are arranged in two groups of ten. Each group is supplied with cooling air and process air from the RES and hydrogen-rich fuel from the FPS. The air is distributed through manifolding to the individual modules. After removing heat from the fuel cell stacks, the cooling air is routed to a return manifold which conveys the cooling air to the steam generation system. Within each module a fraction of the cooling air is extracted to supply oxygen to the cathode side of the module.

The fuel cells consume approximately 83 percent of the supplied hydrogen and 50 percent of the supplied oxygen. The unused fuel and process air are exhausted from the modules through separate lines. The unused fuel is returned to the FPS and the cathode exhaust is directed to the RES for energy recovery. The fuel supply lines, fuel exhaust lines, and cathode exhaust lines to each module are provided with shut-off valves so that individual modules can be isolated.

2.3.1.2 SYSTEM PERFORMANCE CHARACTERISTICS

The FCS steady-state performance is a function of the system operating level, and the condition of the cells as each module ages. Table 2.3.1-1 presents fuel cell parameters over the normal operating range from BOU to EOU.

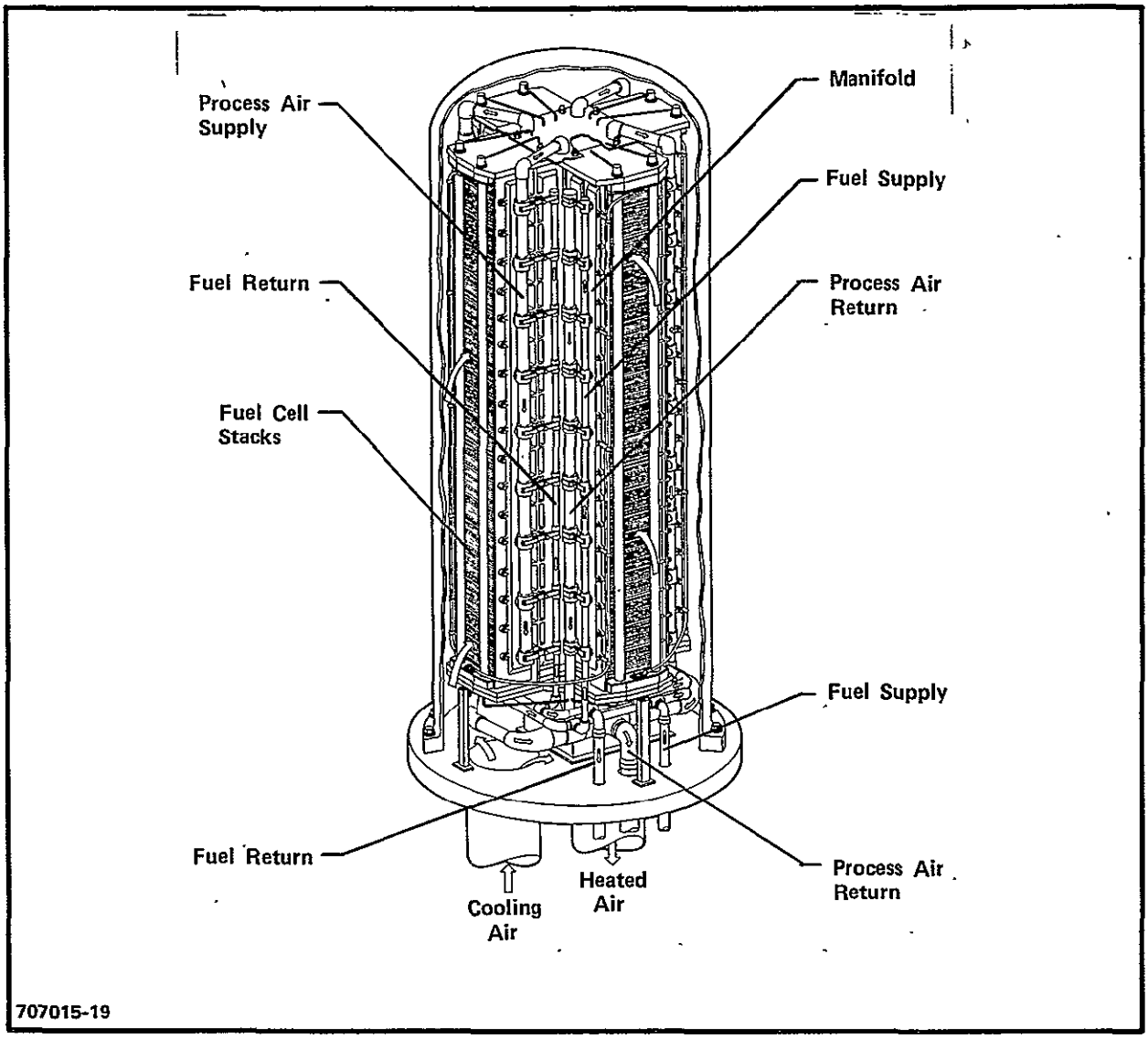

Figure 2.3.1-1. Fuel Cell Module Design

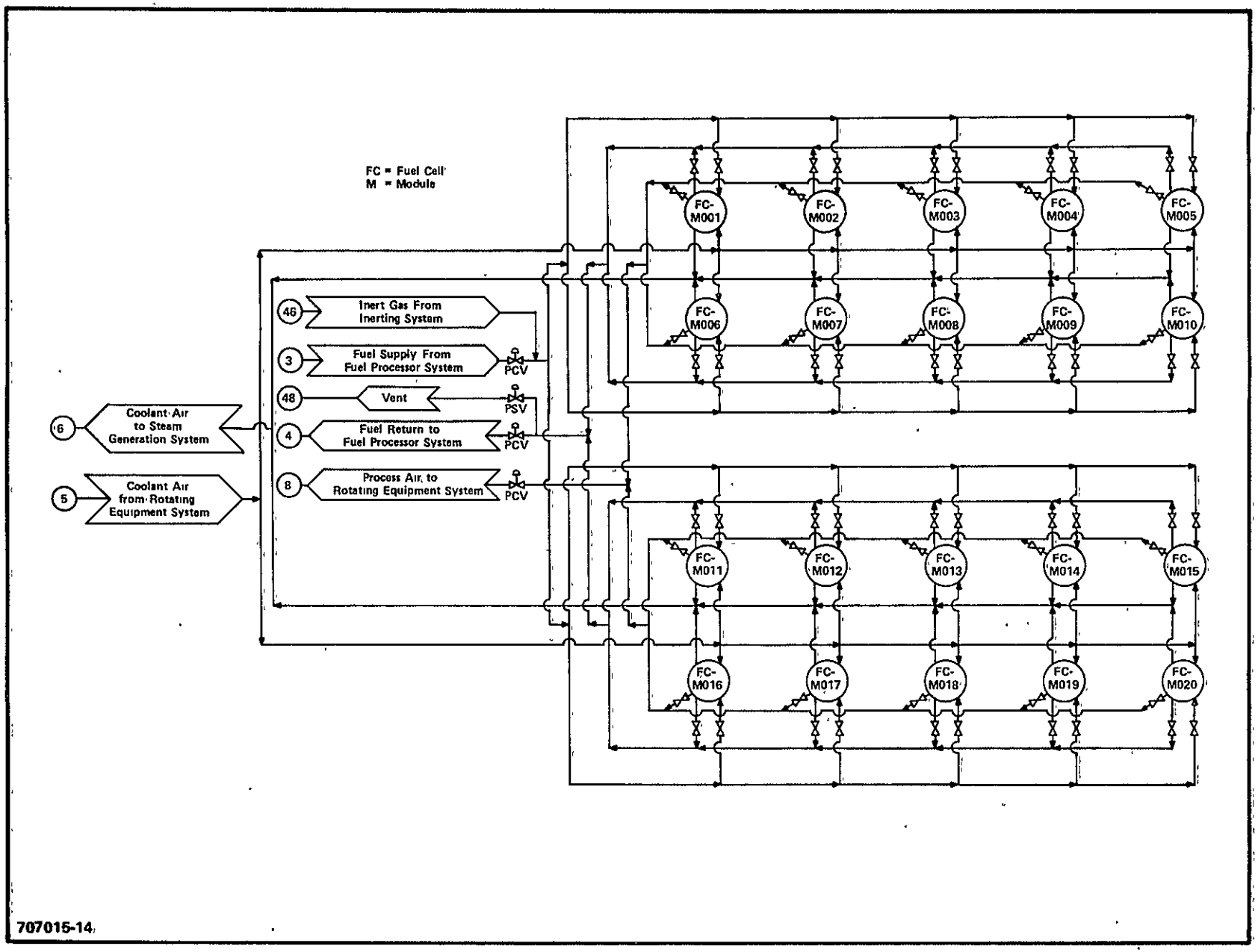

Figure 2.3.1-2. Fuel Cell System Flow Diagram

TABLE 2.3.1-1

FUEL CELL SYSTEM PERFORMANCE SUMMARY

		Beginning of Use		End of Use	
		Full Power	Minimum Power	Full Power	Minimum Power
Gross dc Power	(MW)	7.5	2.10	6.62	1.89
Terminal Voltage	(volts)	1070	1220	940	1090
Heat Rate*	kJ/hr (Btu/kWh)	7900 (7500)	7000 (6600)	9000 (8500)	7800 (7400)
Cooling Air Flow	kg/hr (lb/hr)	0.57×10^6 (1.26×10^6)	0.11×10^6 (0.25×10^6)	0.66×10^6 (1.46×10^6)	0.13×10^6 (0.29×10^6)
Fuel Flow	kg/hr (lb/hr)	3.65×10^3 (8.05×10^3)	0.90×10^3 (1.98×10^3)	3.65×10^3 (8.05×10^3)	0.90×10^6 (1.98×10^3)
Process Air Flow	kg/hr (lb/hr)	2.82×10^4 (6.22×10^4)	0.69×10^4 (1.53×10^4)	2.82×10^4 (6.22×10^4)	0.69×10^4 (1.53×10^4)
Operating Pressure	kPa (psia)	482 (70)	296 (43)	482 (70)	296 (43)
Operating Temperature	°C (°F)	190 (375)	190 (375)	190 (375)	190 (375)

*For FCS alone, based on higher heating value hydrogen utilized in the FCS.

The BOU values represent system performance with all modules operating at their rated operating level, while the EOU values assume that all modules in the system are operational but have fully degraded to the allowable limit. This limit is defined as an average terminal voltage of 0.60 volt per cell at a current density of 325 mA/cm^2, as compared with a BOU voltage of 0.68 volt at the same current density. The heat rate for the FCS decreases at part power because the terminal voltage and the efficiency of the fuel cell modules increases under reduced load.

For off design operation, with one failed fuel cell module isolated, each of the remaining nine modules on the same electrical bank of the system will be carrying about ten percent more current than those in the other bank. The cooling air flow through each of the nine remaining modules is essentially unchanged because the isolated cell still receives cooling flow. The result is that the modules in the nine module bank will be operating at about 3°C (5°F) hotter than the nominal average cell temperature, and those in the ten module bank will be operating at about 3°C (5°F) less than the average. Changes in fuel cell performance due to these temperature differences will tend to equalize the operating temperature somewhat.

For transient operation, the fuel cell operating temperature responds to perturbations with approximately a 15 minute time constant. Response times for other fuel cell system parameters are much faster. The terminal voltage response to electrical disturbances is essentially instantaneous. Responses to changes in fuel flow rate take place with a time constant of slightly under one minute.

2.3.1.3 SYSTEM ARRANGEMENT

The FCS is arranged in two groups of ten modules for the 7.5 MW plant. The conceptual design of one of the ten-module groups is shown in Figure 2.3.1-3. Ten fuel cell modules are supported in two rows of five modules on an elevated platform above the piping system.

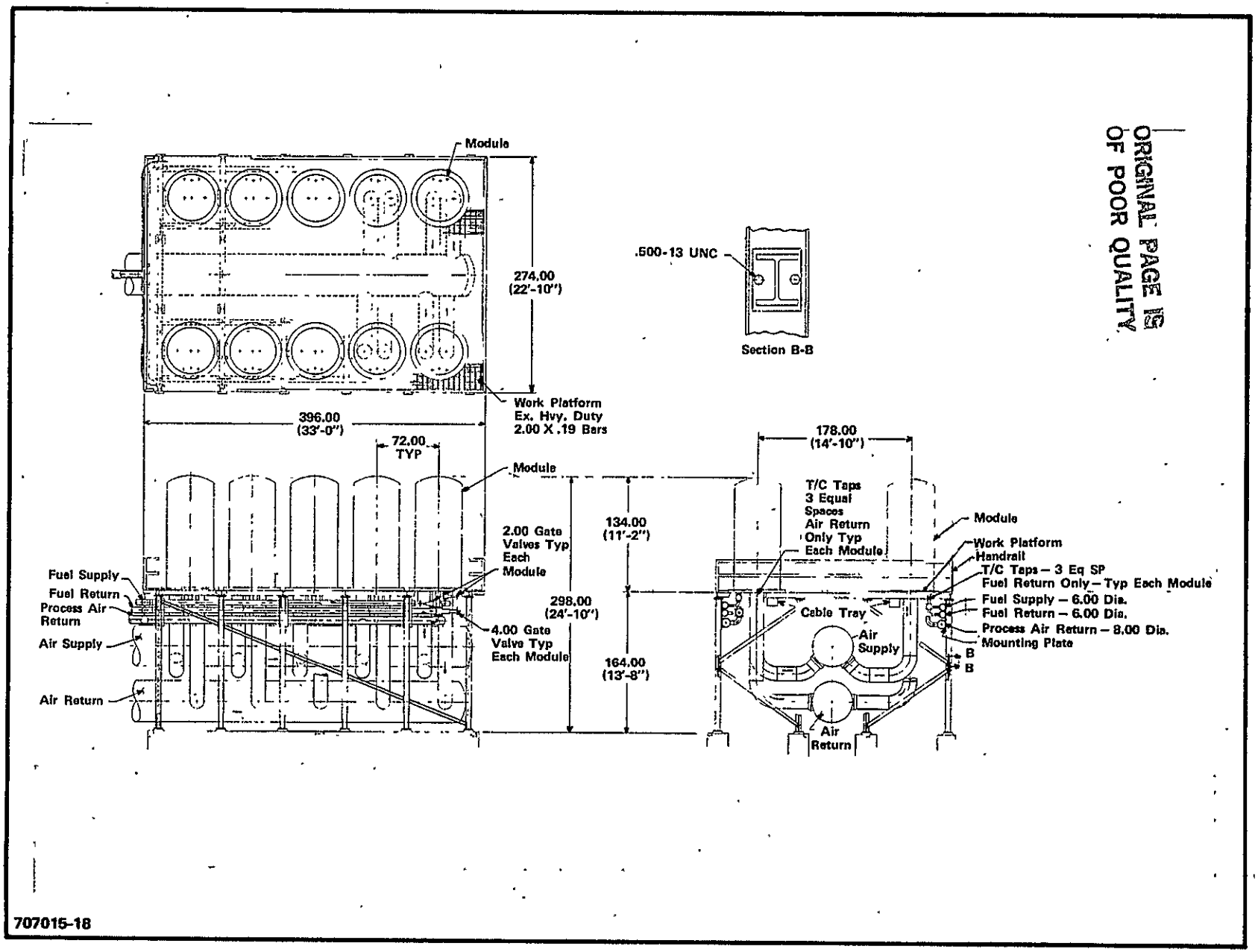

Figure 2.3.1-3. Fuel Cell System Conceptual Design

Cooling and process air are supplied through a 1.2m (4 ft) diameter manifold which traverses the length of the system, immediately below the platform and midway between the two rows of modules. Air is supplied to each module through a short 0.4m (16 inches) diameter branch pipe. The cooling air, after traversing the module internals, is returned through another 0.4m (16 inches) line to a 1.2m (4 ft) diameter air return manifold.

The fuel supply and return lines are 15 cm (6 inches) diameter and are supported in two rows immediately below the outermost edges of the mounting platform. The fuel lines and the 20 cm (8 inches) diameter process air return lines, which are similarly supported, are connected to penetrations at the module pressure vessel lower head, through short lengths of small diameter piping. This piping is 5 cm (2 inches) diameter, for the fuel supply and return, and 10 cm (4 inches) diameter for the process air return. The modules and their piping system and valves are thermally insulated to reduce heat losses to acceptable levels. Gate valves are provided in all the fuel and process air connections to the modules to enable any of the modules to be shut down independently of the system.

The symmetry of the piping arrangement provides for uniform distribution of fuel, and cooling and process air between the modules comprising the fuel cell system. The pipe sizes are selected so that the pressure drops through the fuel cell stacks dominate the flow resistances in the system, thus promoting equal flow distribution between modules as well as between the fuel cells within a module.

The overall height of the FCS is 8m (25 ft). The overall length and width of the ten-module assembly are approximately 10m and 7m (33 ft and 23 ft), respectively. The module support platform is approximately 4m (14 ft) above ground level.

Access is provided to the fuel cell modules from below for attention to electrical and piping connections, and acid replenishment systems. Access is also provided from the sides of each ten-module group and via an aisle between

the two five-module rows within each ten-module group to facilitate replacement of the fuel cell modules.

The physical location of the FCS ten-module groups in relation to the interfacing plant systems is suitably arranged so that thermal expansion effects in the large four foot diameter cooling air pipes can be accommodated by hinged bellows in the piping runs external to the FCS without overstressing the pipes in bending or exceeding limiting axial loads and moments at the fuel cell system interfaces.

Piping thermal expansion effects within the FCS ten-module group are accommodated by bending of the 40 cm (16 inches) diameter branch pipes thus eliminating the need for additional multiple-bellows systems. The feasibility of this approach was verified in a preliminary piping stress analysis performed to evaluate the bending stresses in the branch pipes resulting from thermal expansion of the piping system relative to the ambient temperature supporting structure. The piping configuration analyzed is illustrated in Figure 2.3.1-4. The finite element compute program WECAN (Reference 1) was used in the analysis.

The resultant bending stresses in the branch pipes are presented in Table 2.3.1-2 and were compared with the ANSI B31.1 Power Piping Code (1977) of Reference 2.

2.3.1.4 INSTRUMENTATION AND CONTROL

The overall approach to control of the FCS during plant operations is to individually control current from each fuel cell module. A single overall control is provided for each of these flows. Individual control of the performance of each module is provided by the PCS and the current of each

---

Reference 1. WECAN-Westinghouse Electric Computer Analysis, User's Manual, Westinghouse R&D Center, February 10, 1982.

Reference 2. ANSI B31.1 Power Piping Code, 1977 Edition.

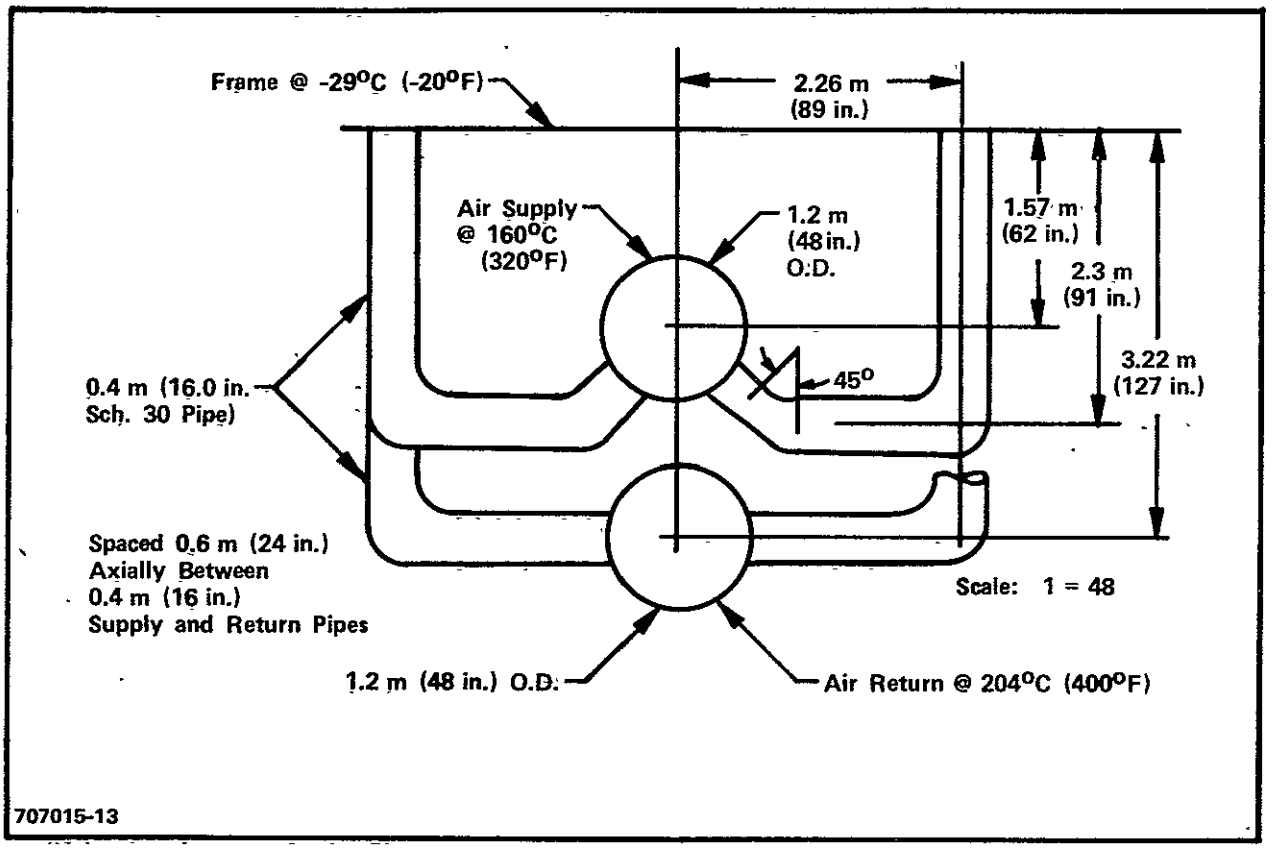

Figure 2.3.1-4. Piping Configuration for the Fuel Cell System 0.4m (16 in.) Cooling Air

TABLE 2.3.1-2

STRESS RESULTS FOR THE 0.4m (16 INCH SCHEDULE 30) AIR PIPES

Location	Return Loop Bending Thermal Stresses MPa (psi)	Supply Loop Bending Thermal Stresses MPa (psi)	Allowable Stresses from Ref. (2) MPa (psi)
At frame	146 (21,172)	161 (23,390)	163 (23,620)
90 Elbow	33 (4,783) 49 (7,111)	68 (9,914) 67 (9,733)	163 (23,630) 163 (23,630)
45 Elbow	--- ---	108 (15,602) 75 (10,896)	163 (23,630) 163 (23,630)
At Large Pipe	79. (11,452)	71 (10,285)	163 (23,630)

module is controlled to maintain its temperature equal to the average temperature for all operating modules in a given electrical bank. This electrical control provides the adjustment necessary to compensate for variations in flow characteristics between modules as well as for variations in electrical characteristics.

The controls for the fuel cell plant will follow the electrical power demand and provide cooling and process air, and fuel as required to match the electrical load. The controls which regulate the cooling and process air are not part of the FCS as such. These control functions are provided by the controls associated with the RES. Overall temperature control is obtained by varying the performance of the circulator, and thus the cooling air flow, in response to the mean temperature of the fuel cell modules. The net mass flow rate of air delivered by the compressor is regulated to be proportional to the total current being generated in the FCS. This is accomplished by varying the compressor speed and/or by adjusting the compressor bypass flow.

The SGS also influences the temperature control. Pressure control valves in the FPS and the RES maintain the saturation pressures in high and low pressure steam generators at the desired values. Control of these pressures, in turn, regulates the sink temperature for the cooling air.

The module operating pressure is regulated by controls directly associated with the FCS. The operating pressure for the FCS, as well as for the RES, is established by the pressure of the cooling air. The pressure drops in the cooling air channels and the cathode channels are small compared to the 483 kPa (70 psia) operating pressure in the system. Therefore, pressures measured at any point in this loop are representative of pressures anywhere on the air side of the system. A pressure control valve regulates the flow of process air to the RES expander and maintains the pressure in the process air return piping at the desired level. This valve and the compressor controls provide complete flow and pressure control for process air under normal operating conditions. For inerting the system, and for abnormal conditions when insufficient flow capacity is available through the expander, an auxiliary valve is provided

which vents the cooling air return ducts directly to the atmosphere. The setpoint for the pressure control loop is a function of the compressor speed.

A flow control valve is provided in the FCS to regulate the flow of fuel to the system. This flow is directly proportional to the current being drawn from the FCS. Pressure control of the fuel in the FCS is established by a pressure control valve between the fuel return manifold and the FPS. This valve operates to maintain a low pressure difference between the fuel return manifold and the process air return manifold under normal operating conditions. For abnormal conditions, or when the system is being purged, an additional valve is provided which vents the fuel return manifold directly to the atmosphere.

No control valves are provided to regulate fuel, cooling air, or process air flow to individual modules. In order to accommodate differences in flow and performance characteristics between individual modules, the inverter system provides for adjusting the current supplied by each module individually. The module current is controlled to maintain the operating temperature of each module equal to the mean temperature of all the modules in the appropriate electrical bank in the fuel cell system. In addition, the current controller maintains the total current equal to the current required to meet the load demand. The temperatures required for this function and to compute the mean temperature required for control of the cooling air circulator are measured at the fuel return manifold for each module. This is representative of the mean operating temperature of all the fuel cells comprising each fuel cell module.

Manually operated shutoff valves are provided on the fuel supply, fuel return, and process air return connections for each fuel cell module. These valves permit isolation of a malfunctioning module from the FCS, and also eliminate the flow of cathode air. With these valves closed, the remainder of the plant can remain operational with minimal impact on the overall plant performance, until a convenient time is found to replace the malfunctioning module.

2.3.2 FUEL PROCESSOR, POWER CONDITIONER, AND ROTATING EQUIPMENT SYSTEMS DESIGNS

This section discusses the conceptual designs developed for the FPS, PCS, and RES.

2.3.2.1 FUEL PROCESSING SYSTEM (FPS)

FUNCTIONAL REQUIREMENTS

The primary function of the FPS is to convert steam and hydrocarbon fuel to a hydrogen-rich gas for use in the fuel cells. Secondary functions of the FPS are: to remove impurities (carbon monoxide, etc) which are detrimental to fuel cell performance from the fuel stream, to remove water from the fuel stream, to provide process heat for steam generation, and to recover combustion gas waste heat to the maximum extent possible to enhance overall power plant efficiency.

The FPS consists of all the necessary equipment, controls, and instrumentation required to perform the functions defined above. Major equipment will include a fuel cleanup system to remove impurities detrimental to FPS and fuel cell performance, a steam reformer to convert the hydrocarbon fuels into CO, CO_2 and H_2, shift converters to convert water and CO into additional H_2 and CO_2, and rotating machinery to deliver compressed air and recover waste stream energy.

Combustion processes to supply heat to the steam reformer will be part of the FPS and will be capable of burning fuel cell anode exhaust gas as the primary fuel. Natural gas or naphtha will be used to supplement this primary fuel as required for stable control of the combustion process. Pressurized combustion is used to increase overall power plant efficiency, by minimizing gas pressure losses, reducing equipment sizes, and permitting the generation of electric power from the furnace exhaust gases. The FPS will be equipped with a turbo-compressor that provides compressed air for combustion. The pressurized furnace exhaust gas will be used to superheat steam and preheat the combustion air before being expanded through a gas turbine to drive the compressor and to generate electric power. Process gas heat exchangers will be used to increase

power plant efficiency. Water for process gas cooling will be supplied to the FPS from the SGS. Air cooling will be used to remove from the product stream before delivery to the FCS.

SYSTEM DESCRIPTION

The FPS flow schematic is shown in Figure 2.3.2-1. The process flow starts at the fuel inlet from the fuel handling system. Pressurized natural gas or naphtha at ambient temperature is heated to 371°C (700°F) by recovering energy from the high temperature shift product stream. In the case of naphtha, preheating consists of vaporization, followed by superheating. The natural gas and naphtha preheating units are arranged in parallel and valves are used to select the desired fuel. The feed stream is then desulfurized by absorption on hot zinc oxide. For naphtha, the feed gas is hydrogenated ahead of the ZnO beds in a hydrodesulfurization reactor using a small product recycle stream to provide the hydrogen. After desulfurization, approximately six percent of the feed gas is taken off for auxiliary furnace firing. The remaining feed gas is mixed with superheated steam and preheated by the reformer product gas to 427°C (800°F). The mixed feed is converted in a catalytic steam reformer to a mixture of H_2, CO and CO_2, plus unreacted CH_4 and H_2O. The reformer is a recuperative tube-in-tube design that recovers approximately 20 percent of the reformer energy directly from the reformer product gases, thus reducing furnace firing requirements. The reformed gases exit the reformer at approximately 593°C (1100°F) and are recuperatively cooled by process preheaters to 382°C (720°F). The gases then enter an adiabatic high temperature shift (HTS) converter where the temperature is raised to 449°C (875°F) and approximately 60 percent of the CO is converted to CO_2. The HTS product is cooled by the feed preheaters and then used to produce approximately 0.26 kg/s (2100 lbs/hr) of low pressure steam. The process gas at 206°C (402°F) then enters a low temperature shift (LTS) converter where the temperature rises to 253°C (487°F) and most of the remaining CO is reacted. The LTS product is used to raise steam and then is cooled by a recuperative heat exchanger and a direct contact condenser. The dried product gas containing 74.2 percent H_2 is reheated to 191°C (376°F) and sent to the fuel cell anode. For operation with naphtha, five percent of the dry fuel gas is recycled to the hydrodesulfurization reactor.

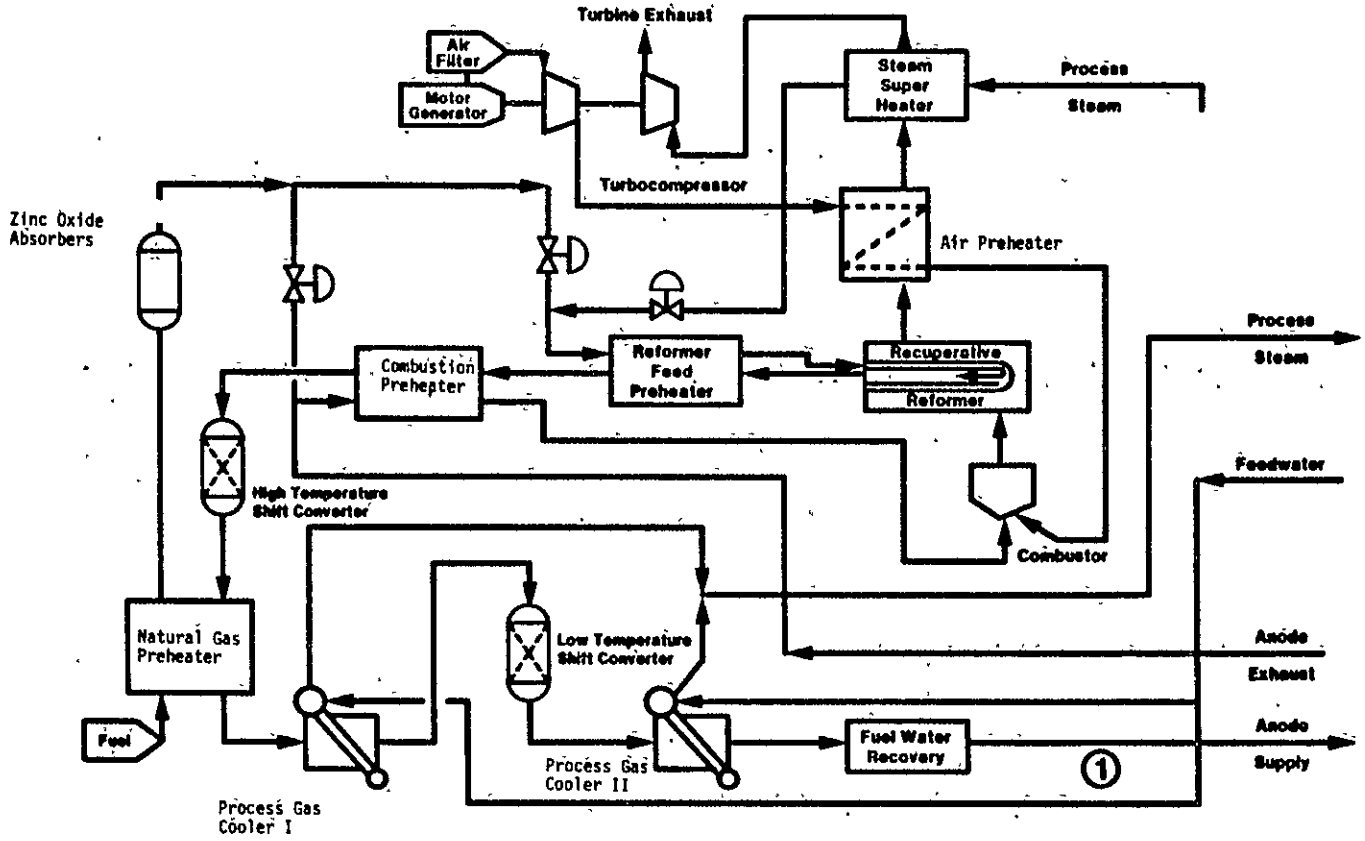

Figure 2.3.2-1. Fuel Processing System (FPS) Flow Schematic (Natural Gas Feed)

On the combustion side of the process, ambient air is pressurized to 469 kPa (68 psia) and preheated to 400°C (750°F). The preheated air is then burned with heated anode exhaust gas and the auxiliary feed gas. Combustion takes place in a pressurized, fluidized bed combustor operating at 900°C (1650°F). The combustion gases leave the fluidized bed and pass through a convective reformer section where they are cooled to 655°C (1210°F). The gases are then further cooled by the air preheater and steam superheater, finally entering an expansion turbine at 505°C (941°F).

Steam for the reforming process is provided by the steam generation system (SGS). Saturated steam at 710 kPa (103 psia) and 166°C (330°F) is superheated to 266°C (511°F) by the combustion exhaust gases and is mixed with the desulfurized feed gas. At the lower temperature end of the system, process gas is used to generate low pressure steam from SGS feedwater. The low pressure steam is returned to the SGS.

Major FPS equipment are listed in Table 2.3.2-1. The FPS is arranged in an area of approximately 16.0 m (52 ft) by 14.3 m (47 ft) as shown in Figure 2.3.2-2. Equipment and piping runs are arranged to provide space for inspection and maintenance. All pipe runs will be located at sufficient height to facilitate movement around the process units. The largest FPS component is the reformer vessel, which occupies a space of approximately 5.3 m (17 ft) in diameter and is 8.8 m (29 ft) high. The anode condensate recovery system and turbine exhaust water recovery system will be located adjacent to the FPS.

SYSTEM PERFORMANCE

Gross hydrogen production is 1.53 Normal m^3/s (4.93 x 10^6 SCFD). Approximately 83 percent of the hydrogen is consumed in the fuel cells and the remainder is returned to the FPS. Net hydrogen consumed is 1.27 Normal m^3/s (4.09 x 10^6 SCFD). Natural gas feed is 0.348 kg/s (2760 lbs/hr). The FPS efficiency, based on the higher heating value of the natural gas and the net hydrogen, is 92 percent. This efficiency does not include the effect of import steam, export steam, or the energy contained in the hot, pressurized combustion gas exhaust.

TABLE 2.3.2-1

FUEL PROCESSING SYTEM (FPS) MAJOR EQUIPMENT

Zinc Oxide Absorbers
Hydrodesulfurization Reactor
Steam Reformer/Reformer Furnace
High Temperature Shift Reactor
Low Temperature Shift Reactor
Turbo Compressor with Motor/Generator
Recycle Gas Compressor
Anode Condensate Recovery System (including air coolers)
Air Preheater
Combustion Preheater
Steam Superheater
Reformer Feed Preheater
Natural Gas Preheater
Naphtha Vaporizer/Superheater
Process Gas Cooler I (Steam Generator)
Process Gas Cooler II (Steam Generator)
Initial Catalyst Charges
Process Piping, Valves and Fittings
FPS Control System and Local Control Station
Flare Gas System

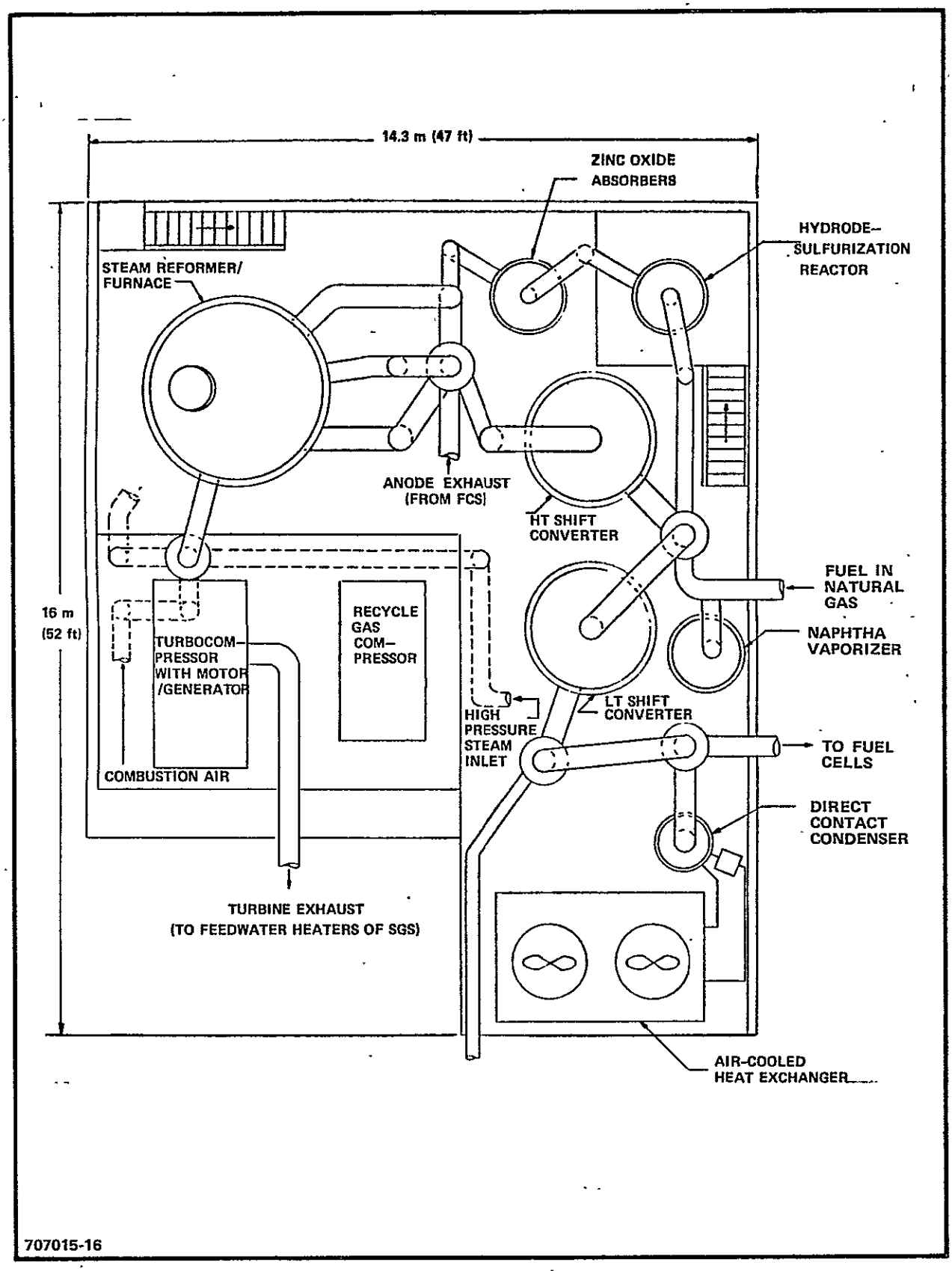

Figure 2.3.2-2. Fuel Processing System (FPS) Layout

Gross and net hydrogen production using naphtha feedstock are maintained constant at 1.53 normal m^3/s (4.93 x 10^6 SCFD) and 1.27 normal m^3/s (4.09 x 10^6 SCFD), respectively. The naphtha feedrate is 0.36 kg/sec (2890 lbs/hr). The FPS efficiency is 96 percent. It should be noted that the higher FPS efficiency using naphtha is partially offset by recycle compressor power requirements and increased steam demands. Overall power plant efficiency using naphtha will be less than when operating on natural gas.

2.3.2.2 POWER CONDITIONING SYSTEM (PCS)

FUNCTIONAL REQUIREMENTS

The conceptual design of the Power Conditioning System is based on the application of state-of-the-art, current sourced, line commutated converter and digital control technologies. The system design combines a second generation, redesigned version of the successful inverter system delivered to the Component Development and Integration Facility (CDIF) in Butte, Montana by Westinghouse. The inverter system is supplemented by newly developed circuitry to consolidate or combine the currents from a number of fuel cell modules. Figure 2.3.2-3 illustrates the relationships between the major system components, the fuel cell modules and the Utility Station Equipment.

SYSTEM DESCRIPTION

FUEL CELL MODULE INTERCONNECTIONS

Twenty fuel cell modules will furnish dc input power to the PCS. These twenty power sources are connected in various series/parallel arrangements to deliver the power at the required voltage and current. A fuel cell module will have a nominal rating of 375 kW and will deliver 351 amperes at 1068 volts.

The twenty modules are divided into two groups of ten. Each group is then arranged in five parallel pairs and connected to one of two inverter inputs. The resulting nominal input to each 3.75 MW inverter will then be:

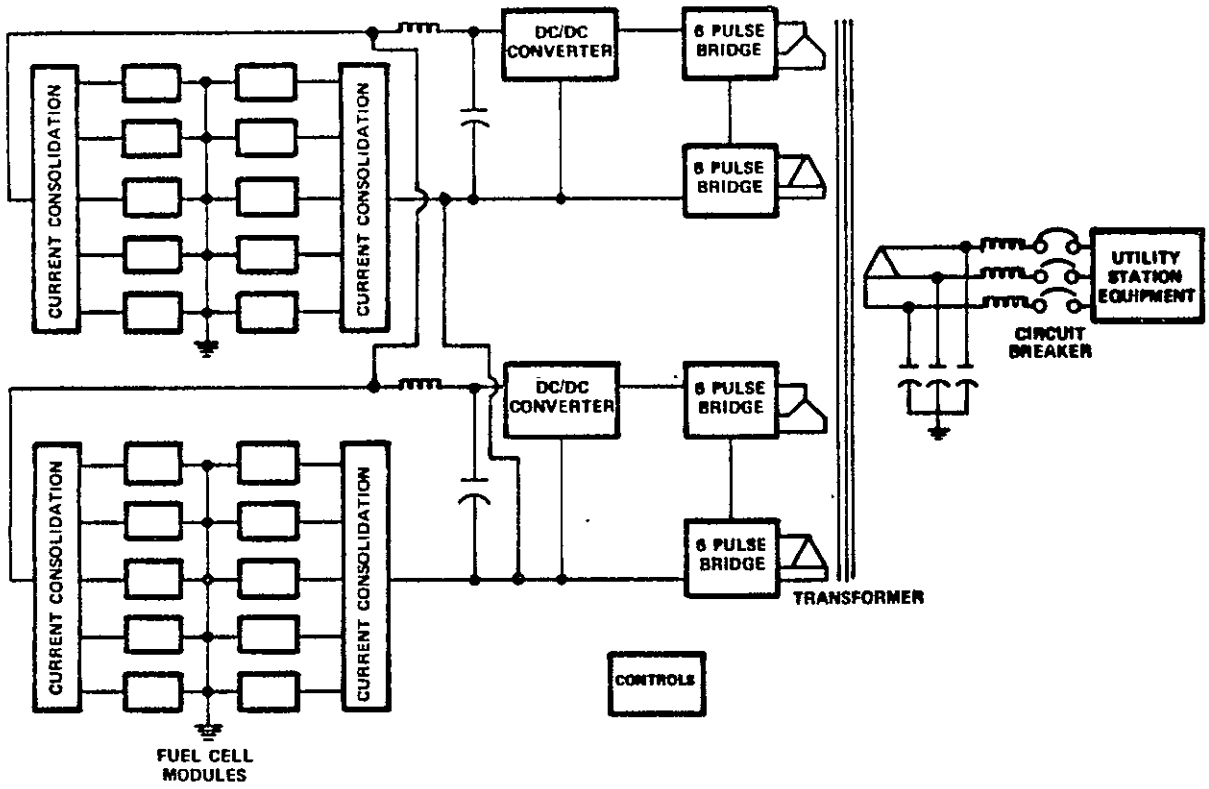

Figure 2.3.2-3. 7.5 MW PAFC Power Plant Power Conditioning System (PCS)

Beginning of Use	Full Power	25% Power
Current (amps)	1755	400
Voltage (volts)	2136	2376
Power (kW)	3750	950

End of Use	Full Power	25% Power
Current (amps)	1755	400
Voltage (volts)	1884	2100
Power (kW)	3330	850

It should be noted that these are nominal values assuming that all modules are matched initially, are of the same age, and degrade with age at the same rate. From a practical standpoint this will not be true. The system design therefore includes consolidation circuitry to compensate for voltage mismatches between modules covering the full spread of possible conditions.

Plant power output is specified between 1700 kW and 7500 kW, but the PCS will be capable of accepting dc power from the fuel cell modules and converting it to ac power at any module power output. The dc input voltage ratio over which an inverter must operate is normally an important inverter design consideration, but is of little concern with the present design. For this application, it has been specified that inversion will take place whenever the modules can deliver current and maintain their terminal voltage at 400V dc or above. This will result in a dc voltage ratio requirement of about three for the inverter system.

CURRENT CONSOLIDATION

The preferred operating mode for the fuel cell modules is to have each module deliver an equal current to its inverter. The currents will be programmed to vary slightly to compensate for differences in module cooling capabilities resulting from tolerances on manufacturing and non uniform aging effects. Manufacturing tolerances and module aging effects will also result in different module terminal voltages for the same module currents. If pairs of modules

were simply connected in parallel as shown in Figure 2.3.2-3, the module terminal voltage mismatches would result in interactions between the modules and in some modules delivering less power than desired. To alleviate this situation, a "current consolidation" design was established to change the module outputs before summing the currents at a common voltage.

Current consolidation, in general, is accomplished as follows. Each of the modules will have a terminal voltage of $V \pm \Delta V$ where V is the average of all terminal voltages and the ΔVs are deviations above or below the average. Adjusting a module's terminal voltage to V at the current summing point requires a device which can add or subtract voltage from a module's terminal voltage without changing the value of the current flowing. To meet such a requirement, increments of power will be transferred between module output current paths.

This transfer is made to a common power point which can act as either a source or a sink depending on the direction of power flow by "differential converters."

Fortunately, current sourced, line commutated circuits meet the requirements for differential converters. Switching devices are gated on in an alternating, timed sequence by low power control circuitry and are gated off naturally by ac from the common transformer. This is a single phase configuration and will result in a 120 Hertz ripple. The required power interchange will take place by electromagnetic coupling in the common transformer and the only power drawn from the ac line will be reactive power and a relatively small amount of real power to make up for any circuit losses. The switch firing times will be adjusted so that the converter either rectifies, and thus adds voltage to the module voltage, or inverts, and thus subtracts voltage from the module voltage while maintaining current flow at the desired level. This will result in equal voltage relative to the fuel cell module common at each of the transformer winding center taps (the current summing point in the circuits).

2.3.2.3 ROTATING EQUIPMENT SYSTEM (RES)

FUNCTIONAL REQUIREMENTS

The primary function of the RES is to provide a supply of clean, pressurized air to the FCS to replace air consumed on the cathode side of the fuel cells. The RES receives steam from the SGS and oxygen depleted cathode exhaust air from the FCS. The energy in this stream is converted into mechanical shaft power to drive circulating and compressing equipment. One of the key RES design objectives is to help minimize the overall power plant heat rate.

SYSTEM DESCRIPTION

The RES consists of a steam turbine, gas turbine expander, two stage centrifugal air compressor, air circulator, and a variable speed electric motor. The rotating machinery equipment is skid mounted, modular, and packaged as a single unit. A process flow schematic for the RES is shown in Figure 2.3.2-4. Key statepoints are summarized in Table 2.3.2-2.

The steam turbine uses low pressure steam from the SGS to produce mechanical shaft power to help drive the circulator and compressor. Steam exiting the steam turbine is sent to an air cooled condensor in the SCS.

The gas expander receives cathode exhaust gas from the FCS. The cathode exhaust gas entering the expander consists of approximately 76 percent nitrogen, 11 percent oxygen, and 13 percent water. This gas is expanded from 483 kPa (70 psia) to 110 kPa (16 psia) to provide power for driving the compressors and circulators. The gas stream after exiting the expander is routed to a WRS. Separation of water from the cathode exhaust stream after the expansion provides approximately 25 percent more power from the expander than can be achieved if water were removed prior to expansion.

The circulator returns the cooling air to the FCS at absolute pressures ranging from 289 kPa (42 psia) up to 490 kPa (71 psia) over the operating range. The pressure rise across the circulator is approximately 6.9 kPa (1 psia) at full power at a recirculating air temperature of 146°C (295°F).

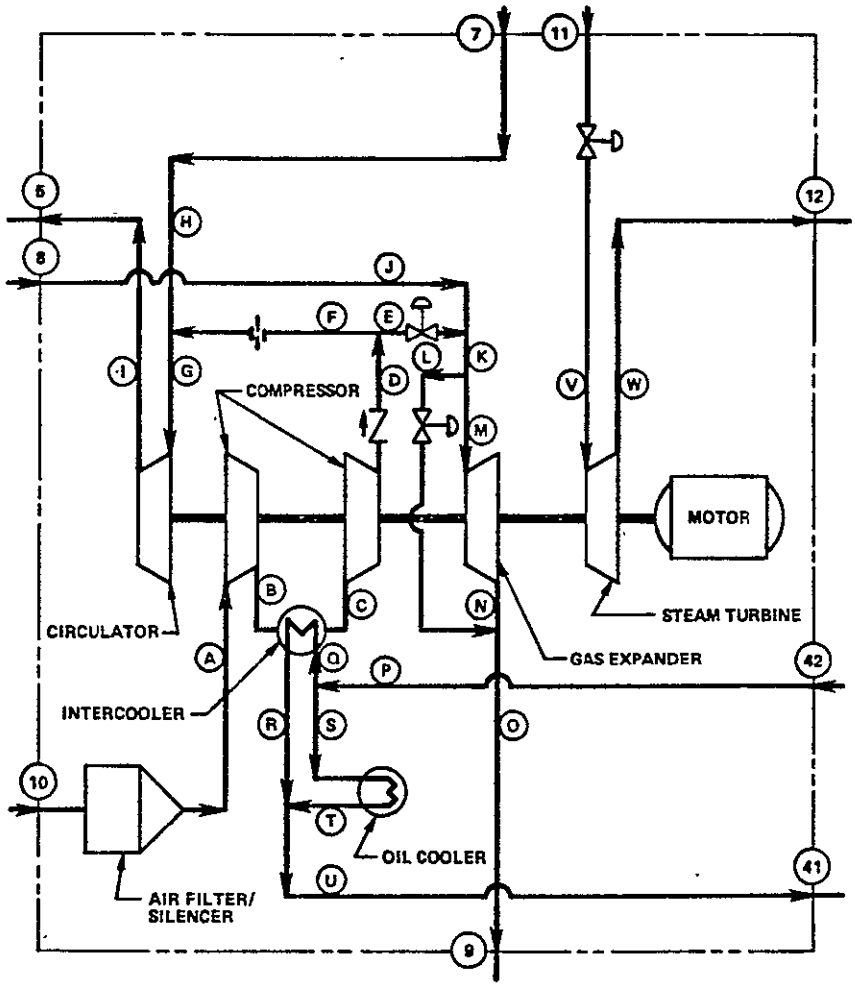

Figure 2.3.2-4. Rotating Equipment System (RES) Flow Schematic

Table 2.3.2-2
ROTATING EQUIPMENT SYSTEM (RES) OPERATING REQUIREMENTS

	Full Power	Part Power
• Air Circulator		
Flow, kg/hr (lb/hr)	662,840 (1,460,000)	115,089 (253,500)
Inlet Pressure, kPa (psia)	482 (70)	296 (43)
Inlet Temperature, °C (°F)	145 (293)	149 (300)
Outlet Pressure, kPa (psia)	489 (71)	296 (43)
Outlet Temperature, °C (°F)	147 (296)	149 (300)
Fluid	Air	Air
• Centrifugal Compressor* (Two Stages)		
Flow, kg/hr (lb/hr)	28,239 (62,200)	18,160 (40,000)
Inlet Pressure, kPa (psia)	101.3 (14.7)	101.3 (14.7)
Inlet Temperature, °C (°F)	26 (80)	26 (80)
Outlet Pressure, kPa (psia)	482 (70)	296 (43)
Outlet Temperature, °C (°F)	143 (291)	114 (237)
Fluid	Air	Air
• Steam Turbine		
Flow, kg/hr (lb/hr)	8,808 (19,400)	1,226 (2,700)
Inlet Pressure, kPa (psia)	365 (53)	365 (53)
Inlet Temperature, °C (°F)	140 (284)	140 (284)
Outlet Pressure, kPa (psia)	21 (3)	21 (3)
Outlet Temperature, °C (°F)	61 (141)	61 (141)
Fluid	Steam	Steam
• Gas Expander**		
Flow, kg/hr (lb/hr)	28,466 (62,700)	18,205 (40,100)
Inlet Pressure, kPa (psia)	475 (69)	289 (42)
Inlet Temperature, °C (°F)	192 (378)	144 (292)
Outlet Pressure, kPa (psia)	110 (16)	110 (16)
Outlet Temperature, °C (°F)	73 (163)	64 (148)
Fluid	Air (O_2 depleted)	Air (O_2 depleted)

*Bypass flow of 11,214 kg/hr (24,700 lb/hr) to the gas expander is required for part power operation to prevent surge.

A two stage centrifugal air compressor is used to replenish the cathode process gas used as the oxidant in the fuel cell system. The air is filtered to remove particulates greater than three microns prior to compression and pressurized to the system operating pressure. A line is added from the compressor outlet head so that excess pressurized flow at low power operation can be sent to the gas expander where some of the compression energy is recovered. This bypass air flow is required to prevent surging of the compressor at low flow rates.

An electric motor is also provided to meet the total RES power requirements. The design incorporates a variable speed (frequency controlled) 400 HP motor.

SYSTEM PERFORMANCE CHARACTERISTICS

Bypass flow from the compressor outlet is required at low power operations to prevent compressor surging to recover some of the compressed air energy. At 25 percent power, for example, the output flow from the compressor is approximately 2.5 times greater than that required for makeup air. Most of this excess compressed air goes to the gas expander. At full power operation a better match with the compressor characteristics is achieved and no compressed air is bypassed. The RES operates at peak efficiency at full power with the compressor arrangement. Efficiency decreases at part power because of the excess air compressed and because the gas expander and compressor are operating at lower efficiencies.

Table 2.3.2-3 gives the power requirements for the RES design for full and part power at BOU and EOU conditions. The BOU part power case requires the most power from the electric motor 169 kW (227 HP).

SYSTEM OPERATION

The RES is designed to operate as a single unit coupled to a common gear arrangement. During plant startup, the compressor and the circulator are driven by the electric motor. When the plant is operating at normal conditions, the steam turbine and gas expander contribute to the driving power requirements.

TABLE 2.3.2-3

ROTATING EQUIPMENT SYSTEM (RES) POWER REQUIREMENTS

	Full Power		Part Power	
	BOU	EOU	BOU	EOU
Steam Turbine (kW)	592	705	52	77
Gas Expander (kW)	1090	1088	442	482
Air Compressors (kW) (two stages)	-1500	-1500	-659	-659
Air Circulator (kW)	-228	-351	-4	-5
Motor Power Required (kW)	46	58	169	105

The operating characteristics of the RES are such that the compressor must follow an anti-surge protection line. Safety margin exists between the protection line and the actual surge line. As plant power is reduced it becomes necessary to bypass excess compressed air not required for fuel cell cathode supply. A compressor by pass valve opens automatically and the excess air is introduced to the expander inlet to recover energy. Figure 2.3.2-5 shows an operating map indicating the surging limits and anti-surge protection line. At part power operation, the compressor can only reduce air flow to 18,160 kg/hr (40,000 lb/hr) at 296 kPa (43 psia) without surging. The amount of makeup air required for the FCS cathode supply at this power rating is only 6,951 kg/hr (15,310 lb/hr). Because the minimum compressor outlet flow at 25 percent power is 18,160 kg/hr (40,000 lb/hr), it is necessary to bypass 11,209 kg/hr (24,690 lb/hr) of compressed air to the expander. The expander will recover some of the energy expended to compress this excess air.

SYSTEM ARRANGEMENT

A compact arrangement of the RES is illustrated in Figures 2.3.2-6 and 2.3.2-7. The area occupied by the RES is 91.5 m (300 ft^2) and the system weighs 25 tons. Overall RES height and width are 3.8 m and 2.8 m (12.5 ft and 9.1 ft), respectively. The equipment is designed for truck transportation to the plant site. However, special shipment permits are needed because height and width exceed normal shipping constraints.

2.3.3 SYSTEM INTERFACE REQUIREMENTS AND CONTROL

The objectives of this task were to define preliminary system interface requirements and to develop a methodology for the documentation and control of the system interfaces.

A hierarchy of requirements documents and interface control documents were developed to define the methods of documenting and controlling interfaces between systems. These interface controlling documents and their relationships are illustrated in Figure 2.3.3-1. The overall plant level requirements are defined in a plant requirements specification with reference to the process

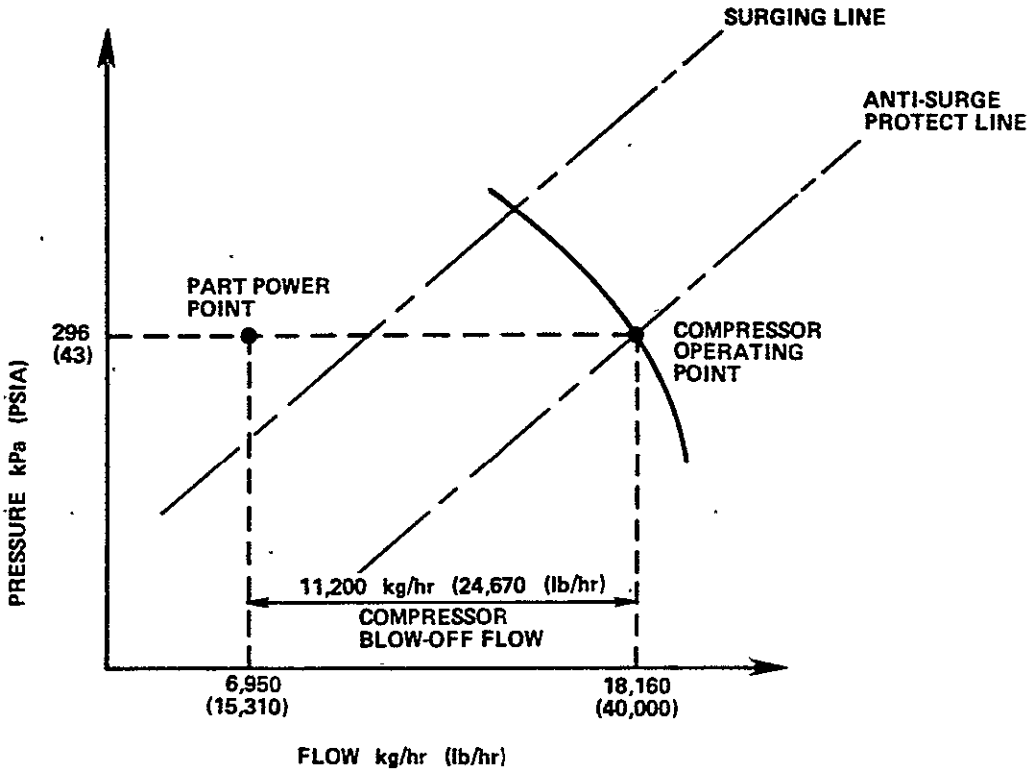

Figure 2.3.2-5. Operating Map of Rotating Equipment System Showing Compressor Surge Limits

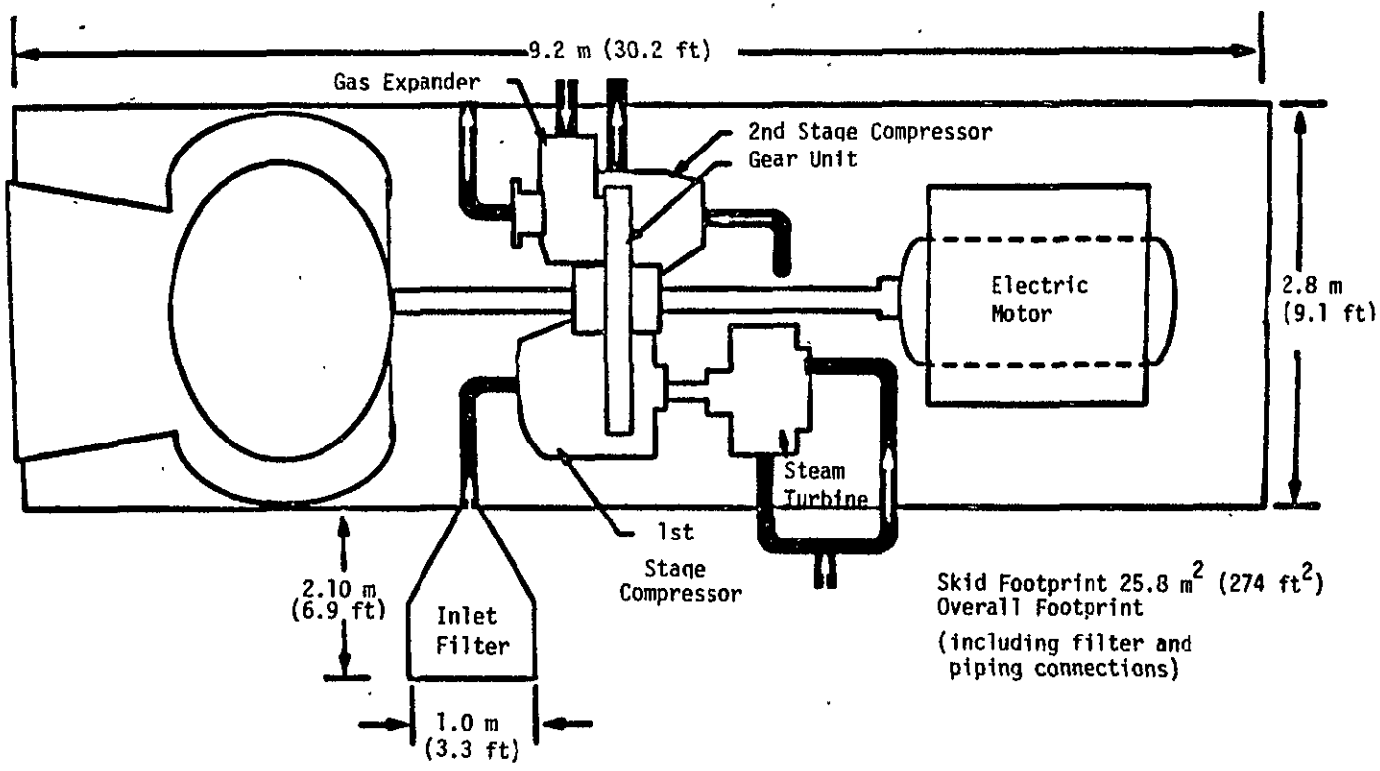

Figure 2.3.2-6. Rotating Equipment System Arrangement (Top View)

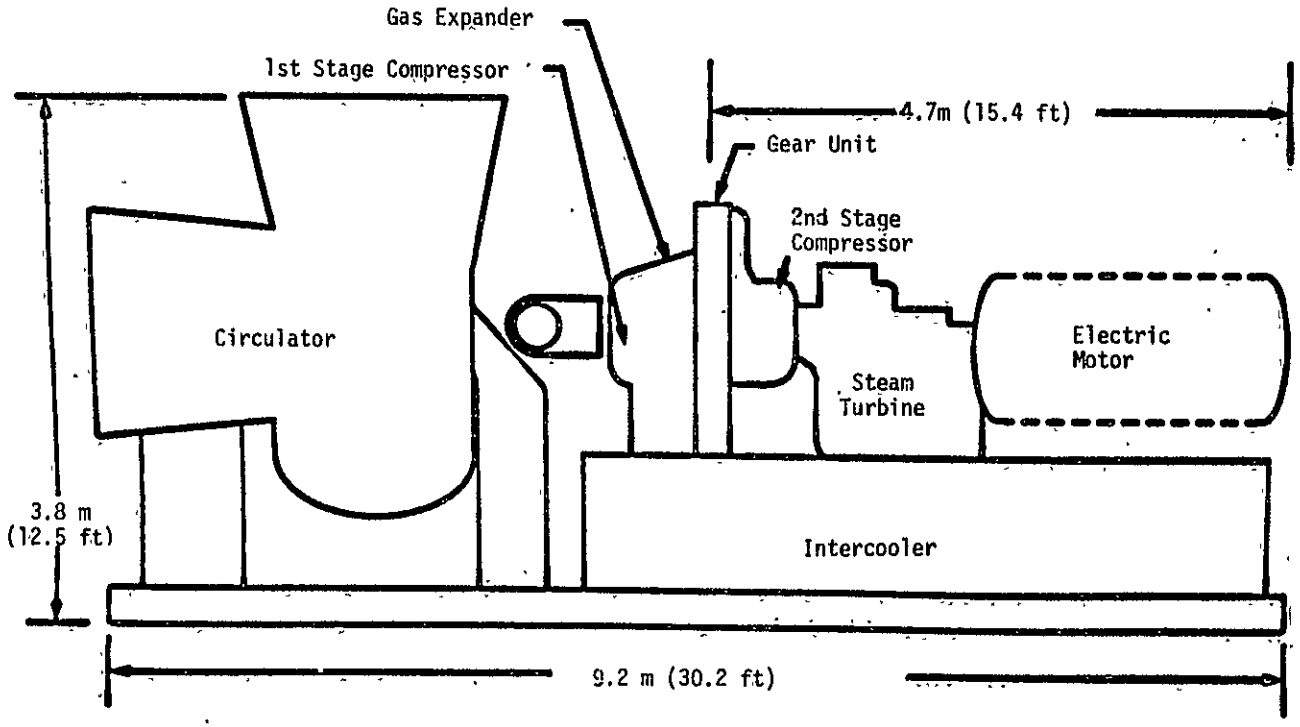

Figure 2.3.2-7. Rotating Equipment System Arrangement (Side View)

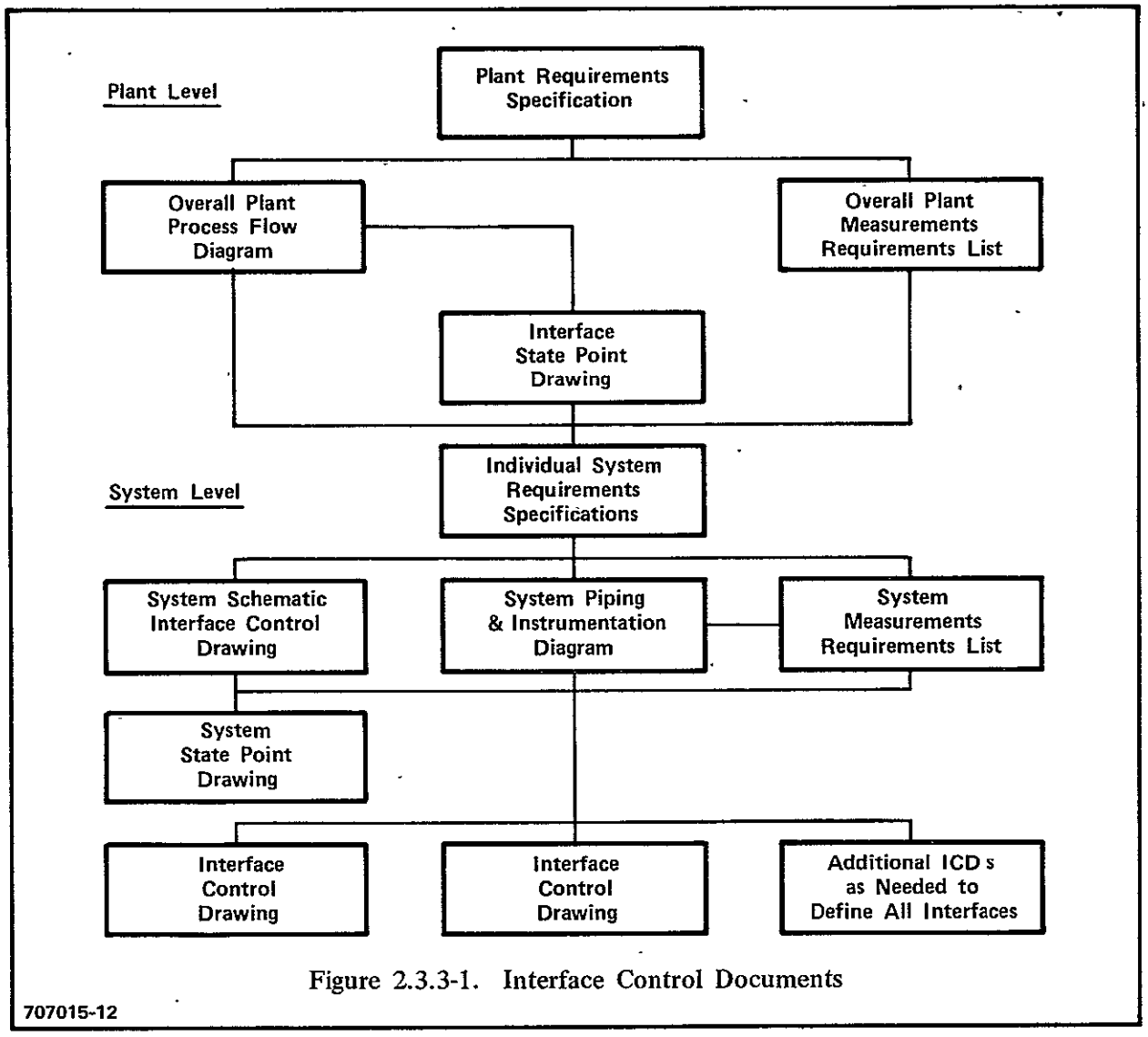

Figure 2.3.3-1. Interface Control Documents

Figure 2.3.3-1. Interface Control Documents

flow diagram and the plant measurements requirements list. The process flow diagram establishes the various system boundaries (schematically) and identifies the statepoints between interfacing systems. The parametric requirements for these statepoints are defined on an interface statepoint drawing. The instrumentation and control system requirements are developed from the plant level measurements requirements list.

At the system level, plant level requirements are amplified in the individual system requirements specifications, the system interface control drawing (schematic), the system piping and instrumentation diagram, and a system measurements requirements list. The latter two documents establish the system interface requirements for instrumentation and control. A system level statepoint drawing and individual interface control drawings are used to define all physical, functional, and procedural interfaces for each system.

A plant level system specification tree was developed and is shown in Figure 2.3.3-2. There are eighteen systems defined for the plant.

An interface management plan was prepared which delineates responsibilities and defines methods for initiating formal interface control documentation for identifying and controlling component and system interfaces. This plan also sets forth the procedural requirements for effecting changes to baseline documents to assure that the impact of proposed changes are considered and changes are acted upon properly.

2.3.3.1 INTERFACE CONTROL DOCUMENT PREPARATION

The interface management plan delineates the functions of the specifications and Interface Control Documents (ICD). Responsibilities and flow of informtion for baselining interfaces are shown in Figure 2.3.3-3.

2.2.3.2 CHANGE CONTROL

Since interface details may change as designs evolve and mature, and may change in actual manufacturing; ICDs will be subject to change control to maintain

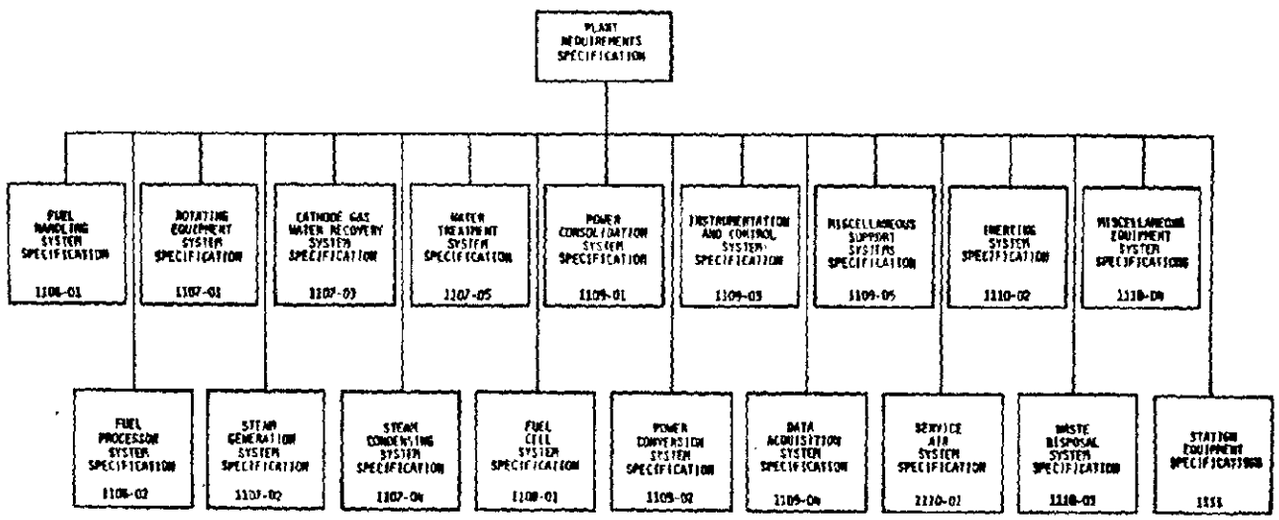

Figure 2.3.3-2 PAFC Plant Specification Tree

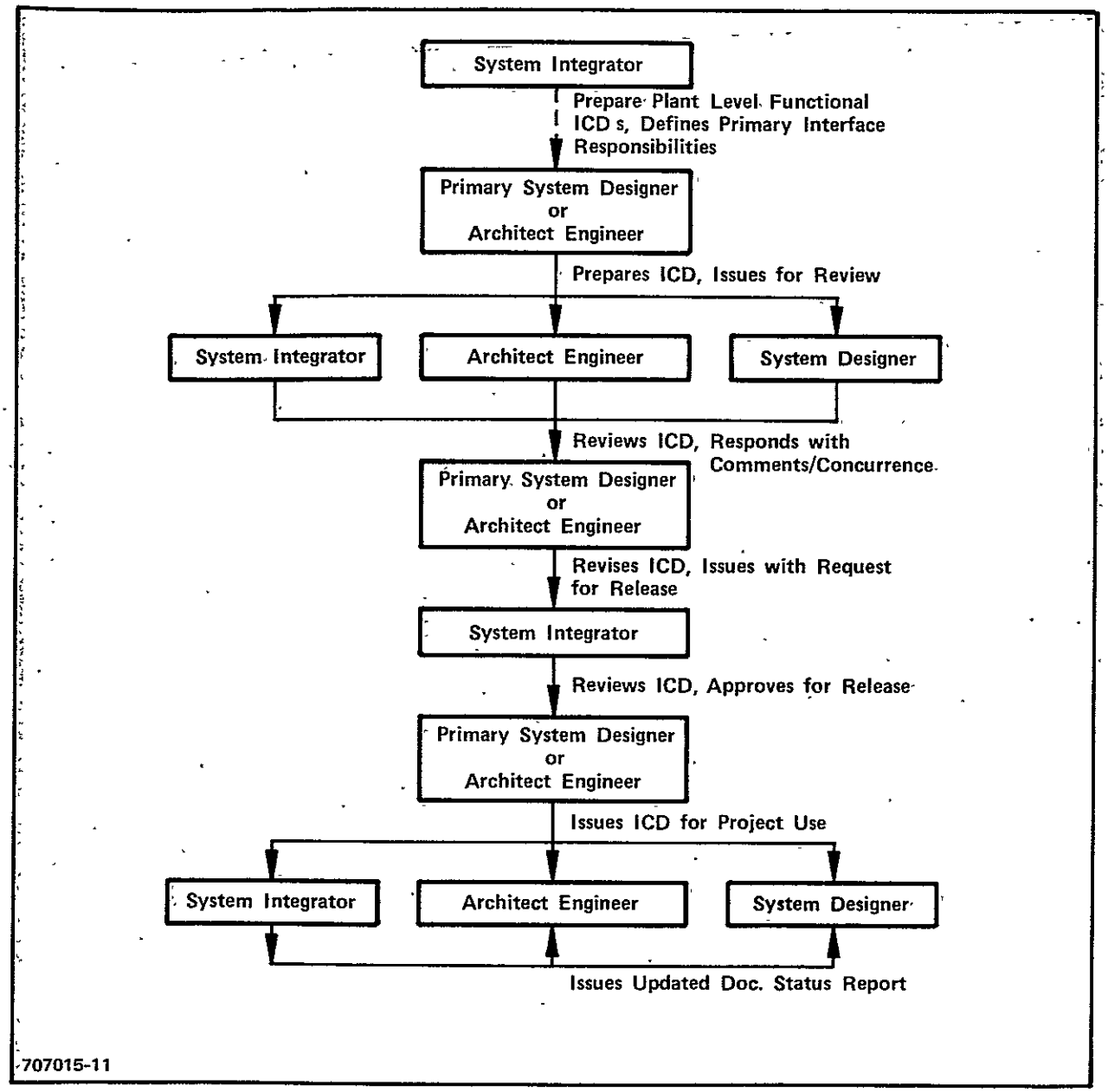

Figure 2.3.3-3. Interface Control Document (ICD) Preparation, Approval and Release Flow Chart

consistency with the equipment and facility designs. This will be accomplished through a change control system which ensures that changes to baseline documents are processed and controlled in a manner that:

- Documents the basis and justification of a proposed change.
- Ensures an impact evaluation of the safety, performance, schedular, interface, and financial effect of a proposed change.
- Assures that the proposed change is not in conflict with other documents or that any conflicts are resolved in the approval process.

The responsibilities and flow of information for revising baseline ICDs are highlighted in Figure 2.3.3-4.

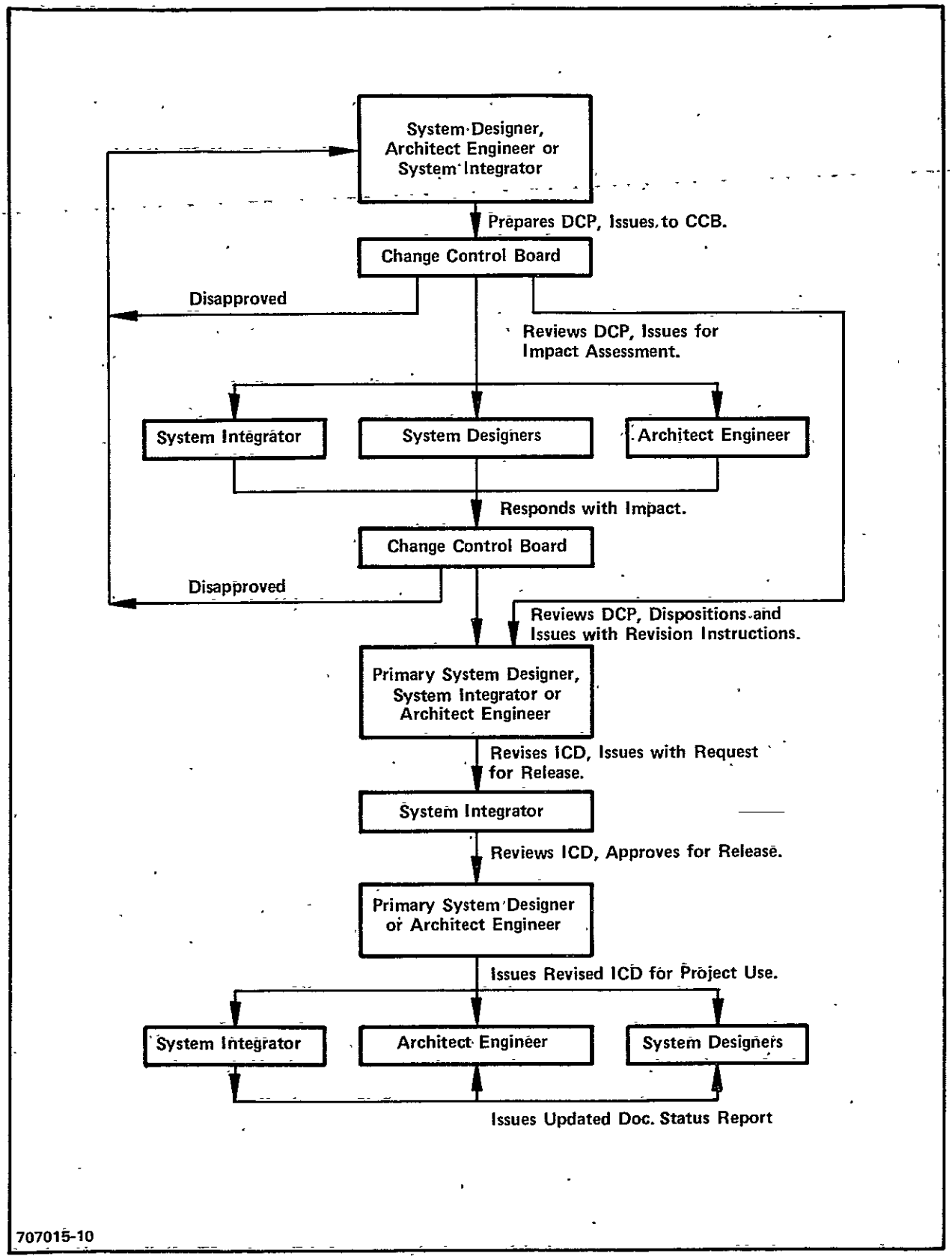

Figure 2.3.3-4. Interface Control Document (ICD) Revision Flow Chart

3.0 FUEL CELL DEVELOPMENT AND TEST

The primary objectives established for fuel cell development and test task were:

- Improve the existing PAFC materials data base and establish baseline materials specifications and process procedures for the electrodes, carbon matrix and silicon carbide layer, and bipolar and cooling plates.
- Establish PAFC component and stack performance, endurance and design parameter data needed for design verification for power plant application.

The balance of this section discusses the achievements made relative to these objectives in terms of the test plans, reports, analyses, design descriptions, final designs and various material, process, and test specifications developed.

3.1 SUBSCALE FUEL CELL DEVELOPMENT

3.1.1 DEVELOPMENT STATUS

The design of the 2 x 2 inch subscale fuel cell, developed under the OS/IES program, was developed into a final working design. The design requirements were defined establishing the functional and operational requirements, and performance goals. Assembly methods were developed and assembly fixtures were designed to control the assembly processes. A detailed assembly procedure was developed that defined the required assembly techniques.

Prior to initiation of the subscale cell test program, a number of cells were fabricated and tested that demonstrated reproducibility of the assembly and testing techniques. While developing this repeatable cell assembly, the design evolved through a series of modifications to eliminate inconsistent test results. Cross leakage problems that occurred with early test cells were corrected by changing the cell edge configuration and eliminating a Teflon gasket. Cell compression requirements were increased from initial values. Various acid application techniques were evaluated and a "wet" cell assembly was selected.

The production of heat treated graphite/resin subscale end plates which had been a problem was successfully resolved. An end plate design with molded grooves was produced without delaminations and excessive curvature. Approximately 50 sets of these plates were produced and used in test assemblies.

Both the design and assembly procedure were verified by the performance reproducibility study in which groups of cells were built and tested for times in excess of 1000 hours. These cells gave a standard deviation of approximately 5 mV and a 95 percent confidence range of $\sim$ 5 mV which is considered adequate for the required subscale testing program. Evaluation of lot No. 3 catalyst, being used for the current nine-cell testing program, was completed and the results gave a subscale IR-free performance of 670 mV at 200 mA/cm^2. A number of subscale performance evaluations were completed including cell transient response, performance decay with cell voltage, kinetic study of oxygen reduction, effect of operational parameters on all performance, effect of air flow rate on cell performance, and the effect of preheating process gases on cell performance.

The first of two Westinghouse provided subscale pressurized subscale test facilities was completed and pressurized testing was initiated. Cell performance was evaluated over the pressure range of from ambient up to approximately 7 atmospheres (100 psia) using electrodes produced with lot No. 3 catalyst. At the proposed plant conditions of 4.74 atm (70 psia), 325 mA/cm^2, 190°C, and 80 percent H_2 utilization a cell terminal voltage of 700 mV and an IR-free voltage of 740 mV were measured for these electrodes.

A total of 65 subscale cells was assembled and tested, acquiring approximately 60,000 hours of operating time.

3.1.2 SUBSCALE FUEL CELL DESIGN DESCRIPTION

An artist's illustration of the subscale cell assembly is shown in Figure 3.1.2-1. To meet the functional requirement that the cell be representative of the full size stack design, the basic stack features, i.e., compression plates,

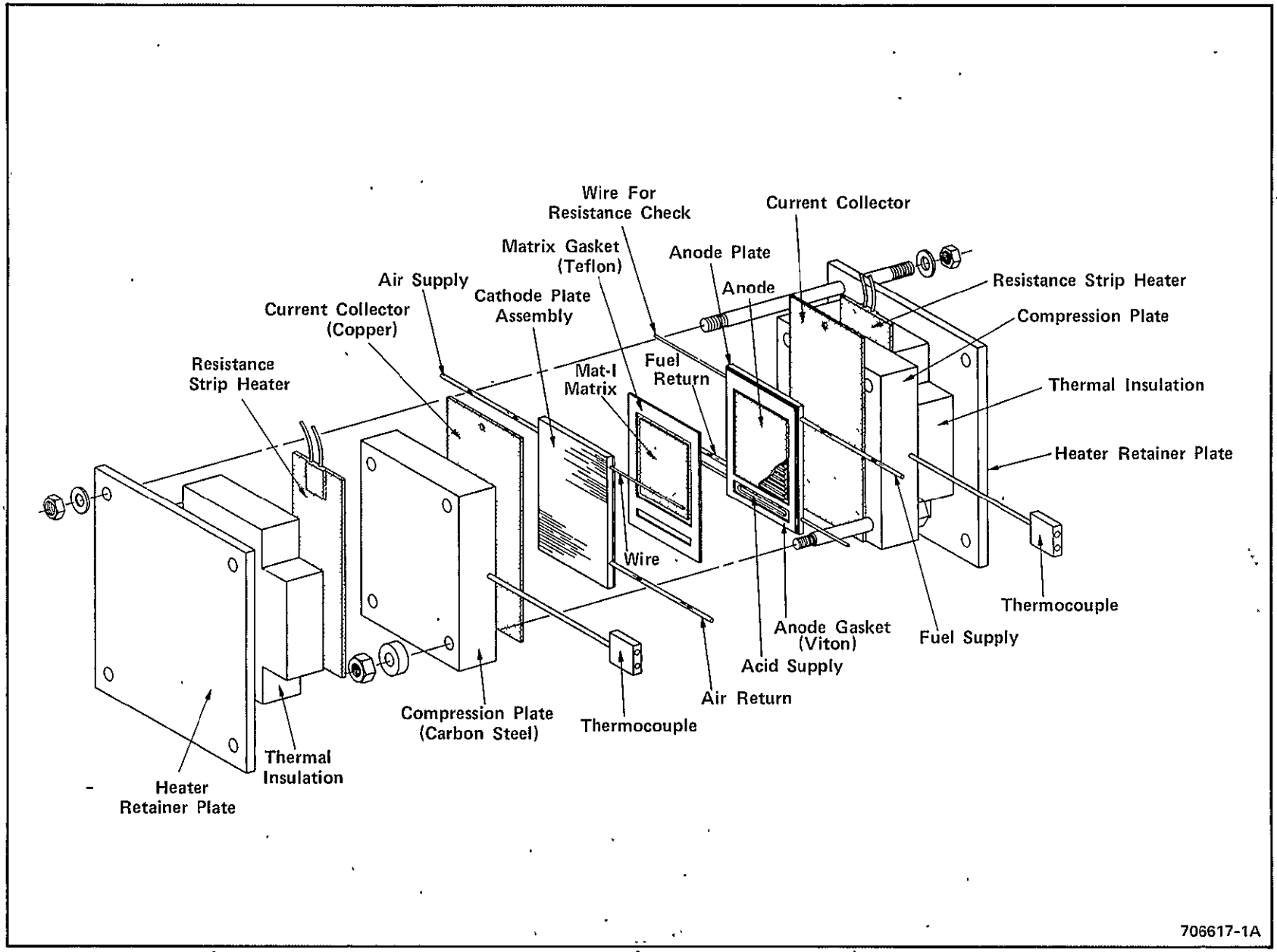

Figure 3.1.2-1. Subscale 2 x 2 Inch Cell Test Assembly

current collectors, tie bolts, and cell components (plates, electrodes and MAT-1 matrix), were incorporated into the subscale cell design. The tie bolts were placed outboard of the cell plates in an arrangement typical of the full size stack design. Cell component seals are an elastomer material (Viton) and the MAT-1 matrix is terminated inside of the seals. The process gas channel patterns on the end plates are molded to the identical cross-sectional geometry of full size plates.

Resistance strip heaters, thermal insulation blocks, and heater retainer plates external to the basic cell are not typical of a full size stack but are required for temperature control. These items are placed outboard of the basic cell components and are held in place with an additional set of tie rods. The tie rods are tightened slightly to hold the heaters in position but not enough to add any additional compression load to the basic cell.

In the subscale cell, the MAT-1 matrix layer and the anode are identical in area. The anode covers the 5 x 5 cm (2 x 2 inch) groove pattern in the anode plate, forming a 0.25 cm (0.10 inch) border around all four sides of the groove pattern. The anode gasket surrounds the anode like a picture frame, with a slot for the acid supply groove. The gasket is bonded to the anode plate with Viton adhesive. The MAT-1 is positioned inside the anode gasket on top of the anode.

The cathode is positioned on the cathode plate in a similar manner to the anode, with a similar picture frame gasket. The cathode is larger in area than the anode, extending beyond the anode edges on all four sides. The cathode extends over the acid supply groove in the anode plate. Because of the size difference, the inside edge of the anode gasket compresses against the cathode surface. This double gasket seal concept provides a very effective seal against acid and process gas cross or external leakage.

The silicon carbide layer of the cathode is exposed directly to the acid supply enabling the acid to wick to the cell components through the porous silicon carbide layer.

Process fuel and air supply and return lines are Teflon tubes attached to the electrode plates with epoxy. Manifold header grooves machined into each plate distribute and collect flows. Permanently attached resistance and voltage probe wires (one to each plate) are provided to monitor operational performance. Sheathed thermocouples located in holes in the compression plates are provided for control of the strip heaters. The electrical resistance load is connected to the cell by attachment to the gold plated copper current collectors which extend from the top of the cell.

3.1.3 SUBSCALE FUEL CELL ASSEMBLY

To meet the objective of providing reliable test data, it was mandatory that the subscale assembly procedure be reproducible. Previous experience with Teflon edge seals was inconsistent in that frequent cell gas leakage was encountered in cells using this approach. To correct this, a design using Viton edge seals coupled with controlled compression was developed. Also, the assembly procedure was modified to use wet assembly of the silicon carbide layer (0.6 cc acid added) as well as a wet (float filled) matrix. The subscale test results using the final version of this assembly procedure are presented in Section 3.1.4.

The assembly procedure used for building cells for pressurized testing is the same as for the unpressurized except for additional hardware and fittings to insure positioning and retention of the gas flow tubing in the area where connections are made to the end plates.

3.1.4 SUBSCALE FUEL CELL TESTING

SUBSCALE PERFORMANCE REPRODUCIBILITY STUDY

To gain experience with the developed subscale cell design, a series of cells SC-006 through SC-028 were built and tested. These cells were all built basically dry with 0.4 ml of 100 percent acid added to the cathode SiC layer during assembly.

In the course of this series of cell builds, a number of assembly conditions and design changes were made. For example, the cell component compression

(electrodes plus matrix) was fixed at 12 percent, the Teflon gasket was omitted, the relative size of the matrix and anode fixed, the method of attaching the electrodes to the end plates established and wet cell build was adopted. In addition, several generations of molded and heat treated (to 900°C) end plate geometries were evaluated. While the results obtained with these cells were somewhat variable, it was concluded that the assembly design and procedure were reproducible and that a series of eight cells could be built to satisfy the reproducibility performance goal.

To demonstrate this, two groups of cells were built (eight in one group) from Westinghouse components and (four in the second group) from ERC repeating cell components using wet assembly; that is, the MAT-1 layer was float filled in 100 w/o acid at room temperature and 0.6 ml of acid was added to the SiC layer of the cathode during assembly. The components used are identified in Table 3.1.4-1. These cells were tested at 190 $\pm$ 2°C for 1000 hours at 200 mA/cm^2, 80 percent hydrogen utilization, and five stoich air flow. The individual cell internal resistance and open circuit voltage after 100 hours of cell operation are given in Table 3.1.4-2. The IR-free cell voltages for all cells tabulated for each 100 hours of operation up to 1000 hours are presented in Table 3.1.4-3. Analysis of the data was performed and the mean performance values, standard deviations, and range for the 95 percent confidence interval are presented in Table 3.1.4-4. Group No. 1 cells, using the Westinghouse produced components, gives a standard deviation of about 5.6 mV which is an acceptable reproducibility.

Polarization curves for Group No. 1 cells are shown in Figures 3.1.4-1 and 3.1.4-2 and are quite similar. Tafel slopes measured over the low current densities (up to about 80 mA/cm^2) range from 95 to 105 mV/decade. Oxygen gain data was determined for Cell SC-039 in Group No. 1 and SC-045 in Group No. 2 and are given in Figures 3.1.4-3 and 3.1.4-4. These data show the voltage gain to be about 70 mV after a test duration of approximately 200 hours.

It should be noted that the intent of this group of tests was to verify the cell design and assembly procedure. The electrodes used in this study are from Lot No. 1 catalyst and were produced in early to mid 1982.

TABLE 3.1.4-1

REPEATING COMPONENT IDENTIFICATION

Group No. 1 Cells

Westinghouse Produced Components

Anode A087-8	0.29 mg Pt/cm^2
Cathode C055-3	0.43 mg Pt/cm^2

Group No. 2 Cells

ERC Produced Components

Anode No. 266	Nominal 0.3 mg Pt/cm^2
Cathode 90-8903-102	Nominal 0.5 mg Pt/cm^2

TABLE 3.1.4-2

CELL RESISTANCE AND OPEN CIRCUIT VOLTAGE AFTER 100 HOURS

	Cell Resistance (mΩ)	Open Circuit Voltage (mV)
Group No. 1 Cells		
SC-036	8.4	915
SC-037	8.4	914
SC-038	7.1	905
SC-039	6.9	904
SC-041	6.8	905
SC-042	7.2	904
SC-043	7.5	911
SC-044	6.8	906
Group No. 2 Cells		
SC-045	7.3	917
SC-046	8.4	920
SC-047	7.2	930
SC-048	7.4	926

TABLE 3.1.4-3

TEST TIME VERSUS IR-FREE VOLTAGE PERFORMANCE (VOLTAGE IN MILLIVOLTS)

		Test Time (Hr)									
Cell Identification	Initial	100	200	300	400	500	600	700	800	900	1000
Group No. 1											
SC-036	645	648*	646	646	644*	652	649	648	647	646	646
SC-037	634	643	644	654	651	649	653	654	656	656	655
SC-038	645	650	654	653	644	647	647	647	646	645	647
SC-039	648	657	657	656	648	648	651	647	646	644	643
SC-041	639	644	648	639	637*	645	647	646	648	650	647
SC-042	648	652	650	646	648	649	647	651	651	646	646(1)
SC-043	643	643	645	647	648	647	645	647	646	643	642
SC-044	651	650	651	652	651	651	649	652	654	653	647
Group No. 2											
SC-045	656	666	669	667	668	668	664	664	661	656	655
SC-046	665	673	669	669	669	668	671	667	664	661	659
SC-047	664	662	666	666	669	668	669	666	665	665	665
SC-048	661	658	658	658	660	656	655	652	653	652	650

*Indicates 100 percent H_3PO_4 added to cell reservoir.

(1)Test terminated after 985 hours.

TABLE 3.1.4-4

ANALYSIS OF RESULTS OF SUBSCALE CELL REPRODUCIBILITY

Time (Hr) Group No. 1 (8 Cells)	Mean (mV)*	Standard Deviation (mV)	Range for 95 Percent Confidence Interval (mV)
Initial	644.0	5.46	644.1 ± 4.6
100	648.8	4.93	648.4 ± 4.1
200	648.8	4.91	648.8 ± 4.1
300	649.1	5.62	649.1 ± 4.7
400	646.4	4.63	646.4 ± 3.9
500	648.5	2.27	648.7 ± 1.9
600	648.5	2.56	648.5 ± 2.1
700	649.0	2.93	649.0 ± 2.4
800	649.3	3.96	649.2 ± 3.3
900	647.9	4.64	647.8 ± 3.9
1000	646.6	3.89	646.7 ± 3.3
Group No. 2 (4 Cells)			
Initial	661.5	4.04	661.4 ± 6.4
100	664.8	6.40	664.9 ± 10.3
200	665.5	5.20	665.5 ± 8.3
300	665.0	4.83	665.5 ± 8.2
400	665.5	4.36	667.0 ± 7.4
500	665.0	6.00	665.0 ± 9.5
600	664.7	7.14	664.6 ± 11.2
700	662.2	6.95	662.4 ± 11.2
800	660.7	5.44	660.7 ± 8.6
900	658.5	5.69	658.5 ± 9.0
1000	657.3	6.34	657.2 ± 10.0

*IR Free (Measured cell voltage gave same standard deviation and confidence intervals as IR Free)

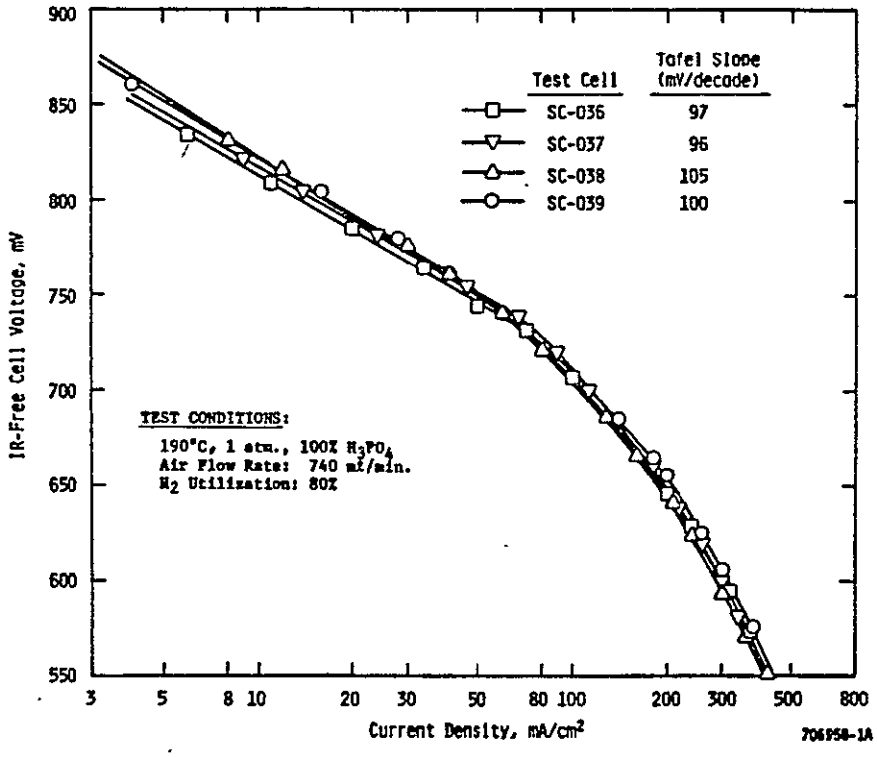

Figure 3.1.4-1. Polarization Curves for Cells SC-036, 037, 038, and 039

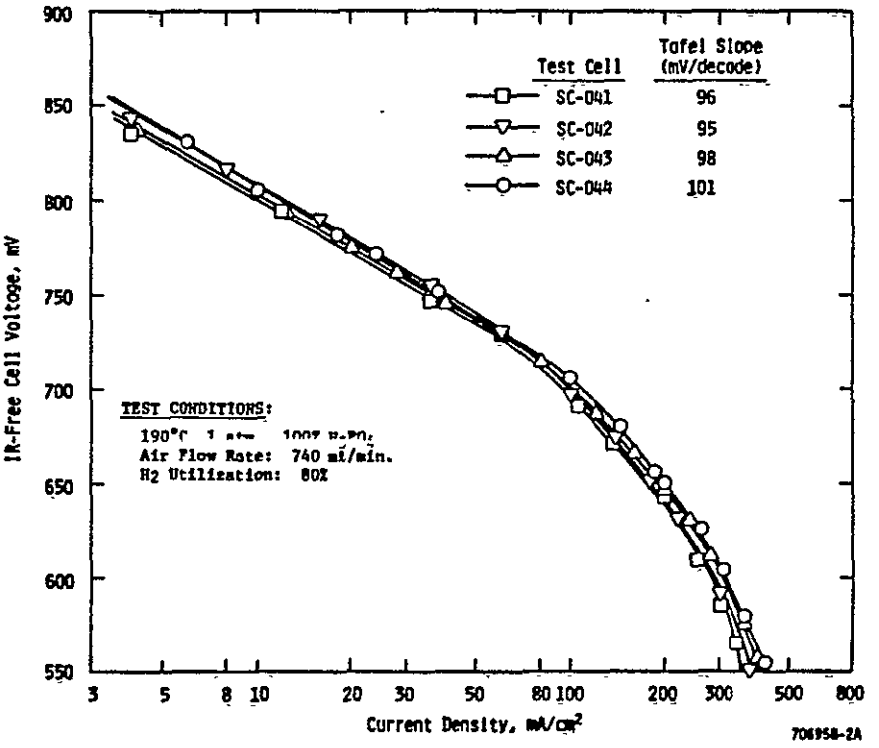

Figure 3.1.4-2. Polarization Curves for Cells SC-041, 042, 043, and 044

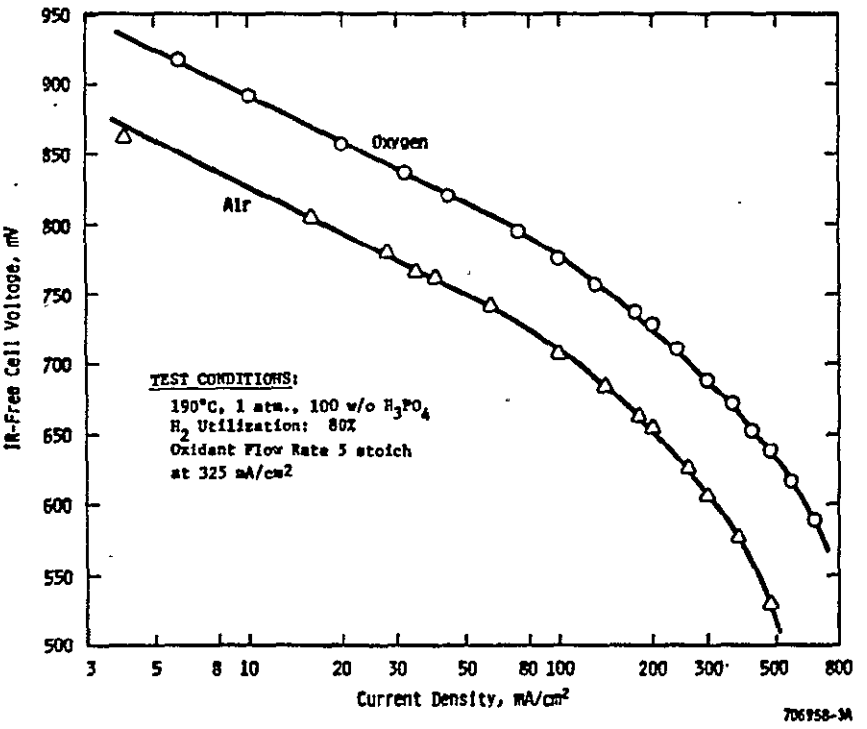

Figure 3.1.4-3. Polarization Curves for Cell SC-039, Air, and Oxygen

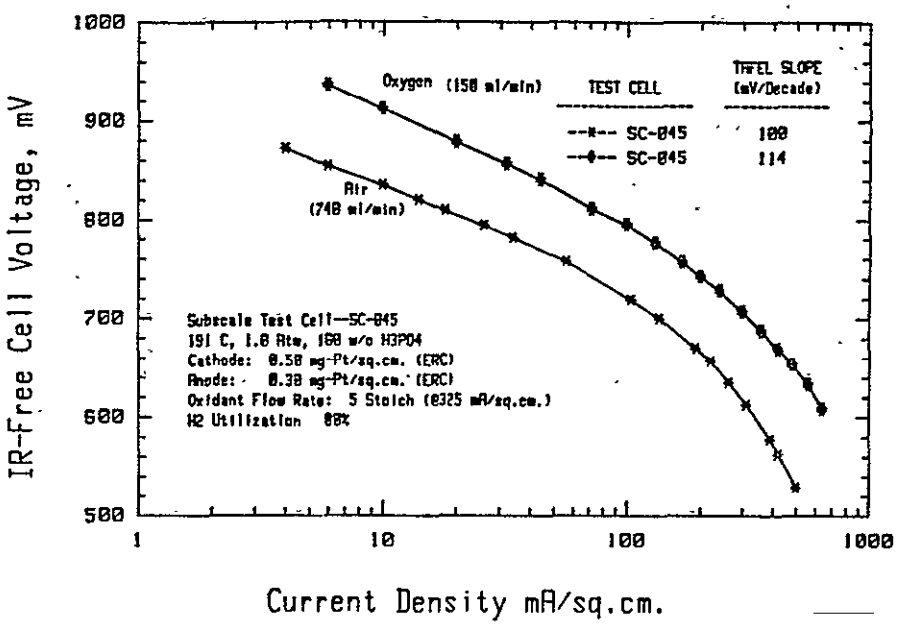

Figure 3.1.4-4. Polarization Curves for Cell SC-045, Air, and Oxygen

SUBSCALE EVALUATION OF LOT NO. 3 CATALYST

A series of six cells was built from electrodes made with Lot No. 3 catalyst and tested at ambient pressure for times in excess of 1000 hours. The electrodes tested and their loadings are shown in Table 3.1.4-5 while the IR-free cell voltage at test intervals of every 100 hours up to 1000 hours is given in Table 3.1.4-6. The average performance for the cells is above 670 mV IR-free and about 20 mV higher than that found for the reproducibility study electrodes.

ALTERNATE MATRIX TEST CELLS

Two cells, SC-068 and SC-072, were assembled and testing initiated to evaluate alternate matrix acid transport materials. Alternates being evaluated are Stackpole PC-206 and Kureha type KCF carbon paper. The laterial acid transport wicking behavior of these materials is presented in Section 3.7.5 and was better than that determined for MAT-1. These cells were built utilizing the standard assembly procedure but with a modified assembly design. The carbon paper was cut to the same size as the cathode, thus permitting it to pick up acid from the acid reservoir. To accommodate this, a 0.13 mm (0.005 in) Teflon gasket was added between the two Viton gaskets normally present.

At 200 mA/cm^2, 190°C, ambient pressure and standard gas flows, the performance shown in Table 3.1.4-7 is essentially equivalent to that obtained using the MAT-1 layer and the same electrode, see Tables 3.1.4-5 and 3.1.4-6. It should be noted that both of these cells had relatively low open circuit voltages, approximately 875 mV, and had relatively large cross leaks when the air is cut off with the cells on open circuit. The modified cell construction is thought to be the cause of the cross leak and not the presence of the alternate acid transport material. Due to the large pore size in these materials, they would not be expected to provide high bubble pressures but the SiC layer on the cathode has been shown to provide a 90 kPa (13 psi) or greater bubble pressure.

TABLE 3.1.4-5

REPEATING COMPONENT IDENTIFICATION FOR EVALUATION OF LOT NO. 3 CATALYST

Cell No.	Cathode	Loading mg/cm^2	Anode	Loading mg/cm^2
SC-050	C119-4	0.49	A123-1	0.29
SC-051	C119-4	0.49	A123-1	0.29
SC-052	C119-4	0.49	A123-1	0.29
SC-053	C119-4	0.49	A123-1	0.29
SC-056	C116-2	0.48	A121-1	0.30
SC-057	C116-2	0.48	A121-1	0.30

TABLE 3.1.4-6

IR-FREE VOLTAGE (mV) FOR CELLS BUILT WITH LOT NO. 3 CATALYST[1]

Cell Ident. No.	Test Time, Hr.										
	INITIAL	100	200	300	400	500	600	700	800	900	1000
SC-050	660	679	680	679	677	671	670	671	668	668	669
SC-051	663	678	680	678	676	678	676	675	674	672	671
SC-052	682	680	681	679	678	676	678	676	675	676	675
SC-053	678	677	680	676	678	676	675	672	671	673	673
SC-056	675	675	674	674	673	672	671	670	668	665	665
SC-057	666	676	677	676	673	674	676	675	675	672	672
Average	670.6	677.5	678.6	677.0	675.8	674.5	674.3	673.2	671.8	671.0	670.

(1) Data for 190°C, 200 mA/cm^2, 80 percent H_2 Util., 20 percent Air Util., Ambient Pressure.

TABLE 3.1.4-7

DATA ON CELLS HAVING ALTERNATE MATRIX MATERIAL

	SC-068	SC-072
Cathode		
Identification	C119-4	C119-4
Pt. Loading mg/cm^2	0.49	0.49
Catalyst Lot No.	3	3
Anode		
Identification	A123-1	A123-1
Pt. Loading mg/cm^2	0.28	0.28
Catalyst Lot No.	3	3
Matrix	PC-206 (Stackpole)	Type KCF (Kureha)
Gasket	2 Viton 1 Teflon	2 Viton 1 Teflon
Assembly	Matrix Wet Cathode SiC Wet	Matrix Wet Cathode SiC Wet
Open Circuit Voltage, mV	880(1)	875(1)
Temperature, °C	190	190
Current Density, mA/cm^2	200	200
Oxygen Utilization, percent	20	20
Hydrogen Utilization, percent	80	80
Internal Resistance, mΩ	6.9	9.8
Testing Time, Hours	500	168
IR-Free Cell Voltage, mV	670	682

(1) Relatively high cross leak with air off-drop of ∿ 30 mV in 30 seconds.

CELLS FOR THERMAL CYCLING

Thermal cycling tests were conducted on two cells, SC-050 and SC-051, which had previously been tested for approximately 1000 hours. The cycle used was from 190 to 150°C at which point the external load and gas flows were removed and the cell allowed to cool to ambient temperature (21 to 24°C). After a hold time of either 16 or 72 hours at ambient temperature, the cells were heated to 140°C, the external load and process gas flow restored, and the cell heated to 190°C. Several cycles were completed and the performance before and after these cycles is given in Table 3.1.4-8. There appears to be no significant performance decrease after this limited cycling. The average loss per cycle would appear to be between 1 and 2 mV. Cycling will be continued until at least ten cycles are accumulated on each cell.

SUBSCALE ENDURANCE TESTING

Endurance tests were initiated on subscale cells SC-003 and SC-005 under the following operating conditions: 200 mA/cm^2, 191°C, ambient pressure, five stoich air flow rate, and 80 percent H_2 utilization. The detailed cell components, testing conditions, and experimental results are summarized in Table 3.1.4-9. These subscale cells used the ERC-designed cell configuration and Westinghouse-produced electrodes with MAT-1 matrix.

After having accumulated about 3000 operating hours, cell SC-003 exhibited a peak voltage of 632 mV at 200 mA/cm^2. Subsequently, the cell performance deteriorated slightly with time. In the first 10,000 hours of operation, the average deterioration rate of slightly less than 2 mV per 1000 hours.

Subscale end plates produced by Westinghouse were evaluated in SC-005 for the first time. Despite poor initial performance, the terminal voltage of SC-005 gradually improved to a peak value of 620 mV.

CORRELATION OF PERFORMANCE DECAY WITH CELL VOLTAGE

After reproducibility testing at 200 mA/cm^2 for approximately 1600 hours, three subscale cells were used to investigate the correlation between

TABLE 3.1.4-8

EFFECT OF CYCLING TO AMBIENT TEMPERATURE ON CELL PERFORMANCE AT 190°C AND 200 mA/cm^2

	Cell Resistance (mΩ)	IR-Free Cell Voltage (mV)	Performance Change (mV)	Time at Ambient Temperature (Hours)
Cell SC-050				
Start of Cycling	7.5	673	-	-
Cycle 1	7.0	673	0	72
Cycle 2	7.6	671	-2	16
Cycle 3	7.7	676	+3	16
Cycle 4	7.9	672	-1	16
Cycle 5	8.0	667	-6	72
Cell SC-051				
Start of Cycling	6.9	674	-	-
Cycle 1	7.5	674	0	16
Cycle 2	7.9	669	-5	72
Cycle 3	8.3	667	-7	16
Cycle 4	8.0	665	-9	72

TABLE 3.1.4-9

COMPARISON OF COMPONENTS AND PERFORMANCES OF SUBSCALE CELLS FOR ENDURANCE TESTS

Cell No.	SC-003	SC-005
DESIGN CONFIGURATION	ERC	ERC
Cathode		
Identification	C014-4 (AESD)	C014-4 (AESD)
Pt Loading, mg/cm^2	0.52	0.52
Anode		
Identification	A015-4 (AESD)	A015-4 (AESD)
Pt Loading, mg/cm^2	0.34	0.34
MAT-1		
Identification	M019-2 (AESD)	M019-2 (AESD)
Gasket		
Type	Two Untreated Teflon	Two Untreated Teflon
End Plates		
Type	Heat Treated (ERC)	Heat Treated (AESD)
Performance at 200 mA/cm^2		
Temperature, °C	191 + 2	191 + 2
Oxygen Utilization, %	20	20
Hydrogen Utilization, %	80	80
Testing Time, Hr	10,262	8,865
Peak Cell Voltage, mV	632	620
Final Cell Voltage, mV	619	571
Internal Resistance, mΩ	4.6	9.6
IR-Free Cell Voltage, mV	642	619

performance decay and cathode voltage at 190°C and ambient pressure. Subscale cells SC-037, SC-038, and SC-039 were operated at 80, 10, and 200 mA/cm^2, respectively, so that their initial IR-free cell voltages were in the range of 700-800 mV, above 800 mV, and below 700 mV.

For Cell SC-038 operating at 10 mA/cm^2, the IR-free cell voltage dropped by 10 mV in the first 950 hours of continuous testing, while its internal resistance increased from 10.6 mΩ to 11.9 mΩ. In the identical period of time, the measured IR-free cell voltage of SC-037 (operating at 80 mA/cm^2) decreased slightly from 724 mV to 722 mV and its internal resistance increased to 11.0 mΩ from 10.0 mΩ. After replenishing the acid reservoirs of these two subscale cells, no improvement was observed in either cell internal resistance or IR-free cell voltage. Although the internal resistance of SC-039 (at 200 mA/cm^2) increased by about 0.7 mΩ in the first 900 hours of operation, its IR-free cell voltage remained practically constant at 655 mV during the test. The replenishment of acid in SC-039 resulted in a reduction of about 0.3 mΩ in the internal resistance. This investigation is still under way.

SUBSCALE CELLS FOR PROCESS VARIATION EVALUATION

Several cells were assembled and testing initiated to evaluate fabrication process variations, namely SC-069, SC-070, and SC-071. Included in this group of cells are variations in the method of electrode lamination to the backing paper and the effect of catalyst heat treatment on cell performance. The combination of modified electrode lamination and catalyst treatment has resulted in IR-free performance as high as 695 mV at 200 mA/cm^2.

TRANSIENT RESPONSE

Studies were performed using subscale cell SC-011, to determine the transient response of performance with respect to the variation of current density. As illustrated in Figure 3.1.4-5, the test cell was prepolarized at 325 mA/cm^2 for about two hours. Instantaneously, the operating current density was reduced to 200 mA/cm^2 and both the cell voltage and internal resistance were monitored as a function of time. Air flow was held constant during the tests,

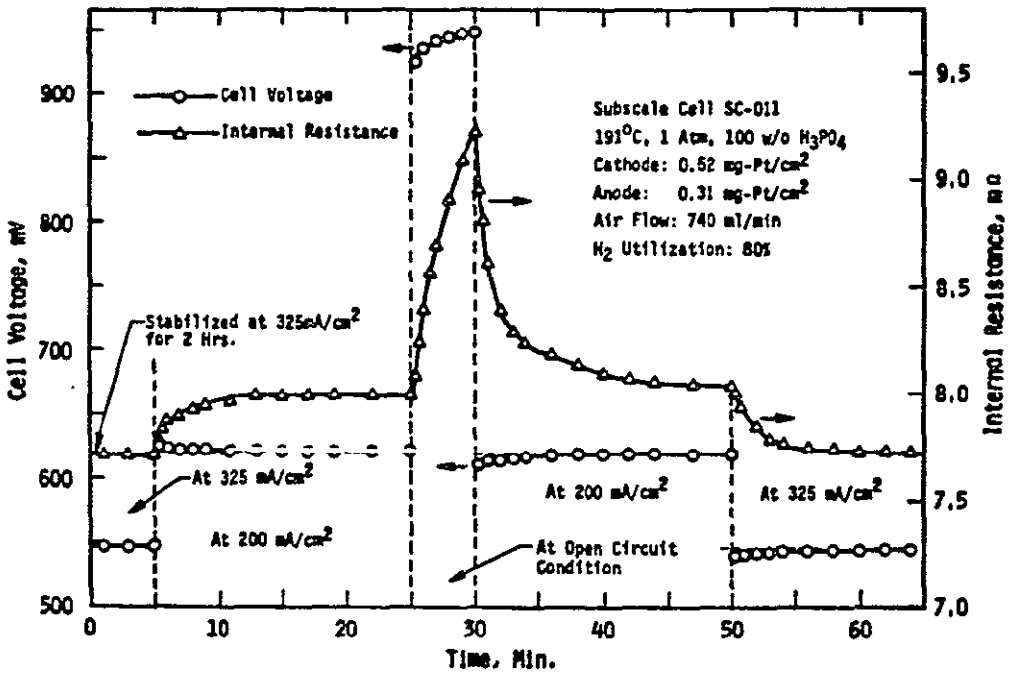

Figure 3.1.4-5. Transient Response of Cell Voltage and Internal Resistance with the Variation of Operating Current Density

which resulted in 20 percent utilization at 325 mA/cm^2 and 12 percent at 200 mA/cm^2. Hydrogen flow was adjusted at the two current densities to maintain 80 percent utilization. Due to the gradual increase of acid concentration at the lower current density, the observed cell voltage decreased slightly and the internal resistance increased with time. After about ten minutes of equilibration, both parameters were considered stable.

Under open circuit condition, the internal resistance increased with time. However, a stable open circuit voltage was obtained in about five minutes. After allowing the test cell to remain at open circuit potential for five minutes, an operating current density of 200 mA/cm^2 was imposed. As seen in Figure 3.1.4-5, the internal resistance and cell voltage stabilized within ten minutes. It is thus concluded that, in the measurement of polarization curves, stabilized cell voltage and electrolyte concentration at a desired operating current density are achievable after about ten minutes of equilibration.

EFFECTS OF VARIATIONS IN KEY OPERATIONAL PARAMETERS ON CELL PERFORMANCES

To normalize the experimental data from subscale cell tests, the effects of minor variations in three key operational variables (temperature, current density, and air flow rate) on cell performances were investigated in cell SC-011. At three constant current densities 100, 200, and 325 mA/cm^2, the cell voltage was measured as a function of temperature in the range of 181 to 201°C. The results are shown in Figure 3.1.4-6, where E_{cell}, $T_{°C}-E_{cell}$, 191°C represents the difference between the cell voltage at T°C and 191°C. As expected, the observed cell voltages did not increase linearly with increasing temperature. At 200 mA/cm^2 and 191°C, for example, the increase in cell voltage with increasing temperature was $\sim$ 1.3 mV/°C.

Figure 3.1.4-7 illustrates variation of measured cell voltage with operating current while maintaining a constant temperature of 191°C and constant flow rates of air and H_2. $E_{cell, I} - E_{cell, Io}$ denotes the difference between the cell voltage at the true operating current I and at the desired operating current I_o. In this study, the desired operating currents were 2.5, 5.0 and 8.12 A, representing the current densities 100, 200 and

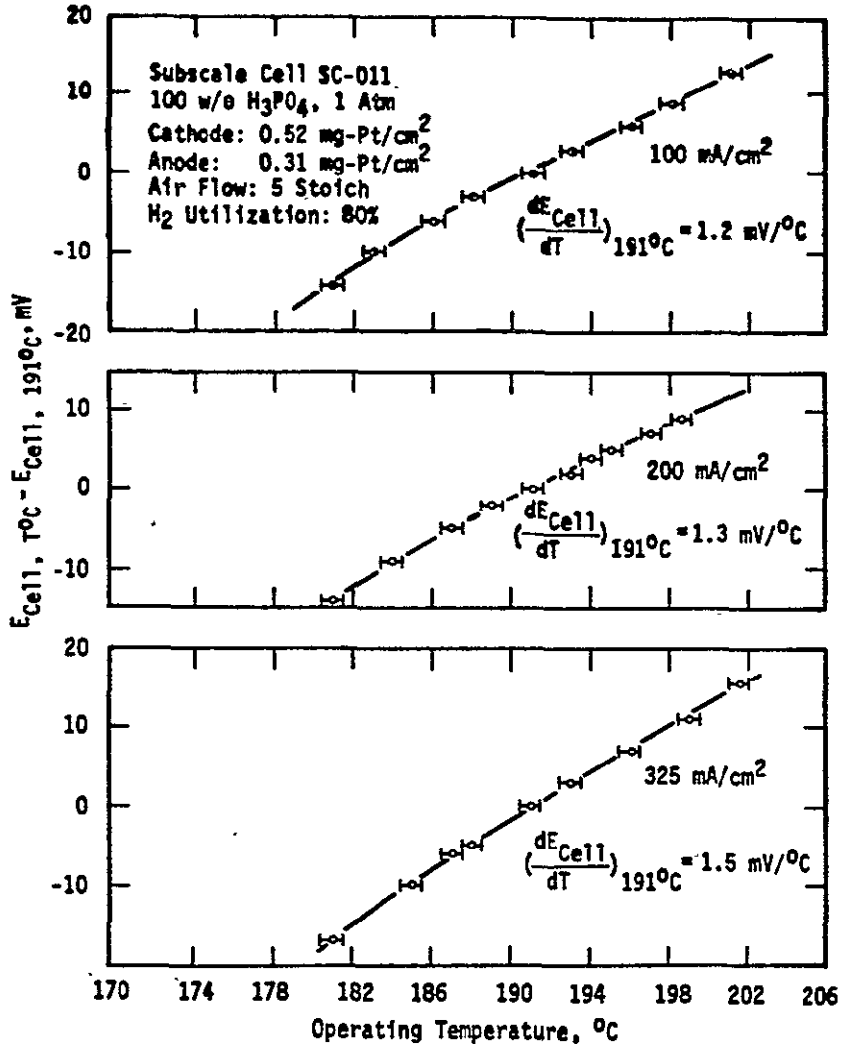

Figure 3.1.4-6. Variation of Cell Potentials at Constant Current Densities 100, 200, and 325 mA/cm^2 with Operating Temperature

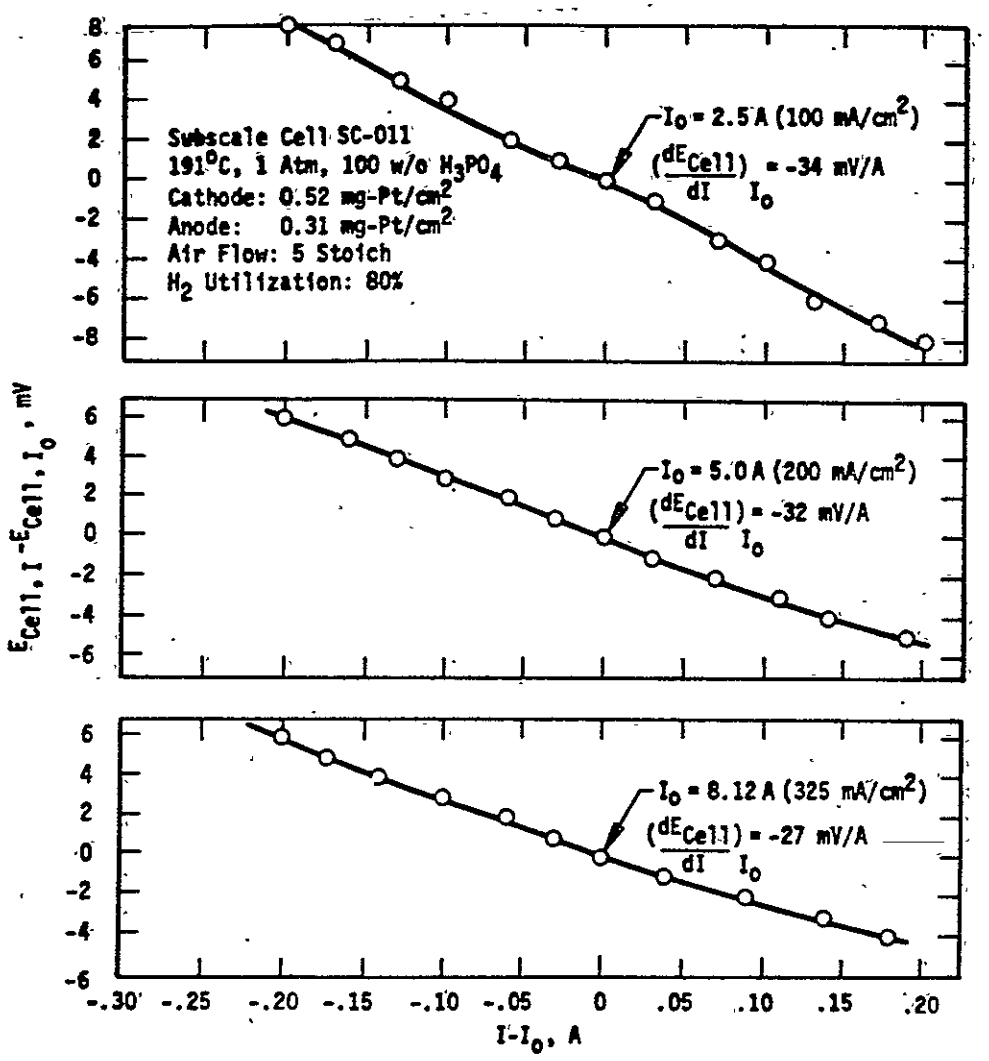

Figure 3.1.4-7. Variation of Cell Voltages with Minor Changes in Operating Currents

325 mA/cm^2, respectively. At 200 mA/cm^2, a two percent increase (about 0.1A) in the desired operating current caused a cell voltage loss of $\sim$ 3 mV.

At constant operating current density and temperature, the measured cell voltages were sensitive to air flow rates below four stoich as evidenced in Figure 3.1.4-8. At increased operating current density, the measured cell voltages became more sensitive to change in air flow rate. At flow rates above five stoich, however, no detectable influence was observed on cell performance. It was decided that all the unpressurized subscale cells should be operated at a minimum air flow rate of four stoich. Consequently, a ten percent system error in the flow meter would have minimal effect on the measured cell voltages.

DEPENDENCE OF KINETIC PARAMETERS FOR OXYGEN REDUCTION ON OXYGEN CONTENT

For oxygen reduction on carbon-supported platinum catalysts of 0.52 mg/cm^2 loading, kinetic studies were performed using subscale test cell SC-018, with air, pure oxygen, and N_2-O_2 mixed gases containing 35 and 49 v/o oxygen. Hydrogen utilization remained at 80 percent and oxidant gas flow rates were kept at three stoich with respect to 325 mA/cm^2. After the correction of anodic overpotentials and ohmic losses, the Tafel plots and kinetic parameters for O_2 reduction are shown in Figure 3.1.4-9 and Table 3.1.4-10, respectively. The measured Tafel slopes ranging from 102 to 105 mV/decade are approximately independent of oxygen concentration in the inlet oxidant gases. Therefore, the variation of oxygen concentration results in no change in the reaction mechanism. However, the observed exchange current densities increase with increasing oxygen concentration (see Table 3.1.4-10). In comparison with air, the use of pure oxygen improves the cathode voltage by 75 mV at current densities in the range of 20-200 mA/cm^2. This voltage gain results from the reduction of activation polarization and a slight increase of the Nernst potential.

EFFECTS OF AIR FLOW RATE ON CELL PERFORMANCES

After continuous operation at 200 mA/cm^2 and three stoich air flow rate for 1800 hours, subscale cell No. 18 was used to investigate the dependence of cell

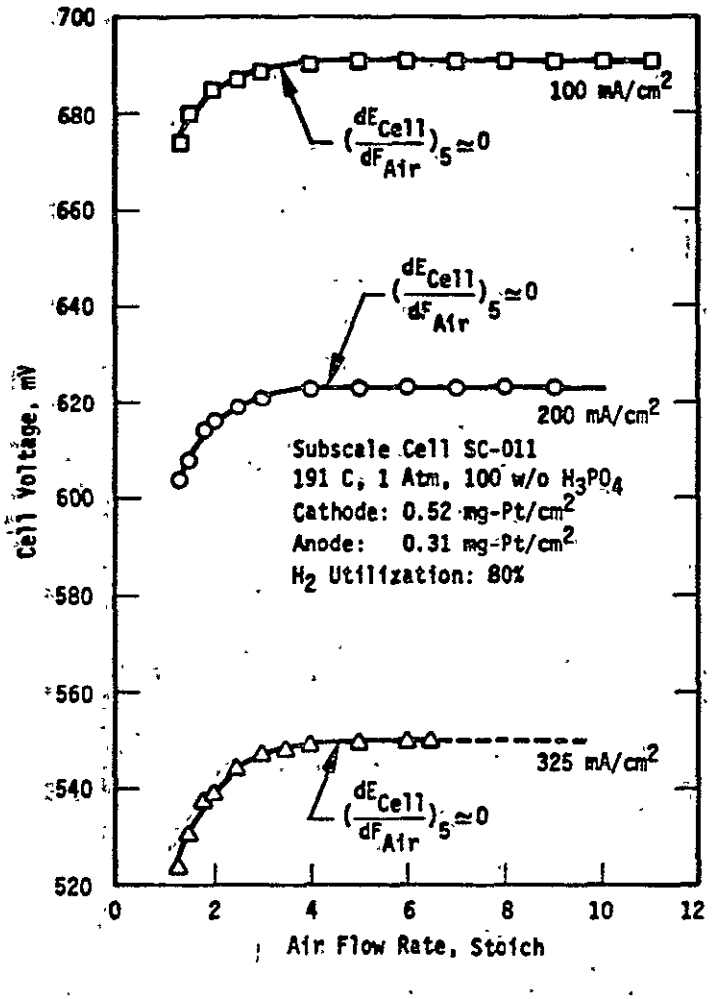

Figure 3.1.4-8. Effects of Air Flow Rate on the Measured Cell Voltages at 100, 200, and 325 mA/cm^2

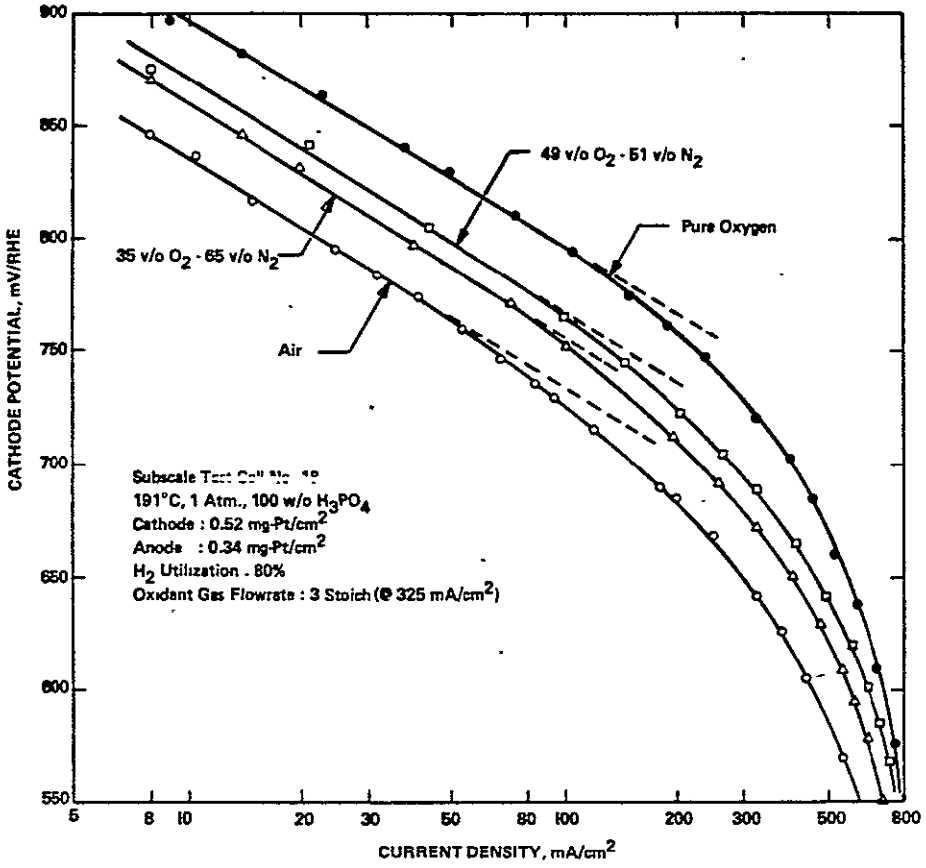

Figure 3.1.4-9. Tafel Plots for Oxygen Reduction in Laminated Porous Cathodes

TABLE 3.1.4-10

EFFECTS OF OXYGEN CONTENT OF KINETIC PARAMETERS FOR OXYGEN REDUCTION AT 191°C AND AMBIENT PRESSURE

Oxidant Gas	Air	35% O_2 - 65% N_2	49% O_2 - 51% N_2	Oxygen
Flow Rate*, mℓ/min	440	262	188	97
Observed Exchange Current Density, mA/cm^2	2.1×10^{-3}	5.4×10^{-3}	7.2×10^{-3}	1.0×10^{-2}
Tafel Slope, mV/decade	102	104	105	102
Cathode Potential at 200 mA/cm^2, mV/RHE	684	710	724	759

*Flow rates were maintained at three stoich at 325 mA/cm^2.

performance characteristics on the air flow rate. By maintaining the hydrogen utilization at about 80 percent, the overall cell potentials at various flow rates were measured as a function of current density. After correcting for ohmic losses and anodic overpotentials, typical polarization curves for oxygen reduction are given in Figure 3.1.4-10. At current densities below 100 mA/cm^2, the polarization potentials of the air electrode were approximately independent of the air flow rate. However, the observed limiting current densities are extremely sensitive to the flow rate. Increasing air flow rate resulted in a large increase in the limiting current density.

In the electrolyte film, the mass transfer resistance of dissolved oxygen molecules produces the so-called concentration overpotential. From the measured limiting current densities, the concentration overpotentials at 325 mA/cm^2 and various air flow rates were calculated and are shown in Table 3.4.1-11. Note that the achievable maximum current densities were predicted on the basis of 100 percent oxygen utilization at different flow rates. The observed limiting current densities were close to the predicted maximum current densities. The concentration overpotentials decreased significantly with increased air flow rate. At the projected air flow rate of about two stoich, there was approximately 7 mV cathode potential loss, resulting from the concentration overpotential in the electrolyte film.

Shown in Figure 3.1.4-11 are the internal resistances as a function of air flow rate in stoichs. At a constant flow rate, for example three stoich, the increase of operating current density from 100 to 325 mA/cm^2 reduced the internal resistance by $\sim$ 0.4mΩ.

For a particular test cell, the decrease of internal resistance resulted from the variation of acid concentration. It is thus concluded that, at constant air flow rate (in stoichs), the electrolyte concentration in phosphoric acid fuel cells is dependent on the operating current density.

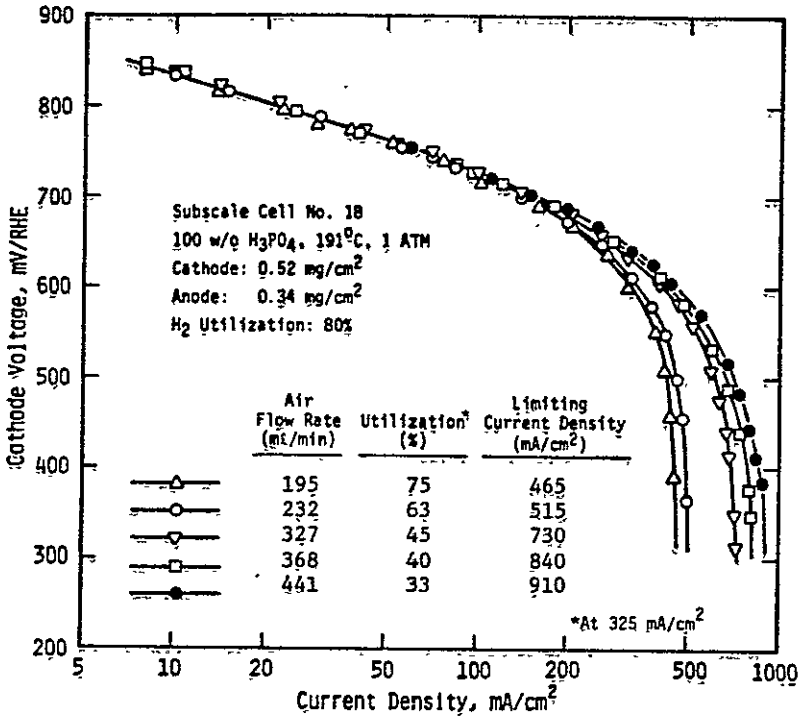

Figure 3.1.4-10. Cathode Performance Characteristics at Various Air Flow Rates

TABLE 3.1.4-11

EFFECT OF AIR FLOW RATE ON CONCENTRATION OVERPOTENTIAL

Air Flow Rate m/min	Air Flow Rate Stoich*	Observed Limiting Current Density (mA/cm^2)	Maximum Achievable** Current Density (mA/cm^2)	Calculated Concentration Overpotential at 191°C and 325 mA/cm^2 (mV)
195	1.33	465	432	12
232	1.58	515	514	10
327	2.22	730	722	6
368	2.50	840	813	5
441	3.00	910	975	4

*Referring to the current density 325 mA/cm^2

**Based on 100 percent oxygen utilization

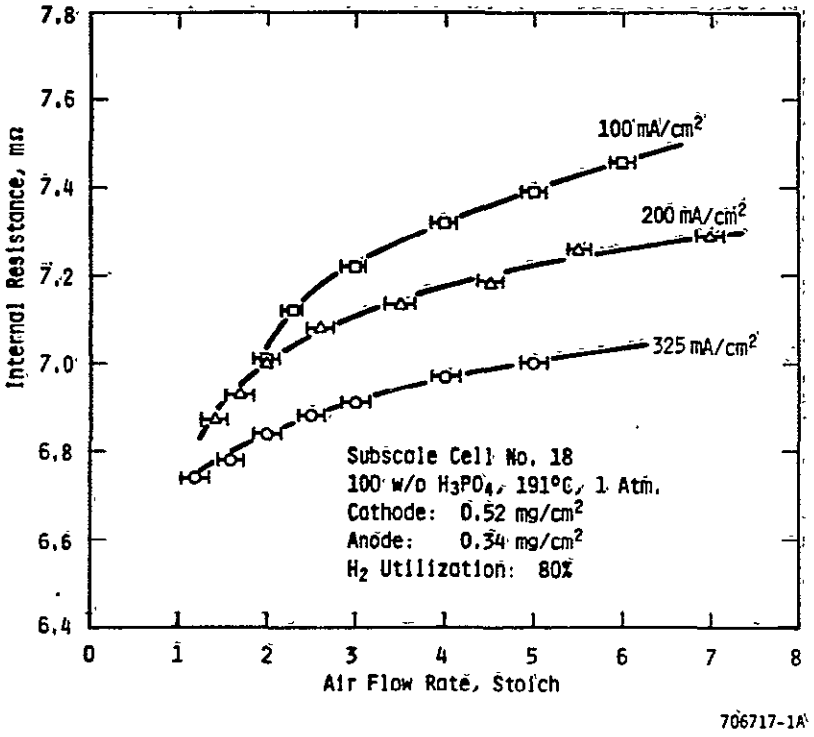

Figure 3.1.4-11. Variation of Internal Resistance with Air Flow Rate at 100, 200, and 325 mA/cm^2

PRESSURIZED SUBSCALE CELL TESTING

The first Westinghouse provided subscale pressurized test loop was completed and checked out in late March, 1983 and is shown in Figure 3.1.4-12. The second system was approximately 90 percent complete at this reporting period. Each system is capable of testing four subscale cells simultaneously at pressures of up to 1,380 kPa (200 psig).

The first four cells tested in the operational system were SC-049, 060, 061, and 062 and their component identification is provided in Table 3.1.4-12. Figure 3.1.14-13 shows the variation of measured terminal voltage and IR-free cell voltage of SC-062 at 325 mA/cm^2 as a function of pressure up to 6.8 atm, 690 kPa (100 psia). The test was conducted at 190°C, 5 stoich air flow rate, and 80 percent hydrogen utilization. At 4.74 atm (70 psia), the initial terminal voltage performance of this cell was about 692 mV, which is 10 mV higher than the projected cell performance goal for the PAFC power plants. In reference to the ambient pressure, the cell voltage gains arising from the pressurization are illustrated in Figure 3.1.4-14 for subscale cells SC-060, SC-061 and SC-062. The linear line depicts the anticipated voltage gain as represented by an equation of the form:

$$\Delta V_{gain} = \frac{2.3\ RT}{4F}\left(1 + \frac{5}{\alpha c}\right) \log P \qquad [1]$$

where P is the operating pressure in atm. At the projected plant operating pressure of 4.74 atm (70 psia), the average voltage gain in these cells is 108 mV, which is in good agreement with the value predicted by Eq. [2].

Under the operating conditious: 325 mA/cm^2, 190°C, 4.74 atm, 5 stoich air flow rate and 80 percent H_2 utilization, long-term performance stability studies were conducted on the four subscale cells. The variation of cell performances with time is presented in Table 3.1.4-13. Subscale cell SC-049 was pre-tested at 200 mA/cm^2 and ambient pressure for over one week. Thus, its internal resistance and cell voltages were relatively stable during the testing. Prior to the pressurization tests, subscale cells SC-060 through

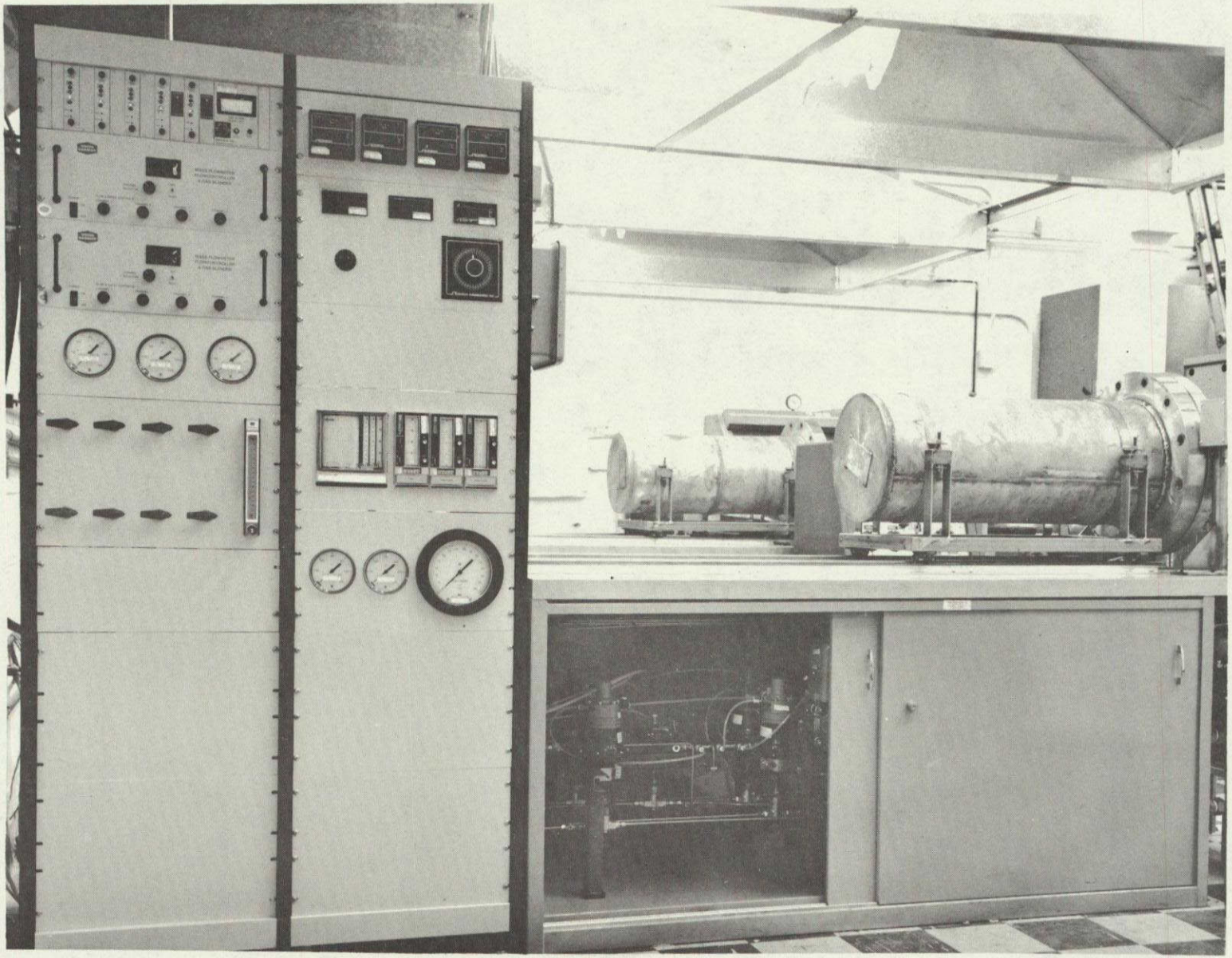

Figure 3.1.4-12. Subscale Pressurized Test Facility

TABLE 3.1.4-12

PRESSURIZED CELL COMPONENT IDENTIFICATION

Cell Ident.	Cathode		Anode		Catalyst Lot No.
	Ident.,	loading mg/cm^2	Ident.,	loading mg/cm^2	
SC-049	C055-3	0.43	A087-8	0.29	1
SC-060	C119-4	0.49	A123-1	0.28	3
SC-061	C116-2	0.48	A121-1	0.30	3
SC-062	C119-4	0.49	A123-1	0.28	3

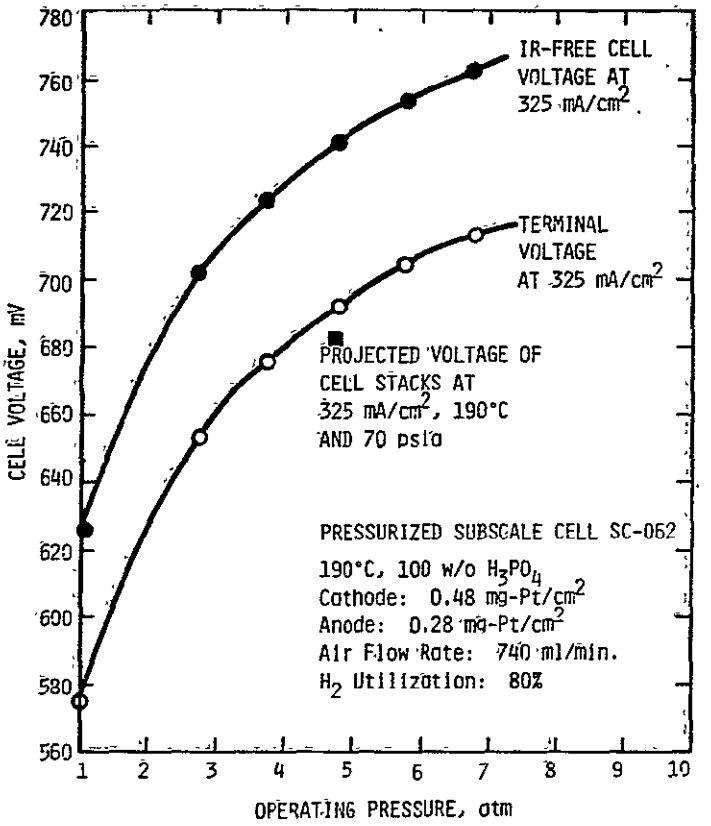

Figure 3.1.4-13. Variation of Terminal Voltage and IR-Free Cell Voltage at 325 mA/cm^2 with Operating Pressure for Subscale Cell SC-062

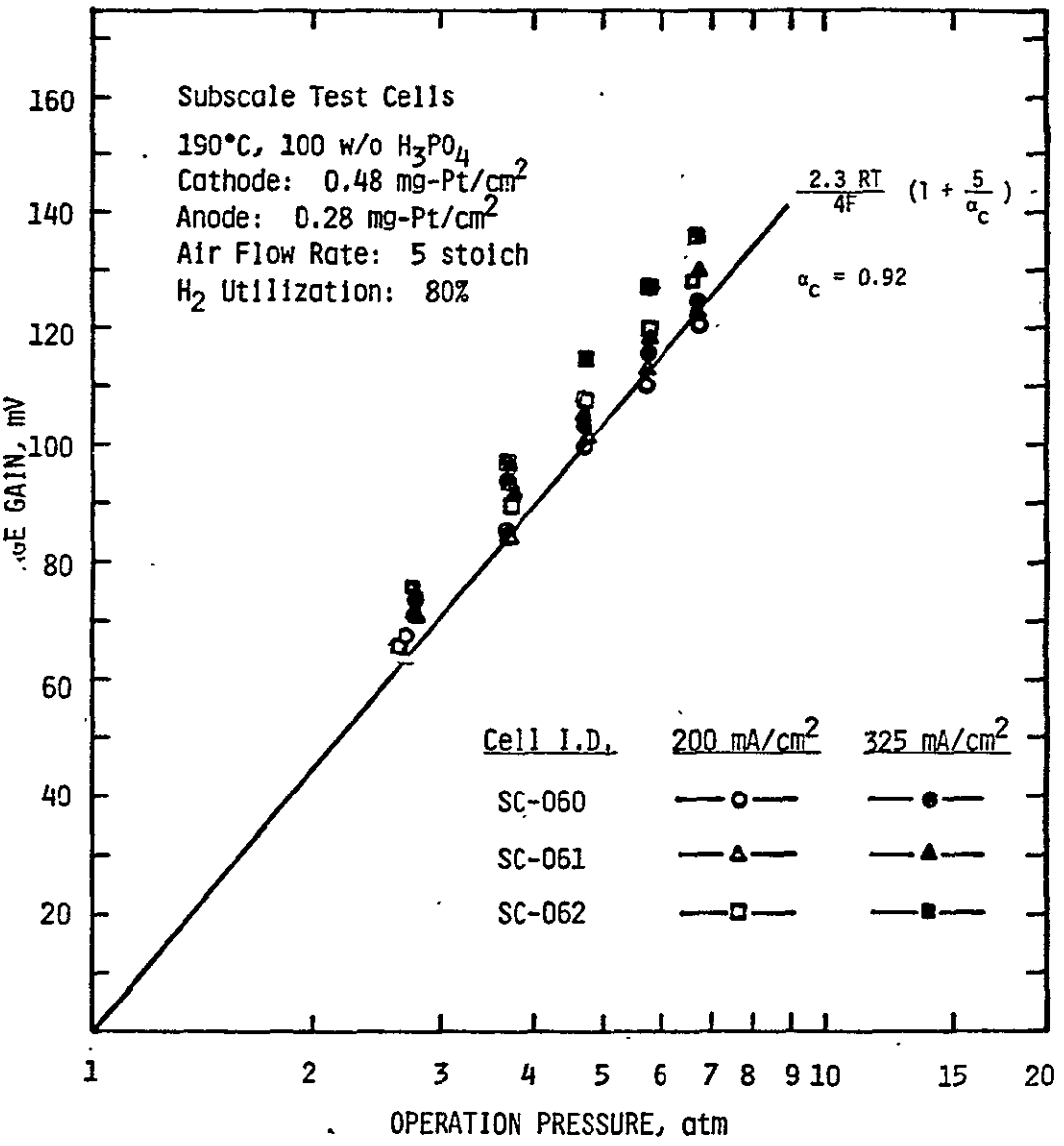

Figure 3.1.4-14. Cell Voltage Gain at 200 and 325 mA/cm^2 as a Function of Operating Pressure

TABLE 3.1.14-13

VARIATION OF PERFORMANCE CHARACTERISTICS OF PRESSURIZED SUBSCALE CELLS WITH TIME

Cell I.D.	Performance	Testing Time* (at 325 ma/cm^2)		
		60 Hours	630 Hours	820 Hours
SC-049	Terminal Voltage, mV	649	666	661
	Internal Resistance, mΩ	7.5	7.5	7.7
	IR-Free Cell Voltage, mV	710	727	723
SC-060	Terminal Voltage, mV	681	668	658
	Internal Resistance, mΩ	7.0	7.9	8.6
	IR-Free Cell Voltage, mV	739	732	728
SC-061	Terminal Voltage, mV	674	653	643
	Internal Resistance, mΩ	7.7	9.1	9.8
	IR-Free Cell Voltage, mV	737	727	723
SC-062	Terminal Voltage, mV	689	676	673
	Internal Resistance, mΩ	6.0	7.1	7.6
	IR-Free Cell Voltage, mV	738	734	735

*Subscale cells were tested at 325 mA/cm^2, 190°C, 4.74 atm, 5 stoich air flow rate and 80 percent H_2 utilization.

SC-062 were operated at ambient pressure for less than 100 hours. The internal resistances of these three cells increased with time, presumably due to the gradual loss of electrolyte. The IR-free cell voltages also decreased in the long-term test. Starting initially in May, 1983, the air flow rate was intentionally reduced to 2.5 stoich and the pressurized stability studies of these four subscale cells are continuing.

3.2 NINE-CELL STACK DEVELOPMENT

3.2.1. DEVELOPMENT STATUS

The nine-cell stack design was completed and sufficient components for seven stacks were manufactured. Procedures for manufacture of the cell repeating components, electrode/plate subassembly, and final stack assembly were developed. Manufacturing and assembly personnel were trained to these procedures.

The nine-cell stack test program was performed utilizing two Westinghouse provided test facilities. Six stacks were assembled of which five were tested. One stack was used to gain stack assembly experience. The ability to conduct two tests simultaneously was demonstrated. The longest test duration was 670 hours.

Operation of each of the five stack tests had to be curtailed due to one or more cells in each stack limiting operation. Primarily, these stacks have provided a better understanding of the stack mechanics during assembly and test operations. They have also provided needed experience in pressurized stack testing. Characterization testing, related to a basic understanding of stack design parameters and interaction effects, was initiated which includes evaluation of acid upset conditions and limited mapping evaluations.

Problems were encountered early in the program with producing flat molded/heat treated bipolar and cooling plates. While development work continued to learn how to produce consistently flat plates, the plates used were machined from molded blank plates and subsequently heat treated to 900°C.

Final reports were issued for the first two stacks and test results for the remaining three stacks are continuing to be evaluated.

3.2.2 NINE-CELL STACK DESIGN DESCRIPTION

The developed nine-cell stack design is shown in Figure 3.2.2-1. This stack is designed to reproduce, functionally, the 10 kW stack design to the extent permitted by reasonable consideration of cost and test facility constraints. All repeating components of the stack are the same as in the 10 kW design. The stack design incorporates a cross tie bar and tie rod arrangement for loading the stack, and other non-repeating hardware features.

The molded bipolar plates are provided to separate the process gases and have a "zee" channel configuration on both sides. The two cooling plates have a "zee" channel configuration on one side and a "tree" cooling channel configuration on the opposite side, the end plates have a "zee" channel configuration on one side and a straight, closed-end groove pattern on the opposite side. Edge seals (flat gasket type) of a fluoroelastomer are compressed between adjacent plates to seal against acid and process gas leakage. The "tree" side of the cooling plates are butted against each other to form the cooling air passages. Fluoroelastomer edge seals fit between cooling plates along the process gas sides, only, to prevent process gas leakage between process manifolds and cooling air leakage into process manifolds. Anode and cathode electrodes are bonded at the edges to their respective surfaces of the bipolar, cooling, and end plates. The ERC MAT-1 layer fits inboard of the edge seals between the anode and cathode. The edge seal surrounding the anode and MAT-1 is narrower than that surrounding the cathode. Thus, the edges of the MAT-1 and anode are compressed by the cathode edge seal to prevent internal process gases cross leakage around the edge of the cell. This design also seals against acid weepage at the outside of the stack since the MAT-1 is completely enclosed by the edge seals.

The plate "zee" process channel faces incorporate 0.038 cm (0.015 inch) thick by 0.794 cm (0.312 inch) wide graphite bridges which span the process gas channels at the edges of the plates. The bridges prevent the edge seals from

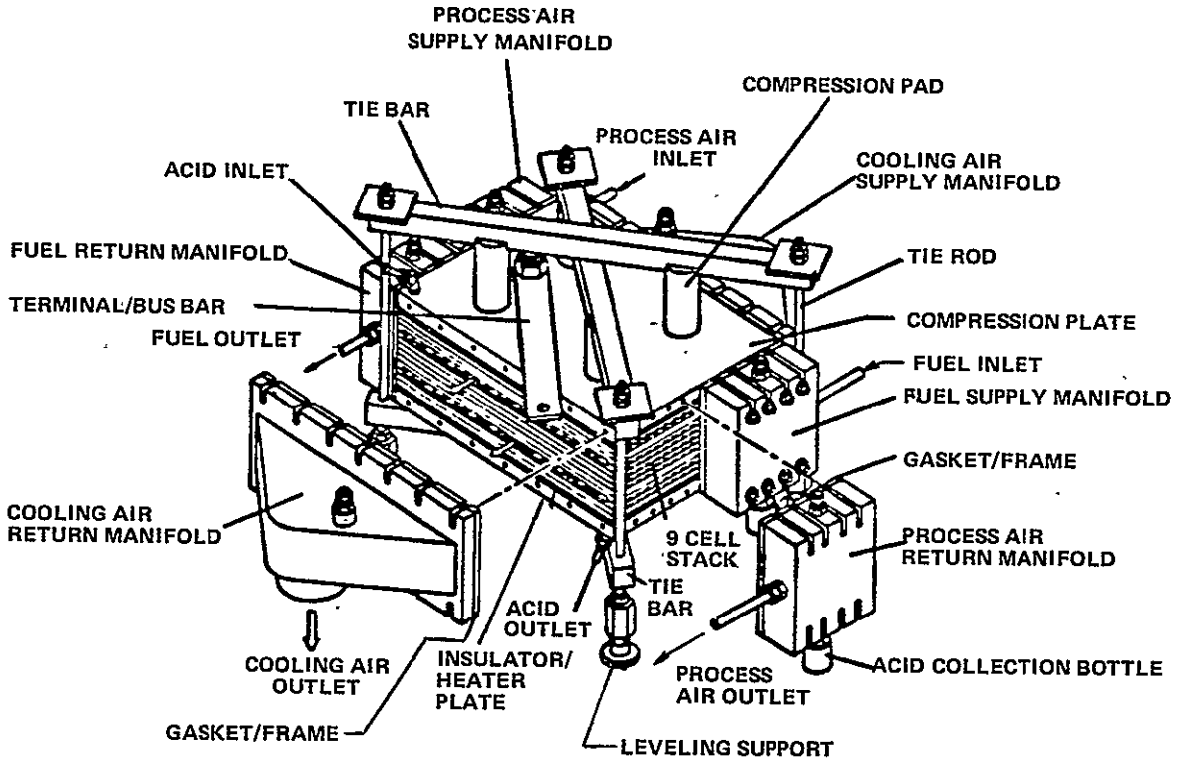

Figure 3.2.2-1. Nine-Cell Stack Assembly

compressing into the grooves and restricting gas flow. The graphite material is compatible with the plate material and is strong enough at stack operating temperatures to withstand the compressive loads caused by the edge seals.

The stack is terminated at each end with a gold/nickel plated copper current collector plate followed by two Micarta insulator plates and a carbon steel compression plate. The electrical connection takeoff is through a centrally located terminal post. Guard heaters, which fit into recesses in one of the insulator plates of each set, are provided to maintain in situ five cell stack temperature conditions similar to repetitive five cell conditions of larger stacks.

The nine-cell stack design uses a cross tie bar stack clamping arrangement with compression plates that are the same size as the cell plates. Therefore, the tie rods are removed from the cooling manifold region allowing manifolds to be used for separate monitoring and control of the cooling air.

The process gas manifolds are aluminum with corrosion resistant Viton coating to protect against phosphoric acid attack. Their design allows for universal installation at either the process fuel or process air inlet or exit locations. Manifold sealing is provided by flat gaskets. A layer of uncured Viton material is applied in contact with the side face of the stack. A Micarta insulator frame and a layer of cured Viton material are placed between the uncured layer and the manifold. At an elevated temperature preconditioning process, the uncured layer cures and conforms to the face of the stack. After preconditioning, subsequent manifold removals are at the separation between the manifold and the insulator frame so that the frame to stack seal remains undisturbed. The process gas manifolds are bolted onto the edges of the top and bottom compression plates. The cooling air manifolds are also Viton coated aluminum and are bolted and sealed to the stack similar to the process gas manifolds.

Other features of the nine-cell stack design include acid fill and drain tubes sealed to the stack end plate by a fluoroelastomer O-ring. The process gas

manifolds have a provision for acid drain tubes to collect acid that may accumulate in the bottom of the manifolds, either through entrainment in the exit gas flow or through leakage at the electrode/edge seal interfaces. All manifolds have ports for attachment of pressure sensing instrumentation. When installed in the test vessel, the nine-cell stack is supported on standoffs connected to the four tie rods.

3.2.3 NINE-CELL STACK TESTING

In order to establish key design parameter data and interaction effects needed to guide stack and module design efforts, nine-cell stack tests were performed that included:

- Performance and mapping characterization
- Transient characterization
  - startup/shutdown
  - cyclic effects on performance
- Endurance characterization
  - cell performance trends
  - acid makeup
- Characterization of stack mechanics
  - stack loading/relaxation
  - cell gasketing
  - stack resistance

Test specifications and test operating plans were developed for the first seven planned nine-cell stacks (identified as stacks W009-01 thru -07). The test objectives for stacks W009-04 thru -07 are summarized in Table 3.2.3-1 and additional data pertaining to the stack configuration on features is shown in Table 3.2.3-2.

TABLE 3.2.3-1

NINE CELL STACKS - W009-04, 05, 06, AND 07

General Objectives

- Establish reference baseline performance and determine reproducibility of existing technology.
- Demonstrate stack operating characteristics and assess repeatability over the operating range.
- Provide screening information to evaluate performance trends of heat treated catalyst and dry bonded electrodes.

Additional Specific Stack Objectives

W009-04	W009-05	W009-06	W009-07
• Determine performance variation within a stack.	• Assess performance trend with heat treat catalyst.	• Provide additional tests to increase confidence limits of stack performance variation.	• Assess performance trend with heat treat catalyst and dry bonded electrodes.
• Evaluate Test Loop #3 repeatability.	• Evaluate Test Loop #3 repeatability.	• Assess the effects of pressure cycling.	• Assess the effects of compressive load cycling.

TABLE 3.2.3-2

STACK TEST PROGRAM

Stack ID: W009	-04	-05	-06	-07
Cells 1 and 2	Baseline	900° Ht Catalyst	Baseline	Dry Laminated and 900° Ht Catalyst
Cells 3 thru 7	Baseline	Baseline	Baseline	Baseline
Cells 8 and 9	Baseline	900° Ht Catalyst	Baseline	Dry Lamination and 900° Ht Catalyst
Bipolar Plates	← Machined →			
Seals	← Teflon →			
Acid	← 93% 42 ml to 46.5 ml →			
Load Instrument	No	Yes	No	Yes
Additional Tests	Start/Stop	Load Var.	Start/Stop	Load Var.
Test Loop	2 → 3	2 → 3	2	3

Summary test results for stacks W009-01 thru -06 inclusive are summarized in Table 3.2.3-3. Test reports for stacks W009-01 and -02 were prepared and issued.

3.3 10 kW FUEL CELL STACK DEVELOPMENT

3.3.1 DEVELOPMENT STATUS

A 10 kW stack design requirements document was developed and a final design in accordance with these requirements was essentially completed. The final detailed design for all long lead components was completed and then released for procurement. Initial cost and delivery difficulty was encountered with the polyethersulfone molded manifolds. After numerous discussions with vendors, however, it was concluded that the manifold could be made from an extruded slab of polyethersulfone and machined as required for the fuel and oxidant manifold chambers.

3.3.2 10 kW STACK DESIGN DESCRIPTION

The 10 kW stack mounted in the test loop pressure vessel is shown in Figure 3.3.2-1. The stack contains 44 cells in eight groups of five with two cells at each end. Each group of five cells is separated by cooling channels. The remaining cell components in the five-cell group are separated by bipolar plates. the Section 3.2.2, nine-cell stack discussion relative to the "zee" and "tree" pattern bipolar and cooling plates, respectively, is applicable for this stack and is therefore not repeated herein.

Viton elastomer seals are provided along the edges of the "Zee" channel faces. The seals are supported at the plate edge by the graphite bridges. The electrodes and matrix are confined to the area inside the seals. Seal thickness is set to accommodate tolerance variations in the electrodes and allow approximately 12 percent compression of the electrodes and assembly.

The cell stack ends in gold/nickel-plated copper collector plates followed by Micarta insulator and carbon steel compression plates. Four stainless steel tie rods, extending the length of the stack and inserted through holes in the

TABLE 3.2.3-3

NINE-CELL STACK SUMMARY

Stack W009-01

- Initial evaluation of stack mechanics
- Developed stack compression procedure
- Utilized for checkout of test facility loop #2

Stack W009-02

- Operated 500 hours (180 hours at 1 atm, 320 hours at 4.7 atm); 603 mV/cell avg. at 325 mA/cm^2, 190°C, 4.7 atm
- Evaluation of acid upset conditions and subsequent impact on corrosion of bipolar plate
- Initial evaluation of electrical transients and ripple effects

Stack W009-03

- Evaluation of modified Viton cell seal design
- Develop cell subassembly and stack assembly procedures

Stack W009-04

- Operated 670 hours (170 hours at 1 atm, 500 hours at 4.7 atm); 620 mV/cell avg. at 325 mA/cm^2, 190°C, 4.7 atm with SRG
- Conducted limited mapping characteristics
- Utilized for checkout of test facility loop #3

Stack W009-05 and W009-06

- Testing initiated and continuing.

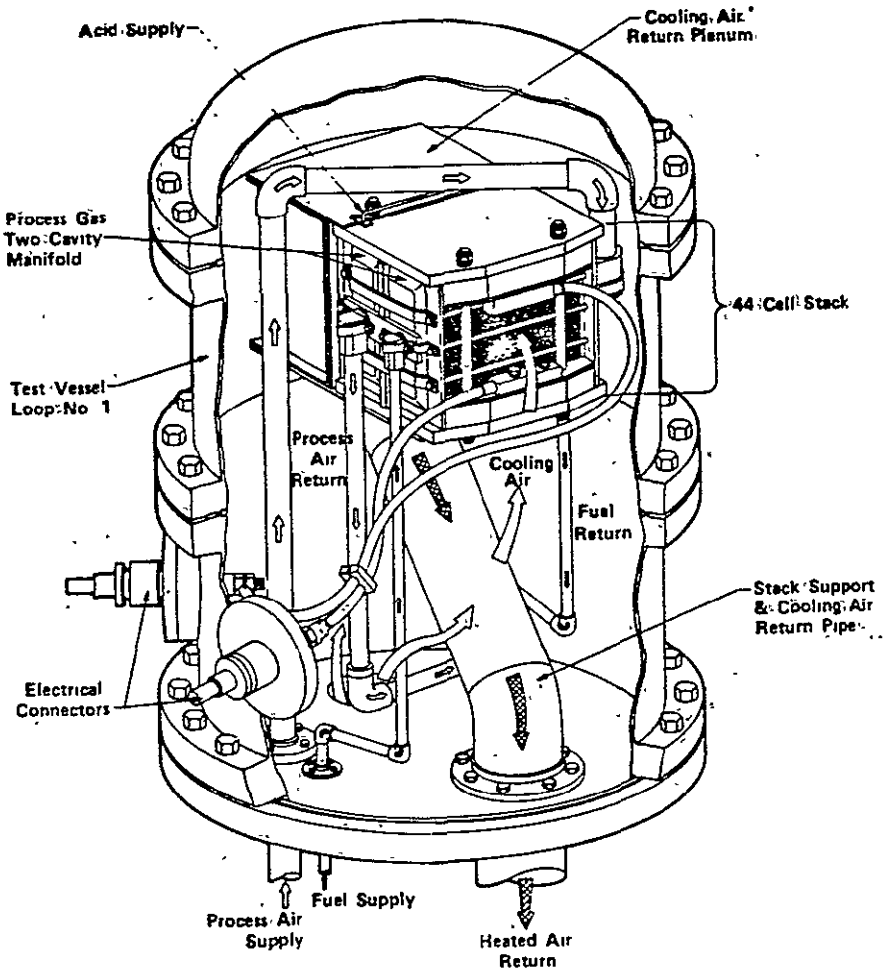

Figure 3.3.2-1. PAFC 10 kW Stack Test Assembly

edges of the compression plates, achieve the required initial clamping pressure of approximately 50 psi. The compression, insulator, and copper collector plates are made somewhat wider than the cell plates to accommodate the clamping rod holes and to provide support for the electrical connections at the edges of the collector plates. The compression plates are also somewhat longer than the insulator and copper collector plates which are the same length as the bipolar plates, in order to locate the process fluid supply manifolds on the end faces of the stack. A shim plate, made of Micarta material of the same shape as the insulator plate, is provided at the top of the stack to allow the distance between the compression plates to be matched with the overall length of the manifolds, while accommodating the overall stack height resulting after compression.

The manifolds are made from a fiberglass filled polyethersulfone material and are held in contact with the end faces of the stack by tie rods. Teflon tubing around the tie rods insulates them from the stack. The manifolds are sealed to the faces of the stack by 0.47 cm (3/16 inch) diameter Viton O-rings. Two O-rings are employed in each manifold, one encircling the fuel cavity and the other process air cavity.

The process gas connections to the manifolds are provided with removable orifices to ensure a controlled pressure drop across the stack. Flow deflectors are provided between the orifices and the stack to prevent impingement of the orifice jet on local plate flow passages and ensure a well-distributed, low velocity, flow of gases into the manifold cavities. The connections are inserted through simple circular holes in the manifolds, sealed by fluorelastomer O-rings and held in place by retainer clamps and bolts threaded into the manifolds. The connections also support the process gas stainless steel piping.

The phosphoric acid is supplied to the stack through a 0.94 cm (0.375 inch) diameter Teflon tube. The tube is clamped to a machined Teflon connector retained in a drilled hole in the compression plate and sealed to the uppermost cell end plate by means of a fluorelastomer O-ring. Provision is made for

shimming at the connector retainer to compensate for variations in the stack shim plate thickness. Excess acid is drained at the bottom of the stack using a similar arrangement. The stack acid supply and drain lines are terminated in Teflon penetrations at the pressure vessel. The penetrations are sealed by steel caps during operation but are accessible after shutdown by removal of the steel caps.

The stack electrical connections consist of copper connectors clamped to the copper collector plates with bolts and supported from the Micarta insulator plates. A 4/0 nickel coated TFE insulated cable is swaged to the copper connectors and routed to insulated pressure vessel penetrations. The cables are supported along their length to prevent whipping under short circuit fault conditions.

Provision is made for instrumentation leads via three 15 cm (6 inch) diameter penetrations in the facility pressure vessel.

3.4 25 kW SHORT STACK DEVELOPMENT

3.4.1 DEVELOPMENT STATUS

The 25 kW stack design requirements document was developed and in accordance with these requirements a design package was completed. This design package consisted of detail and assembly drawings, supporting analysis, and a design description document. A partial release of long lead hardware (i.e., the plastic process distribution manifolds and piping details) was made. To date, all potential vendors contacted have failed to submit unqualified, acceptably priced quotations for injection molding the manifolds. Suggestions were received for performing the work as a development program, with no guarantee of success and at the risk of substantial monetary increments. Consideration is being given to machining the 25 kW stack manifolds from extruded stock and deferring the injection molding process to the 100 kW stack, where larger initial monetary investments could more reasonably be justified.

C-3

3.4.2 25 kW STACK DESIGN DESCRIPTION

The 25 kW stack mounted in the test facility pressure vessel is illustrated in Figure 3.4.2-1. The stack assembly is supported from a carbon steel lower support plate which is mounted on the cooling air outlet pipe and two support columns. Many of the 10 kW stack design features described in Section 3.3.2 are applicable to the 25 kW stack, and thus are not reported herein.

The 25 kW stack contains 104 cells in 20 groups of five with two cells at each end of the stack. Each group of five cells is separated by cooling channels with the design identical to that used for 10 kW stacks.

Figure 3.4.2-2 is an illustration which shows the "Zee" process channel and the "treed" cooling channels geometry.

The cell stack ends in gold/nickel-plated copper collector plates followed by Micarta insulator plates and carbon steel compression plates. Four stainless steel tie rods, extending the length of the stack and inserted through holes in the edges of the compression plates, achieve the required initial clamping pressure of approximately 50 psi. Provision is made for heating the tie rods on the inlet side of the stack to minimize the tendency for the stack to bow due to differential thermal expansion of the rods. Heated air is channeled from the cooling air outlet plenum through grooves machined in the upper insulator plate to the inner diameters of insulating tubes placed around the cold-side rods. The heated air then flows downward in the annular spaces between the rods and the insulating tubes to grooves machined in the lower insulator plate. Reference to Figure 3.4.2-1 should be made for details of these features. The grooves in the lower plates then transfer the air to the process air outlet bobbin connectors.

The manifolds materials and design configuration is also similar to that described for the 10 kW stack. The 25 kW stack manifolds, however, are reinforced by stiffening ribs which also serve to divide up each of the manifold cavities into a number of smaller compartments. Each compartment is supplied from, or supplies, an individual gas connection. The stiffening ribs

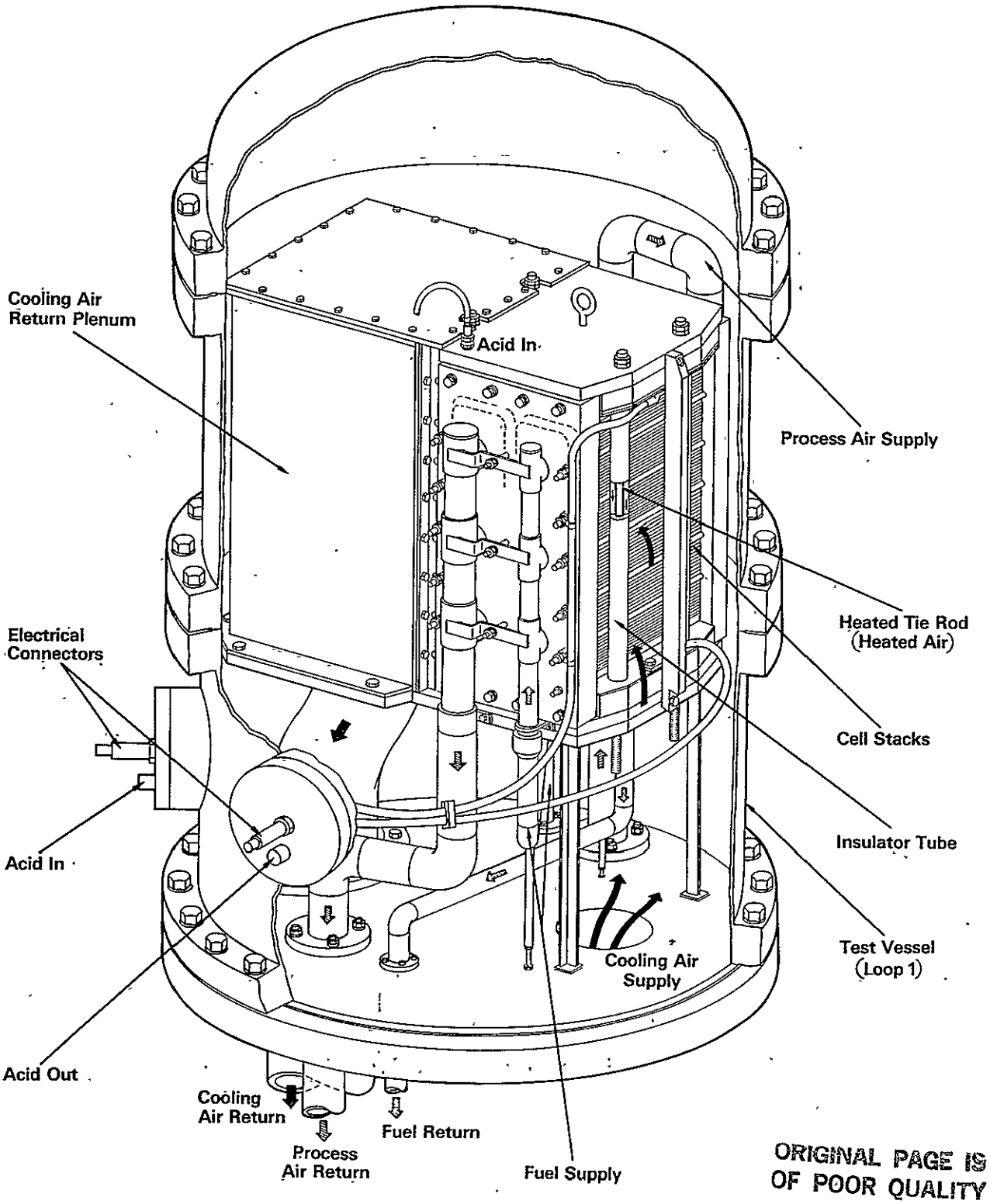

Figure 3.4.2-1. 25 kW Stack Design

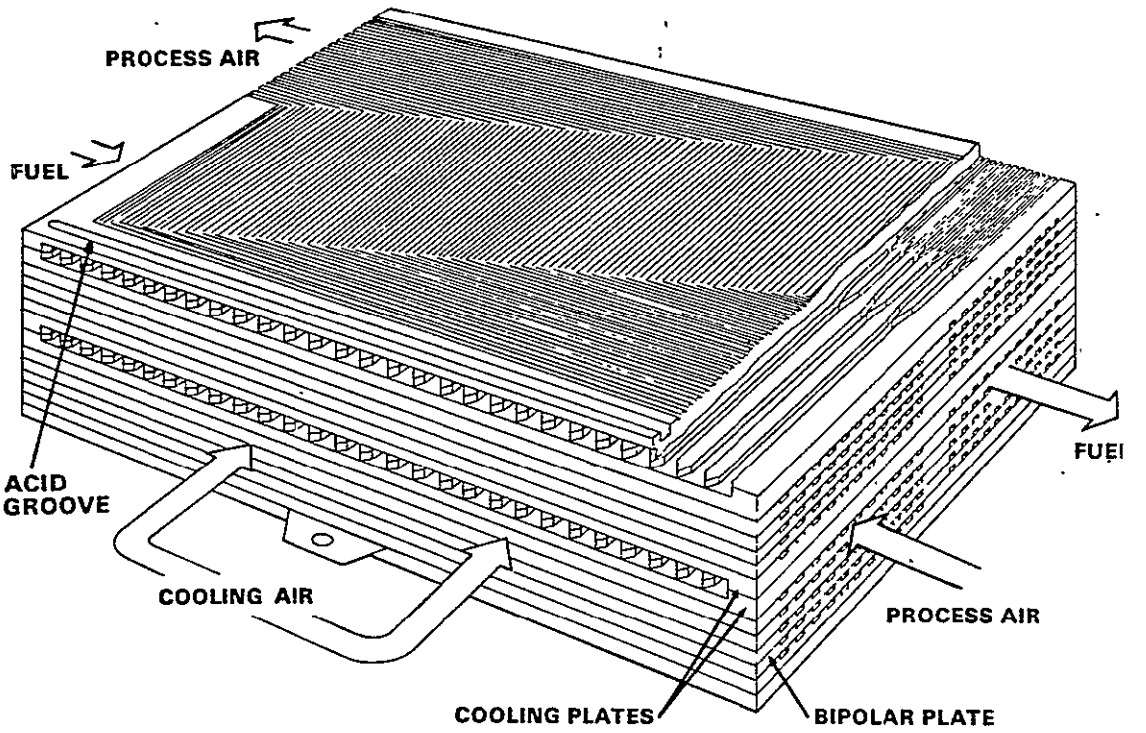

Figure 3.4.2-2. Baseline Fuel Cell Stack

and associated detail and much of the detail described in the following paragraphs, are defined in Figure 3.4.2-1.

The process gas "Tee" connections to the reinforced plastic manifolds are made of unreinforced polyethersulfone and are provided with removable orifices to ensure good distribution of flow along the length of the stack. Flow deflectors are provided between the orifices and the stack to prevent impingement of the orifice jet on local plate flow passages and to ensure a well-distributed, low velocity, flow of gases into the manifold cavities. The "Tee" connections are inserted through simple circular holes in the manifolds, sealed by fluorelastomer O-rings and held in place by retainer bars and bolts threaded into the manifolds. The "Tee" connections also support the process gas piping along the length of the manifolds. Simple polyethersulfone "bobbin" type sections of pipe, supported between the "Tee" connections and sealed by O-rings, are used in the supply and return piping to accommodate thermal expansion motions and misalignment. This arrangement also avoids the application of large forces to the plastic manifolds during the attachment of the piping.

Fuel supply and return, and process air return bobbin connectors are supported between the lowermost manifold "Tee" connections and stainless steel piping weldments mounted from the lower pressure vessel head. Positive support from the stack lower compression plate is provided for these bobbin connectors so that, when the stack is removed from its supporting structure, disconnection of the process fluid lines occurs automatically as the lower ends of the bobbin connectors are withdrawn from the piping weldments mounted on the vessel lower head. The uppermost manifold "Tee" connections are terminated by means of caps held in place by rollpins.

The process air supply bobbin connector at the uppermost manifold "Tee" connection engages at its upper end with a transfer pipe connected at its other end to a penetration at the vessel lower head. Heated and filtered air is supplied to this vessel penetration, from the facility, through an external pipe and is then conveyed to the upper end of the transfer pipe and into the

bobbin connector and "Tee" connections to the manifold. The lowermost manifold "Tee" connection of this piping is terminated by means of a cap held in place by rollpins.

In the particular arrangement illustrated, a continuously operating acid management system, if required, could be incorporated and is being considered. The cap details shown would require modification to provide for this capability. Alternatively, an internal acid reservoir can be accommodated in the pressure vessel if such a system is determined to be more suitable.

3.4.3 STRUCTURAL ANALYSIS

A structural analysis of the 25 kW stack design was completed which included the stack mechanics and the stack-to-vessel interface support structure. A stack mechanics evaluation was performed to determine the component loads, deflections, and stresses. The general purpose structural analysis program, WECAN (Reference 3-1), was used to perform this static analysis. The materials data base was composed of known industrial data, empirical test data, and elastic properties of the current fuel cell stacks.

Anisotropic material properties, directional thermal expansion values, and effective material properties were required to accurately simulate the structural characteristics of the stack. It was assumed that all components (anode-matrix-cathode) and the bipolar plates can be modeled as a structural material with effective material properties. This eliminates individual definition of each cell. Anisotropic material properties are used to simulate large axial deflection with very small lateral deflections. Directional thermal expansion values were employed to simulate the manifold assembly procedure and the negative creep effects in the cell components.

Ref. 3-1 "WECAN-Westinghouse Electric Computer Analysis," 82-7E7-WESUP-R1, Third Edition, Rev. R. Edited by A. W. Filstrup.

3.4.3.1 MODEL DEVELOPMENT

The 25 kW structural model was based on an earlier representation of the 10 kW stack mechanics model. This model was updated to include the following:

- Current effective material properties for the cell components (anode-matrix-cathode).
- Anisotropic (or orthogonal) material properties to simulate the correct lateral displacement response of the stack at the cell component level.
- More accurate representation of the plastic manifold to verify actual manifold stresses and deflections.
- The elimination of belleville springs in the 10 kW stack compression load train.

Due to the element size of the existing 10 kW structural model (785 elements), this model was used with some corrections to account for differences in the overall height of the stack instead of developing a new, larger 25 kW model.

Geometrically, the 25 kW stack contains three planes of symmetry. The three planes of symmetry are: 1) centerline of 41.9 cm (16.5 inch) side, 2) centerline of 29.8 cm (11.75 inch) side, and 3) mid-plane of the overall compressed height.

Generally, 3-D isoparametric solid elements were used with orthotropic material properties. The elements were generated in a manner to permit easy modification of material properties and accurate simulation of the stack geometry. The manifold detail was improved over the 10 kW model to better define the stresses and displacements in the new plastic manifold. The axial and horizontal rib sections were added to simulate the reinforcement of the manifold.

The combined isometric view of all components of the 1/8 section model of the 25 kW stack is shown in Figure 3.4.3-1. The compression plate and insulation plates are shown to be coincident for simplicity.

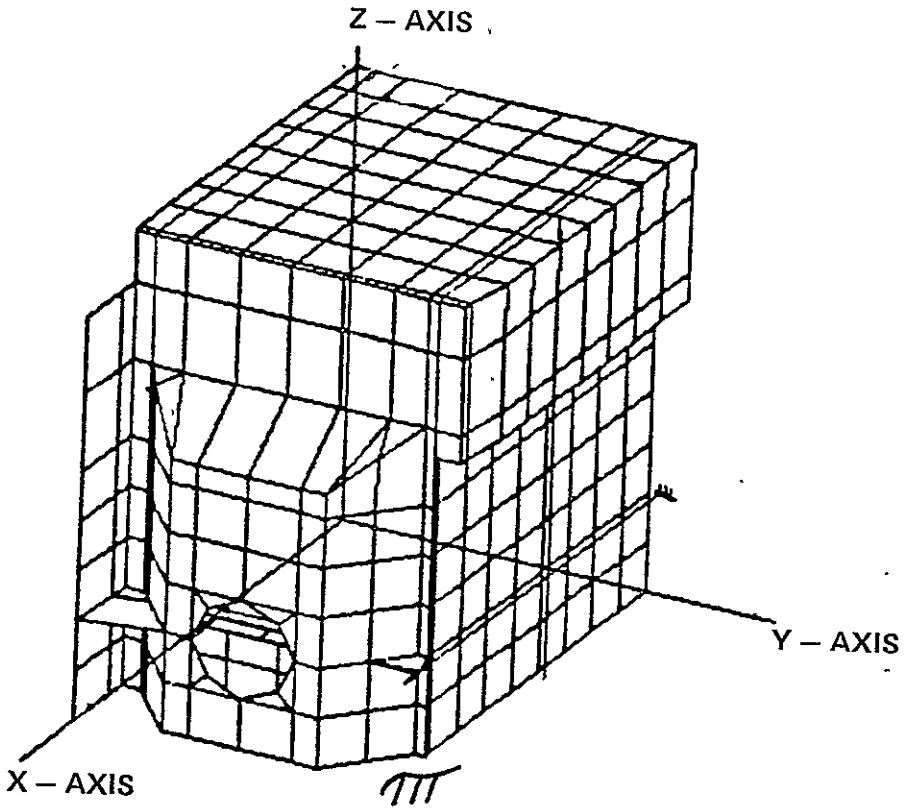

Figure 3.4.3-1. Analytical Model Used for 25 kW Stack Evaluation

3.4.3.2 STACK LOADING CONDITIONS

The purpose of this evaluation was to determine the response of the stack to specific structural and thermal conditions. The following four loading conditions were selected:

- Pre-Assembly Condition - This condition pertains to the situation when the stack has been assembled and heated to approximately 77°C (170°F). The stack is then compressed to an average of 0.344 MPa (50 psi) over the fuel cell area. This assumes that the manifolds have not been installed.
- Assembly Condition - This condition extends the preassembly condition to include the manifold at 77°C (170°F). The worst case condition was evaluated with the assumption that the manifold has a 0.0355 cm (0.014 in) interference between the compression plates.
- Normal Operating Condition - This condition assumes the cell components of the stack to be at normal operating temperature of 190°C (375°F). Cooling inlet air temperature is assumed to be 146°C (295°F) and no gas pressure differential is assumed to exist across the stack.
- Long Term Operation - This case provides a preliminary indication of the possible effect of creep on the cell components. The thermal and mechanical conditions are the same for the normal operating condition except that the cell materials and seals are specified to have a negative coefficient of thermal expansion to represent the dimensional changes due to creep. For this case the assumption was made that each cell interface creeps 0.00846 cm/cell (0.0033 inches/cell) over the operating life of the stack.

The 25 kW stack was designed with a manifold to provide a passive compressive load mechanism. Once the compression loads for the stack and manifold are established, changes in load on the stack are determined by temperature changes and creep effects. The stack was modeled based on this situation. The tie rod displacements are set to produce the preloads desired in the pre-assembly condition and they then remain constant throughout the analysis. Changes in the stack pressure and bolt loads then occur as functions of the temperature changes.

3.4.3.3 ANALYSIS SUMMARY

The pre-assembly and assembly load cases were performed to determine the following aspects of the stack assembly procedure:

- Determine gap between compression plates after the stack was compressed.
- Determine the required bolt deflection and load to produce an average of 0.34 MPa (50 psi) pressure on the stack.
- Determine the distributed loads on stack, manifold and seals when the stack is completely assembled and held at dry room temperature conditions.

The results of these cases indicated low stress with only a minimal amount of load on the manifold. As expected, a stress discontinuity was found between the cell components and the seal region.

The normal operation case indicated loads and stresses which were well within the design limits for this operating condition. The stack bolt loads manifold stresses and cell compressive pressure, all increased due to the change in temperature of 114°C (205°F). The cell compressive pressure only increased from 0.35 MPa (49.0 psi) to 0.36 MPa (52.0 psi). The increased stack bolt load developed due to this temperature change appears to be properly distributed between the stack and manifold. The manifold peak compressive stress increased to 20.7 MPa (3005 psi). This stress is below the short term tensile strength of 76 MPa (11,028 psi) @ 180°C but the long term strength may be closer to 27.6 MPa (4000 psi) which would reduce the margin of safety currently indicated.

The long term operation case represents the initial estimate of the effect of cell component creep on the stack loads and stresses. Data obtained from the nine cell stack program was used to approximate the cell component creep deflection of 0.0084 cm/cell (0.0033 inch/cell). The actual creep is expected to be less than that indicated in the nine cell stack tests.

The stack bolt loads and cell compressive pressures dropped during this case with most of the load shifting to the manifold. The cell compressive pressure

indicates a drop of 44.2 percent near the top of the stack from the beginning of life to the time required to achieve the previously listed creep deflection.

In summary, the results of the static stack mechanics evaluation indicate that the 25 kW stack design meets the design objectives and the calculated stresses are less than the allowables. The results indicate the manifold functions as designed. The stack load appears to be correctly distributed between the manifold and stack at the operating temperature. This is partially due to the high coefficient of thermal expansion of the insulation plate. The cell compressive pressure of approximately 0.345 MPa (50 psi) is maintained during the assembly and normal operating conditions; however, the long term normal operating case indicates a 44.2 percent reduction in the cell compressive pressure due to creep effects. This is based on a conservative estimate of the creep rate and only represents an initial assessment of the creep effect on the loads developed in the stack and the manifold. Additional testing is necessary to verify that the assumed materials' properties used in this analysis and the manifold/stack loads are adequate to preclude gas leakage.

3.4.3.4 ANALYSIS OF STACK-TO-VESSEL INTERFACES

In addition to the stack mechanics evaluation reported above, the structural adequacy of the fuel stack support structures and piping was evaluated. The results of this analysis are listed below and indicate that the stack to vessel interfaces are structurally adequate.

- Support Legs - The two ASTM A36 angle legs were modeled as straight bars pinned at both ends. The maximum load each leg will have to support was found to be 1423N (320 lbs). The legs were found to be structurally adequate for these loads.
- Cooling Air Return Pipe - The 20.3 cm (8 inch), Sch. 40, ASTM-A234 pipe was evaluated for both horizontal loads and vertical loads. The pipe was assumed to be rigidly bolted to the floor and base plate. The force acting normal to the stack and plenum caused both twisting and bending in the pipe. The largest of these stresses was found to be bending and had a maximum value of 7.24 MPa (1,050 psi). The results of this analysis have shown that the cooling air return is adequate to support the weight of the stack and plenum.

- Process Air Pipe - The significant loads on the 6.35 cm (2.5 inch) Sch. 40, ASTM-A312 process air pipes are caused by movement of the fuel stack. These horizontal deflections are transmitted to the process air pipes causing small bending stresses. The maximum bending stress was calculated to be 21.2 MPa (3,073 psi). This is well within the allowable stress limits of the material. In the vertical direction, slip joints between the pipe and fuel stack allow either component to move unrestricted.

- Fuel Pipe - The loads on the ASTM-A312 fuel pipe are similar to those on the process air pipe. The same analytical techniques were used and the maximum stress was found to be 9.8 MPa (1,420 psi), well within the maximum allowed.

- Flange Bolts - The 304 SS flange bolts were evaluated for the various loading conditions imposed on the pipes. The largest membrance stress found was only 9.84 MPa (1,427 psi) and occurred on the process air pipe flange.

- Thermal Stresses - Thermal expansion of the fuel and process air pipes are significant only in the vertical direction and are accommodated for in the pipe slip joints. The calculated worst case bending stress was found to be 4.86 MPa (704 psi). The thermal stresses in these structures are well within the allowable stress values.

3.5 100 kW STACK DEVELOPMENT

3.5.1 DEVELOPMENT STATUS

The 100 kW stack design requirements document was developed and a preliminary design was completed in accordance with these requirements. Also, a narrative description of the design was prepared.

3.5.2 100 KW STACK DESIGN DESCRIPTION

The 100 kW stack test assembly is very similar in concept to the 25 kW stack design described in detail in Section 3.4 and employs identical support structure and piping components, where possible. The main differences are the longer stack, cooling air outlet plenum box, electrical power take-off wires, acid lines, and pressure vessel. In addition, process air in the 100 kW stack is piped directly from the cooling air outlet plenum box (as in the 375 kW module design) instead of via a separate vessel penetration provided in the 25 kW Stack.

The test assembly incorporates maximum component commonality with the Loop 1 test assembly configuration and the 375 kW module design (see Section 3.6). In this arrangement, the 100 kW stack and its cooling air outlet plenum box interface with the module designed internal support structure. Process air is supplied from the cooling air outlet plenum box. A departure was made from the prototypical module piping manifold arrangement on the vessel lower head, to avoid the need for blanking off and, possibly, bleeding the piping legs for the three missing stacks.

The 100 kW stack contains 419 cells in 83 groups of five with two cells at each end of the stack. Each group of five cells is separated by cooling channels and is of a design configuration identical to that described for the 10 kW stack. Many of the 10 and 25 kW stack design features as described in Sections 3.3.2 and 3.3.3 are applicable to the 100 kW stack, and thus are not reported herein.

The reinforced plastic manifolds are each assembled from two identical half-length fiberglass reinforced polyethersulfone moldings, joined at stack mid-height and are held in contact with the end faces of the stack by tie rods. Teflon tubing around the tie rods insulates them from the stack. The manifolds are sealed to the faces of the stack by 0.5 cm (3/16 inch) diameter Viton O-rings. Two O-rings are employed in each manifold, one encircling the fuel cavity and the other the process air cavity. The plastic manifolds are reinforced by stiffening ribs which also serve to divide up each of the manifold cavities into a number of smaller compartments. Each compartment is supplied from, or supplies, an individual gas connection.

The process air supply bobbin connector at the uppermost manifold tee connection engages at its upper end with a transfer pipe connected at its other end to the cover plate of the cooling air outlet plenum box. The plenum box is generally similar in concept to that of the 25 kw stack design, but is longer to suit the 100 kW stack. The 100 kW plenum box is usable in both the facility and the module vessel designs and is sealed to the stack using plastic angle components prototypic of the module design. Heated air from the stack cooling

channels is conveyed to the upper end of the process air supply piping. The lowermost manifold tee connection of this piping is terminated by means of a cap held in place by rollpins. The process air supply penetration in the lower head of the facility vessel is sealed off with a blanking cover.

The stack assembly is supported, in the case of the test facility version, from a carbon steel lower support plate which is mounted on the cooling air outlet pipe and two support columns. These support details and the piping weldments mounted on the facility vessel lower head are identical with those of the 25 kW stack design. In the case of the 100 kW stack in the module vessel, the lower support plate, cooling air outlet ducting and eight support columns are identical with those of the 375 kW module design. The piping weldments mounted on the lower head of the vessel differ from those used in the module in that provision is made for only a single stack.

Provision is made in the facility and module vessel test assemblies for instrumentation leads via three 15 cm (six inch) diameter penetrations in the facility vessel and two in the module vessel.

The resulting 100 kW stack preliminary design is defined to the point from which detail drawings can be prepared. Detail drawings of the plastic process gas manifolds, long lead hardware, were completed and released for use in negotiations with potential vendors. To date negotiations with vendors have not resulted in obtaining a firm commitment to manufacture the half-length manifold by injection molding. As a result, a design layout study was started to investigate the possibility of assembling the manifold by joining together four relatively short sections. The shorter sections should be more suitable for injection molding than the half-length components and should greatly increase the number of potential molding vendors possessing the necessary facilities.

3.6 375 kW MODULE DEVELOPMENT

3.6.1 DEVELOPMENT STATUS

Preliminary equipment specification was developed for the 375 kW module, and in accordance with this specification a conceptual design was completed which is illustrated in Figure 3.6.1-1. The nominal design parameters of the module are presented in Table 3.6.1-1 at beginning-of-use (BOU) of the plant. Although designed to provide an electrical output of 375 kW dc at full power operating conditions at beginning-of-use (BOU) the module is also capable of producing up to 400 kW as a replacement module when combined with degraded modules.

3.6.2 375 kW MODULE DESIGN DESCRIPTION

The 375 kW module consists of four stacks of fuel cells supported inside a containment vessel with their cooling air outlet passages discharging into the space formed between the stacks. Cooling air is admitted to the pressure vessel cavity, surrounding the stack assembly, and flows through passages provided in the stack to the space between the stacks. The cooling air enters and leaves the vessel through the lower head, allowing the vessel cylinder and upper head to be easily removed for maintenance of the fuel cell stacks. Figure 3.6.2-1 illustrates the cooling air flow path schematically. Process air is piped to the stacks from the cooling air outlet cavity through holes in the top plate which separates the inlet and outlet cooling air cavities. Figure 3.6.2-2 illustrates the process air flow path. Fuel is piped to the stacks from a manifold in the lower region of the pressure vessel fed from a supply bobbin passing through a penetration in the lower vessel head. Figure 3.6.2-3 illustrates the fuel flow path. The fuel and process air return lines from the stacks are led into similar manifold and bobbin connections to penetrations through the lower vessel head. Figure 3.6.2-4 illustrates all of the above flow paths in a schematic illustration of the module.

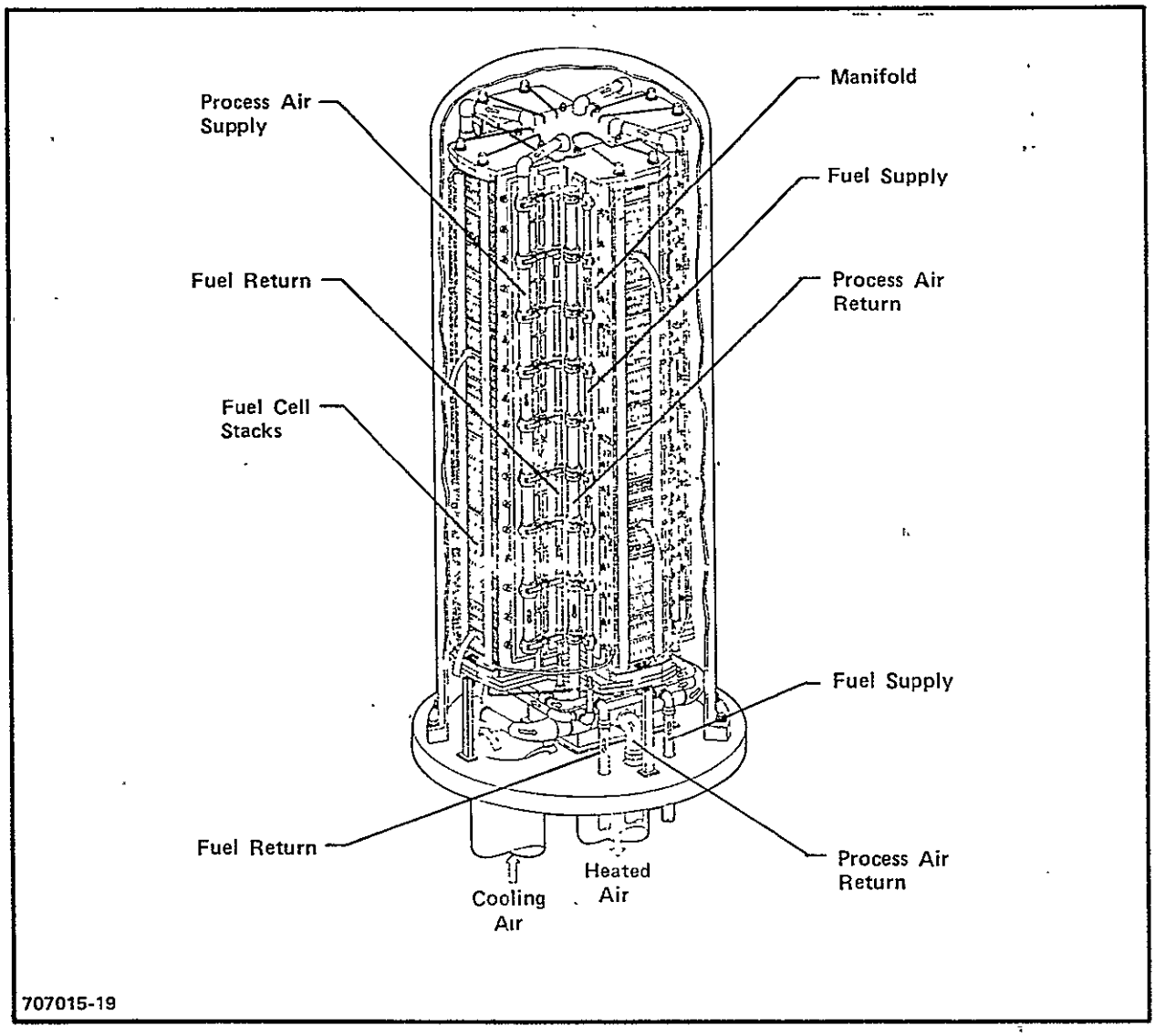

Figure 3.6.1-1. General Seal Test Configuration

TABLE 3.6.1-1
MODULE DESIGN PARAMETERS

Parameter	Nominal
POWER	375 kW dc
TEMPERATURE	
Oxidant Inlet*	185 (365) °C (°F)
Coolant Inlet	147 (297) °C (°F)
Fuel Inlet	191 (376) °C (°F)
Plate Avg.	191 (376) °C (°F)
*Same as coolant outlet.	
PRESSURE	482 (70) kPa (psia)
FLOW	
Fuel (simulated Reformate Hydrogen, 80% Utilization)	183 (403) kg/hr (#/hr)
Oxidant (air 2.0 stoichs)	1423 (3135) kg/hr (#/hr)
Coolant (air)	28,570 (62,930) kg/hr (#/hr)
CELL VOLTAGE	
Open Circuit	920 mV
Operating Limit	800 mV
Operating Point	680 mV
CELL CURRENT DENSITY	325 mA/cm^2
MODULE VOLTAGE	
Open Circuit	1440 Volts
Operating Limit	1260 Volts
Operating Point	1080 Volts
MODULE CURRENT	351 Amps

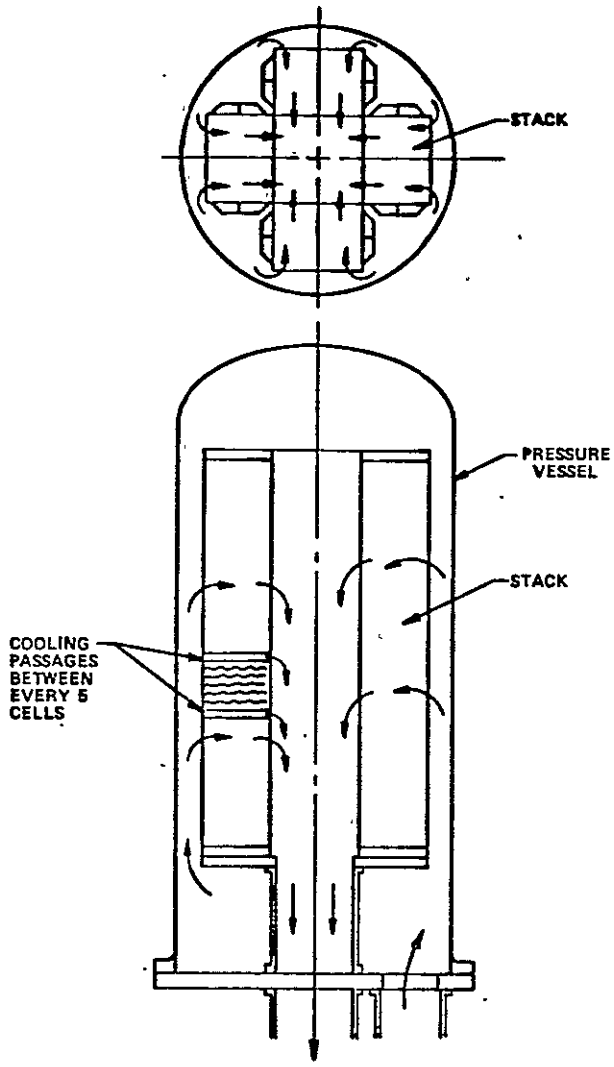

Figure 3.6.2-1. Module Cooling Air Flowpath

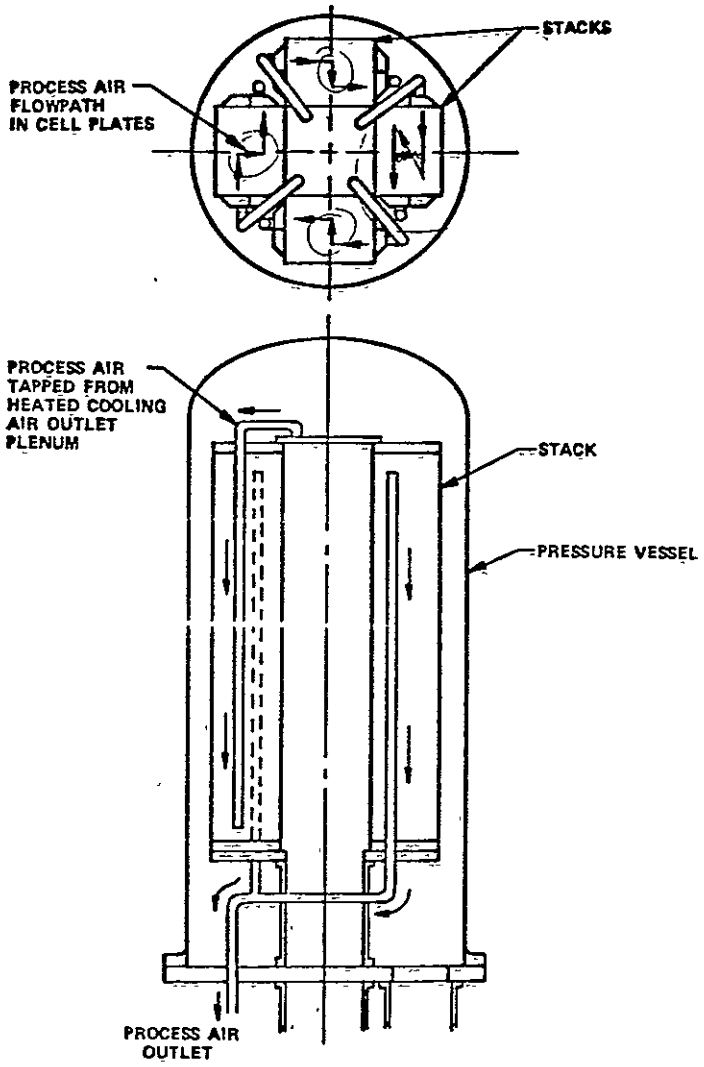

Figure 3.6.2-2. Module Process Air Flowpath

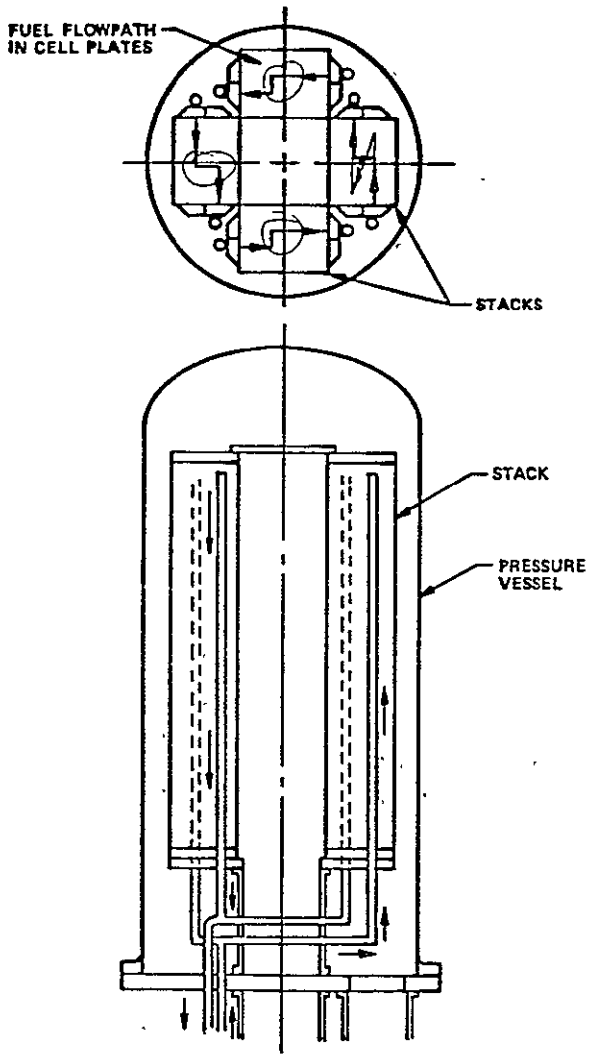

Figure 3.6.2-3. Fuel Gas Flowpath

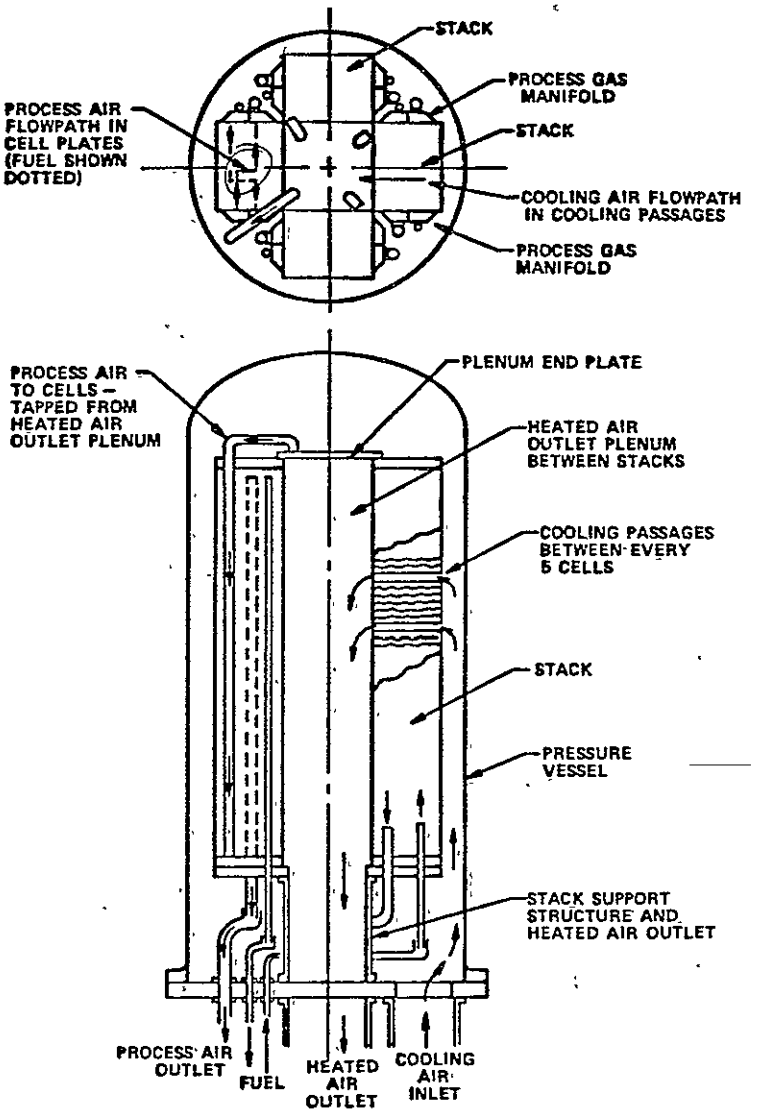

Figure 3.6.2-4. Module Flowpaths

Each fuel cell stack contains 419 cells in 83 groups of five with two cells at each end of the stack and is of a design configuration essentially identical to that described in Section 3.5.2 for the 100 kW stack.

Provision is made for heating the stack compression tie rods on the inlet side of the stack to minimize the tendency for the stack to bow due to differential thermal expansion of the rods. Heated air is channeled from the cooling air outlet plenum through grooves machined in the upper insulator plate to the inner diameters of insulating tubes placed around the cold-side rods. The heated air then flows downward in the annular spaces between the rods and the insulating tubes to grooves machined in the lower insulator plate. The grooves in the lower plates then transfer the air to the process air outlet bobbin connectors.

The four stack assemblies are supported from a carbon steel support plate mounted on the cooling air outlet piping and four support columns. The upper end of the cooling air outlet plenum, formed between the stacks is closed by a carbon steel cover plate. Leakage of cooling air into the plenum between the stacks is limited by corner seals bolted to the adjacent edges of the stack manifolds.

A conceptual definition was developed for a continuously operating acid management system. This system employs an acid reservoir and micropump or pumps to deliver acid to the stacks. The complete system, including micropumps and acid reservoir, would be contained within the pressure vessel environment. The micropump would be energized by means of compressed air lines, penetrating the pressure vessel.

Two 15 cm (6 inch) diameter penetrations are provided in the vessel lower head to accommodate instrumentation. Each penetration has the capability of accommodating several multiple lead compression fittings.

Support for the stacks against seismic loads in the horizontal direction is provided by four adjustable support bolts on a 90 degree spacing around the

upper circumference of the pressure vessel. The supports are individually adjustable to suit the particular dimensions of initial or replacement cartridges following installation of the pressure vessel. Four guide bars supported between the stack compression plates protect the stacks from damage during installation of the vessel.

Some of the major physical characteristics of the module are listed in Table 3.6.2-1. The module external interfaces are listed in Table 3.6.2-2.

Consideration was given to prevent the phosphoric acid from freezing during module storage and transporation periods by keeping the cell environment at a minimum temperature of 37.8°C (100°F) in a dry atmosphere of -12.2°C (10°F) dewpoint or less. A candidate heating concept was developed to achieve this. The approach employs tubular heating elements mounted in the module cooling air outlet plenum between the stacks. Heat is distributed to all cells by natural convection. Design effort was initiated to define the heater provisions in the module.

TABLE 3.6.2-1

MODULE PHYSICAL CHARACTERISTICS

Vessel Height	3.5 m (11 ft, 6 in)
Vessel Diameter	1.37 m (4 ft, 6 in)
Base Plate Diameter	1.68 m (5 ft, 6 in)
Weight	5400 kg (6 tons)
Module Contains four Stacks of 419 Cells	83 5-cell groups 2 2-cell groups
Cell Plate Dimensions (machined)	0.419 m x 0.3 m (16.5 x 11.75 in)
Stack Height	2.44 m (8 ft) (approximately)
Stack Weight	621 kg (1370 lb)
Vessel Cylinder Weight	1088 kg (2400 lb)

Automatic Disconnection of Process
Fluid lines during cartridge replacement

Pressure Vessel - Carbon Steel to ASME Section VIII
Division 1 for 586 kPa (85 psia) and 204°C (400°F) capability

TABLE 3.6.2-2

MODULE EXTERNAL INTERFACES

	Pipe Size	Pressure (psia)	Pressure (kPa)	Temperature (°F)	Temperature (K)	Flow Rate (lb/hr)	Flow Rate (kg/hr)
Cooling Air - In	16" Flanged (150 lb)	71	(489)	297	(420)	69,930	(28,540)
Cooling Air - Out	16" Flanged (150 lb)	70	(482)	365	(458)	59,820	(27,130)
Process Air - Out	4" Flanged (150 lb)	69	(476)	378	(465)	3,135	(1,422)
Fuel - In	2" Flanged (150 lb)	71	(489)	376	(464)	403	(183)
Fuel - Out	2" Flanged (150 lb)	70	(482)	376	(464)	378	(171)
Acid - In (4)	1/4"	N/A		N/A			
Acid - Out (4)	1/4"	N/A		N/A			

Electric Connections

- Vessel feedthrough, two
- Wire connections 4/0 avg stranded nickel-coated copper conductor
- Terminal AMP, Inc., Part No. 325609

Module Voltage

1070 (Operating)
1260 (Operating Limit)
1440 (Open Circuit)

Module Current 351 amps

Module Power 375 kW

Module Heat Rate 7540 BTU/kWh

3.7 FUEL CELL MATERIALS CHARACTERIZATION TESTING

There are many raw materials utilized in the manufacture of the repeating cell components. This section addresses these cell components raw materials. Also, evaluations and/or characterizations performed of these raw materials and resultant cell components including chemical, physical, mechanical, thermal, electrical and corrosion behavior are described.

3.7.1 RAW MATERIAL SPECIFICATIONS

Eleven raw material Purchasing Department Specifications (PDS) were developed and utilized for procurement purposes to manufacture the fuel cell repeating components. These specifications were prepared for the materials listed in Table 3.7.1-1.

3.7.2 PLATE MATERIALS

This section summarizes effort conducted to evaluate the bipolar and cooling plate materials.

3.7.2.1 PLATE FLATNESS

Initial bipolar plate molding efforts resulted in a complex curved surface. The plates were generally concave toward the ribbed section at each of the gas inlet and outlet regions (see Figure 3.7.2-1) such that an "S"-edge profile existed in the 31.4 cm (12.375 in.) direction.

The typical out of flatness was determined to be about 0.1 cm (0.04 in.) in the as-pressed or molded condition. After heat treatment, this edge profile out of flatness increased and ranged from 0.3 to 0.8 cm (0.12 to 0.32 in.). Inspection of plates heat treated in a short cycle revealed the occasional presence of cracks through the thickness in the flow grooves running parallel to the 31.4 cm edge. Plates heat treated using the other longer cycles have not shown these cracks. The heat treated plates were essentially flat in the 44.1 cm (17.375 in.) direction and no cracks were found in the grooves parallel to that edge.

TABLE 3.7.1-1

RAW MATERIAL SPECIFICATIONS

Material (Supplier and Grade)

1. Artificial Graphite Powder (Asbury-A99)
2. Platinum Catalyst (Johnson Matthey-Type ERC)
3. Phenolic Resin Powder (Reichhold-29-703 Varcum)
4. Carbon Black (Cabot-Vulcan XC-72)
5. FEP-Fluorocarbon Resin (DuPont-Teflon 120)
6. TFE-Fluorocarbon Resin (DuPont-Teflon 30)
7. TFE-Fluorocarbon Resin Powder (DuPont-Teflon 6C)
8. Silicon Carbide Powder (Carborundum-1000 grit green)
9. Carbon Sheet Material (Stackpole-PC206)
10. Hydrocarbon Solvent (Guard-All Chem.-Shell Sol 340)
11. Resin, Water Soluble Thickener (Polyox WSR-301)

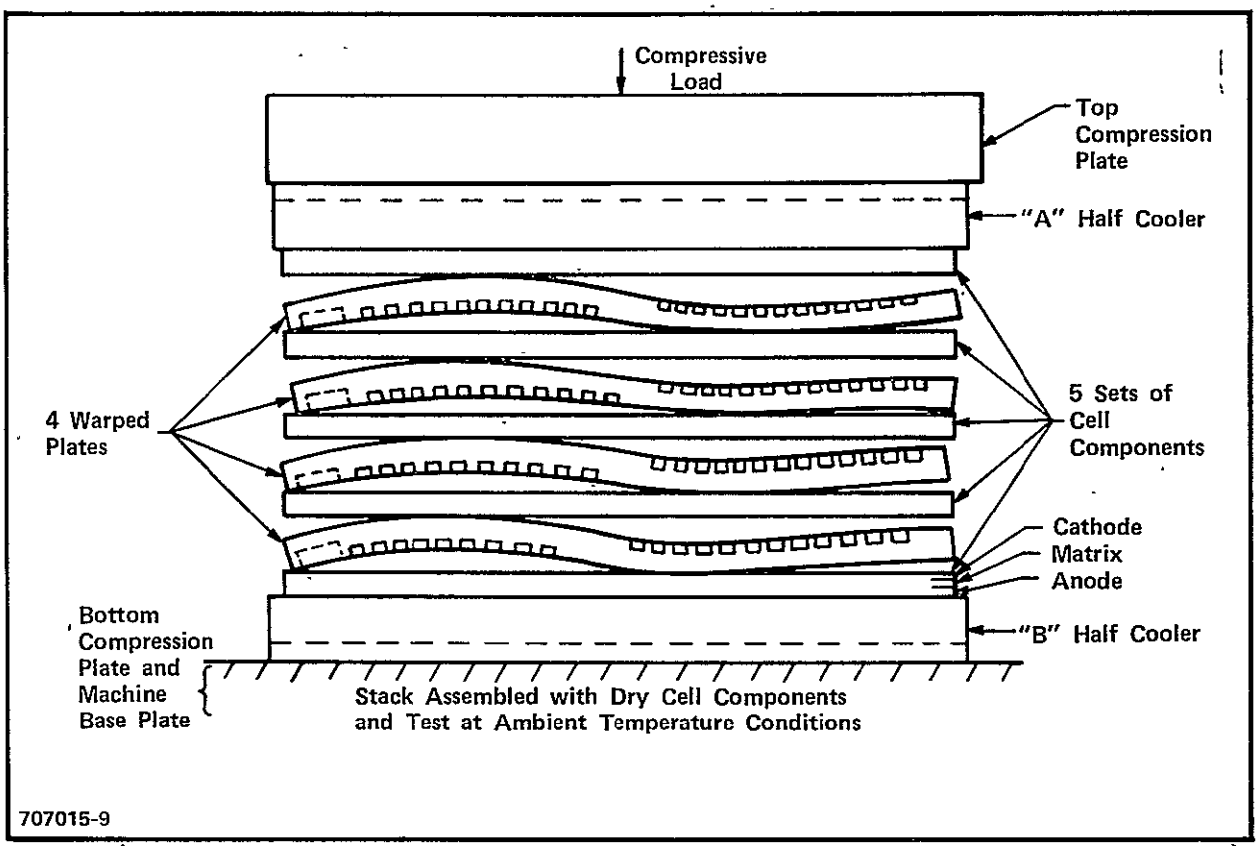

Figure 3.7.2-1. Edge View of Five-Cell Group Test Configuration

Flatness measurement of molded, heat treated cooler plates revealed the typical "S" pattern in the 31.4 cm direction with an out of flatness of up to 0.35 cm (0.13 in.). The curvature in the 44.1 cm length is concave toward the "Tree" pattern side with an out of flatness of up to 0.8 cm (0.32 in.). Also noted was a pronounced rippled surface on the "Zee" side corresponding to the spacing of the "Tree" grooves on the reverse side.

Water immersion density and its variation within the "Zee-Zee" heat treated plates was determined for two molding cycles. Plate ZZ-8 molded using a five-minute cycle showed very little density variation throughout the plate. Of the 18 locations evaluated, all were 1.77 g/cc with the exception of three, and the lowest of these was 1.72 g/cc. Plate ZZ-77 molded using a two-minute cycle resulted in a plate having slightly more density variation, ranging from 1.70 to 1.77 g/cc. The short cycle is, however, capable of producing acceptable plates. Mercury intrusion porosity data on both molded flat and "Zee-Zee" plates in the heat treated condition, presented in Table 3.7.2-1, indicates the two geometries have generally similar pore characteristics.

A mechanical evaluation of the curvature in the molded/heat treated bipolar plates was performed. Various flattening type test configurations were conducted on dry mixed A99 graphite/resin plates to determine whether plates having the typical large "S" curvatures could be flattened sufficiently for use in cell stacks without cracking. Individual warped plates, without and with, dry electrodes placed on each side of the plate, were flattened between steel compression plates to both a pre-selected final dimension and to a maximum load of 345 kPa (50 psi). The results of these initial tests were inconsistent in that some plates cracked while other did not. By considering the deformation effects of the electrodes a simple test criteria was developed. A warped plate would not fail in a stack, if the warped plate survived a compression test between rigid plates to a flatness equivalent to the average plate thickness plus 0.00762 cm (0.003 in). This test also indicated that the warped plate had a tendency to locally imprint on the electrode with the plate groove pattern, as would be expected due to localized high contact loads. In an effort to evaluate this effect and insure that warped plates could be loaded to normal stack loads, a five-cell stack was assembled. Machined cooler plates, warped

TABLE 3.7.2-1

PRELIMINARY POROSITY DATA - BIPOLAR PLATES

(TEST TO 60,000 PSI MERCURY INTRUSION PRESSURE)

Property	Pressed and Heat Treated	
	ZZ Plate	Flat Plate
Void Volume (g/cc)	0.026-0.032	0.026-0.033
Pore Size Distribution Diameter (Å)	< 36-200	< 36 to 200
Surface Area (m^2/g)	16.3	14.6-20.8
Bulk Density (Hg) (g/cm^3)	1.835	1.911
Percent Porosity	5.94	5.89

bipolar plates, and dry electrodes were loaded to 345 kPa (50 psi) while recording load and deflection. This small test unit duplicates the five cell unit which is used in larger stack arrangements. The general test configuration used for the five cell unit is shown on Figure 3.7.2-2. Examination of the bipolar plates after this test revealed that only one plate cracked as a result of this loading. All tests involving electrodes revealed a tendency to locally imprint the electrode backing paper with the groove pattern. This imprint effect was not consistent as to specific areas or intensity. This test confirmed the inconsistent behavior of a curved bipolar plate when mechanically flattened.

Based on the inconsistent results of these tests, it was concluded that reliable cells and cell stacks could not be produced using plates having the "S" curvatures produced using the plate molding technology developed for straight groove bipolar plates.

Major emphasis was placed on examination of processing parameters, raw material evaluations, and heat treatment cycles to establish the reason for the large out of flatness observed and to develop either alternate processing or materials technology or a combination of these to produce an acceptable bipolar plate.

A number of different graphite/carbon materials were procured and evaluated. These materials included Shawinigan Acetylene Black, Vulcan XC-72, A99 Regrind, Airco Speer (-20μ), Texas Wilmington Coke, POCO-PXB-5Q-325, and Stackpole MF958. The various powders were processed into molded and heat treated plates with varying degrees of success. The acetylene and carbon blacks are difficult to process due to their bulk and fine particle size. They do produce flat plates, but their use was discarded due to mixing problems.

The regrind A99 powders in various mesh sizes produce essentially flat plates with an out of flatness of about 0.08 cm (0.030 in.). The POCO and Stackpole graphite powders likewise produce plates which have similar out of flatness values. The Airco Spear powder produced plates which have slightly less curvature than the A99 powder but is much greater than the other materials evaluated and thus marginal with regards to stacking behavior. The electrical

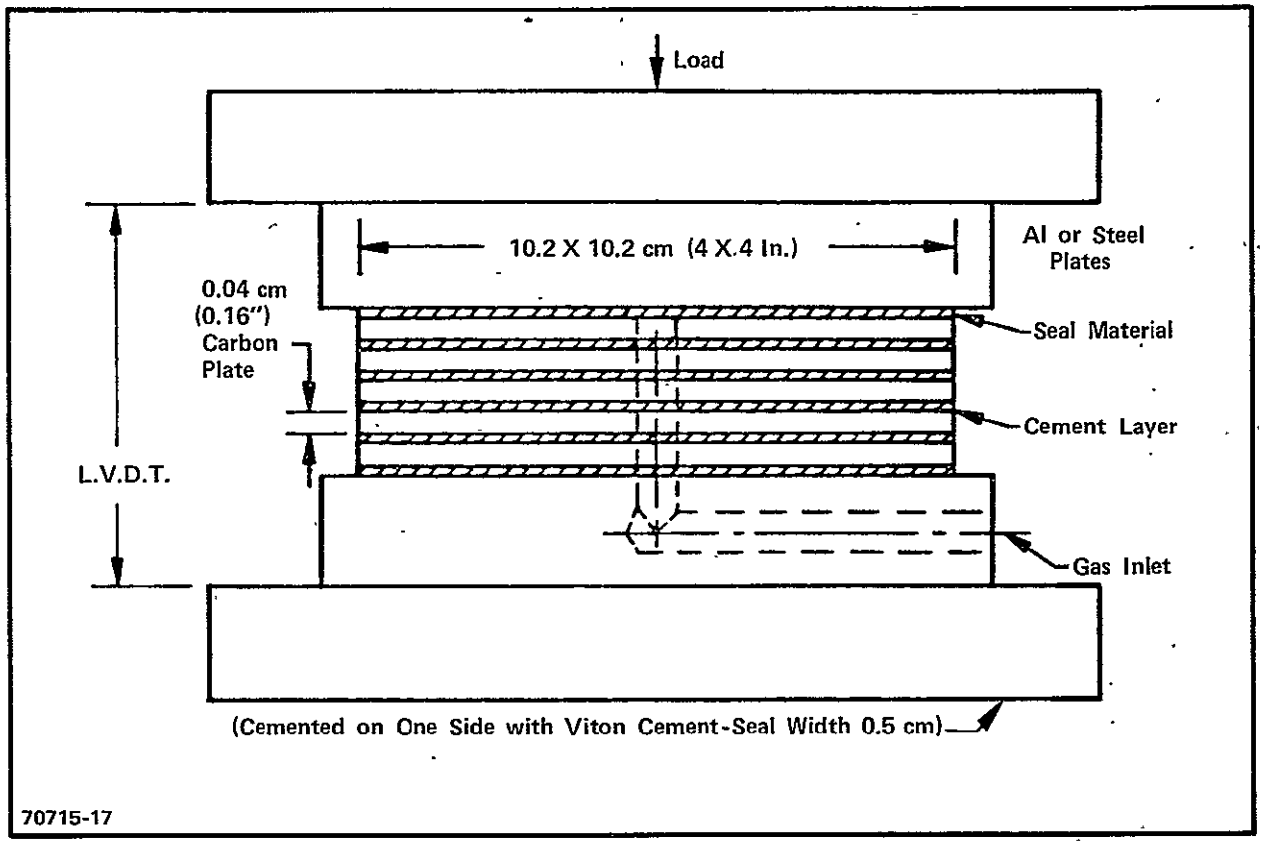

Figure 3.7.2-2. General Seal Test Configuration

resistivity and mercury porosimetry data for a number of the developmental plates is presented in Tables 3.7.2-2 and 3.7.2-3. The resistivity data indicate that those plates which are relatively flat have resistivity ratios of in-plane value to thickness value or vice versa that are about one (approximately 3.2 mΩ-cm in both directions). The porosimetry data indicate that the POCO and Stackpole powders result in plates having bulk densities approximately equal to that of the A99 material, while the regrind A99 results in a plate having a slightly lower bulk density of about 1.70 g/cc. The flatness results together with the density and electrical resistivity indicate that several of the alternate materials are capable of producing a plate that is substantially flatter than the A99 material and should be a satisfactory replacement.

Several other replacement graphite powders are currently being evaluated as well as processing variations involving the forming of the prepressing from the dry mix at high pressing pressures at ambient temperature or at a temperature above ambient but lower than the final plate pressing temperature. These additional process variations together with those materials already evaluated indicate that acceptable plates can be produced. The powder availability in terms of power plant required quantities and overall production cost will dictate which of the various materials and processing variations are chosen.

3.7.2.2 PLATE CORROSION

Post-mortem examinations of the cell components from five cell stack Z-001 revealed the presence of localized but rather extensive corrosion on the cathode side of several of the bipolar plates. This corrosion appears as a localized softening of the plate process channel ribs. Analysis of the corrosion residue and parent plates were performed to provide an understanding of the corrosion mechanism and residue and to provide insight into possible approaches to minimizing or eliminating this corrosion. Included in the analysis of the plates were optical microscopy, scanning electron microscopy, N Methyl Pyrrolidone extraction, infrared spectrographic analysis of the extract, thermogravimetric analysis of the materials, X-ray diffraction, and simulated electrochemical corrosion of selected samples.

TABLE 3.7.2-2

ELECTRICAL RESISTIVITY OF DEVELOPMENT PLATES

Plate No.	Powder	$e_{(Thickness)}$ (mΩ-cm)	$e_{(Plane)}$ (mΩ-cm)	Ratio (e_T/e_p)	Ratio (e_p/e_T)
ZZ59	A99	6.09	1.40	4.35	0.23
ZZ142	A99 Regrind	3.14	3.19	0.98	1.02
ZZ170	A99 Regrind	3.16	3.03	1.04	0.96
ZZ167	A99 Regrind	3.47	3.26	1.06	0.94
ZZ144	Stackpole	2.26	2.05	1.10	0.90
ZZ160	Poco	11.05(1)	3.22	3.43	0.29
ZZ212	Poco	3.07	3.38	0.91	1.10
ZZ219	Poco	3.11	3.59	0.87	1.15
ZZ283	Poco	3.21	3.95	1.09	0.92
ZZ125	Shawinigan Acetylene Black	ND(2)	4.14	ND	ND
ZZ132	Vulcan XC72R	ND	3.88	ND	ND
ZZ256	Airco Spear	3.79	2.25	1.68	0.59
ZZ257	Airco Spear	6.02	3.02	1.99	0.50

(1) Value probably incorrect
(2) Not determined.

TABLE 3.7.2-3

MERCURY POROSIMETRY DATA FOR DEVELOPMENT PLATES

Plate No.	Powder	Skeletal Density (g/cc)	Bulk Density (g/cc)	Specific Pore Volume (cc/g)	Specific Pore Surface (m^2/g)	Porosity Percent
ZZ59	A99	1.94, 1.93	1.86	0.022, 0.020	9.8, 9.4	4.1, 3.7
ZZ63	A99	1.95, 1.95	1.88, 1.87	0.021, 0.022	10.8, 10.3	3.9, 4.1
ZZ142	A99-Regrind	1.80, 1.80	1.69, 1.69	0.037, 0.036	16.0, 15.5	6.3, 6.1
ZZ167	A99-Regrind	1.83, 1.85	1.71, 1.70	0.038, 0.047	17.0, 15.0	6.5, 8.0
ZZ170	A99-Regrind	1.80	1.71	0.030	15.3	5.1
ZZ144	Stackpole	1.91, 1.91	1.86, 1.85	0.016, 0.015	8.7, 9.0	2.9, 2.9
ZZ160	POCO	1.85	1.82	0.011	5.6	2.0
ZZ219	POCO	1.84	1.80	0.012	9.8	2.2
ZZ283	POCO	1.86	1.83	0.007	3.8	1.3
ZZ256	Airco Spear	2.12	2.03	0.020	11.4	4.2
ZZ257	Airco Spear	2.15	2.04	0.025	13.5	5.2

Optical metallography specimens from stack cell number three were washed to remove the acid present, vacuum dried, vacuum impregnated with mounting resin to support the corrosion residue, and polished for examination. These samples revealed that the A99 graphite powder phase of the plate did not appear to be corroded, but that the carbonized resin binder phase was almost completely removed in the corrosion areas. Also, the A99 graphite does not reveal any apparent intercalation. Additional metallography on washed and dried samples of the corrosion residue confirm that the appearance of this residue is identical to that of the A99 graphite powder used to produce the plates.

Evaluation of stack tested versus untested (from same production run) plates reveal no major differences in either density, void volume or emission spectrographic analysis, thus eliminating possible variation in processing from plate to plate or within an individual plate as a major contributor to the observed corrosion.

Penetration of phosphoric acid into a corroded plate from stack Z-001 was further examined using scanning electron microscopy (SEM) and energy dispersive analysis (EDA). Samples prepared from the corroded regions by fracturing rather than sectioning and polishing revealed the presence of phosphoric acid through the entire plate thickness in areas of heavy corrosion while at the edge of corroded regions the presence of acid was detected only near the cathode side of the plate.

N Methyl Pyrrolidone extraction data for samples of stack Z-001 corroded and uncorroded plate material, as heat treated but untested plate material, as cured plate material and pyrolyzed phenolic resin are given in Table 3.7.2-4. These data indicate that the material heat treated to 900°C still contains some organic material after this heat treatment. Additional confirmation of this is provided by the TGA data given in Table 3.7.2-5. These data reveal that both the heat treated plate material and resin were not completely converted to carbon by the 900°C heat treatment cycle, but still contain material which can be pyrolyzed by either higher temperature or for longer hold times at 900°C. Additional TGA and N Methyl Pyrrolidone extractions were performed on flat

TABLE 3.7.2-4

SOLVENT EXTRACTION AND INFRARED SPECTROGRAPHIC DATA

Sample Identification	NMP, Percent Extractable[1]	Infrared Spectrum
Z-001, soft corroded[2] plate area	7.59	Some type of organic material.
Z-001, solid uncorroded[2] plate area	6.00	Same spectrum as above.
NR53, heat treated but not tested in stack	3.33	Same spectrum as above.
As-cured plate. Sum of two extractions. (Plate No. 3417)	15.03	Organic material, but different from the extract found in heat treated plates.
Pyrolyzed, phenolic resin (29-703) 60 seconds as 900°C	2-4	Organic material same as found in extract from as-cured plates.

(1) N Methyl Pyrrolidone

(2) Water washed and dried prior to extraction.

TABLE 3.7.2-5

PLATE/MATERIAL THERMOGRAVIMETRIC ANALYSIS

Material or Plate Identification	250°C	500°C	750°C	900°C	1000°C
Z-001, soft[1] corroded area	0.5	0.75	1.25	2.5	5.5
NR53, heat treated untested plate	0.3	0.3	0.6	2.0	4.0
Phenolic Resin, 29-703	5.25	23.0	45.0	47.5	51.5

(1) Sample washed several times in water and dried before analysis.

plate samples of 70 wt percent A99 graphite/30 wt percent 29-703 resin. These samples were heat treated at temperatures of 900, 1200, 1600, 2300, and 2700°C. The 1200 and 1600°C samples revealed the presence of an extractable organic residue while those heated to 2300 and 2700°C did not. The TGA data at 1000°C indicated that the samples previously heat treated up to 1200°C showed a weight loss of about 2.7 percent, a weight loss of about 1.5 percent at 1600°C, a weight loss of about one percent at 2300°C. It should be noted that weight losses of approximately one percent are most likely associated with the presence of absorbed moisture during sample storage prior to performing the TGA. Combination of the TGA and NMP extraction data leads to the conclusion that the 900°C heat treatment does not completely pyrolyze the resin phase and that a higher heat treatment temperature is required if only a carbon residue (from the resin phase) is to be obtained in the heat treated plate. An alternate to the higher heat treatment temperature may be longer residence time at a lower temperature.

X-ray diffraction data obtained on the A99 graphite powder used in plate manufacture, samples of corrosion product, and various heat treated plate samples are presented in Table 3.7.2-6. The C-interplanar spacing ranges from 6.734 to 6.754 angstoms. While the data range is larger than anticipated for this graphite, it is typical of the range generally found in a manufactured graphite and does not suggest that intercalation of the A99 graphite phase is occurring during the corrosion process. In addition, the data indicate that heat treatment of the plate material over the temperature range of 900°C to 2700°C does not change the C-interplanar spacing, indicating the stability of the A99 graphite over that range of temperature.

With the exception of one plate (Cell 7) from stack W009-02, post-mortem examination of plates from a number of recently tested cell stacks, has failed to reveal the presence of corrosion. In several of these stacks, intentional "defects" or abnormalities were included in an effort to cause corrosion to selectively occur. The one plate from stack W009-02 revealed the presence of minor corrosion on the cathode side in several locations. Metallographic examinations of these regions revealed the same type of residue previously

TABLE 3.7.2-6

X-RAY DIFFRACTION OF GRAPHITE POWDER AND PLATE MATERIAL

Material	C/2, Å	C, Å
A99 Powder	3.367	6.734
Corrosion Residue	3.37	6.74
Plate - 900°C H.T. (AESD)	3.37	6.74
Plate - 900°C H.T. (ERC)	3.377	6.754
Plate - 2700°C H.T. (ERC)	3.377	6.754
Natural Flake Graphite[1]	3.359	6.719
KC Graphite	3.359	6.718

(1) Data from R. E. Nightingale, "Nuclear Graphite," Academic Press, 1962.

described for stack Z-001; namely A99 graphite particles with the carbonized resin phase either completely removed or almost completely removed in the region showing the greatest attack. In areas adjacent to the soft regions, the early stages of corrosion were detected. In these areas, the resin residue phase revealed initial attack on and near the surface but had not been completely removed, and thus still provided skeletal support for the A99 particles.

Based on post-mortem examination of plate corrosion, its occurrence requires the presence of acid at the cathode plate face and an ionic path to the anode. Once this is established corrosion may occur, the rate being dependent on the acid concentration at the cathode graphite surface. The most likely sequence of the plate attack is the selective corrosion of resin phase progressing from the surface into the plate thickness.

3.7.3 SEAL MATERIALS

The stack design relies on effective edge cell-to-cell seals as well as manifold-to-stack seals. Seal tests were conducted to simulate the seal configuration planned for the 10 and 25 kW stacks. The materials selected and tested are based on several specific parameters such as: gas sealability, structural stiffness, acid corrosion resistance, compression set, and stability at 200°C. The commercial availability of stock sheet forms is an important consideration, therefore, the thickness of samples tested are not necessarily the thickness for the stack application. Generally, gas sealability, structural stiffness, short term compression set and operating temperature stability parameters are exhibited via a sealing test at ambient temperature and 200°C. The general seal test configuration is shown on Figure 3.7.2-2. A flowmeter, capable of detecting flow rates as low as 0.003 cc/min (air), is placed in series with the gas inlet to provide a more quantitative measure of seal leakage. The testing was done on a stack of five or six picture frame seals attached to heat treated 10 x 10 cm (4 x 4 inch) graphite/resin plates or one surface with Viton cement. A linear variable displacement transducer (LVDT) is used to define the seal displacement as a function of time. The load and displacement values are recorded continuously on a strip recorder to

evaluate the structural characteristics. Dry nitrogen gas was used to internally pressurize the seal stack to either 7.6 kPa (1 psi) or 34.5 kPa (5 psi). Usually, two stacks were used to evaluate the ambient temperature and operating temperature (200°C) conditions. Table 3.7.3-1 tabulates the seal leakage rates for seal materials tested.

Evaluation of two candidate cell-to-cell fluorelastomer seal materials was completed, namely IER-SV811-3 (24 Shore A, hardness) Viton sponge, 0.32 cm (0.125 inch) thick and Pelmor, PLV-10059 (60 durometer) solid Viton 0.14 cm (0.055 inch) thick. Structural stiffness and seal (leakage) behavior were evaluated for the Viton sponge at ambient temperature and 200°C (395°F) for seal deflections of approximately 32, 50 and 68 percent. The leakage characteristics were determined to be acceptable at both temperatures and for the range of deflections examined for the sponge material. The 32 and 68 percent compressive strain values represent the extremes of the seal compression requirements based on dimensional variations in the repeating cell components. The results at ambient temperatures indicate non-linear compression stress versus seal strain characteristics over the compression range tested. This non-linear curve is evident on Figures 3.7.3-1 and 3.7.3-2 for the 32 percent and 50 percent strain curves, respectively. These curves also indicate ambient temperature and operating temperature stress-versus-strain curves. Figure 3.7.3-2 indicates a relatively linear curve over the range of loading. A low modulus of elasticity value of 496.4 kPa (72.0 psi) is obtained for this load/strain range. This low modulus is also exhibited in Figure 3.7.3-2 over the same load/strain range, however the curve increases sharply between 30 to 50 percent strain. A modulus of elasticity of 1544 kPa (224.0 psi) was calculated for this strain region. These figures also show a significant permanent set after being heated to the operating temperature of 200°C. The sponge material, when compressed and heated up to operating temperature, softens and condenses into a solid material. When this material densifies to a solid, additional loading indicates a significant increase in load for a small displacement (i.e., the modulus of elasticity increases). The ambient temperature modulus of elasticity values, which were calculated after being tested at 200°C, are 2.804 MPa (406.8 psi) and 11.473 MPa (1664.0 psi)

TABLE 3.7.3-1

CELL-TO-CELL SEAL TEST CONFIGURATION AND MATERIALS

(Seal Width = 0.5 cm, Nominal 9.27 cm x 9.78 cm Picture Frame)

Material	Test Temp. °C	Leakage (Nitrogen Gas Pressure) 7.6 kPa (1.1 psi)	34.5 kPa (5 psi)	Compressive Stress on Seal Area (kPa)
Viton Sponge (0.32 cm, IER-SV811-3, 25 Shore A, hardness)	20	1.5%/min	3.0%/min	684.6 (or 60% strain)
Viton Sponge (0.32 cm, IER-SV811-3)	20	None	None	137.8 (or 32% strain)
Viton Sponge (0.32 cm, IER-SV811-3)	20	None	None	351.6 (or 50% strain)
Viton Sponge (0.32 cm, IER-SV811-3)	20	None	None	2347.6 (or 68% strain)
Viton Sponge (0.32 cm, IER-SV811-3)	200	None	None	at 32, 50 to 68% strain values

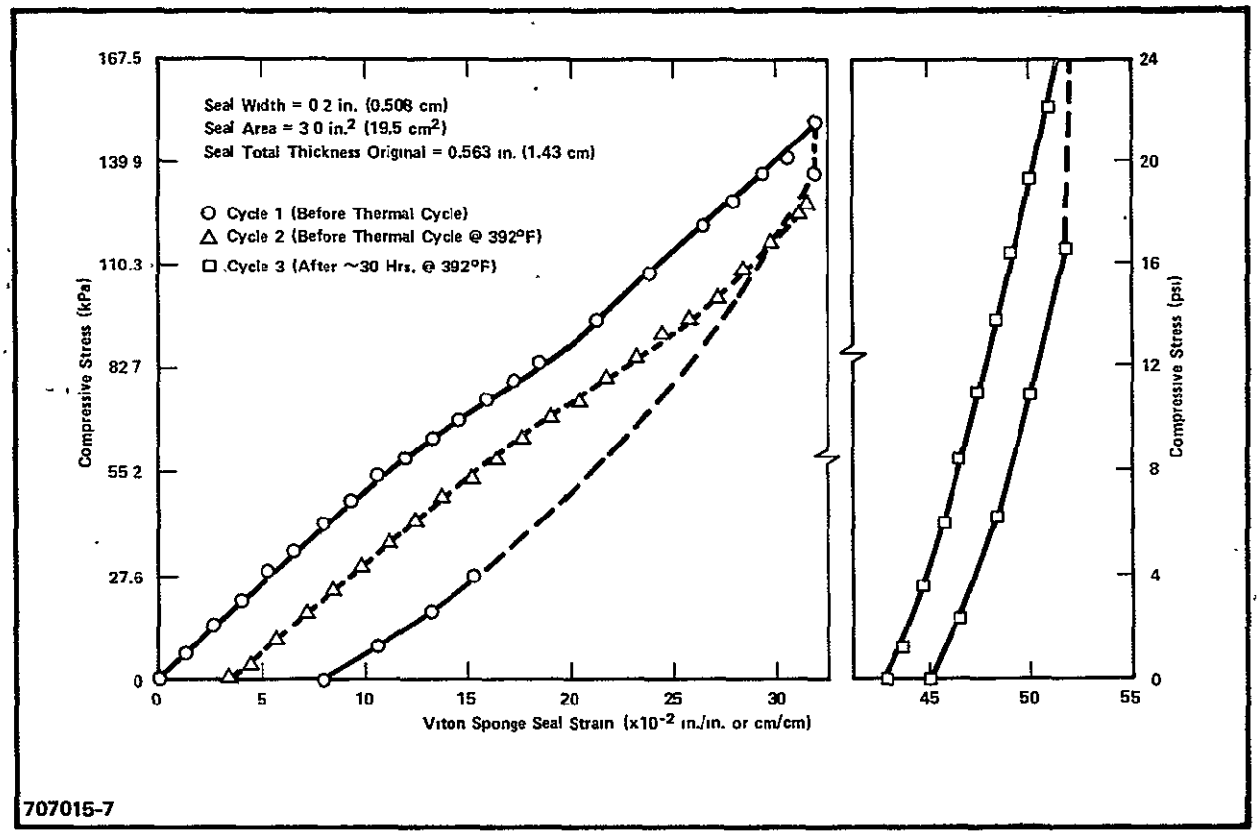

Figure 3.7.3-1. Compressive Stress Versus Seal Strain for Viton Sponge/Viton Cement at Ambient Temperature Before and After Thermal Cycle

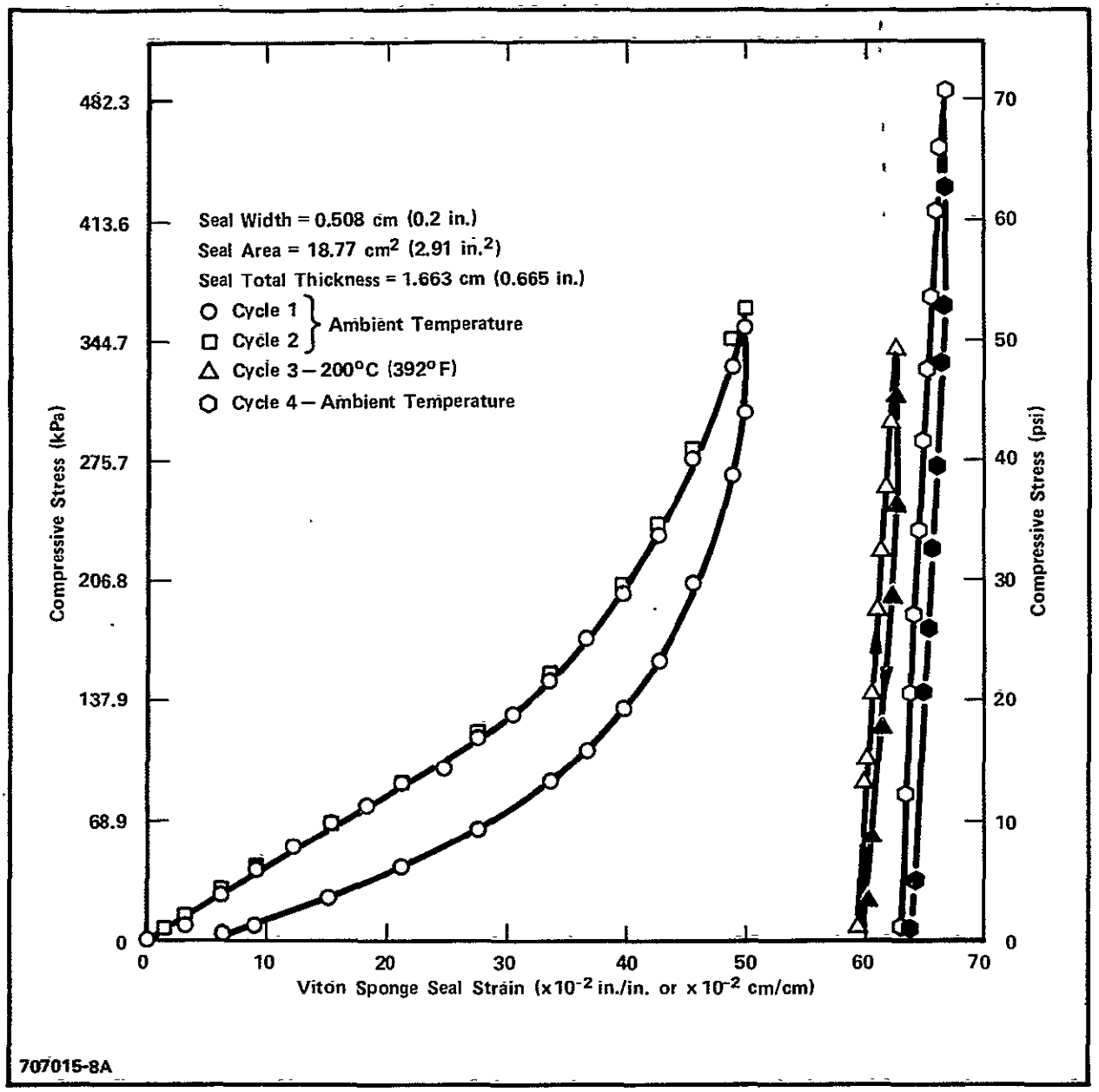

Figure 3.7.3-2. Compressive Stress Versus Seal Strain for Viton Sponge/Viton Cement at Both Ambient and Operating Temperature Conditions

for the 32 percent and 50 percent cases, respectively. These curves also indicate that after being exposed to the 200°C temperature, the resilience or compliance of the material is significantly reduced. This is evident via the large change in load over a small strain value. An additional test was performed using a new seal stack and loaded to obtain 68 percent compression of the seals. This test also indicated nonlinear characteristics with tangent modulus of elasticity values in the high strain range of 25.5 MPa (3700 psi). This modulus value is considerably higher than that obtained for a solid Viton sample of 50 durometer hardware.

The Pelmor Viton seal material was tested in a five unit test stack at ambient temperature to determine structural characteristics. Two loading cycles were performed to define the modulus of elasticity value. This material gives a relatively linear compressive stress versus strain curve over the range of 0 to 2070 kPa (0-300 psi) and a 2070 kPa (300 psi) compression stress produced a 23 percent strain as shown on Figure 3.7.3-3. The chord modulus of elasticity was 9.51 MPa (1380 psi) which is about 28 percent greater than that previously determined for a 50 durometer Viton material.

As previously discussed, the amount of compression set and temperature stability at operating temperature are key parameters which must be verified. The first long-term high temperature evaluation of Viton seal materials was completed using Precision Rubber Viton Compound 19356. The test unit was assembled with only one set of Viton seals attached with Viton cement on one surface. The unit was compressed 30 percent at ambient temperature. The measured modulus of elasticity was 9.88 MPa (1433 psi). Belleville spring washers were placed under the head of each bolt in order to maintain a constant load on the test unit. The assembly was heated to 190°C (375°F) for 2500 hours, then unloaded, measured, and recompressed at ambient temperature to determine the change in modulus and permanent compressive set. A comparison with initial loading curves indicates the ambient temperature modulus increased by a factor of 1.82 to a value of 17.96 MPa (2600 psi) and the dimensional changes indicated an 81 percent compression set after 2500 hours. This compression set is slightly higher than published data would indicate.

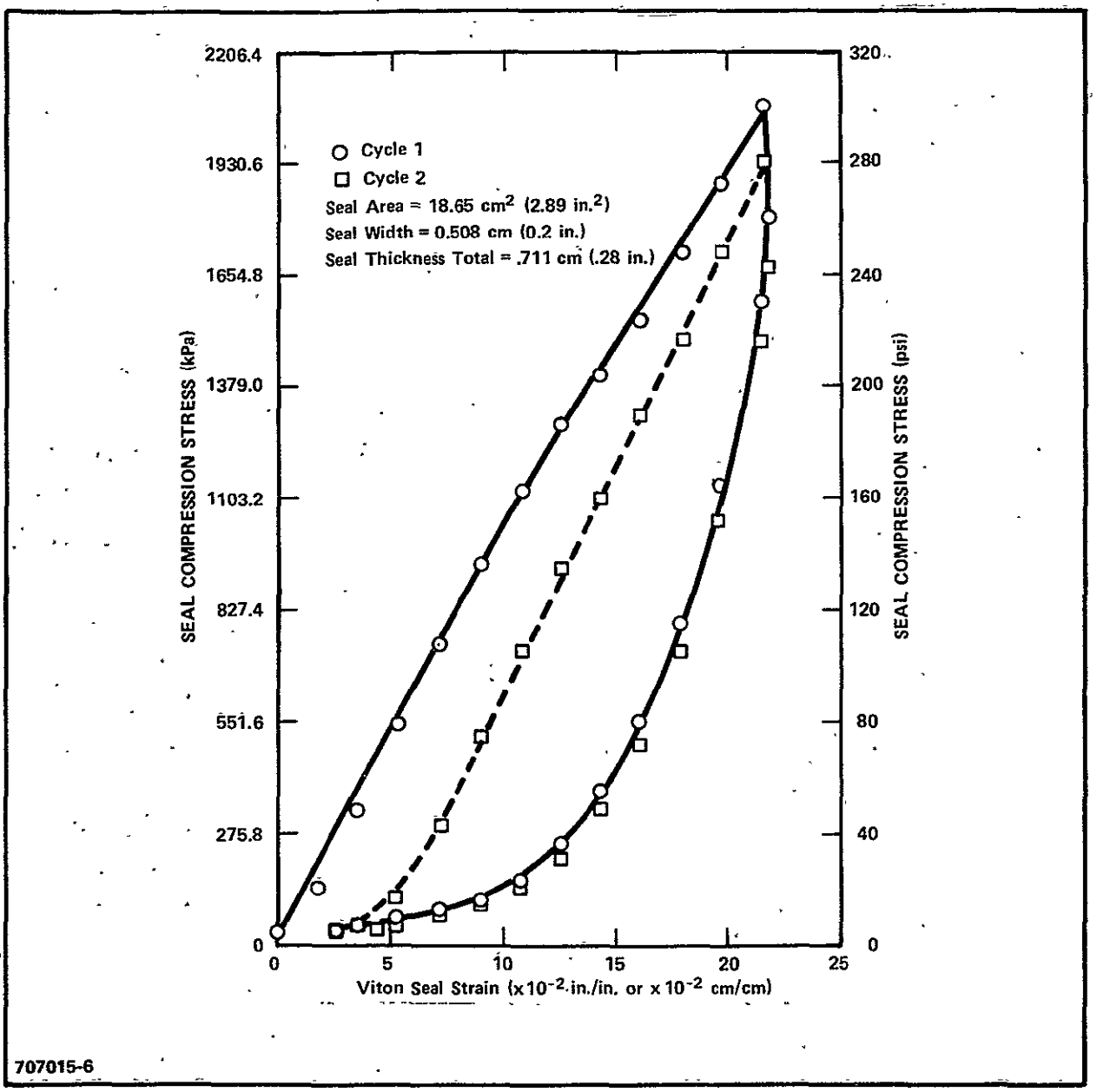

Figure 3.7.3-3. Compressive Stress Versus Seal Strain Pelmor Compound #PLV-10059 Viton 1 Viton/Cement Seal Configuration at Ambient Temperature (60 Durometer Value)

A number of screening tests were run on potential fluorelastomer cell seal materials at 200°C (395°F) in 100 w/o H_3PO_4 for durations of at least 500 hours, without applied potential. The visual observations of the materials are given in Table 3.7.3-2. With the exception of the Kalrez, most of the specimens showed minor reaction with the acid in that they were slightly discolored and the Viton samples revealed some swelling and acid pick up. The Kalrez showed no acid attack, swelling or embrittlement. The acid reaction with the other materials may or may not represent a potential source of cell contamination.

3.7.4 ELECTRODE MATERIALS

Characterization of the dimensional (thickness) and weight variation of electrode components utilized in the construction of stacks DG-001, Z-001 and Z-002 plus five lots each of standard production anodes and cathodes was compiled for analysis of variation and cause of this variation. The data indicated a rather large variation in final thickness and weight, thickness varied by up to 0.1 mm (0.004 in.) in an individual electrode and the average final thickness varied by up to 0.125 mm (0.005 in.) from electrode to electrode. This thickness variation results in corresponding weight variations. The principle cause of this thickness variation is the variability of the backing paper (PC-206) as received from the vendor. This material is used to support the rolled catalyst layer plus the SiC layer in the case of cathodes. Initial variability of this paper is reflected throughout electrode processing and in the final product. Evaluation of individual backing paper sheets indicates thickness variation within a sheet of material of up to 0.125 mm (0.005 in.) and about the some range of variation from sheet to sheet in a vendor supplied lot of material. At present, the only solution to this problem is an inspection of each sheet of material for average thickness to eliminate these sheets having extreme thickness variation. Alternate suppliers are being evaluated to determine if their products are more uniform and can provide an alternate backing paper or replacement for the PC-206 material.

TABLE 3.7.3-2

ELASTOMER ACID COMPATIBILITY SCREENING TEST DATA

Material	Comments
Kel-F, 06-3655 0.15 cm (0.060 in.) thick	Minor acid discoloration. No apparent embrittlement.
Viton solid, PLV-10059, No. 58 Viton solid, PlV-10059, No. 53 0.15 cm (0.060 in.) thick	Minor acid discoloration. No apparent embrittlement. Some swelling and acid pickup.
Viton sponge, IER SV811-3 0.32 cm (0.125 in.) thick	Minor acid discoloration. No apparent embrittlement. Some swelling and acid pickup.
Fluorel, FC 2181 Fluorel, FC 2330 0.15 cm (0.060 in.) thick	Slight acid discoloration. No apparent embrittlement.
Kalrez, K00506, No. 1058 0.15 cm (0.060 in.) thick	No acid attack. No apparent embrittlement or swelling.

3.7.4.1 CATALYST

A large lot of catalyst (18 kgs) referred to as Lot 3 procured for production of nine-cell stack electrodes was received but inspection revealed the presence of contamination in the form of large foreign particles (up to 0.3 cm) such as glass, ceramic, wood and other debris. This material was rejected and returned to the vendor and rejected a number of times.

Radiography of finished electrodes was performed initially to determine if it could be used as a means of assessing variability within a finished electrode. It was performed using a Faxitron unit at 70 kV, ultrafine grain film (Kodak Industrex R) and without intensifying screens. Initial results did not indicate electrode variability, but did indicate the presence of numerous small high density particles (hundreds per electrode layer) scattered throughout the catalyst layer. Particles ranged in diameter from a few hundredths of a millimeter up to 0.75 mm. SEM and EDA analysis of these particles left in the original electrode layer indicated trace amounts of iron and nickel as well as platinum and sulfur as expected. To obtain a more definitive analysis of the dense particles, several of the larger ones were removed from the catalysed layer for EDA examination. The analysis indicated that the particles were high in iron with varying amounts of chromium and nickel present. At this time no definite conclusions can be drawn concerning the source of the particles or their effect on electrode performance.

Chemical analysis of Lot 3 catalyst together with that of previously used Lot No. 1 catalyst, Vulcan XC-72 support, finished cathode layer from Lot No. 1 catalyst and ERC cathode are given in Table 3.7.4-1. As expected, these spectrographic analyses indicate higher Fe, Cr and Ni in the catalyst and finished electrodes than in the Vulcan XC-72. In addition, the emission spectrography indicated the presence of palladium. The increase in the foreign elements are presently thought to be associated with operations performed by the catalyst vendor. The palladium accounts for 1.09 percent of the total platinum present in Lot 1 catalyst and 0.54 percent of the platinum present in Lot 3 catalyst. The overcheck of platinum loading in finished cathodes was determined by both wet chemistry and X-ray fluorescence. The data given in

TABLE 3.7.4-1

EMISSION SPECTROGRAPHIC ANALYSES OF ELECTRODE LAYERS, CATALYST AND CATALYST SUPPORT MATERIAL

	Al	Ag	B	Be	Bi	Ca	Cd	Co	Cr	Cu	Fe	Ga	Ge
ERC Cathode Layer	.02	.003	<.0001	<.0001	<.001	.03	<.003	<.001	.002	.003	.03	<.0005	<.0005
AESD Cathode Layer	.04	.0001	<.0001	<.0001	<.001	.02	<.003	<.001	.001	.003	.06	<.0005	<.0005
Vulcan XC-72, P.O. 55499	.02	<.0001	<.0001	<.0001	<.001	.02	<.003	<.001	<.001	.0001	.003	<.0005	<.0005
Lot No. 1 Catalyst P.O. 56742	.01	<.0001	<.0001	<.0001	<.001	.001	<.003	<.001	<.001	.0004	.01	<.0005	<.0005
Lot No. 3 Catalyst P.O. 64723	.02	<.0001	<.0001	<.0001	<.001	.001	<.003	<.001	.01	.0008	.03	<.0005	<.0005

	La	Mg	Mn	Mo	Nb	Ni	P	Pb	Sb	Si	Sn
ERC Cathode	-	.01	.0002	<.001	<.003	.002	<.005	<.002	<.002	≥1	<.001
AESD Cathode	-	.01	.001	<.001	<.003	.003	<.005	<.002	<.002	.05	<.001
Vulcan XC-72	-	.01	<.0001	<.001	<.003	<.001	<.005	<.002	<.002	.03	<.001
Lot No. 1 Catalyst	-	.0003	.0001	<.001	<.003	.002	<.005	<.002	<.002	.01	<.001
Lot No. 3 Catalyst	-	.0003	.002	<.001	<.003	.01	<.005	<.002	<.002	.03	<.001

	Ti	V	W	Zn	Zr
ERC Cathode	.003	.003	-	.001	<.001
AESD Cathode	.008	.003	-	.001	<.001
Vulcan XC-72	.001	<.0001	-	<.001	<.001
Lot No. 1 Catalyst	<.001	.001	-	<.001	<.001
Lot No. 3 Catalyst	.003	.008	-	<.001	<.001

Table 3.7.4-2 indicate fair agreement between the two methods, but do not indicate acceptable agreement between the calculated and measured platinum loadings. Additional work is required to resolve this difference. Analyses performed on the support and catalysed support are given in Table 3.7.4-3, including sulfur, pH and surface area of the catalyst.

The performance of Lot No. 3 catalyst in subscale tests is reported in Section 3.1.5.

3.7.4.2 SILICON CARBIDE

The processing formulation utilized to apply the silicon carbide layer was altered to incorporate the use of viscosity control for the Polyox WSR-301 (polyethylene oxide homopolymer) water solution and the SiC slurry which is roller bar coated on the cathode. Previously this was done based on controlling the weight of constituents used in formulation of the mix and not on measured viscosity. The previous SiC coating, while giving reasonably good performance, was variable in integrity on the electrode; they frequently were susceptible to cracking and spalling. The bubble pressure of this previous SiC layer as measured using a modified stainless steel Gelman in-line filter (47 mm diameter) gave results which ranged from 110 to 186 kPa (16 to 27 psig). The SiC layer was float filled for 15 minutes in ∿100 w/o H_3PO_4 prior to bubble pressure measurement using helium.

The revised processing using a controlled Polyox viscosity produced electrodes with heat treated SiC layers which were adherent and did not show layer cracks or spalling. The bubble pressure of these layers ranged from 91 to 136 kPa (13 to 19.5 psig). While slightly lower than the earlier coatings, these bubble pressures are considered acceptable based on current design requirements.

Porosity of this revised process SiC coating was determined for two thickness [using 0.18 mm (0.007 in.) and 0.25 mm (0.010 in.) shims]. The porosity for the thinner material ranged from 55 to 58 percent (averaging 56.3 percent) while the thicker material ranged from 56 to 59 percent (averaging 57.7 percent). These

TABLE 3.7.4-2

PLATINUM ANALYSIS OF CATHODES

Cathode Identification	Calculated Pt mg/cm^2	Analyzed Pt wt. chem. mg/cm^2	Analyzed Pt. X-ray Fluorescence, mg/cm^2
ERC-Typical Production Cathode	0.50 to 0.55	0.50	$\sim$ 0.44
AESD-C-055-1	0.43	0.32	$\sim$ 0.37

TABLE 3.7.4-3

MISCELLANEOUS EVALUATIONS OF CATALYST AND SUPPORT

Material	Weight Percentage of Sulfur	pH	Surface Area, m^2/g
Vulcan XC-72	1.4	6.8	217.2
Lot No. 1 Catalyst	1.0	4.5	209.5
Lot No. 3 Catalyst	1.0, 1.1	5.0	198.3

data indicate a relatively small spread in the porosity and are similar to the average value of 58.8 percent previously reported for the old mixing process.

It was determined that the viscosity of Polyox WSR-301 solutions were not in agreement with typical vendor data. Limitation in shelf life of old material as well as a rather wide range in as supplied viscosity (depending on the degree of polymerization of the production lot) became apparent, see Figure 3.7.4-1. A more recent shipment of this material contains a stabilizer and the shelf life now used is suggested to be at least six months.

The resin solutions are non-Newtonian in that the viscosity varies with the shear rate. Thus in measuring the viscosity, the method used to measure it can influence the results especially in the higher Polyox concentration ranges. Figure 3.7.4-2 shows Union Carbide (using a Brookfield Viscosimeter, No. 1 spindle at 2 rpm) compared to AESD (National Instrument Co., Dip-N-Read Model VT-02, Rotor No. 3 at 62.5 rpm) solution concentration of resin versus solution viscosity results.

The acid wicking rate of the SiC layer produced by the previous procedure was evaluated and the rate and acid content are 4.1 mm/hr. This is substantially higher than that of the MAT-1 material, suggesting that the principle lateral acid transport layer is the SiC. While the presently formulated material has not been evaluated, based on the porosity data, it should be quite similar to previous material.

3.7.4.3 AMMONIUM BICARBONATE

A series of experiments were initiated to characterize the particle size and distribution of the ammonium bicarbonate utilized in electrode manufacture. The grinding of this material in production is done in Shell Sol. 340. It was noted that the ground powder once dried is unitable and decomposes relatively quickly at ambient temperature. Thus, dry techniques for particle analysis cannot be utilized. The only reliable techniques for particle analysis that seem practical are wet techniques using a fluid such as alcohol, which does not react with the ammonium bicarbonate. Samples were prepared using anhydrous

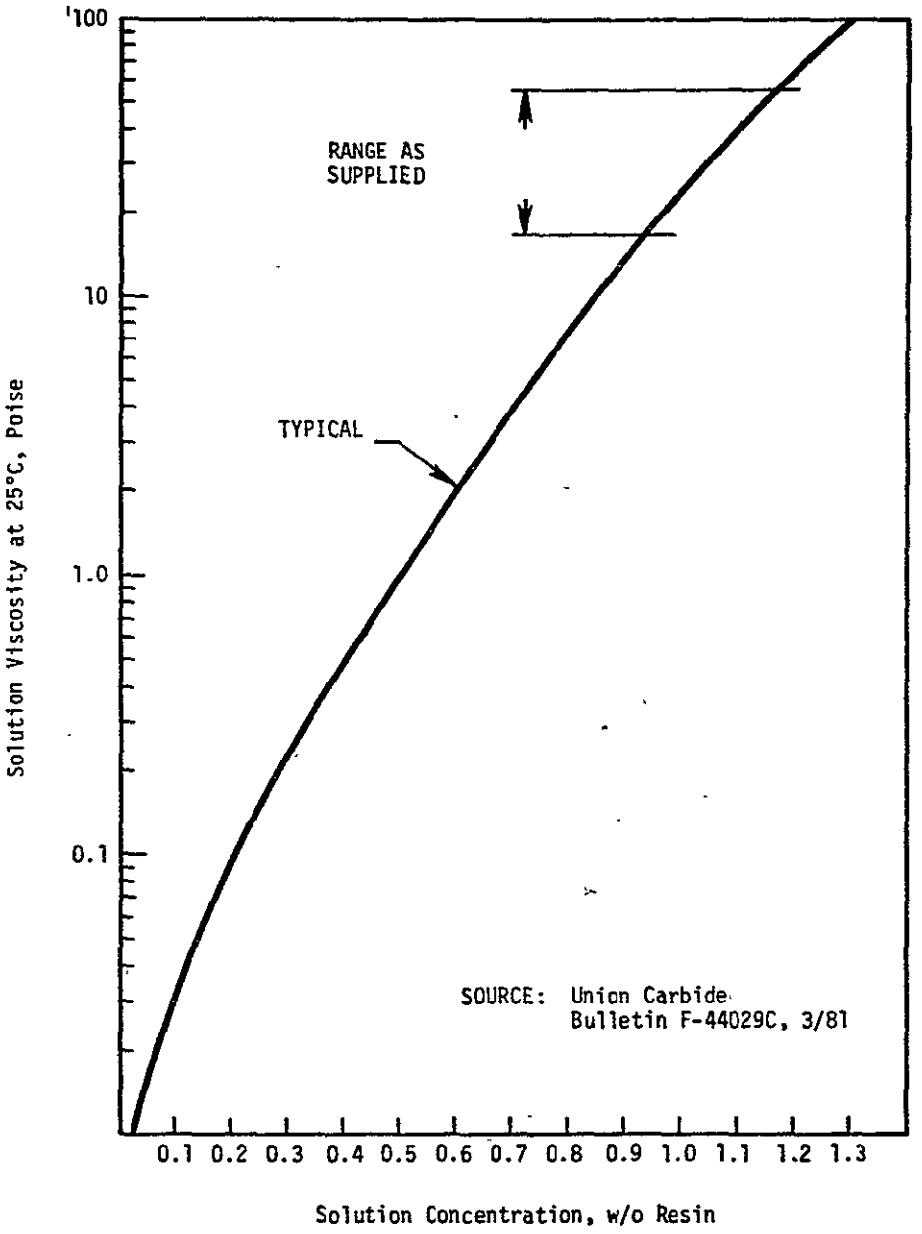

Figure 3.7.4-1 Solution Viscosity Versus Concentration Polyox WSR-301

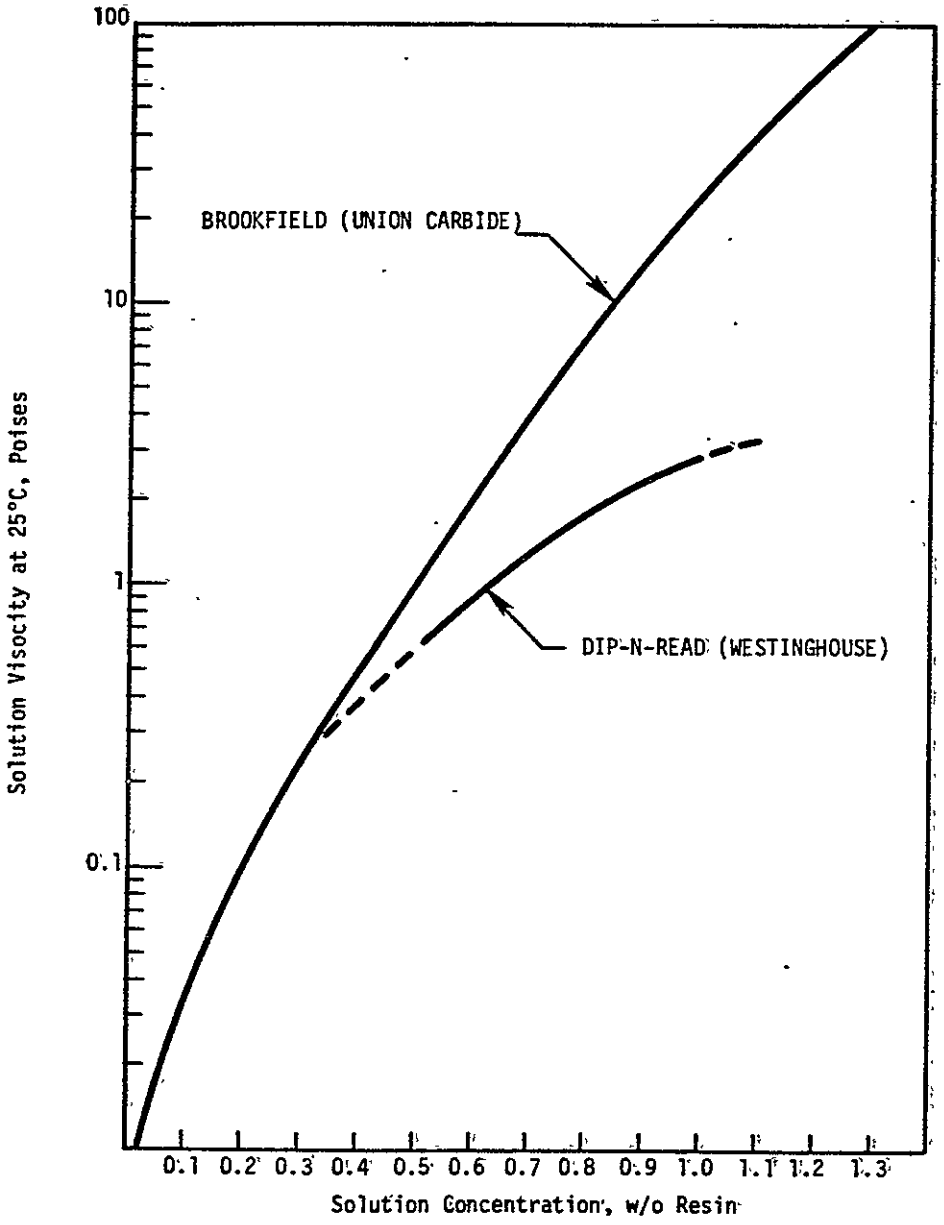

Figure 3.7.4-2. Brookfield Versus Dip-N-Read Viscosimeter Data Versus Polyox WSR-301 Concentration

200-proof ethyl alcohol to remove the Shell Sol 340 and for storage to prevent decomposition of the fine particles. This technique of specimen storage appears satisfactory although the tendency for the bicarbonate particles to agglomerate during storage in the alcohol was noted. The use of alcohol should permit particle size analysis using techniques such as Microtrac or Coulter Counter.

3.7.4.4 BACKING PAPER

Mercury porosimetry of typical wet proofed backing paper samples and its reproducibility in one sheet were determined. These data are given in Table 3.7.4-4 and typical pore volume versus intrusion pressure (pore radius) curves are given in Figure 3.7.4-3.

To determine the effect of compressive stress on the electrical resistance of Teflon impregnated (40 w/o) electrode backing paper, a ten high stack of 7.6 cm square backing paper samples were cyclically compressed up to 690 kPa (100 psi) between gold plated flat end contact plates. While the resistance values presented in Table 3.7.4-5 include the sheet to sheet contact resistance of the paper, contact resistance to the end plates and change in resistance within each sheet of material due to compaction, the data are felt to reflect the relative resistance behavior of this electrode component in cell stacks. Under compressive stresses above about 207 kPa (30 psi), the resistance of the stack shows only a minor decrease with increasing stress and relatively small changes upon multiple loadings. These data suggest that the Teflon layer on the boiling paper fibers is not being damaged by imposition of this stress level or by limited cycling.

3.7.5 MATRIX MATERIALS

Two types of conventional MAT-1 material were evaluated, the older reference material made by mixing in a Ross Blender, limited to about 16 sheets (full cell size) per mix and the second more recent type mixed in a Schold Mixer capable of producing approximately 100 full size sheets per mix. The reason for making this process change is economics of MAT-1 production. MAT-1

TABLE 3.7.4-4

BACKING PAPER MERCURY POROSIMETRY DATA

Material	Specific Pore Volume, cc/g	Specific Pore Surface, m^2/g	Test Pressure Range (kPa)
C-034-4-BP1	0.92	0.19	0-16.5
C-034-4-BP2	0.91	0.20	0-16.5
C-034-4-BP3	0.94	0.22	0-16.5
C-014-2-BP	1.09	0.23	0-16.5

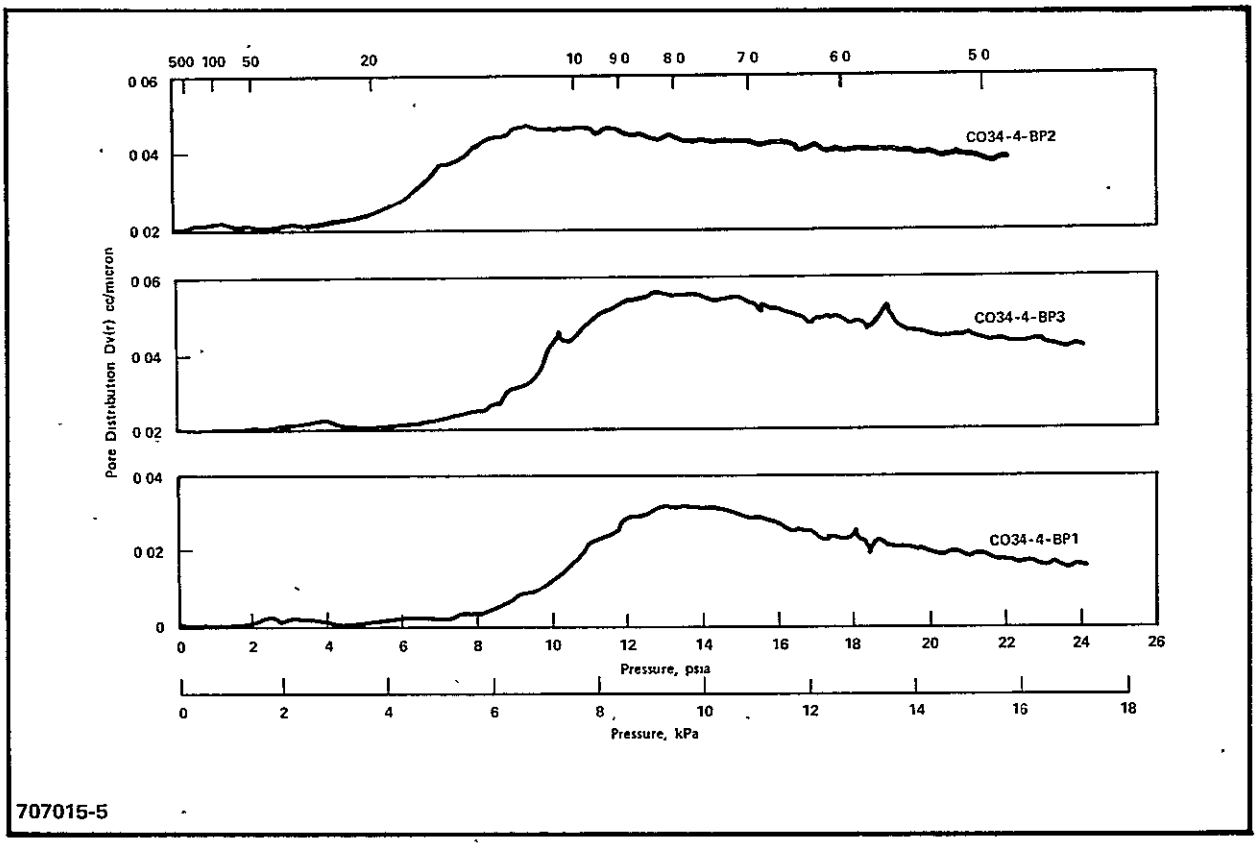

Figure 3.7.4-3. Pore Distribution Versus Mercury Intrusion Pressure for Wet Proofed Backing Paper

TABLE 3.7.4-5

ELECTRICAL RESISTANCE OF COMPRESSIVELY LOADED TEFLON BACKING PAPER (40 wt. percent Teflon)

Stress		Resistance, Milliohms							
		Cycle 1		Cycle 2		Cycle 3		Cycle 4	
kPa	psi	Loading	Unloading	Loading	Unloading	Loading	Unloading	Loading	Unloading
69	10	27.0	12.5	16.5	11.0	14.0	10.2	13.5	10.0
138	20	17.5	8.7	11.0	7.7	9.4	7.3	8.8	7.0
207	30	23.0	7.4	8.4	6.6	7.6	6.2	7.4	6.0
276	40	10.5	6.7	7.4	6.0	6.7	5.7	6.5	5.6
345	50	9.0	6.3	6.6	5.7	6.2	5.4	5.9	5.2
414	60	8.0	6.1	6.3	5.5	5.7	5.2	5.5	5.1
483	70	7.5	6.0	5.9	5.4	5.5	5.1	5.3	4.9
552	80	6.7	5.9	5.7	5.3	5.3	5.1	5.1	4.9
621	90	6.4	5.9	5.5	5.3	5.2	5.1	5.0	4.9
690	100	6.0	5.9	5.4	5.3	5.1	5.1	4.9	4.9

material produced in the Schold Mixer were evaluated after mixing two different times; Exp-002-2-2 was mixed for seven minutes and Exp-002-3-1 was mixed for ten minutes.

Characterization data for the two types of MAT-1 indicate that the materials are quite similar. The minor differences which were found are considered to be within the acceptable limits for the MAT-1 material. Wicking rate and acid content of the material is presented in Table 3.7.5-1, mercury porosimetry data is given in Table 3.7.5-2 and the reactive helium flow rate versus pressure differential for dry matrix material is shown in Figure 3.7.5-1. These data substantiate the above conclusions regarding differences in the two materials.

The bubble pressure determined with helium and using a modified stainless steel Gelman in-line filter (47 mm dia) on float filled material (15 min. in 100 w/o H_3PO_4 at ambient temperature) was 345 kPa (50 psig) or greater for the reference material (M043-15 and 16), 296.5 to 324 kPa (43 to 47 psig) for Exp-002-2-2 material and 338 to 345 kPa (49 to >50 psig) for Exp-002-3-1.

A second process change, the addition of a second heat treatment of the matrix to eliminate possible impurity residues left from the Shell Sol 340, was briefly evaluated. Since it was felt that only minor changes, likely undetectable, would result from this additional heat treatment, detailed characterization was not performed. However, the material was tested in and compared with the reference material in subscale ambient pressure cell tests. No differences in performance attributable to the added heat treat process difference were found.

Evaluation of a replacement for the MAT-1 material having the capability for increased lateral acid transport was initiated. The replacement materials being considered are Stackpole PC-206, Kureha E715, Kureha CP-B-40 and Pfizer FD-33 carbon or graphite papers. As shown in Table 3.7.5-1, all except the Kureha CP-B-40 material have vertical acid wicking rates about 20 times that of the MAT-1 material and acid storage capabilities either equal to or greater than the MAT-1. Due to the relatively large pore size of these materials they

TABLE 3.7.5-1

WICKING RATE AND ACID CONTENT OF MATRIX MATERIALS

Material	Thickness (mm)	Average Wicking Rate (mm/hr)	Acid Content (ml (acid)/cm^2)
Reference Matrix (M043-15)	0.28	1.02	0.0178
New Matrix (Exp-002-2-2)	0.27	1.00	0.0168
New Matrix (Exp-002-3-1)	0.26	1.04	0.0194
Kureha Graphite Paper E715	0.44	22.3	0.0224
Kureha Carbon Paper CP-B-40	0.33	0.95	0.031
Stackpole Graphite Paper PC-206	0.43	37.2	0.0292
Pfizer Carbon Paper FD-33	0.34	20.2	0.0165

TABLE 3.7.5-2

MERCURY POROSIMETRY DATA FOR MATRIX MATERIALS

Material	Skeletal Density (g/cc)	Bulk Density (g/cc)	Specific Pore Volume (g/cc)	Specific Pore Surface (m^2/g)	Median Pore Dia (Angstroms)	Porosity (%)
Reference Matrix	1.73	0.44	1.703	99.4	440-550	74.6
M-043-16	1.70	0.43	1.746	109.9	440-550	74.8
Reference Matrix	1.74	0.43	1.760	104.0	440-550	75.4
M-043-15	1.74	0.43	1.735	99.0	440-550	75.1
New Matrix	1.76	0.40	1.913	105.1	440-600	77.1
Exp-002-2-2	1.70	0.40	1.910	102.6	440-600	76.4
New Matrix Exp-002-3-1	1.81	0.41	1.862	101.4	440-550	77.1

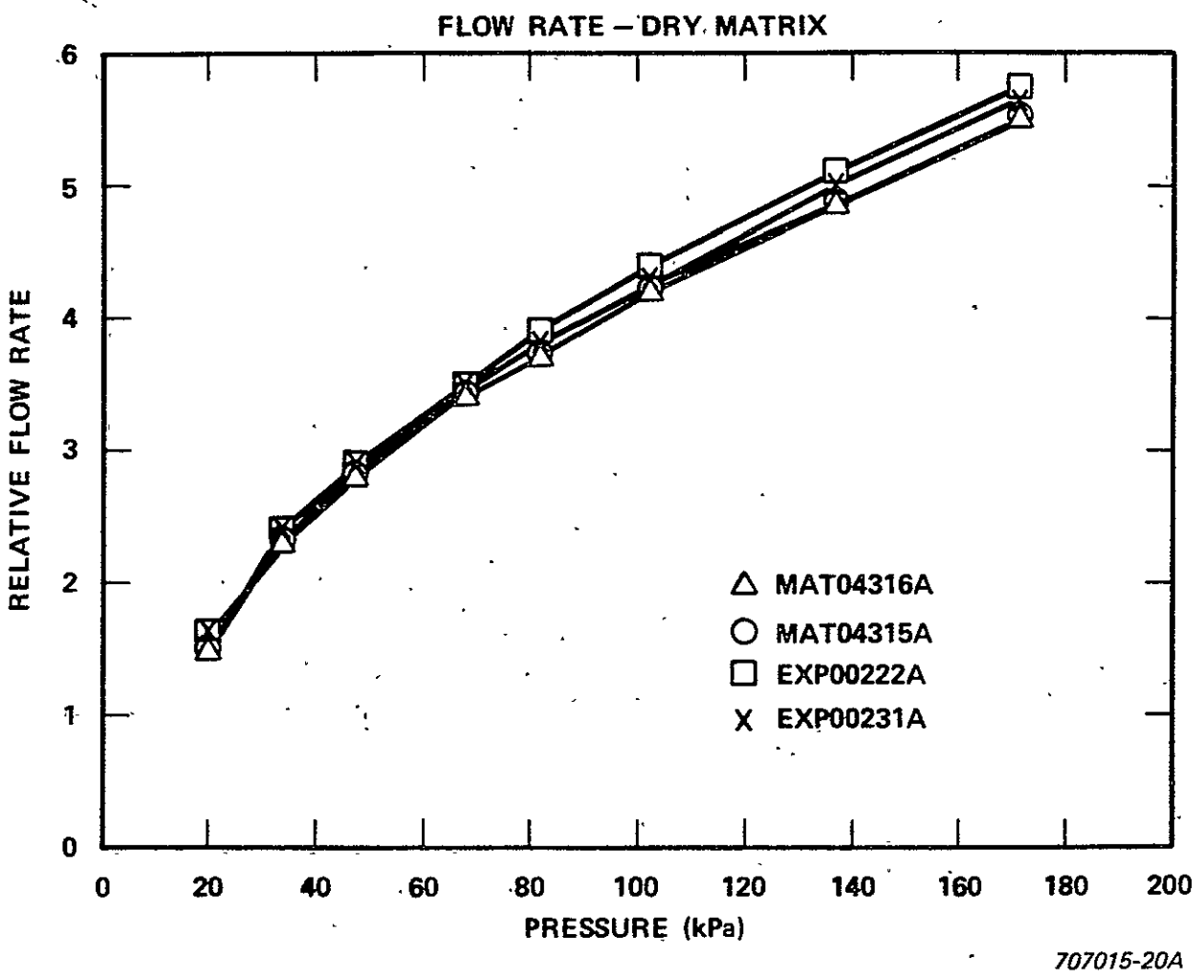

Figure 3.7.5-1. Relative Flow Rate Versus Pressure for Dry Matrix Materials

should exhibit very low bubble pressures and thus the SiC layer on the cathode must provide the gas separation interface in the cell structure. Acid corrosion (100 w/o) with no imposed potential was evaluated for these materials and they were found to be stable for times of 500 hours or greater. Two of the materials were tested in subscale tests; namely PC-206 and Kureha E715. The cell performance of these materials at ambient pressure were presented in Section 3.1.5.

3.7.6 OTHER STACK MATERIALS

3.7.6.1 CURRENT COLLECTORS

Evaluation of plated current collectors was completed. The contact resistance data after approximately 900 hours of 200°C exposure in air for gold and nickel plus gold platings are given in Table 3.7.6-1. The superiority of the duplex plating is apparent, increasing only from 0.75 mΩ to 1.5 mΩ as a result of the thermal exposure. While duplex plating greatly reduces the current collector oxidation, its adequacy in the presence of acid from spills, etc. has yet to be demonstrated.

3.7.6.2 PLATE BRIDGES

A series of tests was initiated to evaluate thin bridge members to prevent the collapse of the cell electrodes backed by fluorelastomer (Viton) seals in the areas of gas inlet and outlet flow channels of the "Zee" bipolar plate geometry. When loaded, the compressible Viton seal backing causes the electrode (anode or cathode) to be forced into the gas flow channels, locally fracturing the electrode and blocking the flow groove in the plate. To correct this problem, a thin, rigid member between the electrode and the plate grooves was examined. The test configuration is shown in Figure 3.7.6-1. Materials evaluated for the rigid bridge members are given in Table 3.7.6-2, and the results of load versus deformation data are given in Table 3.7.6-3. The summary of compressive pressure required to initiate deformation of the bridge support material is given in Table 3.7.6-4. Twelve tests were performed but only the key test results were included on the tables of results. The strain values listed in Table 3.7.6-3 include the deformation of the Viton, anode and

TABLE 3.7.6-1

CONTACT RESISTANCE OF VARIOUS COLLECTOR PLATES

AFTER AIR EXPOSURE AT 200°C

Collector Plate Description	Initial Contact Resistance, mΩ	Exposure Time Hrs	Final Contact Resistance, mΩ
Bare Copper	0.72	72	21.5
Copper + Gold Plate	0.50	888	14.5
Copper + Nickel Plate + Gold Plate	0.75	888	1.5

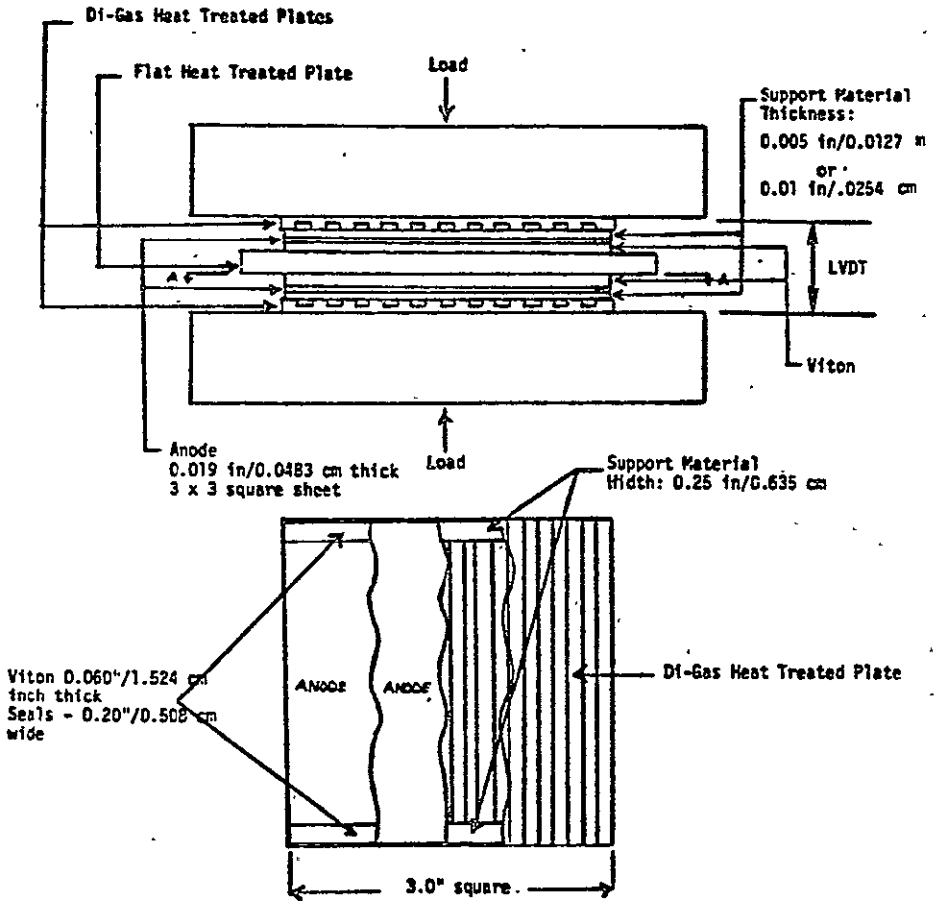

Figure 3.7.6-1. Electrode Seal Interface Test Configuration

TABLE 3.7.6-2
TEST PARAMETERS FOR VITON SEAL AND SUPPORT MATERIALS

Parameter Description	Viton	Teflon	PES-Victrex	Kapton	Graphite
Material Type	Cured and cut from sheet	Cured and skived	Extruded and cut from sheet	Extruded and cut from sheet	Machined from plate
Width (in/cm)	0.20/0.508	0.20/0.508	0.25/0.635	0.25/0.635	0.25/0.635
Thickness (in/cm)	0.60/1.524	0.005/.0127 and 0.01/.0254	0.005/.0127 and 0.01/.0254	0.005/.0127 and 0.01/.0254	0.013/0.033
Attachment Method	Viton cement (one side)	None	None	None	None
Number of Layers	2	2	2	2	2
Supplier	Shields Rubber Co. Pgh., PA	Modern Plastics and Glass, Inc. Bridgeport, CT	Westlake Plastics Company Lenni, PA	DuPont Polymer Products Department Wilmington, DE	Stackpole Grade 2020 Stackpole Carson Co. St. Mary's, PA

TABLE 3.7.6-3

SUMMARY OF LOAD VERSUS DEFORMATION COMPRESSION TEST DATA

Test Number	Support Material and Thickness	Area Nominal in^2 (cm^2)	Maximum Applied Load lbf (Newtons)	Stress σ = Load; Area psi (kPa)	Number of Test Cycles Performed	Number of Test Cycles Avg. Last (1)	$\varepsilon = \frac{\Delta T}{P}$ Total Strain(1) in/in (cm/cm)	Permanent Srain(1) in/in (cm/cm)	Temperature of Test (°F) (°C)	$E = \frac{\sigma}{\varepsilon}$ (1) Tangent Modulus of Elasticity psi (MPa)
1	None	1.2 (7.74)	235 (1045.3)	95.83 (1350.2)	2	1	.245	0.83	77 (25)	1250.2 (8.62)
2	None	1.2 (7.74)	120 (533.8)	100.00 (639.5)	2	1	.159	.057	77 (25)	873.9 (6.03)
3	Teflon (.01"/ .0254cm)	1.2 (7.74)	300 (1334.5)	250.00 (1723.7)	2	1	.231	.100	77 (25)	1846.4 (12.73)
4 2	PES-Victrex (.005"/ .0127 cm)	1.2 (7.74)	312 (1387.8)	260.00 (1792.6)	2	1	.228	.060	77 (25)	2000.0 (13.79)
5	Kapton(2) (.005"/ .0127 cm)	1.2 (7.74)	270 (1201.0)	225.00 (1551.3)	2	1	.229	.081	77 (25)	1628.4 (11.23)
6 2	PES-Victrex .01"/.0254 cm)	1.2 (7.74)	268 (1192.1)	223.33 (1539.8)	2	1	.289	.150	392 (200)	1379.5 (9.51)
7	Graphite (0.013"/ .033 cm)	0.80 (5.16)	244.5 (1087.5)	305.6 (2107.0)	1	1	.228	.060	77 (25)	2566.6 (17.7)

(1) Data based on average of cycles indicated.
(2) Grain of material perpendicular to channels.

TABLE 3.7.6-4

SUMMARY OF COMPRESSIVE PRESSURE REQUIRED TO INITIATE DEFORMATION OF SUPPORT MATERIAL

Material and Thickness	Ambient Temperature		Operating Temperature		
	Cycle 1	Cycle 2	Cycle 1	Cycle 2	Cycle 3
TFE (0.01 in/ 0.0254 cm)	55 psi (379.2 kPA)	73 psi 503.3 kPa)	--	--	--
PES-Victrex(1) (0.005 in/ (0.0254 cm)	110 psi (758.4 kPa)	80 psi (551.6 kPa)	74 psi (510.2 kPa)	103 psi (710.2 kPa)	85 psi (586.1 kPa)
PES-Victrex(1) (0.01 in/ 0.0254 cm)	116 psi (799.8 kPa)	100 psi 689.5 kPa)	116 psi 799.8 kPa)	94 psi (648.1 kPa)	-- --
Kapton(1) (0.005 in/ (0.0127 cm)	124 psi (854.9 kPa)	76 psi (524.0) kPa)	--	--	--
Graphite (0.013 in/ 0.033 cm)	305 psi(2) (2103.0 kPa)	--	--	--	--

(1) Grain perpendicular to channels.

(2) The graphite did not exhibit any real deformation of the support material at this point.

bridge material. Since the actual strain of the assembly is the important aspect, the modulus of elasticity value represents the effective modulus of the bridge region. Both visual and stress-versus-strain curves were used to define a stress at which the bridge material deformed into the grooves of the plate.

In certain cases, the transition point was exhibited via a change in slope on the stress-versus-strain curve. Subsequent load deformed the bridge into grooves and produced indentations into the bridge material surface. The results of this study indicated that the only acceptable material for the long term creep capability would be the Stackpole 2020 graphite machined from stock material.

All of the materials evaluated for bridge member application were given preliminary corrosion tests for 500 hours at 200°C (no applied potential) in 100 w/o H_3PO_4. No major corrosion was visible on any of the materials tested and the 2020 graphite showed no acid interaction.

3.7.6.3 PHOSPHORIC ACID

Modification and checkout of two Teflon-lined autoclaves (750 cm^3 volume) was completed. These two systems capable of operating up to about 230°C are being used for corrosion studies on cell components and materials and for the measurement of physical properties of phosphoric acid at elevated temperatures. An all-Teflon corrosion cell and a conductivity cell were fabricated. Corrosion testing of bipolar plate material (67 w/o A99/33 w/o resin heat treated to 900°C) was done in 94 w/o acid at 190°C and 690 kPa (100 psia). Corrosion current was measured after 24 hours equilibration at each potential. The first cycle data are in good agreement with previously published data. The second cycle data for the same sample resulted in differences in the corrosion current particularly at the lower potentials. These differences are likely associated with changes in the "true" surface area of the sample after being corroded at higher potential in the first cycle. These studies again demonstrate the problem of defining the true corrosion area to be used for data analysis and comparison of materials.

At temperatures above 170°C, published quantative data on the conductivity of phosphoric acid is quite limited. To supplement available data, a limited effort was undertaken to obtain specific conductivity data for this acid over the temperature range from 160°C to 210°C.

3.7.6.4 STACK MECHANICS

Small scale stack mechanics tests were performed to determine the cell components structural characteristics at ambient and operating temperature. A test stack of ten units (electrodes, matrix and bipolar plates) was tested at ambient temperature and 200°C. The 7.6 cm x 7.6 cm x 10 unit high stack used plates cut from heat treated digas configured plates. This provided the first data on cell compression stress as loaded between ribbed plates in the dry condition (no acid).

This configuration produces a contact area equal to 16 percent of the gross area of 58.06 cm^2 (9.0 in^2). This ribbed configuration may cause larger deflections during compression due to this reduced area. It should also be noted that the "zee" bipolar plate design produces constant areas of 16 percent or 40 percent based on the location on the plate. Therefore, the data obtained from this test is directly applicable to 16 percent contact area of the plate. However, the weighted average contact area of the plate is actually 33 percent of the gross plate area. Therefore, full size stack compressed to 344.7 kPa (50 psi) will produce an effective contact pressure on the cell components of 1034.1 kPa (150 psi). This effective contact pressure is critical for maintaining a low contact resistance and precluding the cracking of the backing paper. The test compressive load was limited to 1034.1 kPa (150 psi) contact stress which should occur during actual test conditions.

The test unit was cycled from 0 to 172.3 kPa (0 to 25 psi) stress based on the gross area, three times to remove slack in system and reduce the plastic deformation which may develop in the stack. The stack was then heated to 200°C and cycled one time before being held at temperature for 85 hours. The load relaxation was monitored to determine the amount of creep deformation which may occur at operating temperature.

Figure 3.7.6-2 shows a plot the compressive stress verses cell strain based on gross area. The loading cycle produces a non-linear stress-versus-strain curve. The stack was allowed to relax (cross-head fixed) between cycles 2 and 3. The nominal modulus of elasticity values increased between cycle 1 and cycle 4, which were 4.68 MPa (680.0 psi) and 6.37 MPa (923.9 psi), respectively. With the stack loaded at the end of cycle 4, the test unit temperature was increased to 200°C. Figure 3.7.6-3 shows the results of the high temperature loading cycles. During the heat up phase, a permanent set of approximately 1 percent strain occurred. The modulus of elasticity values for cycles 1 and 2 at operating temperature are almost identical at 7.84 MPa (1137 psi).

These modulus of elasticity values are considerably lower than test data obtained for flat compression samples. This test unit with bipolar plates, arranged in a Digas configuration, only provides a contact area of 9.29 cm^2 (1.44 in^2) rather than the nominal 58.06 cm^2 (9.0 in^2). The ambient test data for cycles 1 through 4 are shown on Figure 3.7.6-4 using the effective contact area. The cycle 1 and cycle 4 modulus of elasticity values for the effective area case become 32.57 MPa (4725.0 psi) and 38.61 MPa (5600 psi), respectively. The first cycle modulus values are consistent with the results obtained for flat tests using dry components. The total strain exhibited by these tests is smaller than that exhibited by previous tests using flat plates. Since the ribbed plate loading is more prototypic of the actual stack conditions, these values will be used for future evaluations and studies.

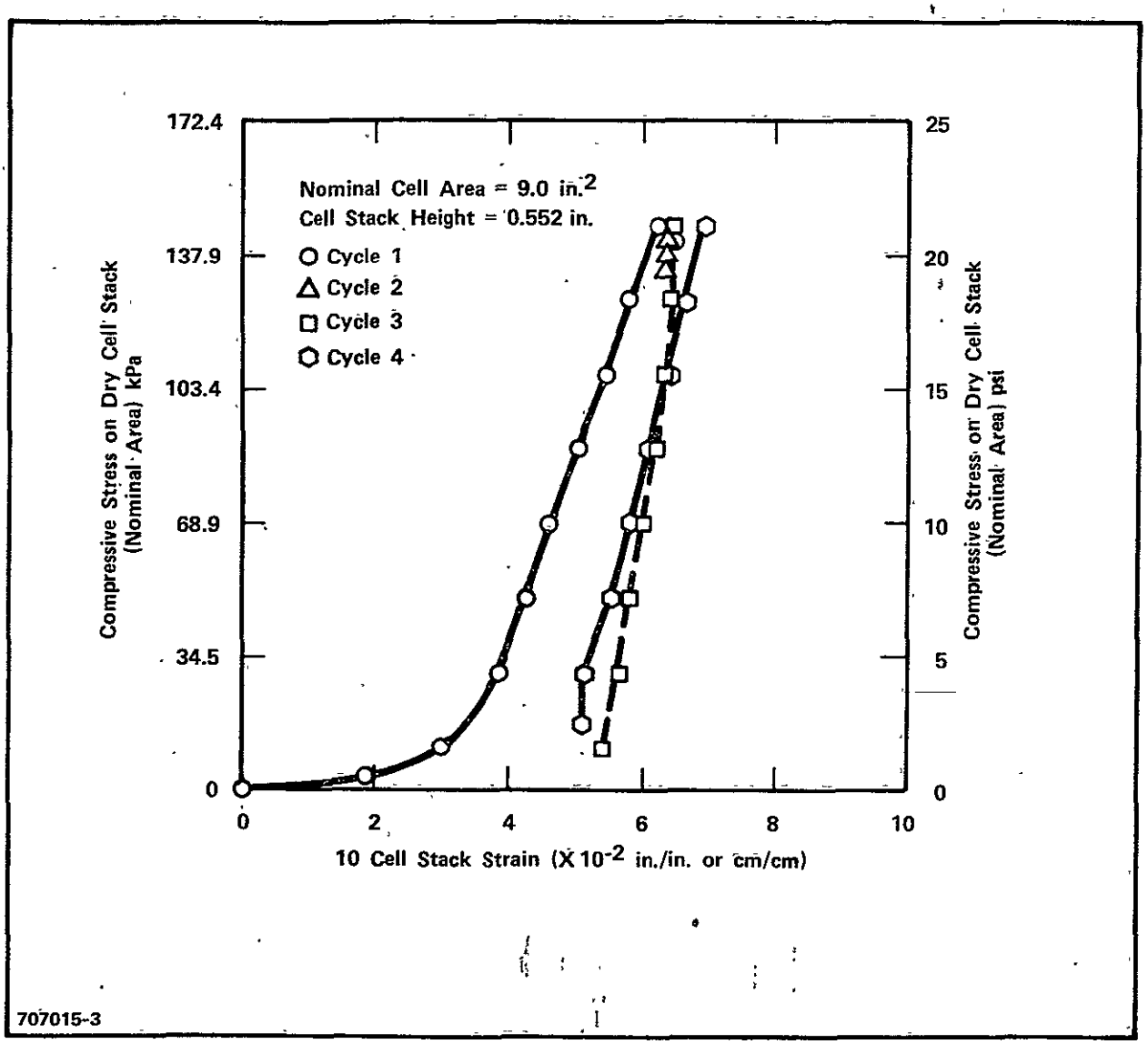

Figure 3.7.6-2. Nominal Compressive Stress Versus 10-Cell Stack Strain for Dry Stack with Heat Treated Bipolar Plates at Ambient Temperature for Cell Group VI

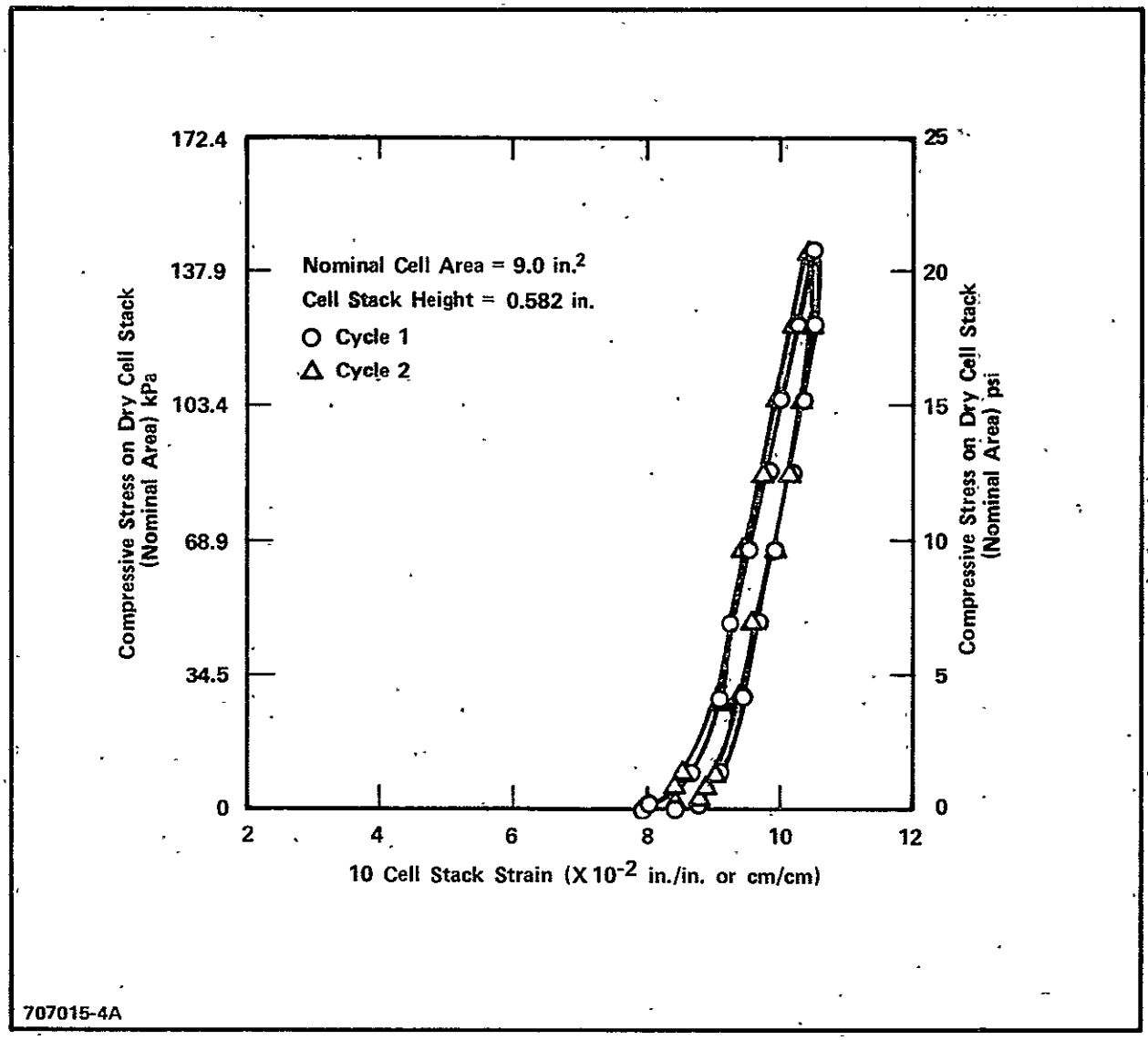

Figure 3.7.6-3. Nominal Compressive Stress Versus 10-Cell Stack Strain for Dry Stack with Heat Treated Bipolar Plates at Operating Temperature of 200°C for Cell Group VI (includes ambient cell pre-conditioning)

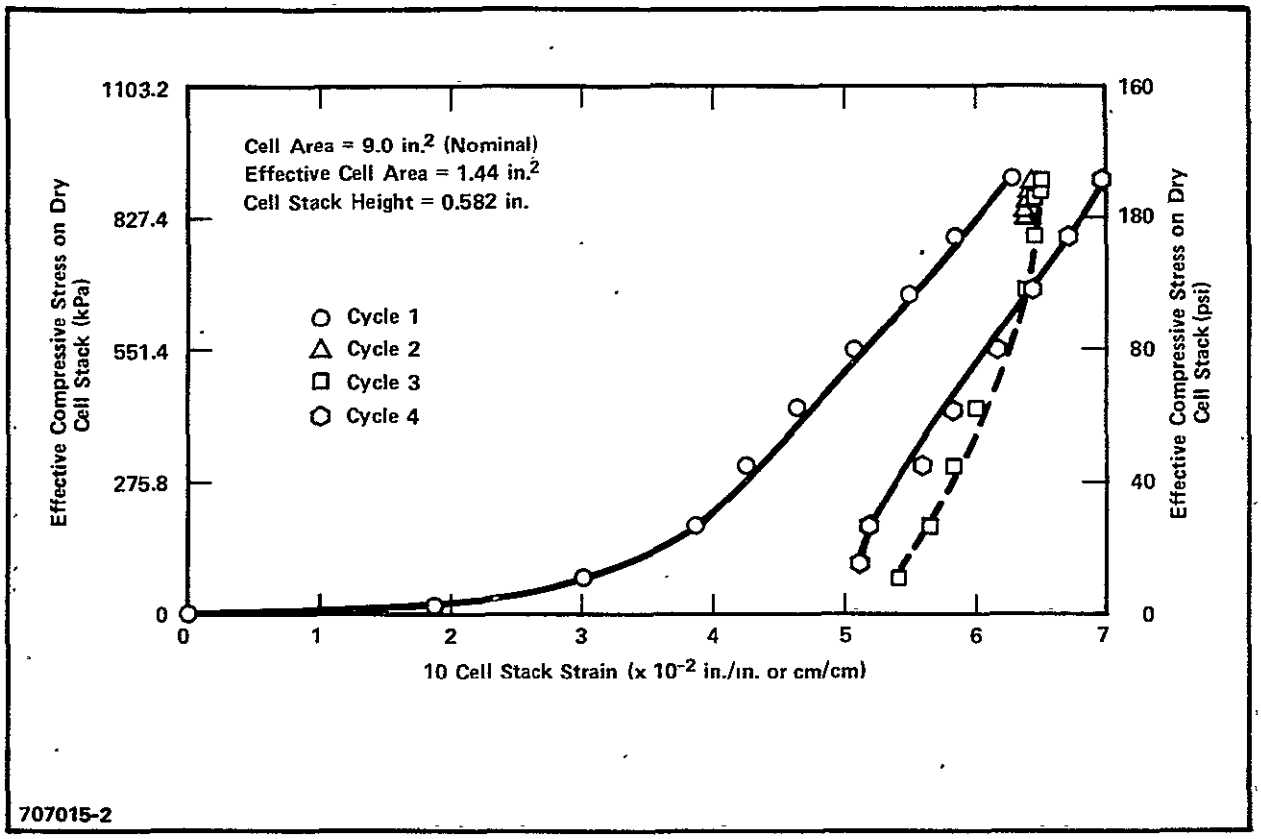

Figure 3.7.6-4. Effective Compressive Stress Versus 10-Cell Stack Strain for Dry Stack with Heat Treated Bipolar Plates at Ambient Temperature Cell Group VI (ambient cell pre-conditioning)

3.8 ADVANCED FUEL CELL DEVELOPMENT

3.8.1 CATALYST AND SUPPORT

Two cells with 900°C heat-treated Pt (Cells 3009 and 3010) and two with standard Pt (Cells 3011 and 3012) were tested to compare the stability of the heat-treated versus non heat-treated catalyst. Atmospheric IR-free performance of the heat-treated catalyst cells was ∿ 676 mV at 200 mA/cm^2 while that of the standard Pt cells was ∿ 673 mV. All these cells showed a good stability during the testing period. Based on these experiments, no significant difference between the stability of heat-treated Pt and standard Pt was evident; however, long term stress testing is required to clearly differentiate the stability of the two materials. It should be noted that the Pt surface area of the heat-treated catalyst is lower than the standard catalyst.

Eight cells (3017 through 3024) were assembled and tested to study the performance of Pt catalyst on heat-treated carbon supports. These cells showed ∿ 17 to ∿ 44 mV lower IR-free performance in comparison to the cells containing standard Vulcan support. These cells also showed ∿ 10 mV higher oxygen gain than the cells built with a standard Vulcan catalyst support. These results confirm the results obtained under the NASA LeRC DEN3-205 program, however the cells tested under the DEN3-205 program did not contain Mat-1 layers.

Six of these cells were tested at 70 psia and 325 mA/cm^2. Pressurized performance of these cells was also lower than the pressurized performance of the standard Vulcan cells. This difference in performance is attributed to a difference in the wetting characteristics of the heat-treated and non heat-treated supports.

It is concluded that further effort is required to optimize the electrode structure with respect to the heat-treated catalyst support materials.

3.8.2 ACID MANAGEMENT

Effort was directed at standardizing the method for calculating the acid volume change between various operating conditions. After examining the available

literature for the vapor pressure and temperature data* the following conclusions and assumptions were made:

- Although the accuracy of the MacDonald and Boyack* equations is limited at low temperatures (∿ room temperature) and operating temperatures (∿ 190°C), they are probably the best choice.
- It is assumed that the electrolyte in the cell package is in thermodynamic equilibrium with the reactant gases. This is a very simplified assumption and it may not be strictly applicable.
- Average water partial pressure determines the average electrolyte concentration in the cell package.

The MacDonald and Boyack equations were used to develop constant concentration curves (Figure 3.8.2-1) and constant volume curves (Figure 3.8.2-2). These curves facilitate the determination of electrolyte concentration and electrolyte volume (in the cell package) for the desired operating conditions.

Several acid inventory control members (AICM) were fabricated by stamping an FEP solution on one face of the backing paper and spraying an FEP solution on the opposite face (Figure 3.8.2-3). The dotted wetproofed areas allow gas flow through the backing paper to the electrode layer. The sprayed-on face of the backing paper remains in contact with the bipolar plate. The FEP content for fifteen AICMs was ∿ 43 percent ± 3 (one standard deviation). Table 3.8.2-1

---

* References for Vapor Pressure of H_3PO_4

(1) MacDonald, D. I., and Boyack, J.R.; "Density, Electrical Conductivity, and Vapor Pressure of Concentrated Phosphoric Acid," Journal of Chemical and Engineering Data, Vol. 14, No. 3, July 1969, pp 380-384.

(2) Brown, E.H., and Whitt, C.D.; "Vapor Pressure of Phosphoric Acids," Industrial and Engineering Chemistry, Vol. 44, No. 3, March 1952, pp. 615-618.

(3) Fontana, B.J.: "The Vapor Pressure of Water Over Phosphoric Acids," Journal of American Chemical Society, Vol. 73, 1951. p. 3348.

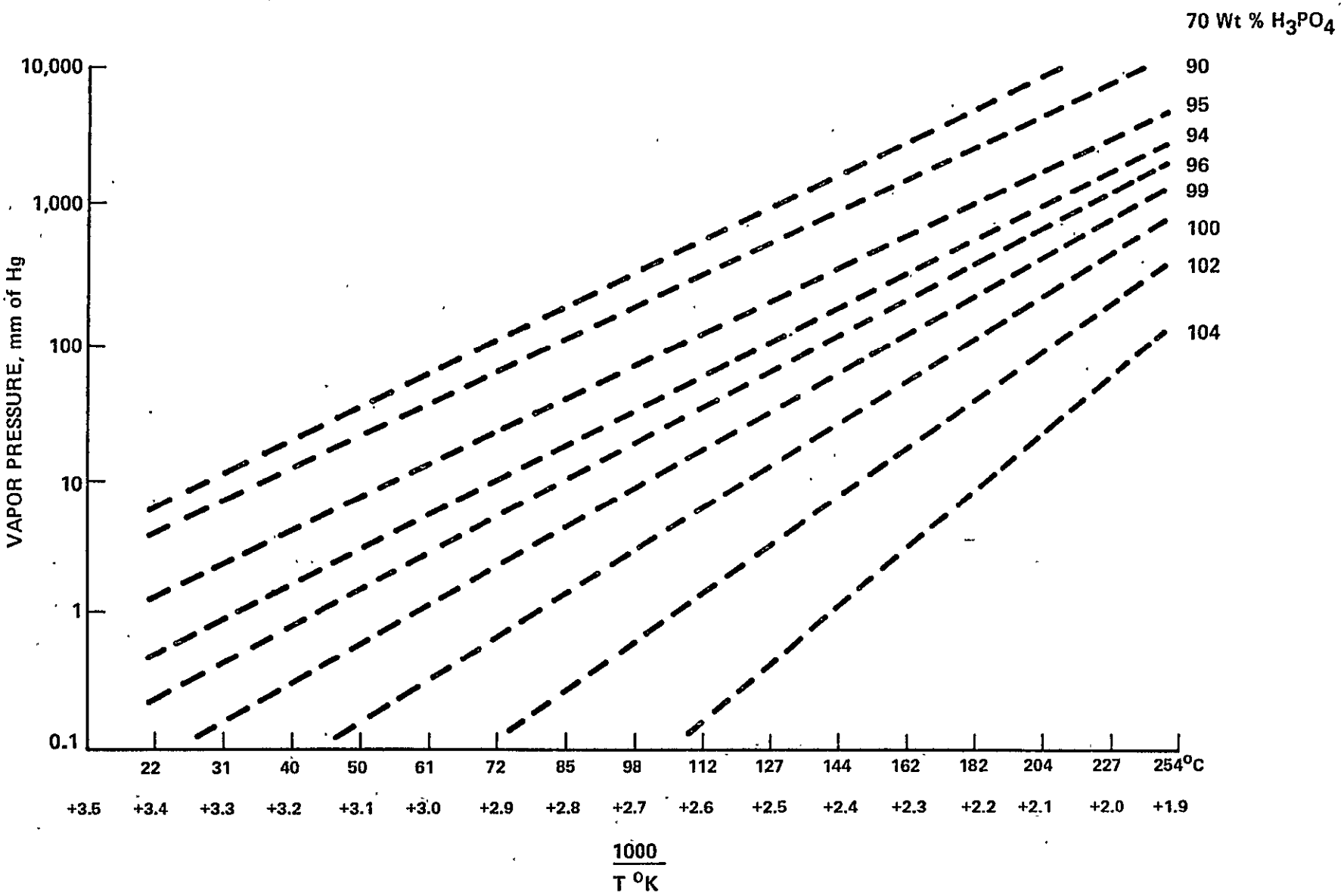

Figure 3.8.2-1 Water Vapor Pressure Versus Temperature for Constant Concentrations (System: H_3PO_4 and Water)

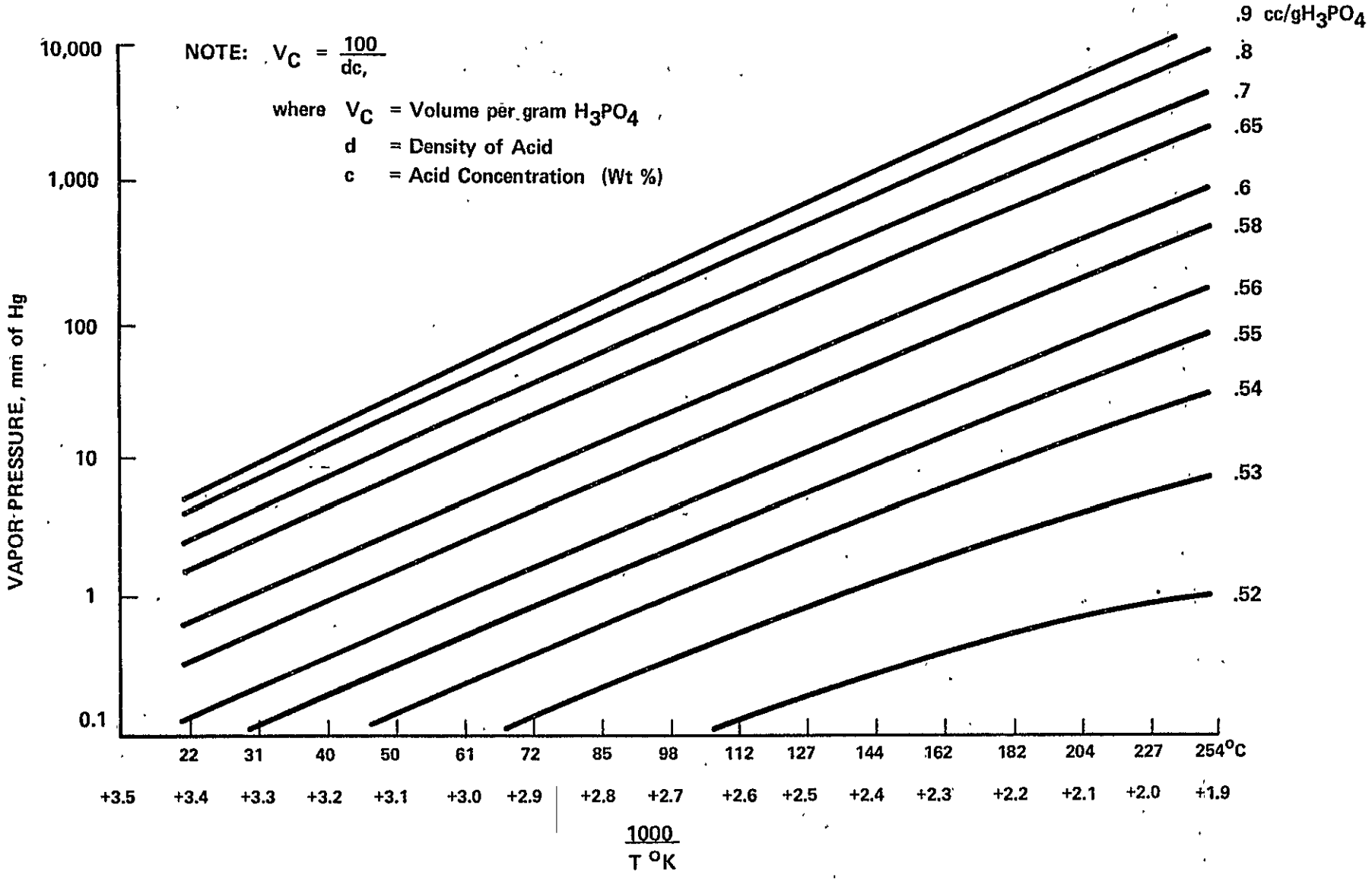

Figure 3.8.2-2 Water Vapor Pressure Versus Temperature for Constant Volume (System H_3PO_4 and Water)

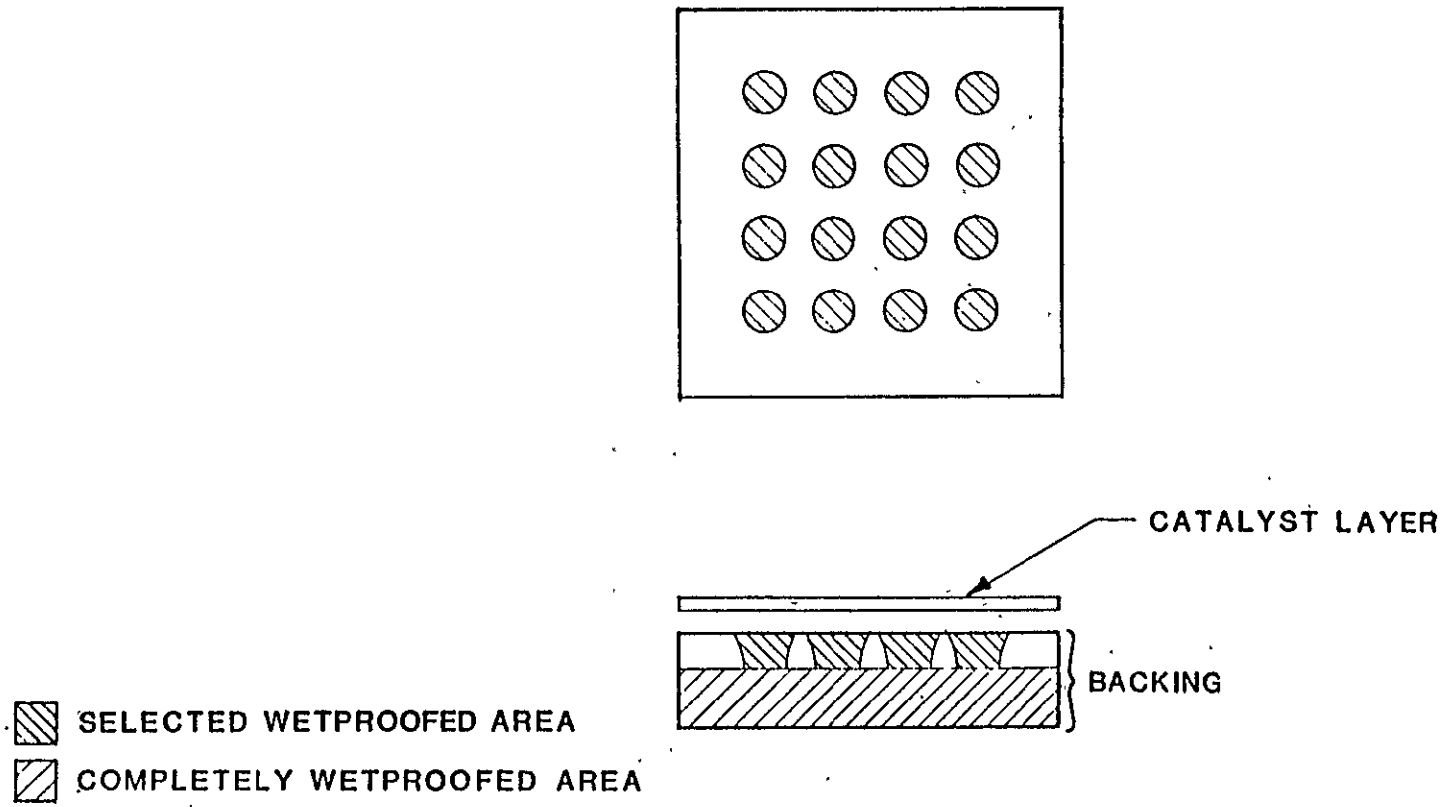

Figure 3.8.2-3 AICM-Anode Backing

TABLE 3.8.2-1

REPRODUCIBILITY OF THE AICM MANUFACTURING PROCESS

AICM #	INITIAL THICK (IN.)	INITIAL WEIGHT (GR.)	DOTTED AREA WT% FEP
W33	.014	18.20	40
W34	.015	19.12	44
W43	.016	19.79	40
W45	.015	20.50	46
W46	.015	19.77	44
W47	.014	20.23	39
W53	.015	20.18	38
W54	.015	19.65	43
W55	.015	20.04	46
W56	.014	19.73	43
W57	.012	19.90	45
W58	.015	19.41	43
W59	.014	20.20	41
W60	.014	18.77	47
W61	.015	20.00	39

BACKING SIZE = 17.75" x 12.75"

STAMPED AREA = 16.50" x 10.50"

NUMBER OF FEP DOTS = 1265

DOT AREA = .29 cm^2

demonstrates that the manufacturing process is reproducible. The electrolyte pick-up for these AICMs was measured by float filling samples at 160°C (electrolyte concentration ∿ 100 percent at 20°). Table 3.8.2-2 compares the electrolyte pick-up of the AICMs, non-wetproofed backing paper and fully wetproofed backing paper. It is apparant that the AICM member has the capability to absorb the electrolyte volume expansion. These AICMs will be tested in a 12 inch x 17 inch nine-cell stack. Additional work is required to optimize AICM with respect to the following parameters:

- Range of the electrolyte volume expansion
- Spacing and the size of the dot pattern
- Effect of the AICM configuration on the contact resistances
- Lateral transfer of the electrolyte

A test apparatus for measuring gas flow resistance through porous media (e.g., backing paper) was designed and fabricated (Figure 3.8.2-4). This apparatus will be used to characterize the various cell components.

3.8.3 POISON EVALUATION

Various materials were selected for chemical analysis under the poison evaluation plan. These materials are listed in Table 3.8.3-1.

The amount of hydrofluoric acid solubles found in the silicon carbide is cause for concern because it can react with the electrolyte and change its properties. Significant levels of sulfur were found in Vulcan carbon and backing paper.

A sample of Stackpole backing paper was heat treated to 900°C to determine if this could remove some impurities. Table 3.8.3-1 shows that sulfur was not removed after heat treatment.

TABLE 3.8.2-2

COMPARISON OF ACID PICKUP IN WETPROOFED, NON-WETPROOFED, AND AICM BACKING PAPER

MATERIAL	SAMPLE	PICKUP* (cc)	PERCENT OF TOTAL** VOLUME FILLED
Non-FEP Backing	1	.699	71.0
	2	.663	72.2
	3	.657	71.6
	4	.621	67.7
	5	.611	71.2
	Mean	.650	
	Std. Dev.	.035	
FEP Backing	1	.021	2.1
	2	.021	2.3
	3	.042	3.8
	4	.031	2.8
	5	.037	3.3
	Mean	.031	
	Std. Dev.	.009	
AICM	1	.39	37.4
	2	.44	42.3
	3	.47	44.8
	4	.41	39.3
	5	.43	40.8
	Mean	.43	
	Std. Dev.	.03	

* Acid pickup determined by float filling 2 x 2 inch samples in 160° phosphoric acid (acid concentration was ∿ 100 percent at 20°C).

** Percent of total volume filled equals

$$\frac{\text{Acid Pickup (cc)}}{\text{Sample Bulk Volume (cc)}} \times 100$$

NOTE: In a 12 x 17 inch fuel cell with an initial electrolyte volume of 50cc, an AICM backing has the capacity for an additional 22cc (a 44 percent volume increase of the initial 50cc).

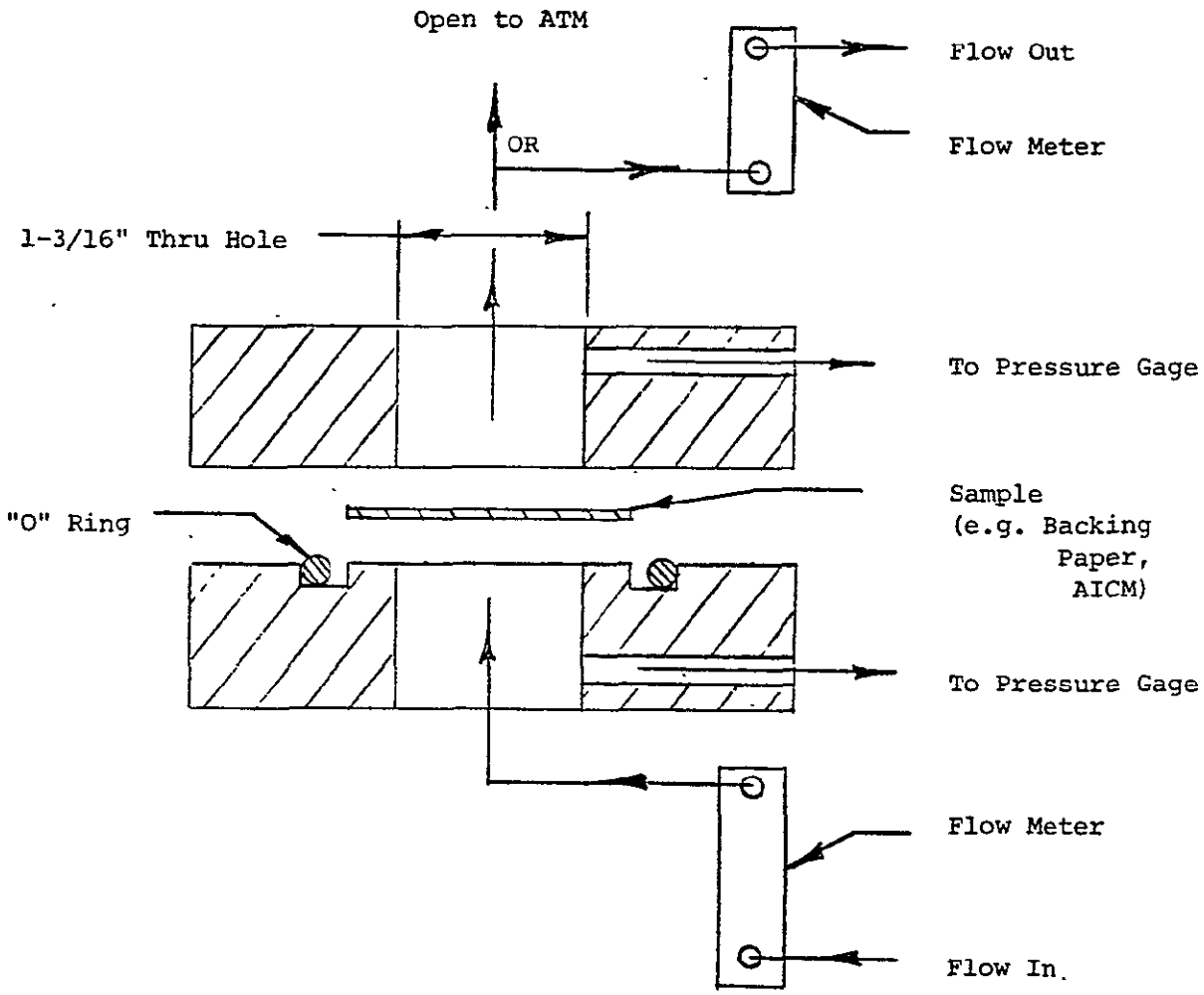

Figure 3.8.2-4 Apparatus for Characterizing Gas Flow Through a Thin Porous Sheet (e.g. Backing Paper)

TABLE 3.8.3-1

CHEMICAL ANALYSIS OF FUEL CELL COMPONENTS AND MATERIALS SELECTED FOR POISON EVALUATION

Semiquantitative Emission Spectrographic Analysis

MATERIAL OR COMPONENT	SULFUR	CHLORIDE	>1%	.1 - 1%	.01 - .1%	.005 - .01%	0 - .005%	REMARKS
tackpole Paper s Received	0.08%	0.13%			Si	B, Mg, Ca	Cu, Fe	Sulfur & Chlorine need to be reduced. Metallic impurity levels seem ok.
tackpole Paper 00°C Heat-treatment	0.046%	.034%				Si, Mg, Ca	B, Fe, Cu	Metallic impurities about the same as previous. Would like further reductions on sulfur and chlorine levels.
eflon 30 s Received	ND < .01%	.042%						Analysis on dry wt. basis. ND-not detected.
sbury A-99 raphite As Received	.016%	ND <.01%			Si,Fe,Mg, Al,Ca,Cu	Mn, Ni,Ti	B, Pb,Sn, V, Cu	Iron 0.33% by Atomic absorption ND-not detected.
ilicon Carbide s Received			Si		Al	Fe,Mg,Ti,Cu, Ca	B, Ni,V	HF Soluble Si-3.96%
arcum Resin s Received	.04%	.027%					Si,Fe,Mg	All levels in prefabricated material look ok.
ulcan Carbon s Received	1.00%	.046%			Mg	Si,Cu,Al	Fe	Sulfur & Chlorine need to be reduced
ulcan Carbon * 00°C Heat Treatment	0.98%	.038%				Si,Mg,Ca	Fe,Al,Cu	
Pt/Vulcan	0.96%*	ND <.01%*	Pt	Pd		Si,Mg,Ce	Fe,Cu,Ag	Ag-10ppm by Atomic Absorption Pd-821 ppm by Atomic Absorption
Pt/Vulcan 00°C Heat Treatment	0.98%*	ND <.01%*	Pt	Pd		Si,Fe,Mg,Cu, Ca, Ag		

Chemical analysis of 900°C heat-treated Vulcan also shows negligible reduction in the sulfur content. An acid leached Vulcan sample was sent for analysis. Discussions were held with Cabot Corporation regarding the removal of the sulfur from Vulcan XC-72. They indicated that most of the sulfur was bound in the structure of the carbon due to their manufacturing process and could not be removed without affecting the structure of the carbon. Chemical analysis of catalyzed Vulcan also shows negligible reduction in the sulfur content due to catalyzation. X-ray dispersion analysis of the catalyst identified some silver and palladium particles.

Four subscale (2 inch x 2 inch) cells (numbers 3025 through 3028) with "cleaned" Mat-1 layers were assembled and tested. Two of these cells were built with the Mat-1 layers manufactured with 900°C heat-treated Vulcan XC-72 and the other two with the Mat-1 layers manufactured with 190°C phosphoric acid leached Vulcan XC-72. The IR-free performance of the "cleaned" Mat-1 cells was $\sim$ 682 mV at 200 mA/cm^2 and 1 atm. pressure, while the corresponding standard Mat-1 cells (3001, 3002, 3005, 3006 and 3010) showed an average of 672 mV. The difference of $\sim$ 10 mV does not clearly indicate that the "cleaned" Mat-1 was responsible for the improvement. Further testing is required to confirm these results. Cell 3029 was built without using the Mat-1 layer. This cell had an IR-free performance of $\sim$ 701 mV at 200 mA/cm^2 and 1 atm. pressure. Figure 3.8.3-1 presents the polarization curves for Cell #3029. Figure 3.8.3-2 presents the polarization curves for the "cleaned" Mat-1 Cell #3028 and no Mat-1 Cell #3029. A close examination shows that the performance of both cells (3028 and 3029) is equivalent (885 mV) at low current density (20 mA/cm^2). The cell containing the Mat-1 layer (3028) has lower IR-free performance at 200 mA/cm^2.

It is suspected that the Mat-1 layer (10 mil thick) adds an extra ionic resistance to the cell package, which is not measured by the conventional resistance measurement techniques. This will be investigated in the next logical unit of work.

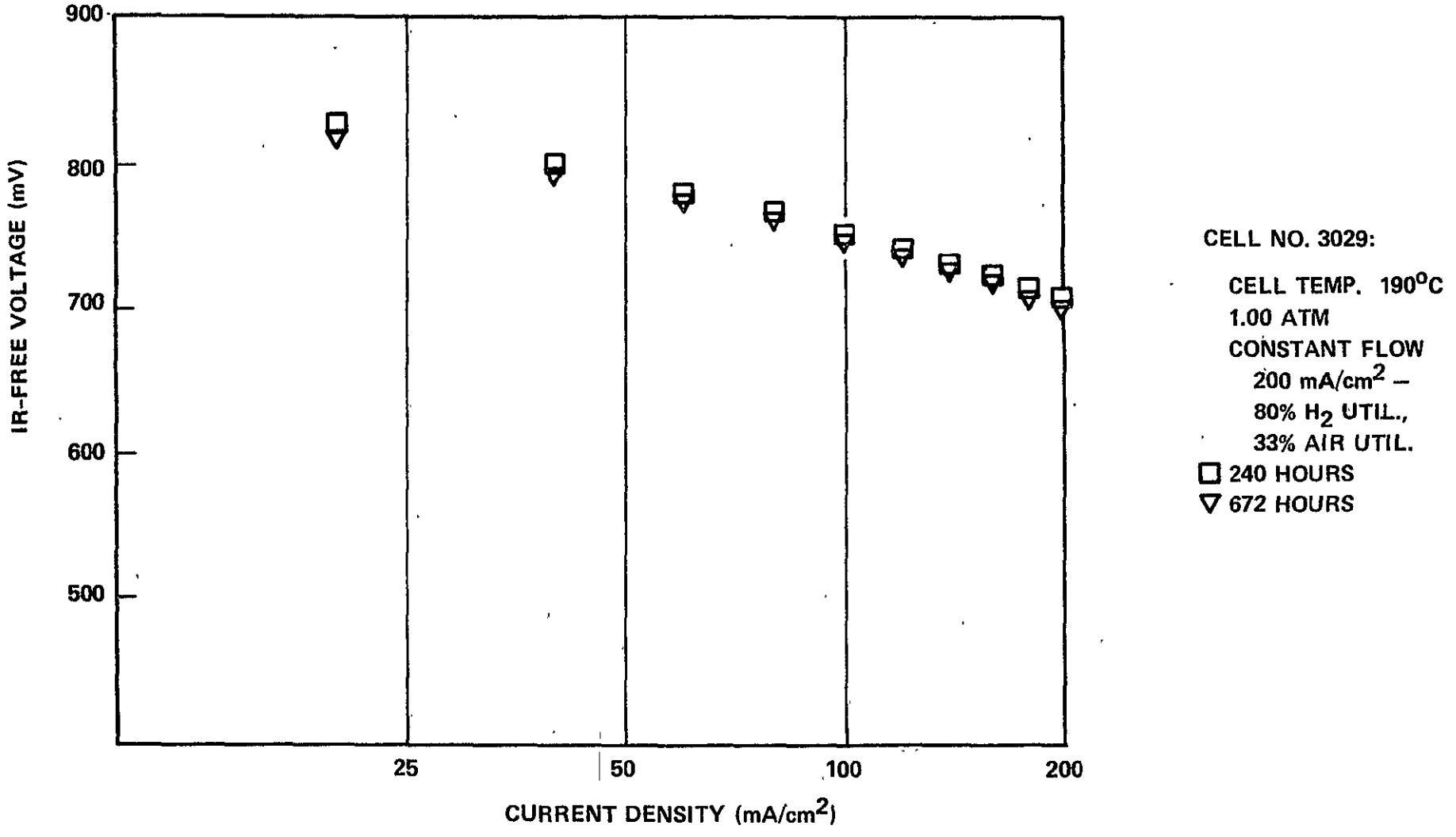

Figure 3.8.3-1 Polarization Curves for No-MAT-1 Cell

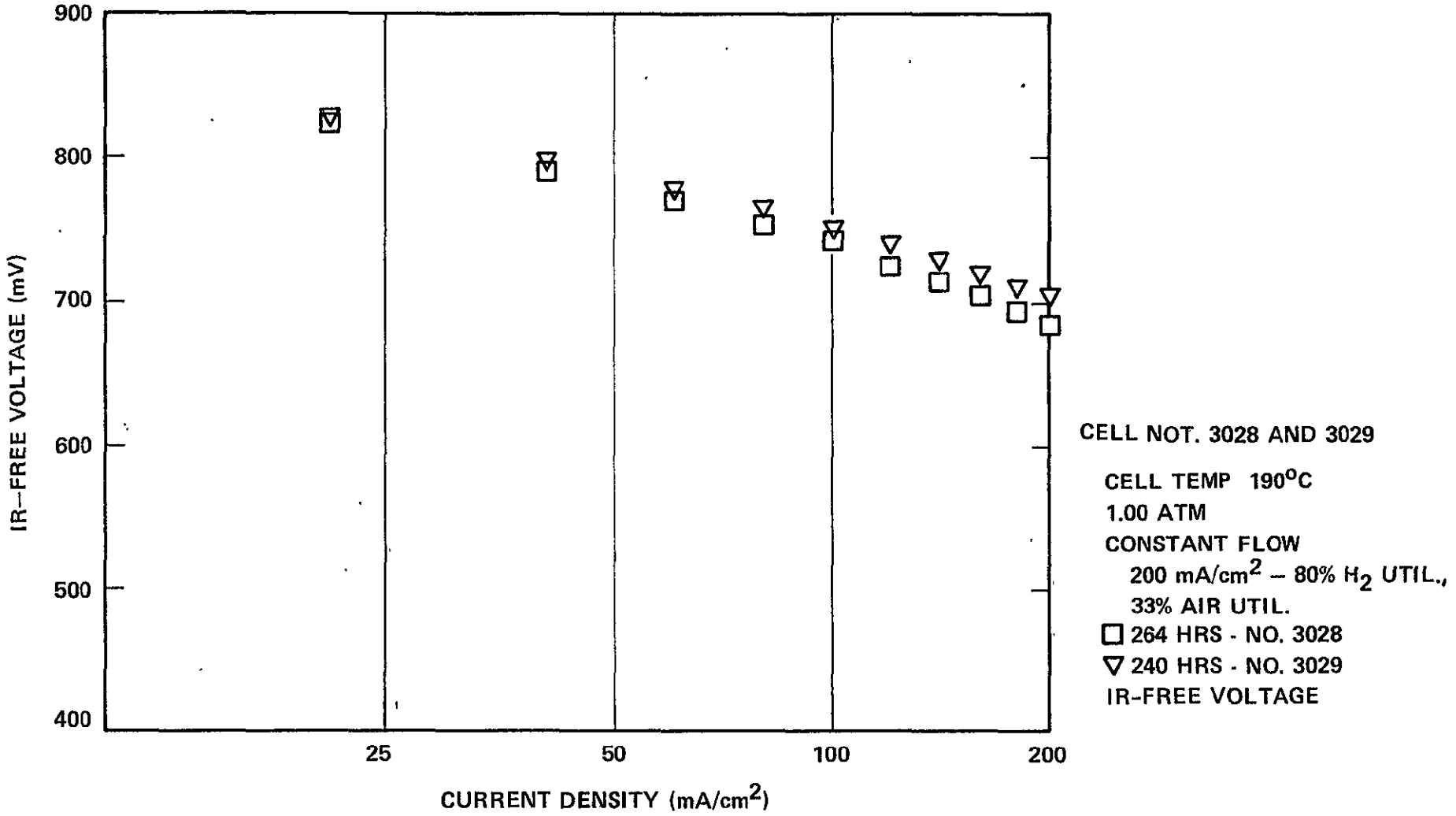

Figure 3.8.3-2 Comparison of Polarization Curves for No-MAT-1 and Cleared-MAT-1 Cells

3.8.4 CORROSION ANALYSIS

3.8.4.1 VITON SEALS

Corrosion testing of Viton samples was completed during this period. The data (Table 3.8.4-1) indicates that neither material may be acceptable for long term use in phosphoric acid fuel cells. During the test, both the Viton sponge (SV811-3) and Viton sheet (PLV-10059) absorbed large amounts of acid (8.3-29.0 percent) while at the same time the Viton was corroding. After extraction of the acid, the sample showed a weight loss of between 1.3 and 7.6 percent. The Viton sponge samples which showed the greatest acid absorption and attack, also showed dimensional instability. The samples grew as much as 2 millimeters in length and width during immersion. This expansion was mostly recovered after acid extraction. PLV-10059 (Viton Sheet) which showed the greater dimensional stability and less weight loss, changed color from grey to black, and developed small blisters on the surface. Pictures of the PLV-10059 (Viton Sheet) in Figure 3.8.4-1 show the change in surface condition during testing. No physical property testing was performed on any samples before or after testing, so it is not known if any significant change in physical properties occurs after exposure to phosphoric acid at 375°F. Previous analyses performed on Mosite 1028 Viton showed a weight loss of 3.2 percent after 336 hours and 7.7 wt. percent acid absorption (no quantative data is available for this sample's dimensional stability). Reviewing this data poses a serious question about the use of Viton in phosphoric acid fuel cells as gasketing material. While this test is severe, it is indicative of problems that may arise due to long term exposure of Viton gaskets such as a loss of elastic properties. Organic poisons may also be liberated from the corroding Viton which may affect fuel cell performance.

3.8.4.2 SEPARATOR PLATES

Atmospheric corrosion testing of heat-treated graphite Resin/molded with the following graphite materials was conducted.

- A-99
- Asbury 4421
- Poco

TABLE 3.8.4-1

RESULTS OF CORROSION TESTING AND ACID TOLERANCE CHARACTERISTICS OF VITON SEAL MATERIALS

MATERIAL	AGING TIME, HRS. / ACID TEMP.	INITIAL WT, g	WT AFTER AGING, g	WT AFTER AGING AND EXTRACTION, g	WT GAIN AFTER AGING, mg	WT LOSS AFTER EXTRACTION, mg	REMARKS
PLV 10059 Pelmor Laboratories Newtown, PA 18964 ~60 Durometer	168 / 375°F	1.7899	1.9344	1.7667 = wt loss=13%	144.5	23.5	Blistering and darkening of surface
	352 / 375°F	1.7826	1.8985	1.7524 = wt loss=1.6%	115.9	30.2	Blistering of surface increased
Viton Sponge Industrial Electronic Rubber Company IER Compound SV811-3 1/8" Thick	168 / 375°F	1.5491	1.8770	1.4548 = wt loss=6%	327.9	94.3	Noticeable Dimension change aft aging
	352 / 375°F	1.4911	1.8402	1.3769 = wt loss=7.6%	349.1	114.2	Noticable Dimension Change aft aging

PLV 10059 (Sheet) After 168 Hours
in ~100% H_3PO_4 at 375°F

PLV 10059 (Sheet) After 352 Hours
in ~100% H_3PO_4

PLV 10059 (Sheet) As Received

Figure 3.8.4-1 Results of Corrosion Testing of PLV 10059

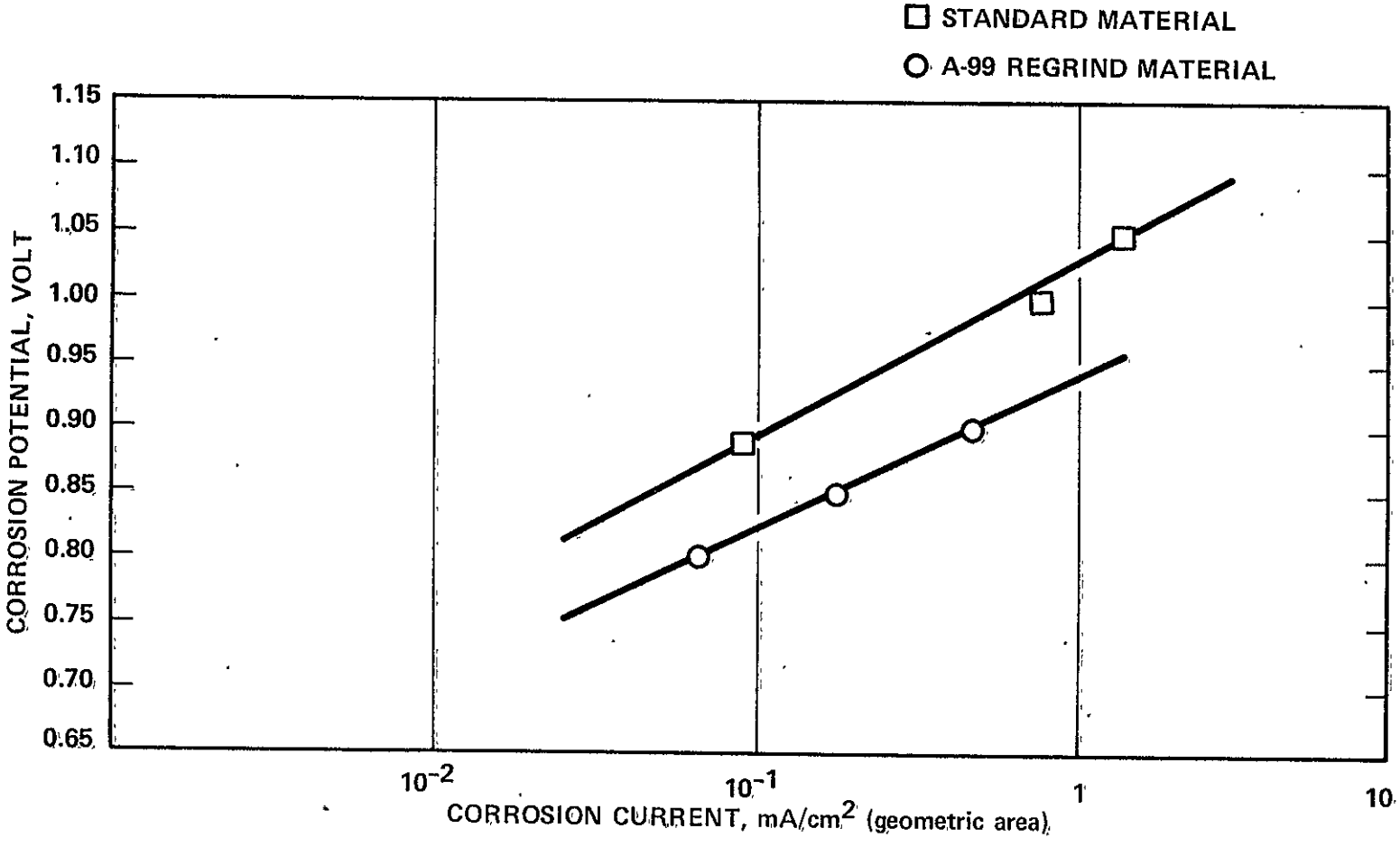

Figure 3.8.4-2 Comparison of Corrosion Behavior for A-99 Regrind Material and Standard (A-99) Plate Material

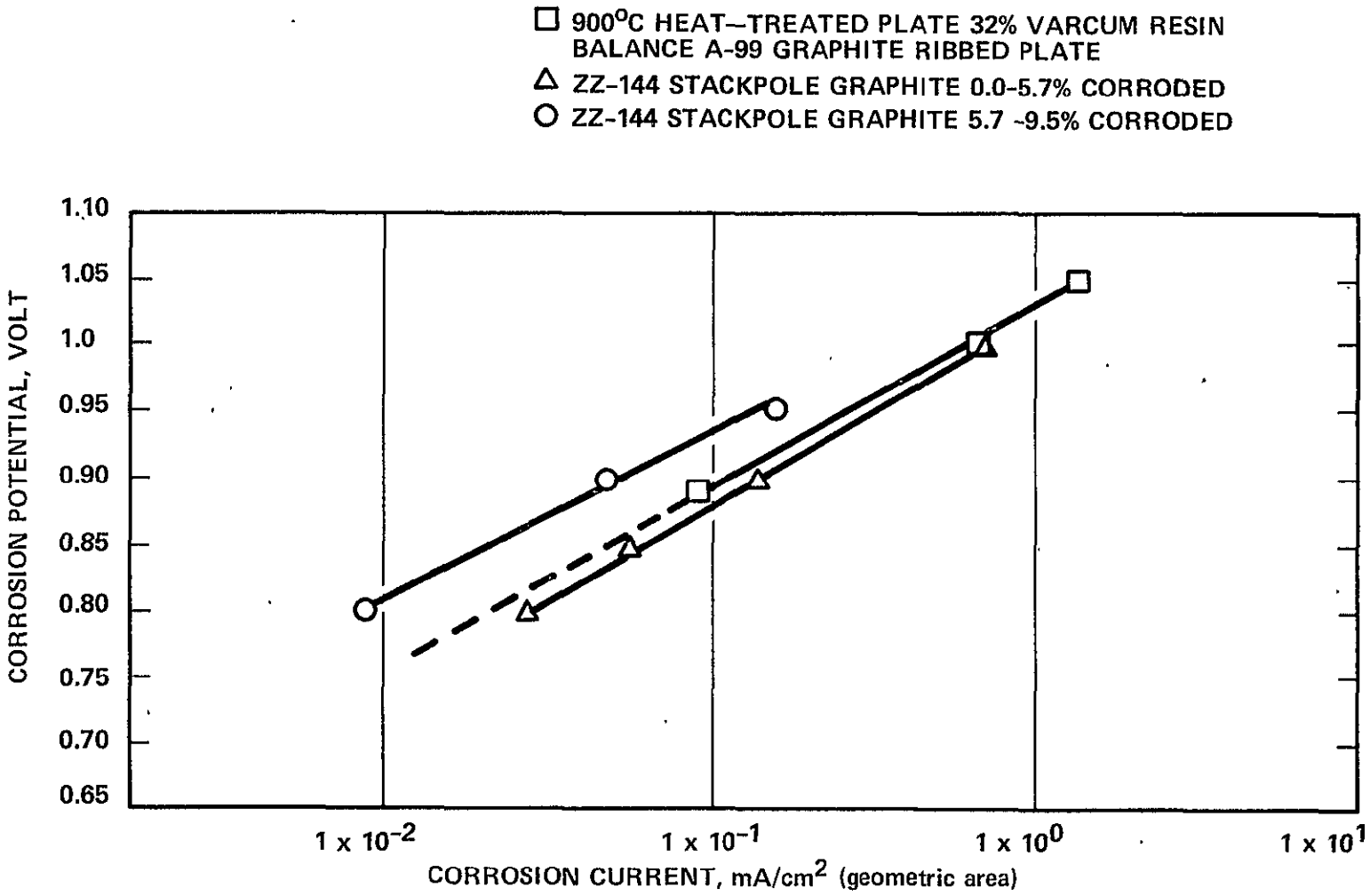

Figure 3.8.4-3 Comparison of Corrosion Behavior for Stackpole Graphite ZZ-144 and Asbury A-99 Plate Material

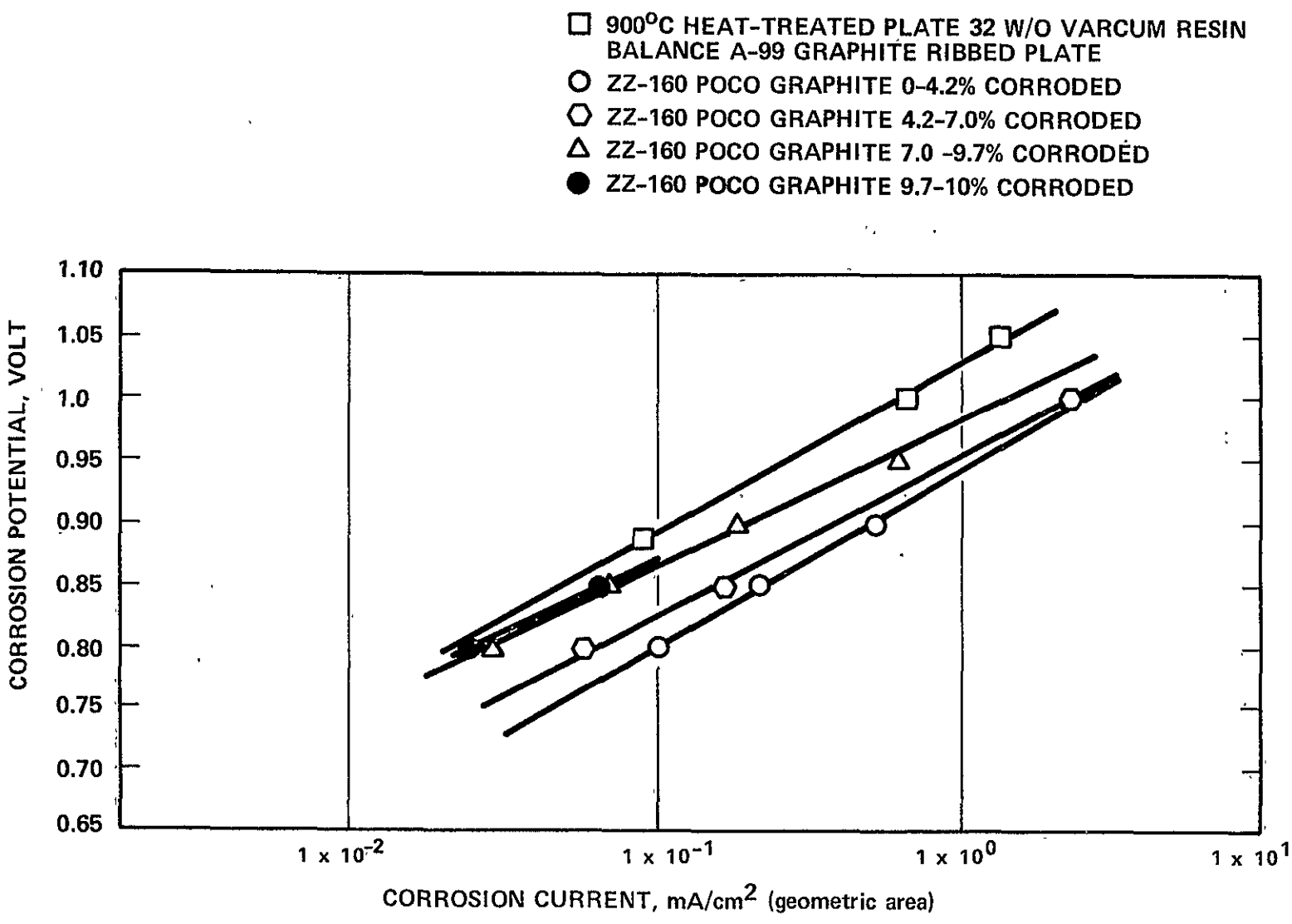

Figure 3.8.4-4 Comparison of Corrosion Behavior for Poco Graphite and Standard (A-99) Plate Material

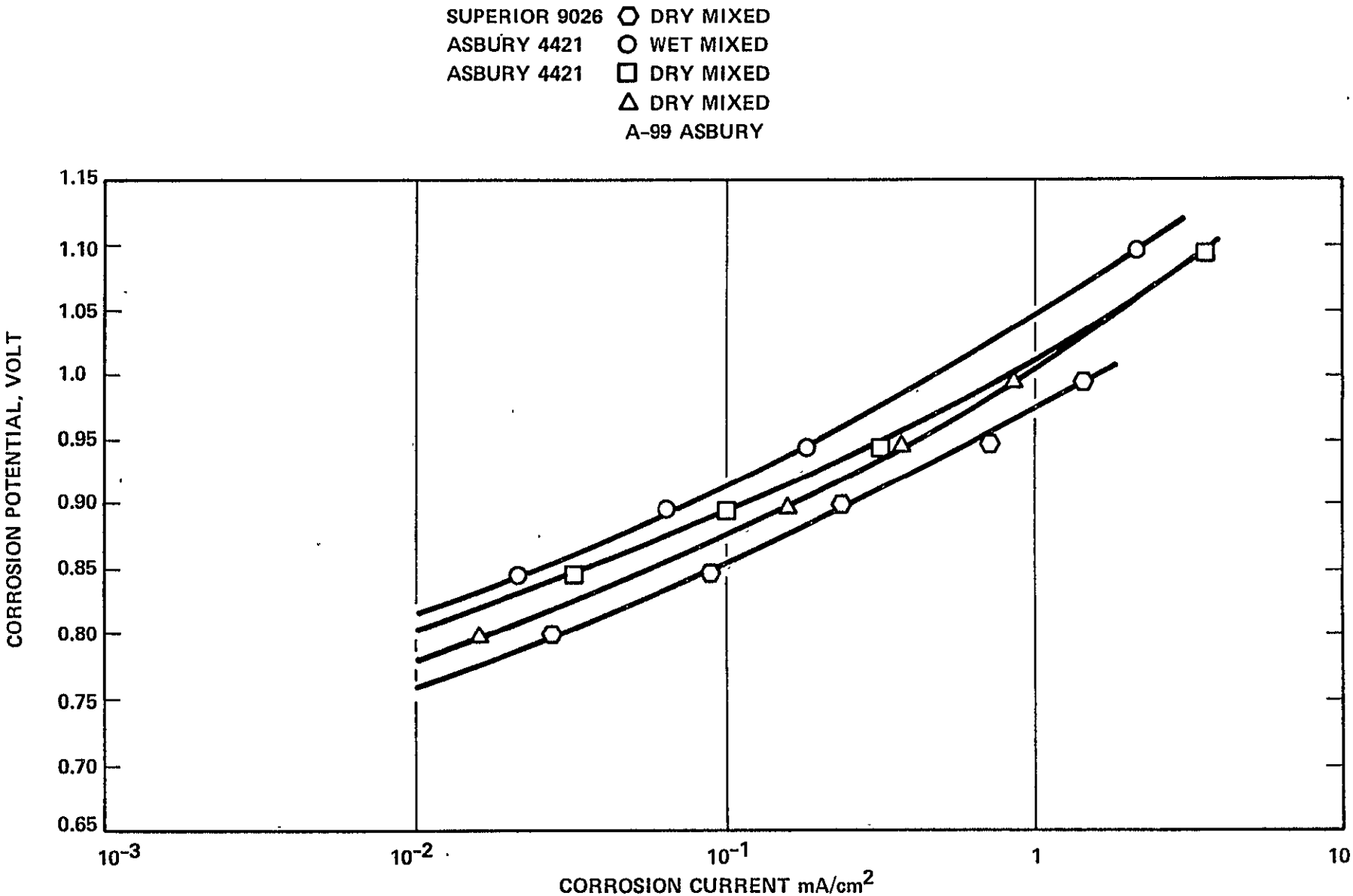

Figure 3.8.4-5 Corrosion Tafel Plots for Miscellaneous Materials

From the above tests it is concluded that except for the Poco material all the other materials tested under this program are very similar in their corrosion behavior.

3.8.4.3 STACK CORROSION EVALUATION TESTS

Two stacks (12-cell and 6-cell) were assembled at Westinghouse and tested at ERC to evaluate the possible corrosion causing mechanism(s). Details of these stack assemblies are provided in Tables 3.8.4-2 and 3.8.4-3.

Several experiments were conducted prior to stack fabrication to arrive at the procedures for introducing possible corrosion causing modes in the cells, such as crossleaks and continuous ionic short circuits. Procedures to create the crossleaks and continuous ionic path were developed and are presented in Figures 3.8.4-6 and 3.8.4-7, respectively.

Preliminary experiments were also conducted to apply corrosion resistant coatings on the bipolar plates so that their effect could be tested in the 12-cell and 6-cell stacks. The test results indicated that the coatings which were applied, significantly increased the contact resistance between the electrode backing and the bipolar plate. It was therefore concluded that the coatings should not be used in these stacks.

Test plans for the 12-cell and 6-cell stacks were finalized in consultation with NASA. The 12-cell stack was assembled at Westinghouse and tested at ERC to evaluate the effects of the following stack defects on bipolar plate corrosion:

- Less than "normal" acid in a cell
- More than "normal" acid in a cell
- Oxidant flow maldistribution
- Built-in crossleaks

TABLE 3.8.4-2

RANDOMIZED CELL ARRANGEMENT
FOR THE 12-CELL STACK Z-004

CELL NO.	CONDITION
1	10cc Less Acid
2	Normal Cell*
3	Normal Cell*
4	Oxidant Flow Maldistribution
5	10cc Excess Acid
6	Built in Crossleak
-	Cooler
7	Normal Cell*
8	10cc Less Acid
9	10cc Excess Acid
10	Normal Cell*
11	Oxidant Flow Maldistribution
12	Built in Crossleak

* Acid Concentration 96 percent

35cc on MAT-1 Layer
13cc on SIC layer
2 cc in the acid channel

TABLE 3.8.4-3

RANDOMIZED CELL ARRANGEMENT FOR THE
6-CELL STACK Z-003

Cell No.	Condition
1	Cathode Backing and Plate Wet
2	Anode and Cathode Backings and Plates Wet
3	Normal Cell
4	Cathode Backing and Plate Wet
5	Anode and Cathode Backings and Plates Wet
6	Normal Cell

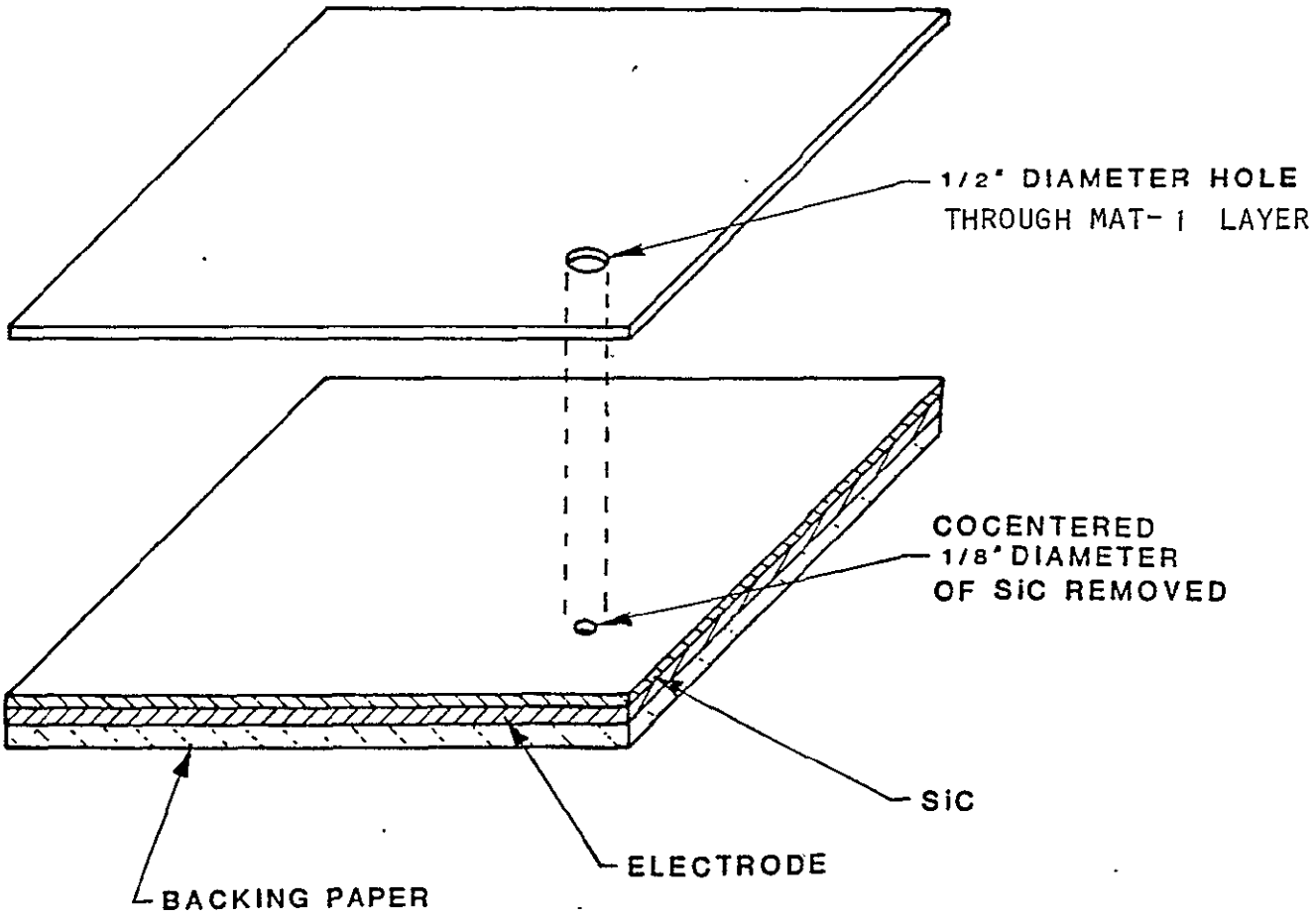

Figure 3.8.4-6 Procedure for Introducing a Cross Leak in a Cell

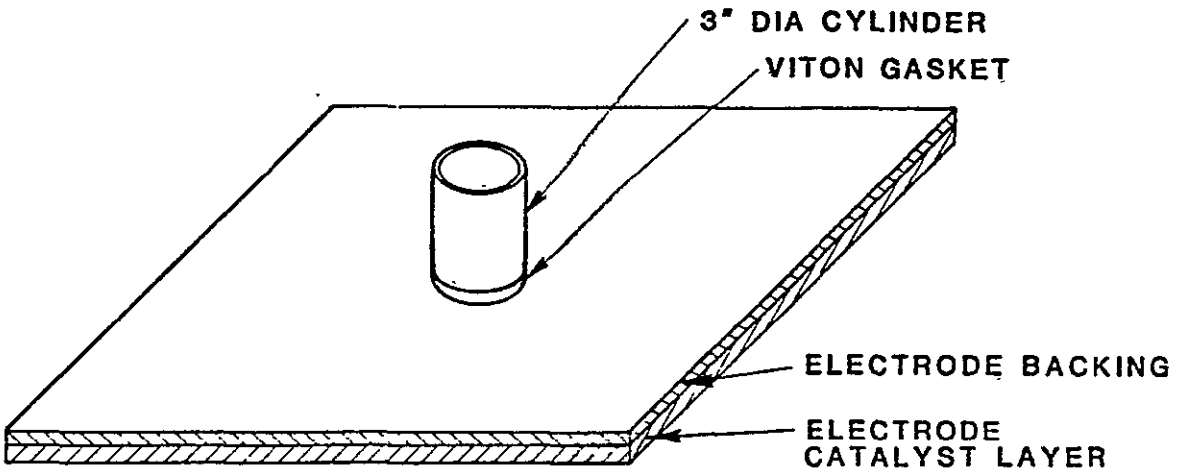

PROCEDURE:

1. Electrode Catalyst Layer placed face down on flat surface.
2. Etch area to be wetted with Chemgrip Treating Agent.
3. Apply Viton Glue to cylinder rim and place gasket on rim.
4. Place cylinder with gasket on area to be wetted. Place ∿4 lbs. of weight on top of cylinder.
5. Fill cylinder with enough Isoproponal and water (Ratio 50:50) to create a 1.25" static head.
6. After 5 minutes siphon off Isopropanol and water.
7. Fill cylinder with H_3PO_4 to create a 1.25" static head.
8. After ∿1 hr. disassemble.

Figure 3.8.4-7 Procedure for Wetting Backing to Create a Continuous Ionic Path

The stack was disassembled after ∿ 420 hours of testing (out of which 400 hours were logged at 5 atm. and ∿ 200 mA/cm^2). No evidence of apparent bipolar plate corrosion was found. Based on this effort, it can not be concluded that the above mentioned defects do not in some unknown way affect the bipolar plate corrosion. It is possible that the degree of severity of the defects was not sufficient to cause corrosion. Table 3.8.4-4 presents a summary of the major events which occurred during testing. Figure 3.8.4-8 presents the life graph of Stack Z-004.

The six-cell stack (Z-003) was assembled at Westinghouse and tested at ERC to evaluate the possible effect of an ionic path connection between two or more cells on bipolar plate corrosion. Table 3.8.4-5 presents a summary of test events for this stack. Figure 3.8.4-9 presents the life graph of Stack Z-003.

The stack was disassembled after 600 hours of testing (out of which 574 hours were logged at 5 atm. and 190 mA/cm^2). No evidence of apparent bipolar plate corrosion was found. Based on this effort it could be concluded that plate and/or backing paper wetting by itself does not drastically affect the bipolar plate corrosion rate. It is possible, however, that the degree of wetting was not sufficient to create enough of an ionic short to accelerate the corrosion.

TABLE 3.8.4-4

SUMMARY OF TESTING FOR STACK Z-004

Total hours tested ∿ 420
Total hours tested at 5 atm. pressure ∿ 400

Start Up

Average OCV ∿ 860mV
Average Cell Voltage ∿ 561mV at 140 mA/cm2, 1 atm., 170°C

20 hours

Pressurization and Stabilization

Endurance Started 40 hours

Average Cell Voltage ∿ 661mV at ∿ 200 mA/cm2, 5 Atm., 189°C, 80% H2 utilization, 50% Air utilization
Average Cell Resistance = 0.22 mΩ

Maximum Voltage 707 Cell #2
Minimum Voltage 628 Cell #11

54 hours	Momentary-10 psia drop on anode loop due to anode condensate drain malfunction. No loss in performance after resetting.
90 hours	System lost 35 psi pressure momentarily due to failure mode control system malfunction. No loss in performance after resetting.
290 hrs.	System lost 8 psi pressure momentarily due to failure more control system malfunction. No loss in performance after resetting.
420 hours	Stack depressurized automatically due to H2 supply distrubance while unattended Stack shutdown and disassembled.

Average Cell Voltage 676 mV at ∿ 200 mA/cm^2 5 atm., 196°C, 80% H_2 utilization, 50 percent Air utilization
maximum voltage = 707 Cell #2,
minimum voltage = 641 Cell #6
Avgerage Coil Resistance = 0.24 mΩ

OPERATING CONDITIONS

PRESSURE:	5 Atm.
TEMPERATURE:	190°C
FUEL/ OXIDANT:	H_2/Air
FUEL UTILIZATION:	80%
OXIDANT UTILIZATION:	50%
CURRENT DENSITY:	2 200 mA/cm^2

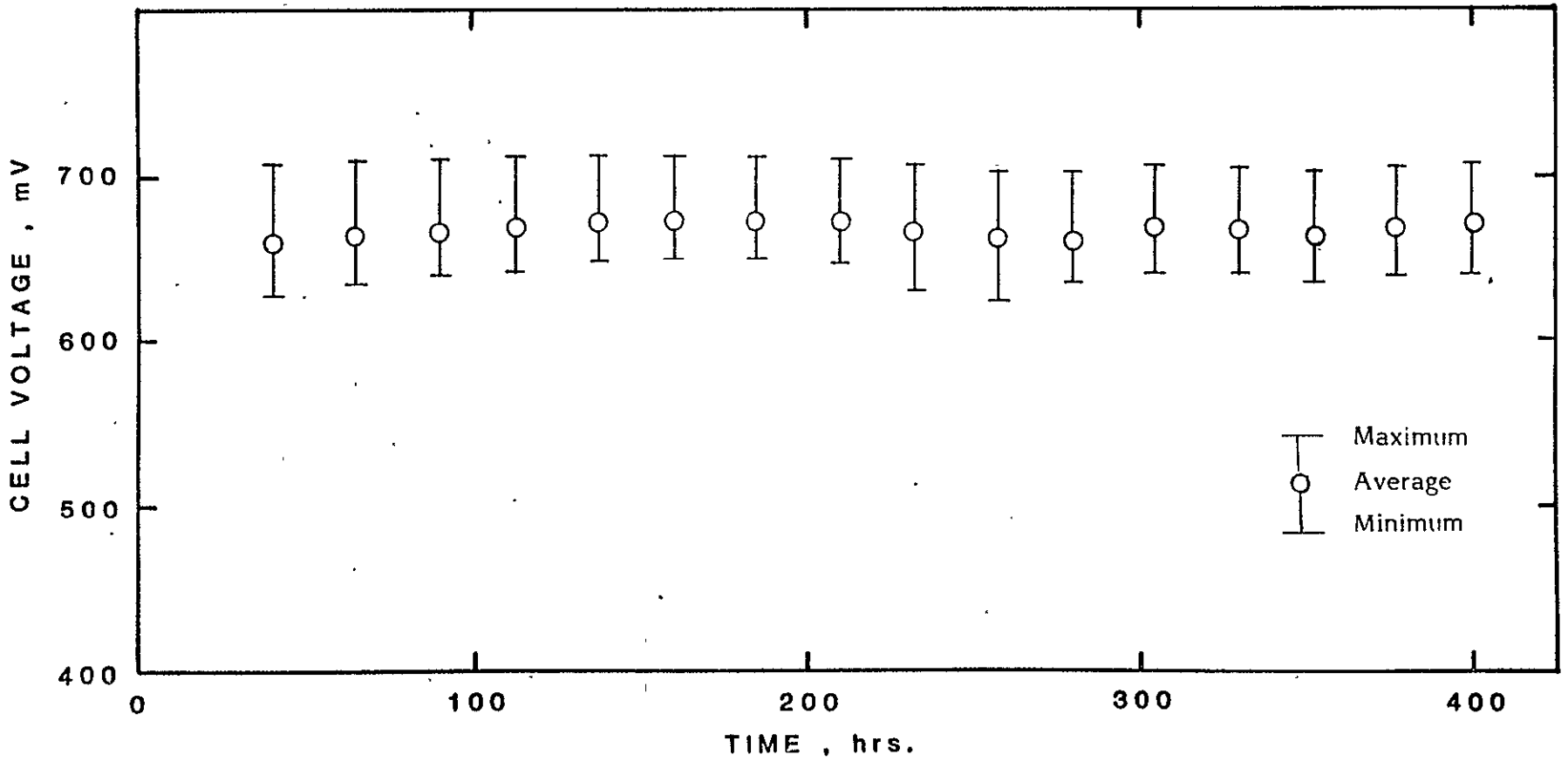

Figure 3.8.4-8 Life Graph of 12-Cell Stack Z-004

TABLE 3.8.4-5

SUMMARY OF TESTING FOR STACK Z-003

TOTAL HOURS TESTED: 600
TOTAL HOURS TESTED AT 5 ATM. PRESSURE: 574

Start

Carbon Dioxide purged through the anode loop for 10 minutes

Cell 1 showed gas flow sensitivity Possible cases: blocked flow channels in the end cells. The stack was stabilized by increasing the oxidant flow through the stack.

Average PCV = 880 mV (1 atm., 174°C)

Average Cell Voltage = 728 mV at 15 mA/cm^2, 1 atm., 144°C

4 hours

Pressurization and Stabilization

Effort was made to run the stack at an electrical load higher than 190 mA/cm^2. Since there was no cooling plate in the stack, it tended to overheat. Hence, lowered to 190 mA/cm^2.

Endurance started at 25 hours

Oxidant inlet temperature and utilization were set at 78°C and 33 percent respectively, to control the stack operating temperature.

Average Cell Voltage = 673 mV at 190 mA/cm^2, 5 atm., 199°C, 80 percent fuel utilization, 33 percent oxidant utilization

Average Cell Resistance = 0.20 mΩ

Maximum Cell Voltage = 694 mV (Cell 4)

Minimum Cell Voltage = 627 mV (Cell 6)

300 hours

Fuel inlet (Cell 4) and oxidant outlet (Cell 5) temperatures increased and remained high (216-246°C) for 11 hours. This may have been caused by a crossleak

TABLE 3.8.4-5 (CONTINUED)

SUMMARY OF TESTING FOR STACK Z-003

	between the fuel inlet and oxidant outlet manifolds. The electrical load was reduced from 190 to 180 mA/cm^2 to control the above temperatures. Because of the malfunction, however, the average terminal cell voltage dropped by 32 mV and average cell internal resistance increased by 0.06 mΩ.
Endurance completed at 599 hours	
Average Cell Voltage = 667 mV at 180 mA/cm^2, 5 atm., 197°C, 80% fuel utilization, 33% oxidant utilization	
Average Cell Resistance = 0.25 mΩ	
Maximum Cell Voltage = 678 mV (Cell 3) Minimum Cell Voltage = 647 mV (Cell 1)	
Depressurized at 600 hours	Avg. cell resistance increased from 0.48 (5 atm.) to 0.63 (1 atm.) mΩ, 142°C, no load
Disassembly	Findings: • No apparent corrosion of graphit plates • No significant wetting of plates even though the temperature near the oxidant inlet was 120-130°C • Gas channels of Cells 1 and 6 in the inlet and outlet manifolds appeared to be severely blocked by Viton Gaskets • Deposits, mostly reaction produce of Aluminum and Phosphoric Acid were found in the oxidant outlet manifold.

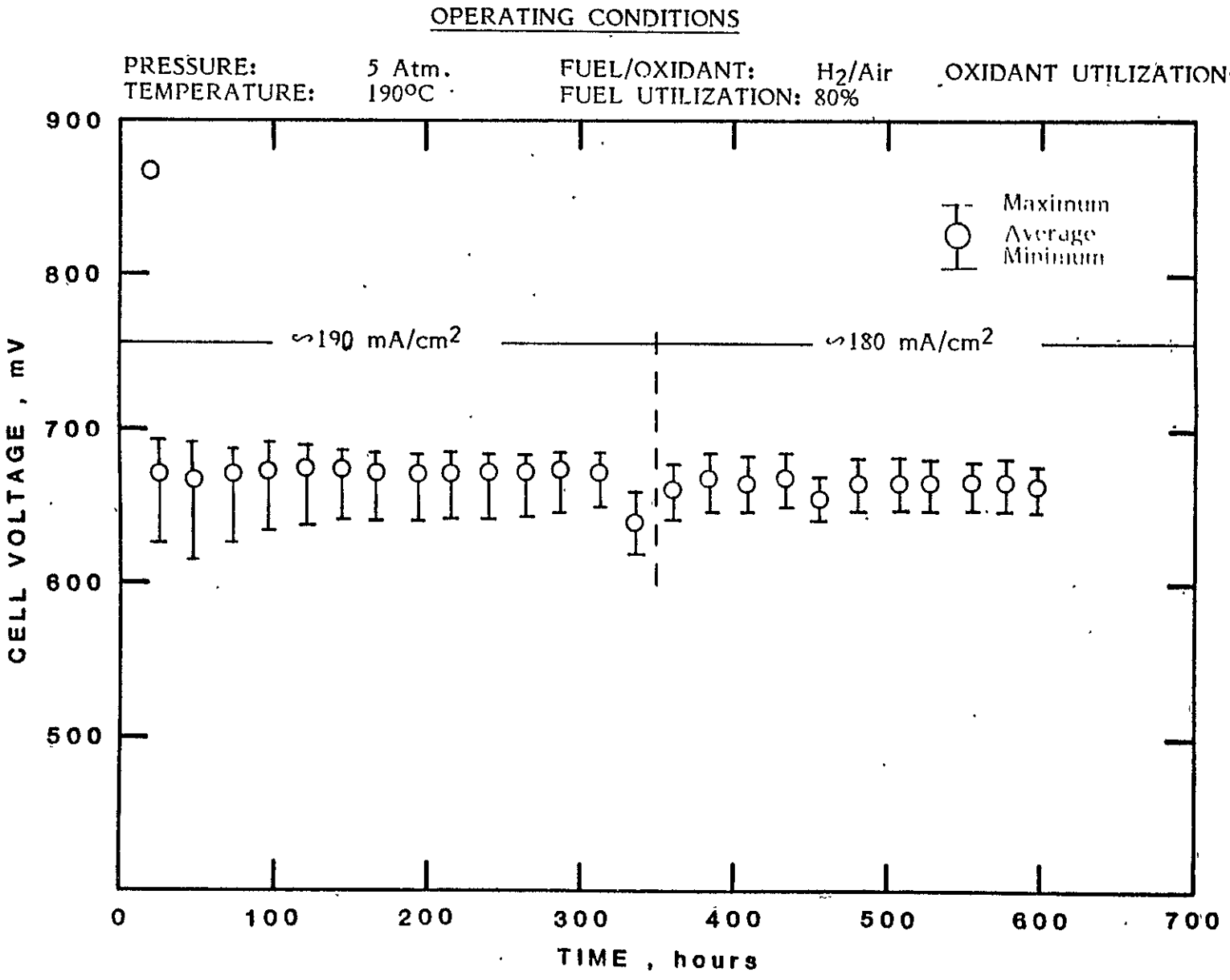

Figure 3.8.4-9 Life Graph of 6-Cell Stack Z-003

3.8.5 PLATE MOLDING

3.8.5.1 MOLDING OF FLAT MK-II PLATES WITH SHOULDERS

Molding trials were conducted for flat MK-II plates with shoulders. A number of experiments were conducted to establish the relationship (molding parameter surface, MPS) between the mold temperature, preheat time and the amount of flash generated (Figures 3.8.5-1 and 3.8.5-2). It should be pointed out that the MPS changes with the preform weight and thickness, plate design, mold clearances and the molding procedures. Mold temperature and preheat time are selected from the MPS diagrams so that the amount and the variation in the amount of flash generated is limited. Experiments were also conducted to adjust the material distribution in the preform (eggcrate distribution) to achieve the required dimensional tolerances. Table 3.8.5-1 summarized the physical property measurements of the molded plates. Twenty 0.245 inch thick and twenty 0.170 inch thick plates were molded after these experiments.

Dies for MK-II pattern plates were received and inspected. These dies were further modified to incorporate recent design modifications. The reworked dies were received and found to be satisfactory.

Flat plates were machined and heat-treated to 900°C. Table 3.8.5-2 shows the dimensions of the plates after heat-treatment. The flatness and dimensional tolerances of these plates were very good. This procedure will be used until a process for molding the Z-Z and Z-Tree plates is finalized.

Molding experiments demonstrated the feasibility of molding the plates with decreased cycle times. The current cycle is of five minutes duration and the experimental plates were molded in as short as 30 seconds cycle time. The properties of the plates molded with the shortened cycle times require further evaluation to determine the effects of fuel cell operation. Table 3.8.5-3 presents a comparison of the physical properties of the plates molded with varied molding cycle times.

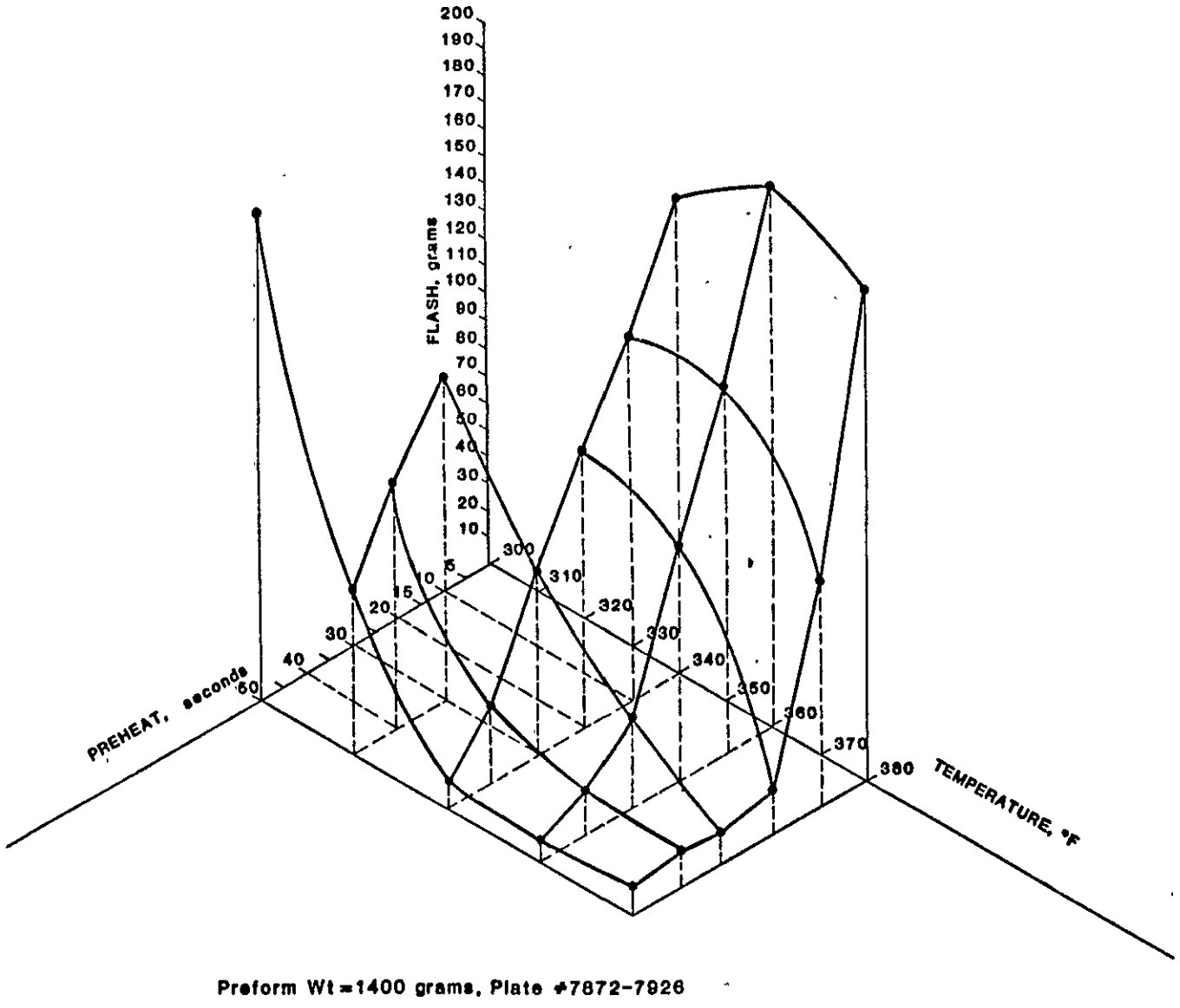

Figure 3.8.5-1 Molding Parameter Surface (MPS) for the Z-Pattern Flat Plates (Graphite/Resin) with Shoulders (Plate Thickness 0.245 Inch)

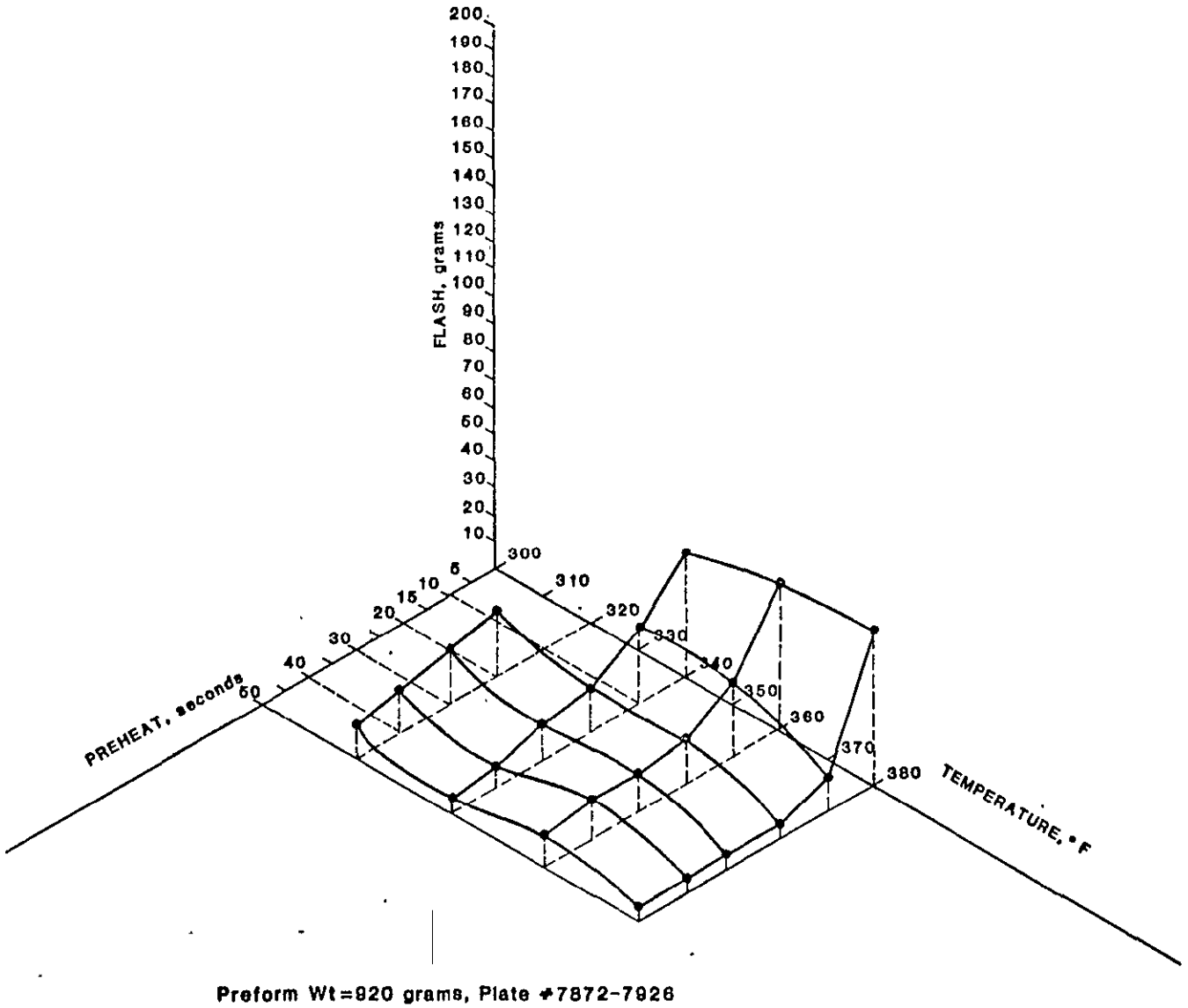

Figure 3.8.5-2 Molding Parameter Surface (MPS) for the Z-Pattern Flat Plates (Graphite/Resin) with Shoulders (Plate Thickness 0.170 Inches)

TABLE 3.8.5-1

PHYSICAL PROPERTY MEASUREMENTS OF FLAT Z-PATTERN PLATES MOLDED WITH VARIED CONDITIONS

Z PATTERN FLAT DIES (AO-BO)
32% VARCUM 29703/.68%-A99 GRAPHITE
PREHEAT LINE CALCULATED SO TOP DIE IS 1/32" INTO PREFORM
TOTAL MOLDING TIME = 2 MINUTES

Plate No.	Pre-Form Weight G	Temp. °F	Pre-Heat Sec.	Bulk Density G/CC	Flash G	Length In.	Width In.	Corn. Thick Mil.	ΔC Mil.	ΔM Mil.	ΔE Mil.
7922	1400	320	30	1.75	119	17.36	12.32	--	--	9	11
7921	1400	320	40	1.77	91	17.35	12.37	240	--	12	13
7920	1400	320	50	1.79	61	17.3	12.35	239	--	9	13
7912	1400	340	0	1.81	175	17.32	12.34	222	25	20	27
7910	1400	340	10	1.81	120	17.32	12.34	228	21	17	24
7911	1400	340	10	1.79	148	17.32	0	234	26	21	35
7909	1400	340	20	1.81	101	17.32	12.33	232	17	18	20
7908	1400	340	30	1.81	67	17.32	12.34	238	19	18	21
7907	1400	340	40	1.81	27	17.32	12.33	245	10	11	13
7906	1400	340	50	1.81	9	17.33	12.34	247	6	11	10
7879	1400	360	0	1.80	169	17.31	12.33	224	5	7	8
7882	1400	360	0	1.82	199	17.31	12.33	217	24	24	26
7877	1400	360	10	1.81	132	17.32	12.34	228	5	11	8
7878	1400	360	10	1.80	139	17.32	12.34	228	5	8	9
7881	1400	360	10	1.83	140	17.32	12.33	225	20	19	22
7876	1400	360	20	1.81	88	17.32	12.34	235	10	12	12
7875	1400	360	30	1.81	34	17.32	12.33	243	12	15	13
7874	1400	360	40	1.80	16	17.33	12.33	246	14	19	19
7872	1400	360	50	1.80	5	17.33	12.34	247	6	15	13
7873	1400	360	50	1.80	9	17.34	12.34	247	3	11	10
7898	1400	380	0	1.83	182	17.32	12.33	218	21	21	23
7896	1400	380	10	1.81	84	17.33	12.34	235	20	20	21
7897	1400	380	10	1.80	86	17.33	12.33	236	17	15	20
7894	1400	380	20	1.82	16	17.33	12.34	245	3	9	8
7895	1400	380	30	1.81	13	17.33	12.35	248	7	8	11
7893	1400	380	30	1.80	8	17.33	12.34	247	8	11	12
7892	1400	380	40	1.79	15	17.35	12.35	250	4	8	9
7891	1400	380	50	1.75	12	17.36	12.36	252	21	16	23
7926	920	320	20	1.80	24	17.32	12.35	169	4	7	5
7925	920	320	30	1.80	20	17.31	12.33	171	6	10	8
7924	920	320	40	1.79	16	17.31	12.34	172	4	7	7
7923	920	320	50	1.78	12	17.36	12.38	174	--	3	3
7919	920	340	0	2.82	45	17.32	12.34	164	13	16	18
7917	920	340	10	1.82	27	17.33	12.34	167	9	11	13
7918	920	340	10	1.82	29	17.33	12.34	167	10	12	14
7916	920	340	20	1.82	17	17.33	12.34	167	6	11	10
7915	920	340	30	1.82	13	17.33	12.34	169	9	13	13
7914	920	340	40	1.83	8	17.33	12.34	169	2	9	7
7913	920	340	50	1.82	5	17.33	12.34	169	5	12	11
7890	920	360	0	1.83	54	17.33	12.34	162	12	15	15
7888	920	360	10	1.82	31	17.33	12.34	166	10	13	14
7889	920	360	10	1.82	24	17.34	12.34	166	7	13	12
7887	920	360	20	1.82	16	17.32	12.34	170	4	8	8
7886	920	360	30	1.81	13	17.34	12.35	169	1	8	9
7885	920	360	40	1.77	15	17.35	12.35	172	5	13	12
7884	920	360	50	1.75	11	17.36	12.37	175	10	14	17
7905	920	380	0	1.84	58	17.32	12.34	163	16	13	19
7903	920	380	10	1.82	12	17.32	12.34	169	4	9	10
7904	920	380	10	1.83	12	17.33	12.34	170	2	7	8
7902	920	380	20	1.80	5	17.33	12.33	173	5	7	10
7901	920	380	30	1.78	6	17.32	12.33	175	5	8	11
7900	920	380	40	1.78	5	17.33	12.34	177	4	5	7
7899	920	380	50	--	5	17.33	12.34	180	1	--	4

Δc = Difference between the highest and lowest corner measurement.
Δm = Difference between the highest point in the middle of plate and the lowest point around the edge of plate (Includes the corners).
Δe = Difference between the highest and lowest point around the edge of plate (Includes the corners).
NOTE: All measurements are expressed in mils. (.001").

2151E-1

TABLE 3.8.5-2

DIMENSIONAL MEASUREMENTS OF 900°C HEAT-TREATED
MACHINED MK-II PLATES
(32 wt% Varcum 29-703/68 wt% Asbury A99)

Type of Plates	N	Average Length (Std. Dev.)	Average Width (Std. Dev.)	Average % Shrinkage (Std. Dev.)		Average[1] ΔC (Std. Dev.)	
				Length	Width	After Machining	After HT.
AB Bipolar	8	16.734 (0.007)	11.888 (0.12)	3.43 (.043)	3.49 (.032)	.0027 (.002)	.00233 (.002)
AC Cooler	8	16.728 (.011)	11.910 (.012)	3.43 (.071)	3.30 (.037)	.0068 (.002)	.0054 (.002)
BC Cooler	9	16.734 (.003)	11.907 (.004)	3.41 (.025)	3.35 (.036)	.0047 (.002)	.0063 (.004)
BD End Plate	4	16.730 (.007)	11.910 (.006)	3.39 (.040)	3.30 (.033)	.0043 (.001)	.0041 (.002)

[1] ΔC is the maximum corner thickness, minus the minimum corner thickness.

TABLE 3.8.5-3

COMPARISON OF DIMENSIONAL AND PHYSICAL PROPERTIES FOR PLATES WITH VARIED MOLDING CYCLES

PLATE #	TOTAL CYCLE MIN.	DENSITY G/CC	LENGTH IN INCHES MEAN	STD.DEV.	N	WIDTH IN INCHES MEAN	STD.DEV.	N
ZZ-41	5	1.77	17.327	.003	4	12.343	.003	6
ZZ-42	"	1.77	17.325	.004	4	12.338	.006	6
ZZ-43	"	1.77	17.325	.005	4	12.342	.005	6
AVERAGE	=		17.326	.004		12.341	.005	
ZZ-38	2	1.77	17.320	.004	4	12.338	.003	6
ZZ-39	"	1.77	17.323	.006	4	12.337	.004	6
AVERAGE	=		17.321	.006		12.337	.003	
ZZ-50	1/2	1.77	17.312	.008	4	12.331	.008	6
ZZ-51	"	1.71	17.318	.017	4	12.341	.008	6
AVERAGE	=		17.315	.013		12.336	.009	

* THESE PLATES WERE MOLDED AT WESTINGHOUSE AND CHARACTERIZED AT ERC.

N IS THE NUMBER OF MEASUREMENTS FOR THE PLATE REFERENCED.

3.8.5.2 MOLDING OF MK-II COOLER AND BIPOLAR PLATES

MK-II cooler and bipolar plates were successfully molded with Asbury A-99 graphite and Varcum resin. Visual appearance of the as-molded plates was very good; however, it was noticed that these plates did not remain "flat" after heat treatment. Figures 3.8.5-3 and 3.8.5-4 represent exaggerated characteristics of the molded and subsequently heat-treated MK-II bipolar and cooler plates. The warpage was larger than desirable and therefore methods were investigated to produce acceptable plates.

Visual examination of the machined heat-treated MK-II bipolar and cooler plates did not show these characteristics. To investigate the reason for the warpage micrographs were obtained for cross sections of the machined and molded plates. These micrographs (Figures 3.8.5-5 and 3.8.5-6) indicated that the orientation of the graphite particles is different in these two plates. This was attributed to the "Anisotropic shape" of the A-99 graphite particles.

It was decided that the following process and material variations should be evaluated to improve the flatness of the heat-treated plates.

- Wet mixing of graphite/resin powders
- Alternate graphite and carbons

Several experimental trials were conducted with various materials. Table 3.8.5-4 summarizes the results and physical property measurements for these plates. The following conclusions were made.

- Regrind material yield acceptable MK-II plates.
- Wet mixing improves the isotropic nature of the composite plate. This is supported by the electrical resistivity measurements perpendicular and parallel to the pressing directions.
- Shrinkage after heat-treatment is higher for plates molded with wet-mixed materials.

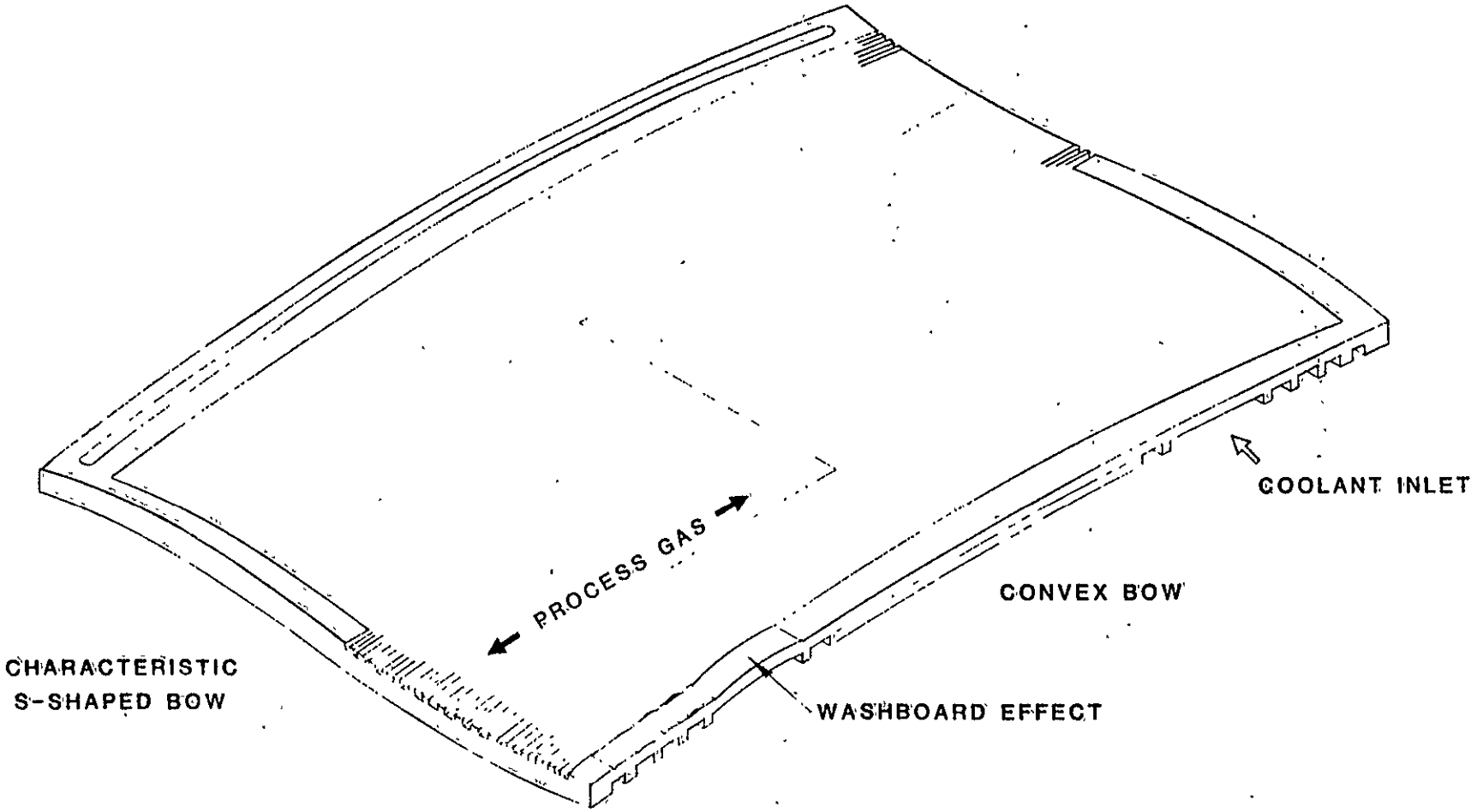

Figure 3.8.5-3 Warping Characteristics of the Molded and Subsequently 900°C Heat-Treated MK-II Cooler Plate (Materials - A-99 Graphite, Varcum Resin)

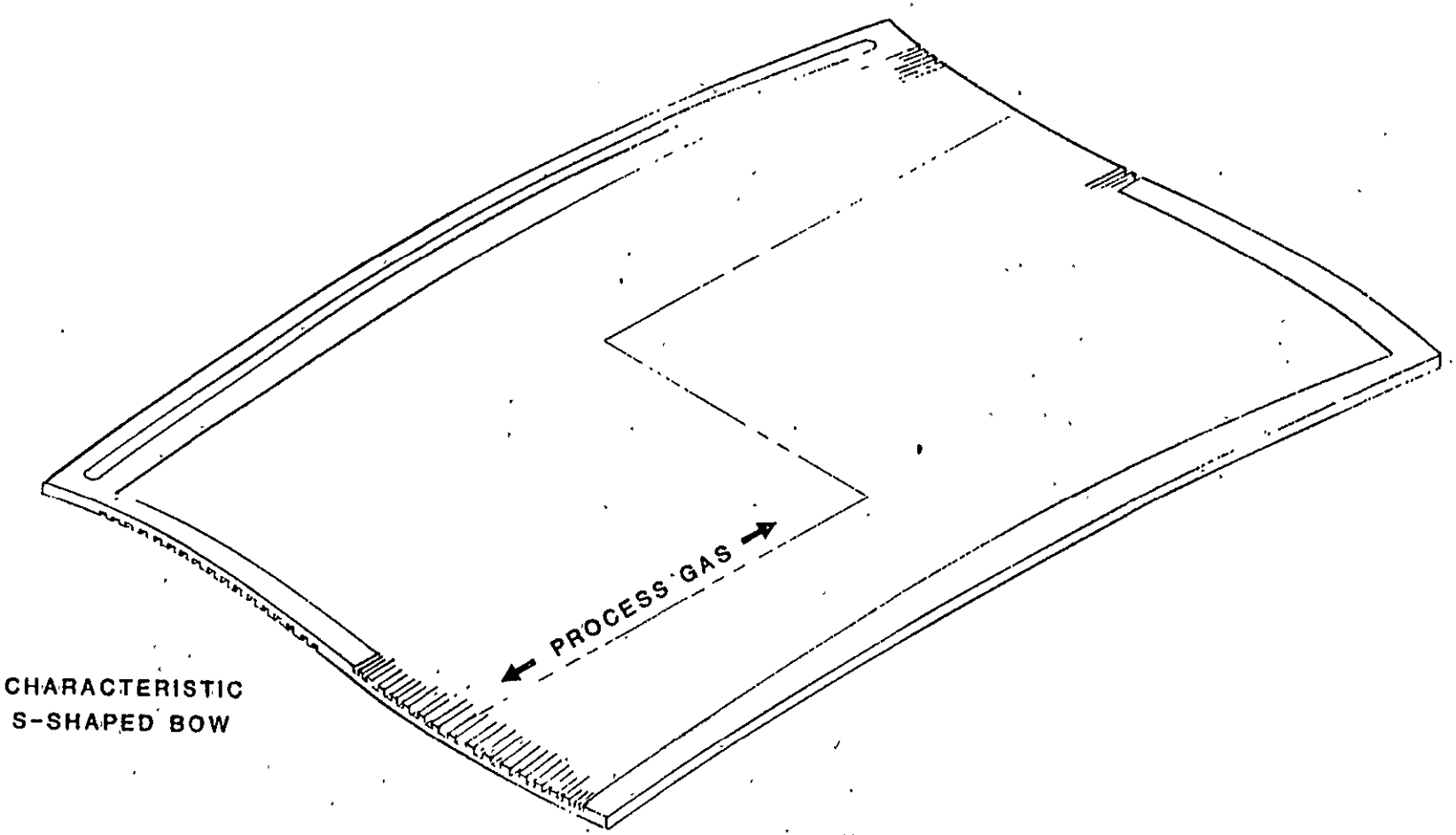

Figure 3.8.5-4 Warping Characteristics of the Molded and Subsequently 900°C Heat-Treated MK-II Bipolar Plate (Materials - A-99 Graphite and Varcum Resin)

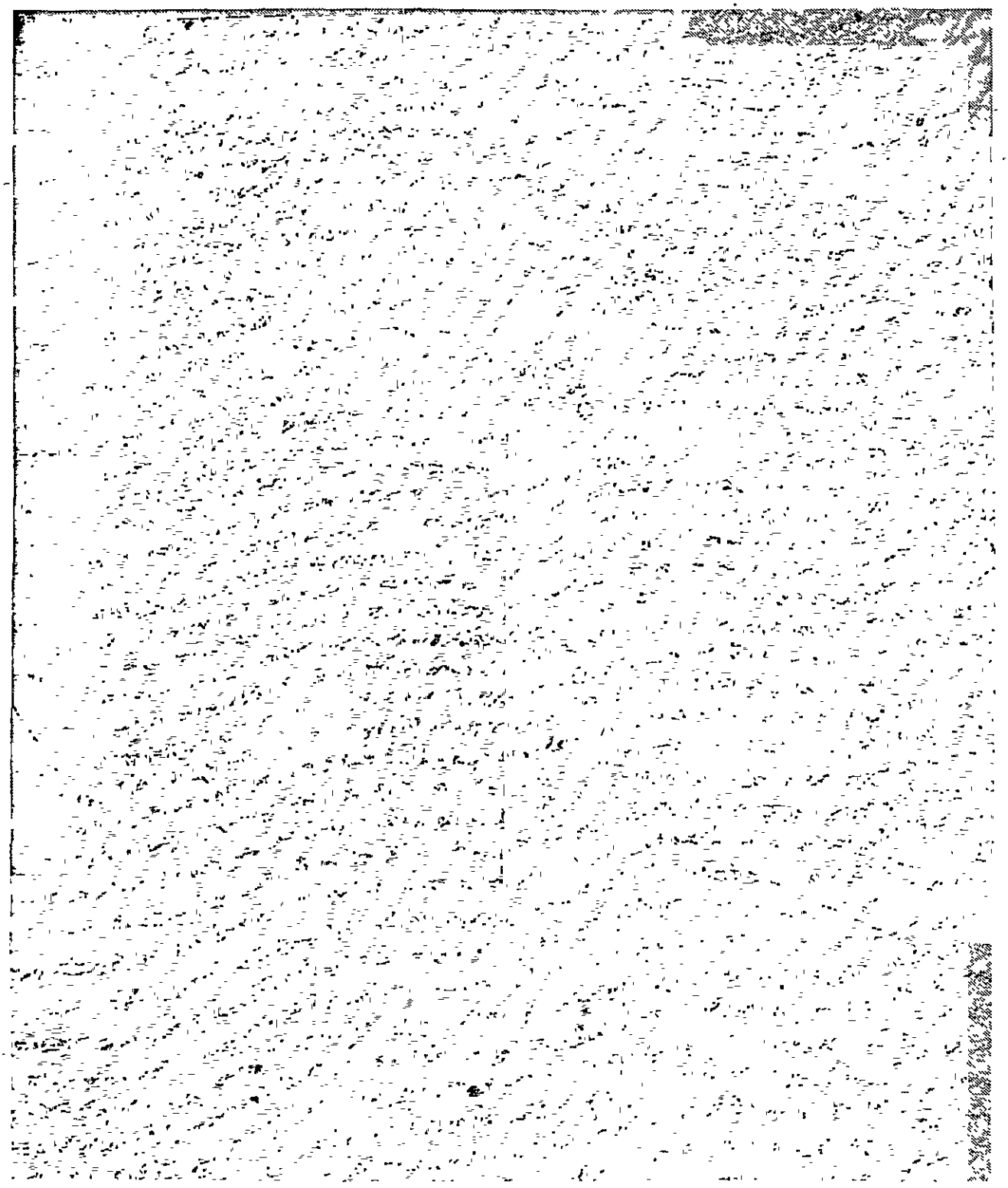

Figure 3.8.5-5 Micrograph of a Cross-Section of the Rib of a Machined Graphite/Resin Composite Plate

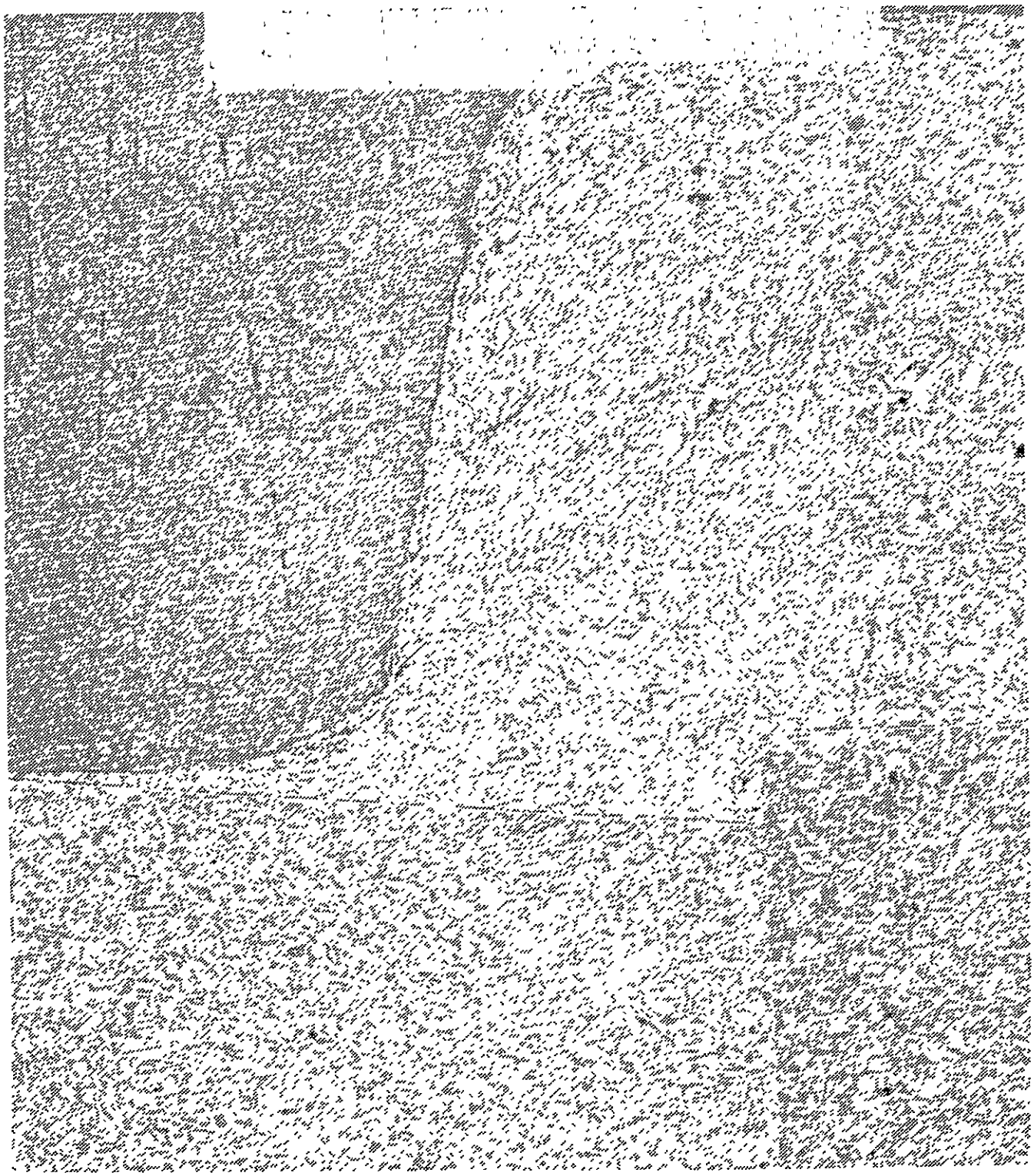

Figure 3.8.5-6 Micrograph of a Cross-Section of the Rib of a Molded Graphite/Resin Composite Plate

TABLE 3.8.5-4

SUMMARY OF HEAT TREATED EXPERIMENTAL PLATES MOLDED WITH ALTERNATE GRAPHITES (SEE APPENDIX C FOR DETAIL INFORMATION)

"COOLER" PLATES

GRAPHITE	% SRINKAGE		FLATNESS (IN.)		RESISTIVITY (MILLIOHM-CM)			BULK DENSITY (G/CC)
	LENGTH	WIDTH	LENGTH LARGE BORDER	WIDTH	PERP.	PARALLEL	RATIO	
MACHINED A-99 PLATE	-	-	0.02	0.00	-	-	-	-
REGRIND	4.60	4.54	0.05	0.02	3.70	6.45	1.74	1.59
AIRCO	4.39	4.30	0.08	0.02	2.40	3.60	1.47	1.52
4421 WET	4.70	4.17	0.09	0.05	1.40	2.25	1.61	1.74
DRY	3.21	3.01	0.16	0.03	1.30	4.65	3.58	1.68
9039 WET	3.27	3.33	0.19	0.05	2.50	3.85	1.54	1.33
DRY	3.16	3.08	0.17	0.06	2.10	5.60	2.79	1.40
A-99 WET	4.46	4.15	0.14	0.03	1.80	2.55	1.42	1.69
DRY	3.67	3.20	0.13	0.05	3.70	5.40	3.38	1.70

"BIPOLAR" PLATES

GRAPHITE	% SRINKAGE		FLATNESS (IN.)		RESISTIVITY (MILLIOHM-CM)			BULK DENSITY (G/CC)
	LENGTH	WIDTH	LENGTH LARGE BORDER	WIDTH	PERP.	PARALLEL	RATIO	
REGRIND	4.33	3.77	0.00	0.01	4.20	3.75	0.89	1.68
9026	3.09	2.97	0.05	0.02	2.70	4.95	1.83	1.68
AIRCO 20	4.52	4.71	0.03	0.04	4.60	6.95	1.51	1.37
4421 WET	4.85	5.24	0.01	0.04	1.40	3.30	2.36	1.80
DRY	3.22	3.52	0.03	0.09	1.20	3.85	3.21	1.76
4735 DRY	3.45	3.22	0.02	0.06	0.86	3.35	3.90	1.80
9039 WET	4.46	4.76	0.01	0.08	2.30	4.80	2.09	1.58
DRY	3.23	3.28	0.04	0.09	4.30	6.90	1.60	1.35
A-99 WET	4.71	5.14	0.04	0.09	1.70	1.92	1.13	1.69
DRY	3.63	3.94	0.02	0.10	1.30	3.50	2.69	1.68
5035	3.67	3.93	0.03	0.09	1.70	4.10	2.41	1.76

1. ALL GRAPHITE OR CARBON MATERIALS MIXED WITH 32 WT% VARCUM 29-703 PHENOLIC RESIN.
2. % SHRINKAGE IS CALCULATED FROM THE DIMENSIONS OF THE PLATES AFTER COMPRESSION MOLDING VERSUS AFTER 900°C HEAT TREATMENT.
3. WET MIXES WERE MADE BY DISSOLVING THE RESIN IN A SOLVENT, THEN ADDING THE GRAPHITE OR CARBON, MIXING, DRYING, THEN GRINDING THE DRIED MATERIAL.
4. ALL MOLDING CONDITIONS CONSISTANT WITH PAFC 003 REV#3 EXCEPT THAT: 2 MINUTE MOLDING CYCLES WERE USED, AND PREFORM PRESSURE WAS INCREASED TO 50 TONS.
5. PERPENDICULAR TO PRESSING SAMPLES WERE 5 BY 5 INCH BARS CUT FROM A PLATE'S EDGE. THE PARALLEL TO PRESSING SAMPLES WERE CUT FROM THE BARS AND MACHINED ROUND (.4" DIA.) A FOUR POINT MEASURING METHOD WAS USED FOR BOTH TYPES OF SAMPLES. THE RATIO IS THE PARALLEL VALUE DIVIDED BY THE PERPENDICULAR RESISTIVITY VALUE.
6. AFTER HEAT TREAT TO 900°C FLATNESS IS MEASURED BY TRACING AN EDGE, CONNECTING THE END POINTS (LINE L1), DRAWING TWO LINES (LINES L2 and L3) THAT ARE TANGENT TO THE PROFILE AND PARALLEL TO THE LINE L1. THE DISTANCE BETWEEN LINES L2 AND L3 IS USED TO CHARACTERIZE FLATNESS.

A) S-TYPE CURVATURE

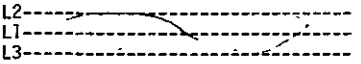

B) BOWED CURVATURE

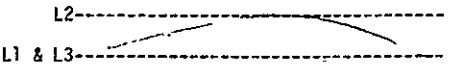

It is believed that the regrind process reduces the anistropy (shape) of the graphite/carbon composite. Figure 3.8.5-7 represents a simplified explanation of this behavior. The number of plates molded with the regrind material was small due to the limited availability of material. The following three materials were selected for further work: Asbury 4421, Superior 9026, and Regrind Asbury 4421.

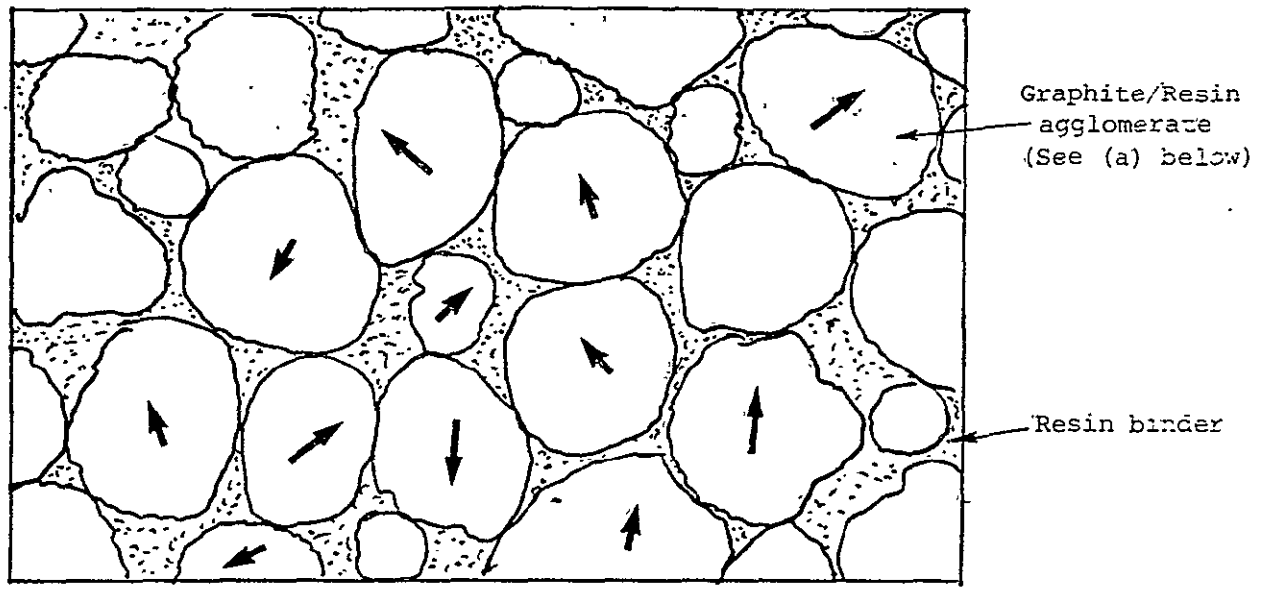

b) Graphite/Phenolic Resin Composite Molded with the Regrind Material.

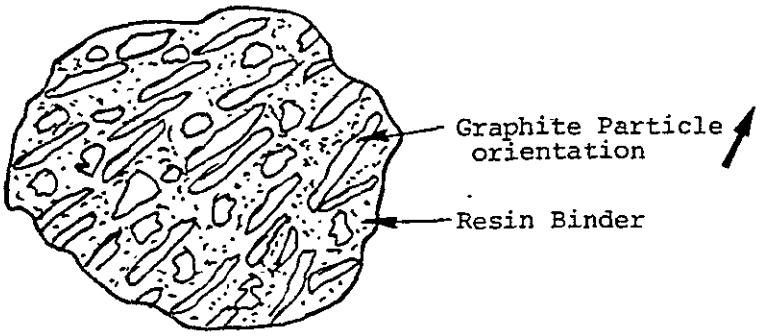

(a) Graphite/resin Agglomerate Cured or Partially Cured before Compression Molding.

Figure 3.8.5-7 Random Graphite Particle Orientation in a Regrind Material/Resin Composite

4.0 FACILITIES DEVELOPMENT

4.1 SUBSCALE 2 x 2 INCH CELL PRESSURIZED TEST FACILITIES

Assembly and checkout of two 2 x 2 inch subscale cell pressurized test facilities was completed. Table 4.1-1 lists the capabilities of these facilities. Each of these facilities is capable of testing four 2 x 2 inch cells independently and simultaneously. Figure 4.1-1 is a photograph of the completed facility in operation. Table 4.1-2 lists the verified operating conditions during the check-out.

Cells numbered 3001 to 3008 were primarily assembled for checking out the new 2 inch x 2 inch cell pressurized test facilities. Performance of these cells at various pressures is presented in Tables 4.1-3 and 4.1-4. At 325 mA/cm^2 and 70 psia, the best cell terminal voltage was 691 mV (IR-free 736 mV) for 80 percent fuel utilization (H_2) and 50 percent Air Utilization. The corresponding terminal voltage at 400 mA/cm^2 and 70 psia pressure was 658 mV (IR-free 723 mV). At 120 psia and 325 mA/cm^2, the maximum terminal cell voltage was 716 mV (IR-free 768 mV), and at 400 mA/cm^2 the corresponding terminal cell voltage was 695 mV (IR-free 759 mV).

4.2 NINE-CELL STACK TEST FACILITIES DEVELOPMENT

Design of a new 12 inch x 17 inch nine-cell stack pressurized test facility was completed. The materials for fabricating this facility were ordered. This facility will be fabricated during the second logical unit of work.

Table 4.2-1 lists the capabilities of the new design. Table 4.2-2 lists the range of the design operating conditions. Table 4.2-3 presents details of the specifications of the failure mode control system for the 12 inch x 17 inch stack pressurized test facility. Table 4.2-4 presents the summary of the materials ordered and received for fabrication of the test facility.

TABLE 4.1-1

2 x 2 INCH CELL PRESSURIZED TEST FACILITY CAPABILITIES

- Capable of testing up to four cells simultaneously
- Independent flow control of process gases for each cell
- Open circuit tests with fuel and/or oxidant off can be performed
- Load transients with greater than 3 millisecond switching time can be studied
- Automatic individual cell shut-down if cell voltage or temperature is outside the set ranges (ranges can be changed)
- Automatic system shut-down if hydrogen detected in vessel

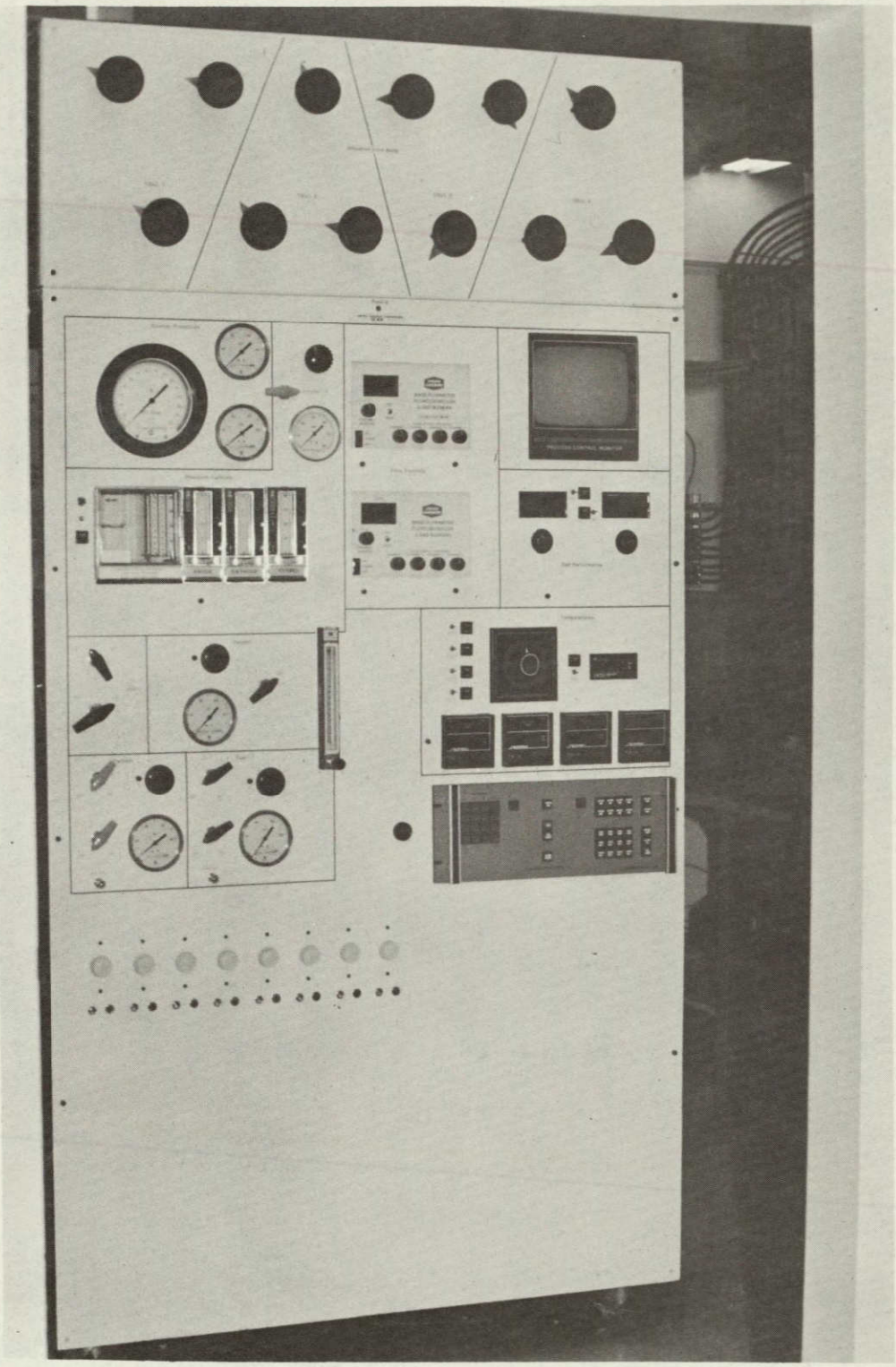

Figure 4.1-1 2 x 2 Inch Pressurized Test Facility in Operation

TABLE 4.1-2

2 x 2 INCH CELL PRESSURIZED TEST FACILITY VERIFIED OPERATING CONDITIONS

		Limitation
Pressure Range	0 to 135 psig (1 to 10.2 atm.) (pressurization rate of ∿ psi per minute)	Present procedure and control equipment
Standard Gases	H_2 fuel, air oxidant, auxiliary inputs for special gases	
Current Range	15 to 600 mA/cm^2 (0.37 to 15 amps)	Amp meter
Fuel Flow Range	Up to 80 percent utilization at mA/cm^2	Flow measuring equipment
	60 percent to 100 percent at 600 mA/cm^2 for H_2 450 mA/cm^2 for SRF (dry)	
Oxidant Flow Range	Up to 50 percent utilization at 50 mA/cm^2	Flow measuring equipment
	27 percent to 100 percent utilization at 600 mA/cm^2	
Temperature Range	30 to 250°C (Independently controlled for each cell)	Fuel Cell Parameters

TABLE 4.1-4

2 x 2 INCH PERFORMANCE DATA OBTAINED DURING TEST FACILITY CHECKOUT (IR-FREE VOLTAGE)

CELL NO	1 ATM.(14.7 PSIA)*			4.76 ATM.(70 PSIA)+			8.16 ATM.(120 PSIA)+			
	IR FREE VOLTAGE @ 20 mA/cm^2 mV	IR FREE VOLTAGE @ 200 mA/cm^2 mV	IR FREE VOLTAGE @ 50 mA/cm^2 mV	IR FREE VOLTAGE @ 200 mA/cm^2 mV	IR FREE VOLTAGE @ 325 mA/cm^2 mV	IR FREE VOLTAGE @ 400 mA/cm^2 mV	IR FREE VOLTAGE @ 50 mA/cm^2 mV	IR FREE VOLTAGE @ 200 mA/cm^2 mV	IR FREE VOLTAGE @ 325 mA/cm^2 mV	IR FREE VOLTAGE @ 400 mA/cm^2 mV
3001	809	672	799	764	734	714	***	***	***	***
3002	812	670	829	772	739	723	***	***	***	***
3003	812	672	815	760	736	713	***	***	***	***
3004	806	665	---	746	725	706	***	***	***	***
3005	803	668	---	765	731	722	858	797	764	751
3006	814	672	831	766	734	719	851	797	769	755
3007	808	669	806	761	726	---	831	798	768	759
3008	810	673	791	754	726	706	800	784	760	---

* CONSTANT FLOW DATA
\+ 80% FUEL (H_2) 50% OXIDANT (AIR) UTILIZATION
*** CELLS NOT TESTED AT THIS PRESSURE

TABLE 4.2-1

12 x 17 INCH STACK PRESSURIZED TEST FACILITY CAPABILITIES

- Capable of testing up to a nine-cell stack
- Measurement of Fuel, oxidant and cooling flow pressure drops
- Cooling inlet temperature control
- Backup flow monitoring
- Fine control of electrical load
- Automatic failure mode control system
- Load transients with greater than 3 milliseconds switching time can be studied

TABLE 4.2-2

12 x 17 INCH STACK PRESSURIZED TEST FACILITY

DESIGN OPERATING CONDITIONS RANGE

		Limitation
Pressure Range	0 to 135 psig (1 to 10.2 atm) pressurization rate of approximately 2 psi per minute	Present procedure and control equipment
Standard Gases	H_2 fuel, air, oxidant, auxiliary inputs for special gases	
Current Range	50 to 460 mA/cm^2 (50 to 500 amps)	Amp meter
Fuel Flow Range	Up to 80 percent utilization at 50 mA/cm^2 50 to ∿ 100 percent utilization at 460 mA/cm^2	Flow measuring equipment
Oxidant Flow Range	Up to 50 percent utilization at 50 mA/cm^2 20 to ∿ 100 percent utilization at 460 mA/cm^2	Flow measuring equipment
Temperature Range	30 to 250°C Independently controlled end plate temperatures	Stack parameters
Cooling	100 scfm air Ambient to 200°C	Blower & heater elements

TABLE 4.2-3

SPECIFICATIONS OF THE FAILURE MODE CONTROL SYSTEM FOR

12 x 17 INCH STACK PRESSURIZED TEST FACILITY

Problem	Trip Point (Adjustable)	Action
Stack Undervoltage (group of 2 or 3 cells)	0.5-3.0 volts	Remove Load
Stack Over Temperature	150-250°C	Remove Load
Vessel Over Temperature	100-175°C	Remove Load Stop Process Flows Depressurize System
H_2 in Vessel Gas	1 percent or 4 percent	Remove Load Stop Process Flows Depressurize System
Power Failure	Longer than 1 minute	Remove Load
	Longer than 30* minutes	Remove Load Stop Process Flows Depressurize System

* Due to Loss of Back-up Power and Supply Air

TABLE 4.2-4

PROGRESS REPORT

12 x 17 INCH PRESSURIZED STACK TEST FACILITY

ITEM	DATE ORDERED	DATE RECEIVED	*DATE MOUNTED	+DATE INSTALLED	#DATE CALIBRATE	COMMENTS
PANEL FRAME	**	**				----
PANEL ALUMINUM						
MAIN VESSEL	**	**				----
VAPORIZER						
WATERTRAP	**	**				----
CONDENSER						
VOLTMETER & SWITCH	**	**				----
AMMETER & SHUNTS	**	**				----
PYROMETER & SWITCH	**	**				----
TEMP JACK PANEL	**	**				----
TEMP CONTROLLERS	**	**				----
AIR PREHEATER	03-04-83	05-13-83				Q-4 E23114
RECIRC. HEATER	03-31-83					Q-2 E23217
DATA MONITOR	03-03-83	03-17-83				Q-1 E23140
DIMMER SWITCHES						
UTILITY BOX	**	**				----
REGULATORS	**	**				----
PRESSURE GUAGES	**	**				----
FLOW CONTROLLERS	03-22-83	04-21-83				Q-4 E23117
RECIRC. FLOWMETER	04-05-83					Q-2 E23301
ROTAMETER	03-10-83	04-15-83				Q-3 E23146
HIGH VOL ROTAMETER	03-09-83					Q-2 E23118
3x6 3-PEN RECORDER	02-28-83	04-12-83				Q-2 E23057
6x6 3-PEN RECORDER	**	**				----
PRES CONTROLLERS	02-28-83					Q-3 E23057
PRES TRANSMITTER	02-28-83	05-16-83				Q-8 E23057
CONTROL VALVES	03-03-83	05-19-83				Q-5 E23129
SOLENOID VALVES	03-04-83	03-18-83				Q-6 E23092
BUTTERFLY VALVES	03-28-83	05-02-83				Q-2 E23280
SUPPLY VALVES	03-08-83	03-17-83				Q-18 E22710 R-6
CHECK VALVES	03-08-83	03-17-83				Q-5 E22110 R-6
RECIRC LOOP PIPING	04-11-83					E23343-E23336-E23219
RECIRC BLOWER	03-09-83	04-28-83				Q-4 E23116
VARIABLE FREQ CNTL	02-28-83	03-22-83				Q-2 E23046
VAPORIZER PUMP	02-28-83	03-24-83				Q-1 E23058
VARIAC	**	**				----
CNTL VALVE TRIMS	03-04-83	04-26-83				Q-3 E23098
VESSEL FITTINGS						
HOUR METER						
DEW PT. HYGROMETER	02-23-83	03-17-83				Q-2 E23110
SAFETY CIRCUIT	04-24-83					
BATTERY	**	**				----
LOAD BANK						
SCANNER/APPLE	**	**				----

* DATE INSTRUMENT WAS MOUNTED INTO PANEL OR FRAME
+ DATE INSTRUMENT WAS WIRED AND/OR PLUMBED INTO SYSTEM
# DATE INSTRUMENT WAS CALIBRATED (TEST OPERATIONAL)
** - AVAILABLE FROM PREVIOUSLY PLANNED FACILITY

1. Report No.	2. Government Accession No.	3. Recipient's Catalog No.
NASA CR-174732		

4. Title and Subtitle	5. Report Date
Gas Cooled Fuel Cell Systems Technology Development	August 1983
	6. Performing Organization Code XAL-78010-AL

7. Author(s)	8. Performing Organization Report No.
J.M. Feret	
	10. Work Unit No.

9. Performing Organization Name and Address	11. Contract or Grant No.
Westinghouse Electric Corporation Advanced Energy Systems Division P.O. Box 10864 Pittsburgh, PA 15236-0864	DEN 3-290
	13. Type of Report and Period Covered Contractor Report
12. Sponsoring Agency Name and Address U.S. Department of Energy Morgantown Energy Technology Center Morgantown, West Virginia 26505	14. Sponsoring Agency ~~Code~~ Report No. DOE/NASA/0290-1

15. Supplementary Notes

Final Report for First Logical Unit of Work. Prepared under Interagency Agreement DE-AI01-80ET17088. Project Manager, Robert B. King, Energy Technology Division, NASA Lewis Research Center, Cleveland, Ohio 44135.

16. Abstract

The work described in this report addresses the first phase of a planned multiphase program to develop a Phosphoric Acid Fuel Cell (PAFC) for Electric Utility Prototype Power Plant Application. This report describes the efforts performed that culminated in the (1) Establishment of the preliminary design requirements and system conceptual design for the nominally rated 375 kW PAFC module and is interfacing power plant systems; (2) Establishment of PAFC component and stack performance, endurance, and design parameter data needed for design verification for power plant application; (3) Improvement of the existing PAFC materials data base and establishment of materials specifications and process procedures for the cell components; and (4) Testing of 122 subscale cell atmospheric testa for 110 000 cumulative test hours, 12 subscale cell pressurized tests for 15 000 cumulative test hours, and 12 pressurized stack test for 10 000 cumulative test hours.

17. Key Words (Suggested by Author(s))	18. Distribution Statement
Fuel cells; Phosphoric acid; Energy conversion; Energy systems; Advanced power; Carbon corrosion; Carbon compounds; Alloy catalyst	Unclassified - unlimited STAR Category 44 DOE Category UC-97d

19. Security Classif. (of this report)	20. Security Classif. (of this page)	21. No. of pages	22. Price*
Unclassified	Unclassified	328	A15

*For sale by the National Technical Information Service, Springfield, Virginia 22161